Oxidative Medicine and Cellular Longevity

Effect of Nutraceuticals and Pharmaceuticals on Oxidative Stress in Vascular Aging and Cardiovascular Disease

Lead Guest Editor: Albino Carrizzo
Guest Editors: Gabriele G. Schiattarella and Sabato Sorrentino

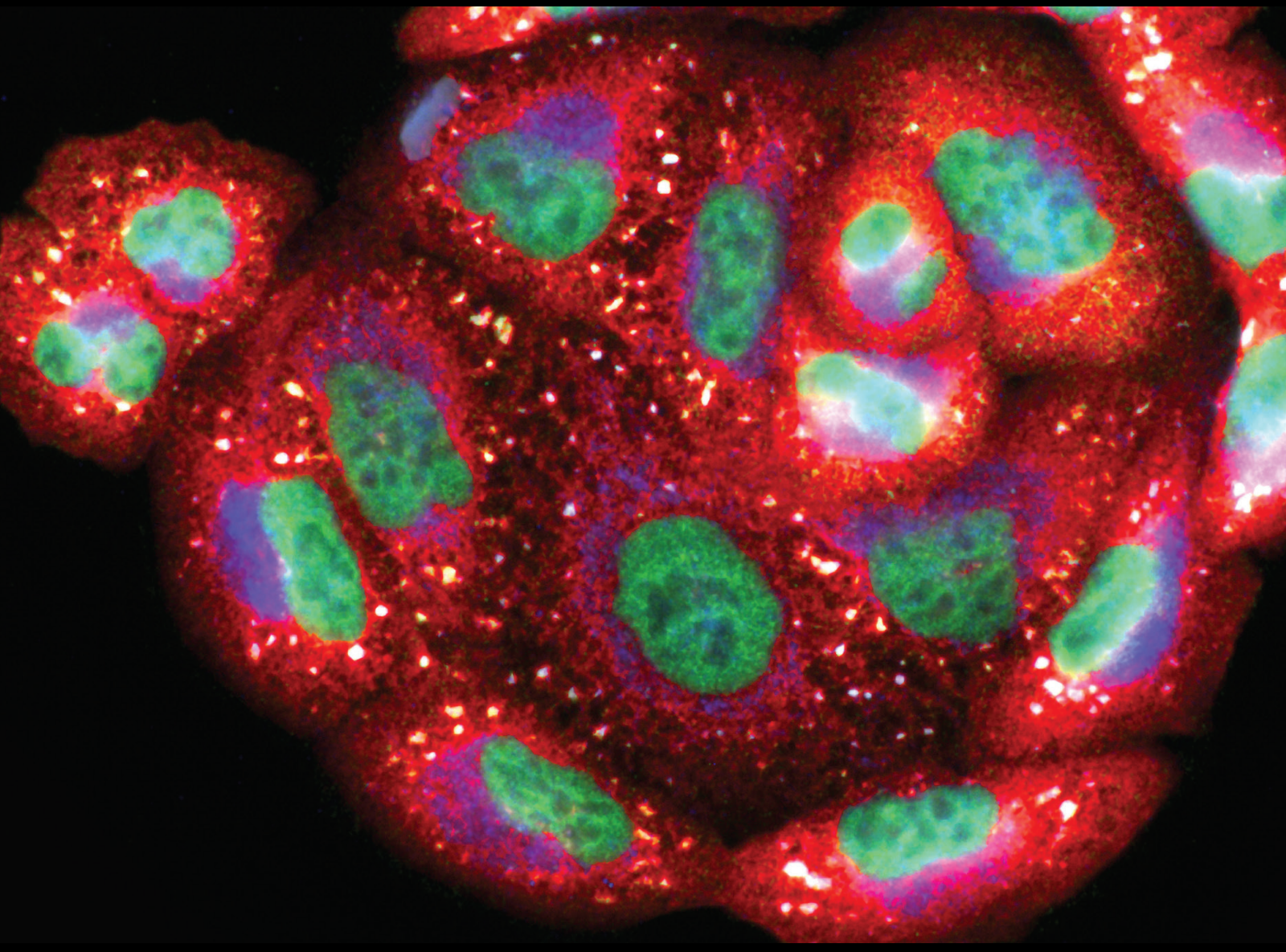

Effect of Nutraceuticals and Pharmaceuticals on Oxidative Stress in Vascular Aging and Cardiovascular Disease

Oxidative Medicine and Cellular Longevity

Effect of Nutraceuticals and Pharmaceuticals on Oxidative Stress in Vascular Aging and Cardiovascular Disease

Lead Guest Editor: Albino Carrizzo
Guest Editors: Gabriele G. Schiattarella and Sabato Sorrentino

Contents

Hindawi
Oxidative Medicine and Cellular Longevity
Volume 2020, Article ID 2176728, 20 pages
https://doi.org/10.1155/2020/2176728

Review Article

Cardioprotective Effects of Dietary Phytochemicals on Oxidative Stress in Heart Failure by a Sex-Gender-Oriented Point of View

Klara Komici,[1] **Valeria Conti**,[2] **Sergio Davinelli**,[1] **Leonardo Bencivenga**,[3] **Giuseppe Rengo**,[3,4] **Amelia Filippelli**,[2] **Nicola Ferrara**,[3,4] **and Graziamaria Corbi**[1]

[1]*Department of Medicine and Health Sciences, University of Molise, Via Francesco De Sanctis, 1, 86100 Campobasso, Italy*
[2]*Department of Medicine, Surgery and Dentistry "Scuola Medica Salernitana", University of Salerno, Via S. Allende, Baronissi, 84081 Salerno, Italy*
[3]*Department of Translational Medical Sciences, University of Naples Federico II, Via Pansini, 5 -, 80138 Naples, Italy*
[4]*Istituti Clinici Scientifici Maugeri SpA Società Benefit" (ICS Maugeri SpA SB), Via Bagni Vecchi, 1, 82037 Telese Terme (BN), Italy*

Correspondence should be addressed to Sergio Davinelli; sdavinelli@hsph.harvard.edu

Received 31 May 2019; Revised 3 November 2019; Accepted 29 November 2019; Published 10 January 2020

Guest Editor: Sabato Sorrentino

Dietary phytochemicals are considered an innovative strategy that helps to reduce cardiovascular risk factors. Some phytochemicals have been shown to play a beneficial role in lipid metabolism, to improve endothelial function and to modify oxidative stress pathways in experimental and clinical models of cardiovascular impairment. Importantly, investigation on phytochemical effect on cardiac remodeling appears to be promising. Nowadays, drug therapy and implantation of devices have demonstrated to ameliorate survival. Of interest, sex-gender seems to influence the response to HF canonical therapies. In fact, starting by the evidence of the feminization of world population and the scarce efficacy and safety of the traditional drugs in women, the search of alternative therapeutic tools has become mandatory. The aim of this review is to summarize the possible role of dietary phytochemicals in HF therapy and the evidence of a different sex-gender-oriented response.

1. Introduction

Despite recent advances in clinical/diagnostic tools and therapies, the incidence and prevalence of heart failure (HF) show a steady increase [1]. From the pathophysiological point of view, this condition is associated with chronic overactivation of the adrenergic system [2–4], endothelial dysfunction, increased oxidative stress [5], and mitochondrial dysfunction; all these abnormalities are involved in the development and the progression of HF [6]. Nowadays, although drug therapy and the implantation of devices have demonstrated to increase survival, their use is limited by important side effects [7] that worsen the HF patients' quality of life. Moreover, the demographic changes in population composition have recently determined an increasing difficulty in the therapeutic approach of HF. Starting with the evidence of the feminization of the world population and the scarce efficacy and safety of the traditional drugs in women, the search for alternative therapeutic tools has become mandatory. Despite sex referring to biological factors and gender to psychosocial, cultural, and environmental factors, it is difficult to separate one from each other. Both are multidimensional, entangled, and interactive factors that may influence the pharmacological response. Then, it has been suggested that the simultaneous use of sex-gender terms is more appropriate [8]. From this view, the dietary phytochemicals appear, thanks to their safety and efficacy, the ideal candidate for the HF therapy in women. The aim of this review is to summarize the cardioprotective effects of natural products in HF therapy and the evidence of a different sex-gender-oriented response to oxidative stress modulation.

2. Sex-Gender and HF

2.1. Sex-Gender Differences in HF. The prevalence of HF affects about 2.6 million women and 3.1 million men in the

USA [9], with higher prevalence in advanced age. However, women tend to be older than men at diagnosis and exhibits a different phenotype: the HF with preserved ejection fraction (HFpEF) is more frequent in women and new onset of HF with reduced ejection fraction (HFrEF) in men [10]. Moreover, despite women with present HF at an older age, where comorbidities are more frequent, some studies showed that women have a lower cardiovascular and all-cause mortality [11, 12], suggesting that the phenotypic differences in HF presentation and prognosis between women and men may be the consequence of progressive, sex-specific changes in cardiac and vascular physiology. Furthermore, the menopausal transition may influence the development of cardiovascular risk factors in women [13]. Women demonstrate greater, body-size-adjusted increases in the left ventricle (LV) wall thickness and concentric remodeling than men, which predispose to myocardial stiffness and diastolic dysfunction. Furthermore, the age-related increase in left ventricle ejection fraction (LVEF) is more pronounced in women [14]. Animal models indicate that female rats are more likely to develop concentric myocardial hypertrophy [15]. These differences in LV remodeling are consistent with the highest likelihood of women to present HFpEF. On the other hand, men are more likely to show age-related increases in the LV cavity dimension and LV systolic dysfunction, which are hallmarks of HFrEF [14]. Consistent with these observations, male rats generally develop eccentric myocardial hypertrophy and fibrosis [15]. These different underlying processes could be responsible for the potential differences in drug tolerance and toxicity [16] to therapeutic interventions in women. Indeed, the most common therapeutic modalities for HF currently include therapies effective in the treatment of HFrEF; conversely, their efficacy in the treatment of HFpEF, the most common HF type in women, has been largely inconclusive [17]. Then, the understanding of the differences in pathophysiological response requires also the study of the different molecular pathways implicated in the different phenotypes of HF.

While HFrEF is linked with ischemia and cardiomyocyte loss [18], HFpEF is associated with advanced age [19], obesity [20], and hypertension [21]. These comorbidities induce the extensive myocardial expression of endothelial adhesion molecules [22]. A progressive reduction in the capillary density (i.e., microvascular rarefaction) in HFpEF hearts [23] activates a transforming growth factor-β- (TGFβ-) signaling cascade that is profibrotic and leads to myocardial collagen accumulation [24, 25].

2.2. Role of Oxidative Stress in HF. Activation of the sympathetic nervous system and the renin-angiotensin-aldosterone axis in HF is associated with oxidative stress, and it is already well-established that, in the genesis of HF, reactive oxygen species (ROS) production within the myocardium and the vasculature is substantially increased [5, 26, 27]. Oxidative stress is defined as an imbalance between the production of ROS and the endogenous antioxidants defense system [28, 29].

ROS are high reactivity oxygen-based chemical species that include free radicals, such as superoxide ($O2^-$), hydroxyl radical (OH), and nonradical molecules capable of generating free radicals, such as hydrogen peroxide (H2O2). The role of the antioxidant defense system is to scavenge and degrade ROS to nontoxic molecules. Well-known enzymes with antioxidant properties are superoxide dismutase (SOD), glutathione peroxidase, and catalase [30]. Mitochondria, nicotinamide adenine dinucleotide phosphate (NADPH) oxidases (NOXs), and uncoupled NO synthase (NOS) are considered relevant sources of ROS generation during HF development. Under physiological conditions, NADH and FADH2 generation is required for sequential redox reactions in mitochondria and ATP production, and minimal quantity of ROS is produced. In HF models, increased generation of $O2^-$, hydroxyl radicals, and H2O2 has been identified an [31, 32]. Moreover, the myocardial expression of ROS correlates with left ventricular contractile dysfunction. Although the majority of experimental models are performed on mice or rats following myocardial infarction induction [33], data from clinical studies in patients with ischemic cardiomyopathy also confirmed the relationship between increased levels of ROS and left ventricular dysfunction [34]. In fact, in conditions such as hypoxia or ischemia where oxygen availability is reduced, mitochondrial generation of ROS is enhanced and this can contribute to cardiomyocyte damage [28, 35]. In addition, increased ROS levels influence mitochondrial DNA damage which may lead to additional mitochondrial ROS generation [36]. Ca^{2+} signaling alternations are other hallmarks for HF, and systolic Ca^{2+} transient amplitude is reduced with a slower rate-of-rise. Consequences of these modifications are decreased cardiomyocyte shortening, slower contractile kinetics, and delayed relaxation. At the molecular level, these findings are explained by an increased leak of Ca^{2+} from the sarcoplasmic reticulum via ryanodine receptors, downregulation of sarcoplasmic reticulum ATPase (SERCA2A) together with upregulation of Na/Ca^{2+} exchanger [37]. These perturbations at the mitochondrial level affect the NADH and NADPH activity, enhancing the prooxidative state and increasing mitochondrial ROS production [38].

NADPH oxidase has been reported as a major source of ROS generation in HF [39]. Endothelial cells and activated leukocytes are main sources of NADPH oxidase ROS generation. Different studies over the last decade have tried to investigate the role of specific catalytic units of NADPH oxidase such as Nox2 and Nox4 in HF development and progression [40, 41]. Indeed, genetic deletion of Nox2 in animal models of systolic dysfunction improved left ventricular remodeling. Pressure overload models of HF triggers NOS uncoupling, generation of ROS, and its inhibition-attenuated cardiac dilatory remodeling and reduced ROS level [42]. Of interest, a crosslink between NADPH oxidase activation and mitochondrial dysfunction mediated by Angiotensin II has been also described [43]. Angiotensin II initially activates NADPH oxidase and production of $O2^-$ and H2O2, which induces mitochondrial generation of ROS and modulates endothelial NO production.

As previously described, whereas in HF genesis and progression, a prominent role is ascribed to ROS production and accumulation, exhaustion of endogenous antioxidants

defense system has been reported in myocardial infarction animal models [43], and inversely, overexpression of antioxidant enzymes such as glutathione peroxidase improves left ventricular remodeling in ischemia/reperfusion HF model [44, 45].

Several murine models of systolic HF have showed reduction of other antioxidative defenses as SOD and NAD [33, 46–49]. Of interest, depleted blood glutathione levels were significantly associated with symptomatic status in patients with ischemic cardiomyopathy [50]. In contrast, in pacing induced HF experimental model, no modification of antioxidant defense enzymes including SOD, glutathione peroxidase, and catalase was described indicating that oxidative stress in this type of HF might be primarily caused by the enhancement of ROS generation rather than the decline in antioxidant defenses [51]. Preclinical studies have revealed the existence of an uncoupled sNO enzyme state where NO release was replaced by $O2^{-}$ production, and inhibition of eNOS resulted in decreased ROS generation [52, 53]. Furthermore, AT1 receptor blockage reduced ROS production, improved NO release, and cardiac remodeling in idiopathic-dilated cardiomyopathy experimental model [54]. Interestingly, in an experimental model of HFpEF, decreased myocardial NO levels lead to increased cytosolic Ca^{2+} and diastolic dysfunction and these effects were restored by supplementation with eNOS cofactor tetrahydrobiopterin [55]. It is believed that in HFrEF, major generation of ROS occurs in cardiomyocytes and this process induces maladaptive remodeling through the activation of cardiomyocyte necrosis, apoptosis, and reactive cardiac fibrosis, while HFpEF, a chronic proinflammatory state induced by comorbidities, is responsible for ROS generation in endothelial cells. Further, this process effects cardiac remodeling by inducing cardiomyocyte hypertrophy and myocardial stiffness.

2.3. Sex-Gender Differences in Oxidative Stress. Notably, clinical and experimental data suggested a greater antioxidant potential in females over males [56]. In particular, ROS production is higher in the vascular cells from males than in the cells from females [57, 58], suggesting that women are less susceptible to oxidative stress. Indeed, oxidative stress occurs as a result of an imbalance between ROS production and the antioxidant defense system. Brandes et al. [59] found that, under normal conditions, the male rat aortas generated more superoxide radicals than the female aortas. In contrast, a study [60], comparing coronary artery disease (CAD) in postmenopausal women with males, demonstrated that, even in the control group who did not have CAD, postmenopausal women had higher oxidative stress levels than men, with women with CAD having ROS levels almost three times higher than men with CAD [60]. This suggests the possibility that estrogen lowers oxidative stress in premenopausal females. These findings could explain, at least in part, the different HF phenotype between genders.

A difference in the expression and/or activities of antioxidant enzymes between males and females may also be explained by the different antioxidant response. Regarding superoxide dismutase (SOD), there is no uniform consensus on gender differences. Chen et al. [61] reported no significant difference in SOD activity levels between male and female mice in the heart, while Barp et al. [62] in female rats' heart found higher SOD activity levels than in males. Interestingly, the SOD activity levels in both male and female rats were significantly decreased after castration compared to their respective controls [62], suggesting a possible association between sex hormones and SOD activity levels. It is more likely that males could have higher levels of superoxide production due to NADPH oxidase activity. A study [63] found no gender difference in the vascular response to hydrogen peroxide, thus suggesting that the difference between male and female ROS production could be due to NADPH oxidase activity. In particular, NADPH oxidase subunits were found to exhibit gender discrepancies. Expression of Nox1 and Nox4 was higher in males than in females, suggesting that gender differences in superoxide formation could be due to the activity of these two subunits [63]. Stimuli that activate Nox4 include ischemia, hypoxia, and adrenergic stimuli, all present and enhanced in the setting of HF. The implications of Nox4 for HF are still controversial. Kuroda et al. [41] demonstrated that, in cardiac-specific Nox4 knockout mice, the upregulation of Nox4 was primarily responsible for the increased mitochondrial O2− production in response to pressure overload. Furthermore, Nox4 played a critical role in mediating mitochondrial dysfunction, apoptosis in cardiac myocytes, and eventual LV dysfunction in response to pressure overload [41]. On the other hand, other evidence [64, 65] showed that both Nox2 and Nox4 contribute to the increase in ROS and injury by ischemia/reperfusion. However, low levels of ROS produced by either Nox2 or Nox4 regulate HIF-1α and PPAR-α, thereby protecting the heart against the ischemia/reperfusion injury, suggesting that Nox also act as a physiological sensor for myocardial adaptation [64, 65].

Higher levels of Nox1 and Nox2 in porcine isolated coronary arteries (PCA) were found in males, although Nox4 was higher in females [66]. It could be possible that higher expression of Nox subunits in men could in part explain why males exhibit higher levels of oxidative stress than females. Wong et al. [66] also showed that the Nox subunits played a role in endothelium-derived hyperpolarization in PCAs of males but not females, which could further show that an increased level of Nox activity is indicative of more oxidative stress in males. Also, ovariectomy of female rats NADPH oxidase activity treatment with 17b-estradiol restored NADPH-oxidase activity to normal levels [63]. These data further suggest that estrogen may contribute to decreased oxidative stress, possibly via the regulation of NADPH oxidase activity especially the Nox1, Nox2, and Nox4 subunits. It has also been suggested that males have higher NADPH oxidase activity levels due to an angiotensin II-mediated mechanism. In endothelial cells, 17b-estradiol receptors (E2-R) signaling exerts anti-inflammatory effects by augmenting eNOS-induced NO signaling [67], attenuating the major cellular source of ROS and NADPH oxidase [40, 68], and inhibiting the expression of endothelial leukocyte adhesion molecules such as vascular cell adhesion molecule 1 (VCAM1) and intercellular cell adhesion molecule

(ICAM1) [69]. In cardiomyocytes, E2 stimulates the expression of the prosurvival kinase, Akt, which inhibits cellular apoptosis in women [70] and promotes cell survival [71]. Moreover, E2 attenuates CM remodeling in response to pressure overload [72] and augments myocardial angiogenesis, thereby increasing capillary density [25, 73].

The different response to ROS could partially also explain the difference in the therapy's efficacy. A study on spontaneously hypertensive rats shows that females are less susceptible to angiotensin II-mediated increases in oxidative stress [27]. Another study with wild-type mice showed that superoxide production decreased in male Nox2 knockout mice, but not in females, suggesting that Nox2 plays a role in mediating ROS generation in response to angiotensin II in males but not in females [74]. Another study [75] found that males have higher levels of p47, which is a cytoplasmic subunit of NADPH oxidase. This subunit is connected to the angiotensin II system as angiotensin II binds to the angiotensin type I receptor, which then induces the phosphorylation of p47. Then, there is a translocation of the phosphorylated p47 into the plasma membrane, which is an essential step in the assembly of the NADPH oxidase complex and the initiation of ROS production. This study found that p47 levels did not change with estrogen levels, thus representing an estrogen-independent mechanism, suggesting that regulation of NADPH oxidase activity may be more complex and likely the result of a combination of estrogen-dependent and estrogen-independent mechanisms [75]. Male spontaneously hypertensive rats were found to have higher levels of superoxide generation than female rats [76]. Gender differences associated with NADPH oxidase activity are responsible for the higher levels of superoxide in males. Male spontaneously hypertensive rats also have lower levels of nitric oxide (NO) due to its degradation by superoxide, thus contributing to oxidative stress [76]. In a study with lipopolysaccharides (LPS) to induce inflammation and oxidative stress [77], it was found that female rats treated with LPS had a greater stroke volume and cardiac output compared to male rats, while male rats with LPS treatment were found to have systolic dysfunction after 24 hours whereas female rats did not [77]. These data reveal a significant sex difference associated with LPS injection and that female rats seem to recover cardiac function faster than male rats. Sun et al. [78] have reported that females have increased levels of eNOS associated with the cardiomyocyte-specific caveolin and that after ischemia/reperfusion, females have increased translocation of nNOS to caveolin-3. Sun et al. [78] further showed that in females showing less ischemia/reperfusion injury than males, females have increased S-nitrosylation of the L-type-calcium channel, which results in decreased calcium entry via the L-type calcium channel. The increase in NOS in females under conditions associated with increased calcium (which activates NOS) results in increased S-nitrosylation of the L-type calcium channel, less calcium entry, and therefore less calcium loading during ischemia. Previous studies [79–81] have shown that reducing calcium levels during ischemia is cardioprotective. Overall, the results of all these studies have demonstrated that there is a clear association between gender, oxidative stress, and HF. The question remains whether these gender differences with oxidative stress explain the gender differences in overarching diseases [82].

Moreover, recently, some studies [83–85] have been carried out to decipher whether a disparity in the response to stress could take place in cells coming from males and females concerning the chromosomal asset. XX and XY cells, independently from their origin (e.g., mice, rats, and humans) and histotype (e.g., muscular and endothelial vessel cells, cardiomyocytes, neurons, fibroblasts), display different responses to stress: XX cells are more prone to autophagic cytoprotection and senescence, whereas XY cells are easier and undergo apoptosis. Under the same stress, e.g., oxidative, a sex disparity can be found in intracellular parameters of importance in cell fate [86]. This has been attributed to sex-biased miRNAs, which are regulated by estradiol or are expressed from loci on the X chromosome due to incomplete X chromosome inactivation [25]. Interestingly, whereas estradiol-induced miRNAs predominantly appear to serve protective functions, many X-linked miRNAs have been found to challenge microvascular and myocardial integrity. Thus, menopausal estradiol deficiency, resulting in protective miRNA loss and the augmentation of X-linked miRNA expression, may contribute to the female-specific cardiovascular etiology in HF with near-normal/normal LVEF [25].

3. Dietary Phytochemicals and HF

Dietary phytochemicals include a large group of nonnutrient compounds from a wide range of plant-derived foods and chemical classes [87, 88]. Polyphenols are the most commonly studied classes of dietary phytochemicals. They are considered an innovative nutritional strategy that helps to reduce cardiovascular risk factors, with a beneficial role in endothelial function and oxidative stress as demonstrated by experimental and clinical models of cardiovascular impairment [89, 90]. Importantly, investigation on phytochemical effect on cardiac remodeling appears to be promising [91]. Indeed, a large number of experimental models report that phytochemicals acting through the modulation of oxidative stress response to ischemic injury reduce cardiomyocyte apoptosis, necrosis, and cardiac fibrosis [92, 93]. Dietary phytochemicals are commonly present in fruits, vegetables, nuts, spices, coffee chocolate, cacao, and wine. Although these compounds are well presented in nature, some limits characterize their bioavailability: it is affected by food preparation techniques, gastrointestinal metabolism, and microbial flora. Also, data regarding phytochemicals active metabolites in tissues are rare and difficult to apply [94]. In this section, we initially describe the characteristics of polyphenols and phytosterols and their role on oxidative stress and endothelial function, and then we discuss the most relevant findings of their applications in experimental and clinical models of HF.

3.1. Polyphenols

3.1.1. Classification. Polyphenols include a large class of natural compounds of plant origin found in fruits, legumes,

vegetables, cereals, spices, nuts, olives, chocolate, tea, coffee, beer, and wine [95]. They are water-soluble compounds characterized by one or more phenolic rings classified in flavonoid and nonflavonoids.

Flavonoids chemically consist of two phenyls and one heterocyclic ring and are further subdivided into flavones, flavanols, flavanones, flavonols, isoflavones, and anthocyanidins. Well-known examples of flavonoids are quercetin, catechin, epigallocatechin, genistein, hesperidin, delphinidin, apigenin, and luteolin. Blueberries, parsley, black tea, wine, and cocoa are rich in flavonoids [96, 97].

Nonflavonoids include phenolic acids, stilbenes, and lignans, comprising products like curcumin, resveratrol, tannins, chlorogenic acid, gallic acid, and caffeic acid.

Polyphenols are secondary plant metabolites characterized by astringent color, bitterness, and protection against ultraviolet radiation and pathogens [98]. They are firstly hydrolyzed by intestinal enzymes or by colonic microflora and poorly absorbed. However, it is reported that resveratrol is characterized by a good absorption rate and by a very low bioavailability: 92% of the administered dose was excreted in urine and feces [99]. Their plasma concentration depends also on their ability to bind to metal cations and proteins. Once reaching the colon, they are metabolized by microbiota producing several bacterial metabolites [95]. During phase I metabolism, isoflavones and flavonoids undergo O-demethylation and hydroxylation catalyzed by CYP1A1, CYP1A2, and CYP1B1 [100]. Phase II metabolism is characterized by methylation, glucuronidation, sulfation, and ring-fission metabolism. Catechol-O-methyltransferase (COMT) and sulfotransferase SULT1A1 and SULT1A3 are described as key enzymes involved in this process in mice, rats, and humans [101]. A considerable number of studies [102–104] report that in phase III metabolism, dietary phytochemicals influence ATP-dependent efflux pumps such as multidrug resistance-associated glycoprotein (MGP), p glycoprotein (PGP), and organic anion transporters (OAT) by inhibiting their activity.

3.2. Mechanisms on Oxidative Stress. Polyphenols have strong antioxidant properties, and their activity on oxidative stress is determined by their capacity to (a) upregulate antioxidant defenses, (b) scavenge and interact with ROS, and (c) inhibit enzymes involved in ROS generation. Polyphenols interact with the hydrophobic core of the membrane layer avoiding ROS access. In the same way, they affect the oxidation rate of proteins and lipids [105]. Furthermore, structural features of polyphenols, as hydroxyl groups, catechol group on the B-ring, and carbonyl group in the C-ring influence the scavenging of metal ion chelation and free radicals. Indeed, quercetin is characterized by iron-chelating properties [106]. Modification of hydrogen peroxidase, nitric oxide synthases (NOS), cyclooxygenase (COX), and lipoxygenase (LOX) has been demonstrated, and their inhibition significantly reduces the level of key mediators and regulators of proinflammatory response as NO, leukotrienes, and prostaglandins [107].

It has been proposed that an indirect antioxidant enzymatic defense is due to hormetic mechanisms where polyphenols induce an adaptive cellular response to oxidative stress [108–110]. Different investigations have reported that the physiological action of polyphenols on endothelium is related to (a) endothelial NO synthase activity production, (b) increase of eNOS expression, (c) inhibition of endothelin-1 synthesis, (d) attenuation of PGI2 synthesis, and (e) intracellular Ca2+ pathways. Several pioneer studies have reported that polyphenols produced endothelium-dependent vasorelaxation that was generally associated with increased NO release and cyclic GMP formation and blunted by inhibitors of NO synthase, indicating that it was mediated by the NO-cyclic GMP pathway [111]. All these pathways are involved in the HF genesis and progression, suggesting a possible role of dietary phytochemicals in this syndrome.

3.3. Polyphenols and HF in Experimental Models

3.3.1. Quercetin. Quercetin is abundant in grains, red onions, apples, and citrus fruits, with antioxidant, anti-inflammatory, and anticlotting properties [112]. In rodent models of hypertension, it has demonstrated a dose-dependent antihypertensive effect [113]. In particular, quercetin treatment reduces vascular production of ROS and was associated with downregulation of NADPH oxidase subunit [114]. It has been reported that, in experimental models of hypertension, quercetin attenuates left ventricular hypertrophy, pressure overload, and isoproterenol-induced cardiac hypertrophy [113, 115, 116]. Then, from these results, it may be hypothesized that there is a plausible effect of quercetin in HFpEF. Indeed, quercetin demonstrated to reduce plasmatic levels of ROS, angiotensin, aldosterone, TGFβ1 myocardial expression, and collagen deposition [116]. Panchal et al. [117] indicated that quercetin's positive effect on collagen deposition is also related to the inhibition of the NF-κB signaling pathway and the activation of nuclear factor erythroid 2-related factor 2 (Nrf2). Furthermore, in metabolic syndrome experimental models, quercetin showed positive effects on left ventricular relaxation by preventing E/A reduction, mediated by enhancing SOD and glutathione peroxidase activity, inducing Nrf2 nuclear translocation, and increasing ATP myocardial levels [118]. In a mouse model of cardiac toxicity induced by doxorubicin [119], where the modulation of oxidative stress activity was mediated by pAkt pathway, ischemia/reperfusion (I/R) experiments revealed that quercetin improves parameters of left ventricular relaxation and contraction. Another investigation focused on the protective role of quercetin on myocardial I/R injury revealed reduction of infarct size and enhanced myocardial contractility and coronary flow. These results were explained by the role of quercetin on inhibiting the nonhistone DNA-binding protein pathway [120]. Peroxisome proliferator-activated receptor γ (PPAR-γ) inhibition attenuated the effects of quercetin on ROS production, SOD and glutathione peroxidase activation, suppression of NF-κB pathway, and myocardial apoptosis. These modifications suggested that the underlying protective mechanism of quercetin on myocardial injury is related to the inhibition of the NF-κB pathway by PPAR-γ activation. In a study [121], after 10 days of intraperitoneal and oral administration of quercetin, a notable amelioration of LVEF was

demonstrated. Other molecules similar to quercetin, such as taxifolin, in both *in vitro* and *in vivo* experimental models of cardiac hypertrophy, have demonstrated significantly reduced ROS production and phosphorylation of MAPK-activated protein kinase 2 and attenuated cardiac fibrosis and left ventricular remodeling [122]. It seems that taxifolin in diabetic cardiomyopathy improves diastolic dysfunction by reducing angiotensin II levels, inhibiting NADPH oxidase activity and inducing JAK/STAT3 activity [123]. The above-mentioned results suggest that in HFpEF quercetin and similar molecules may improve left ventricular relaxation at least in part by modulating oxidative stress response which in turn influences cardiac remodeling development. Then, the study of the therapy with quercetin and similar molecules in combination with well-known drugs, as ACE inhibitors/sartans, beta blockers or other modulators of adrenergic system activity, in experimental models of HFrEF would be of interest.

3.3.2. Resveratrol. Resveratrol is a stilbene present in grapes, blueberries, and peanuts produced when plants undergo infections or ultraviolet radiation. Based on the beneficial cardiovascular effect of red wine consumption, many interesting studies [124–126] have investigated the protective mechanism of resveratrol against endothelial dysfunction and myocardial tissue injury. In endothelial cells culture, isolated by bovine aortic rings cultured, red wine extracts increased the intracellular Ca2+ level, enhanced eNOS activity and, as a final result, attenuated NO release [127]. Further studies showed that red wine polyphenols are responsible for the phosphorylation of Akt and eNOS which in turn activate NO release. However, in the presence of PI3 inhibitors, polyphenols failed to induce vasorelaxation, suggesting that the PI3-kinase/Akt pathway is crucial [128]. Both resveratrol pretreatment and treatment in ischemia/reperfusion (I/R) injury has shown to reduce the generation of ROS, to scavenge ROS and to modulate the activity of SOD [129, 130].

Activation of SOD and glutathione peroxidase and reduction of proinflammatory biomarkers as myeloperoxidase by resveratrol were correlated to the activation Nrf2/ARE pathway [131]. Other data indicate that resveratrol reduced the production of TNF-α, attenuated the expression of TLR4/NF-κB in the ischemic area, and enhanced the synthesis of NO. Of note, application of sNO inhibitors abolished the positive effects of resveratrol [132]. Moreover, resveratrol significantly improves left ventricular-developed pressure and aortic flow and reduces infarct size area, with a significant amelioration of LVEF [131]. Of interest, a recent meta-analysis performed on preclinical studies concluded that in small animal models of I/R injury resveratrol significantly improves infarct size and the benefits were not affected by the duration of reperfusion [133]. Other pathways involved in the modification of the oxidative stress pathway by resveratrol seems to be attributed to MAPK signaling, Sirt1 and Sirt3 activation, and FoxO/NAD activity. Indeed, experiments [134] have demonstrated that resveratrol induced upregulation of Sirt1 expression and downregulation of FoxO1 and these modifications were associated with restoration of the severe diastolic impairment, inhibition of iron-induced profibrotic effect, and increased expression of myocardial SERCA2 protein. Importantly, the examination of Ca2+ homeostasis, in cardiomyocytes isolated from early iron-overloaded mice, demonstrated elevated diastolic Ca2+ levels and prolongation of Ca2+ decay. These changes were corrected by in vivo SERCA2a gene therapy and resveratrol [134]. The modifications in Sirt1 signaling and oxidative stress response were described also in doxorubicin-induced cardiotoxicity, where resveratrol upregulated the expression of Sirt1 protein by attenuating the acetylation of p53 protein [135]. Other associated findings were reduction of myocardial apoptosis, alleviation of oxidative stress, and reduction of left ventricular end-diastolic pressure [135]. Similar results regarding components of reactive cardiac fibrosis, such as cardiomyocyte apoptosis and collagen accumulation in the extracellular matrix of myocardial tissue, were reported in pressure overload-induced hypertrophy [136]. It should be mentioned that resveratrol can attenuate the transition of cardiac fibroblasts phenotype in myofibroblasts acting through TGFβ-Smad3 signaling and inhibiting ROS/ERK/TGFβ/periostin pathway [137]. Riba et al. [126] recently reported that resveratrol treatment showed a protective effect on oxidative stress as indicated by the reduction of iNOS, COX-2 activity, ROS generation. Regarding left ventricular dysfunction, resveratrol-treated rats increased LVEF and reduced left ventricular mass. These beneficial effects were associated with the interaction of resveratrol with cellular survival (e.g., Akt-1, GSK-3β) and stress signaling pathways (e.g., p38-MAPK, ERK 1/2, MKP-1) [126, 133]. Therefore, resveratrol administration seems to have high potentials regarding restoration of left ventricular relaxation and reduction of myocardial apoptosis and infarct size area in HF models. The modulation of oxidative stress response appears cardinal. However, further investigation regarding survival and in-depth signaling pathway interactions are necessary.

3.3.3. Curcumin. Curcumin is a polyphenol found in turmeric plants which exhibits anti-inflammatory, antioxidant, and antifibrotic properties. Several studies have tested the hypothesis of a possible cardioprotective role of this compound [138].

Curcumin showed to be effective in inhibiting maladaptive cardiac remodeling and preserving cardiac function after I/R injury. In particular, Wang et al. [139] demonstrated that, after oral administration of curcumin during reperfusion, collagen synthesis was reduced and the expression of TGFβ1 and phospho-Smad2/3 was downregulated. Moreover, stroke volume, LVEF, and left ventricular end-diastolic volume were significantly improved. Toll-like receptor-2 (TLR2) inhibition by curcumin was also described in I/R experiments, and this effect was associated with preservation of cardiac contractility [140]. It has been proposed that the cardioprotective role of curcumin against myocardial injury is related to the activation of JAK2/-STAT3 signaling pathway [141]. Other pathways related to curcumin effects in HF are the modulation of AT1/AT2 receptors and NF-κB [142, 143]. It is also reported that curcumin-reduced acetylation has a beneficial effect against myocardial injury [144].

Curcumin pretreatment in myocardial infarction models induced by left coronary artery ligation attenuated the expression of Sirt1 and reduced collagen deposition. In vitro experiments revealed that the genetic inhibition of Sirt1 by small interfering molecules blocked the effects of curcumin on cardiac fibroblast proliferation and migration [145]. It has been suggested that curcumin cardioprotective role is also related to Sirt1-dependent activation of eNOS. Indeed, in vitro treatment of endothelial cells with curcumin, protected against premature senescence, increased the Sirt1 activation and reduced the production of ROS [146]. Curcumin administration of 5 mg/kg/day and 50 mg/kg/day during 6 weeks in myocardial infarction experimental model resulted in a significant dose-dependent improvement of left ventricular fractional shortening [147]. Recently, the use of curcumin nanoparticles showed promising results regarding cardiac remodeling and antioxidative and anti-inflammatory properties in isoproterenol-induced myocardial infarction model [148]. Therefore, nanotechnology curcumin delivery may be a future application in HF experimental and clinical models. Table 1 summarizes the abovementioned studies, describing molecular modifications and phytochemical effects on the cardiovascular system.

3.4. Polyphenols and HF in Humans. Despite the preclinical studies reporting excellent results of quercetin, curcumin, and resveratrol on infarct size reduction, diastolic function, and cardiac remodeling, the application of these compounds in clinical HF models is limited. Quercetin administration in hypertensive and obese patients initially reported some positive effects in blood pressure control without showing any modulation of oxidative stress or endothelial function [149, 150]. However, other studies failed to show similar results. A recent study reports that quercetin administration for 12 months in patients with gout and hypertension, normalized the blood pressure control and improved left ventricular diastolic function [151]. In a randomized study [152] on patients with stable angina under optimal drug therapy, 120 mg twice/day of quercetin reported amelioration of left ventricular systolic and diastolic function, with a reduction in the circulatory level of proinflammatory cytokines as IL-1β, TNF-α, and NF-κB [153]. In patients undergoing [154] CABG surgery, the incidence of in-hospital myocardial infarction was decreased from 30.0% in the placebo group to 13.1% in the group treated with 4 g/day of curcuminoid (adjusted hazard ratio 0.35, 0.13 to 0.95, $p = 0.038$) and postoperative C-reactive protein; N-terminal pro-B-type natriuretic peptide levels were also lower in the curcuminoid than in the placebo group. It should be mentioned that the incidence of drug-related adverse events was not different between the placebo and curcuminoid groups, and gastrointestinal symptoms were the main drug-related adverse events.

Although the administration of resveratrol has revealed beneficial anti-inflammatory effects and amelioration of blood pressure control in a different population, no data are available on its effects on left ventricular relaxation or diastolic function [155]. A triple-blind placebo control trial [156], investigating the role of resveratrol and magnesium stearate administration, did not find inflammatory profile reduction. Participants were randomized in homogenous groups for age, gender, comorbidities, cardiovascular risk factor, and LVEF. This study also did not describe changes in diastolic function after resveratrol therapy [156]. In contrast, Milatrau et al. [157] describe not only a reduction of triglycerides and total cholesterol level but also less angina pectoris episodes during and after a short-term follow-up, with a significant reduction of NT-proBNP levels after resveratrol therapy, that could suggest an amelioration of left ventricular function.

Some studies suggest that resveratrol may have an impact on myocardial function in HF patients. Resveratrol administration in a population of myocardial infarction patients [158] resulted in improvement of left ventricular diastolic function, endothelial function measured by flow-mediated vasodilatation, and LDL cholesterol, without improvement in LVEF. Indeed, a positive trend in LVEF amelioration was assessed without achieving a statistical significance (mean LVEF at baseline and after 3-month treatment with 10 mg of resveratrol in placebo and resveratrol group were respectively $52.42 \pm 1.55\%$, $51.33 \pm 1.84\%$ and $54.77 \pm 1.64\%$, $55.83 \pm 1.94\%$). Another randomized placebo-controlled study [159], on the effect of flavanol-rich chocolate in HF patients, reported an improvement of endothelial function and inhibition of platelet activation in HF patients. In Table 2, we report studies focused on the phytochemicals use in human HF models.

By these results, it could be speculated that polyphenols might have a more pronounced role in HFpEF than HFrEF. However, in complex, investigation of polyphenol efficacy in patients with cardiovascular disease or cardiovascular risk factors has not reported the same fascinating results as in experimental models. The most updated meta-analysis on this topic [160], in fact, reports that there is no significant amelioration of the lipid, atherosclerotic, and glycemic profile and no significant reduction of blood pressure. It should be mentioned that these studies are characterized by important limitations, as small sample sizes, differences in doses, and protocols. Second, the structural and physiological differences between polyphenols make challenging their short- and long-term health effects. Third, different metabolism of polyphenols can differently affect physiological functions, producing high interindividual differences in the biological response. Indeed, pharmacokinetic studies of polyphenols on humans are very few. Moreover, biotransformation of polyphenols is still debatable and should be considered that drug-metabolizing enzymes in phase I, II, and III represent potential sites of interactions between drugs and polyphenols.

3.5. Phytosterols. Phytosterols are bioactive components of plant origin, not synthesized in the human body, that regulate the membrane fluidity of plant cells. The main food sources for phytosterols are vegetable oils, nuts, and cereals. Based on their chemical structure, they are classified in plant sterols and plant stanols. Plant sterols are distinctive for the presence of a double bond in the sterol ring and the most studied sterols are campesterol, sitosterol, and stigmasterol.

Table 1: Phytochemical effects on animal models of heart failure.

Experimental model	Phytochemical class	Dose	Treatment	Molecular pathway	Cardiovascular effect	References
Obesity, male rats	Quercetin	2 mg/kg/day 10 weeks	10 weeks	↓ TNF-α, ↓ adiponectin	↓ SBP	Rivera L. et al. 2008 [112]
Hypertension, male rats	Quercetin	10 mg/kg	5 weeks	↓ MDA	↓ SBP, improves endothelial function	Duarte J. et al. 2001 [113]
Hypertension, male rats	Quercetin	11 mg/kg	13 weeks	↑ eNOS activity, ↓ NADPH generation, ↓ p47	↓ SBP, improves Endothelial Function	Sanchez M. et al. 2006 [114]
Pressure overload, male rats	Quercetin	5-10 mg/kg day	3 weeks	↓ MDA, ↓ ERK1/2, ↓ p38,	↓ HW/BW	Han JJ.et al. 2009 [115]
ISO induced cardiac fibrosis, male rats	Quercetin /rutin	25-50 mg/kg day		↑ SOD, ↓ angiotensin II, ↓ TGFβ1	↓ HW/BW	Li M. et al. 2013 [116]
Metabolic syndrome, male rats	Quercetin	0.8 mg/kg	8 weeks	↑ Nrf2, ↓ NF-κB	↓ SBP, ↑ LVEF, ↑ E/A ratio	Panchal SK. et al. 2012 [117]
Dyslipidemia, male rats	Quercetin /ezetimibe	0.5% w/w	4 weeks	↓ GSH/GSSG ratio, ↑ Nrf2	↑ E/A ratio	Castillo LR. et al. 2018 [118]
Doxorubicin and I/R, male rats	Quercetin	15 mg/kg/day	6 weeks	↑ MMP-2,↑ pAkt	↓ apoptosis, improves LV relaxation	Bartekova M. et al. 2015 [119]
I/R injury, male rats	Quercetin	50 mg/kg/day	5 days	↓ HMGB1/ TLR/NF-κB activity	↑ myocardial contractility, ↑ coronary flow,↓ infarct size	Dong LY. et al. 2018 [120]
I/R injury, male mice	Quercetin	250 mg/kg/day	10 days	↑ PPAR-γ activation, ↓NF-κB pathway	↑ LVEF, ↑ FS	Liu X. et al. 2016 [121]
I/R injury, male rats	Resveratrol	100 μmol/l	Before reperfusion	↑ SOD,↓MDA,↑ Nrf2	↑ LVEF, improves LV relaxation, ↓ infarct size	Cheng L. et al. 2015 [131]
I/R injury, male rats	Resveratrol	100 μmol/l	Before reperfusion	↓ TNF-α, ↓MPO, ↓NF-κB, ↓ TLR4	↓ infarct size, ↓ myocardial apoptosis	Li J. et al. 2014 [132]
Iron-induced cardiomyopathy, male mice	Resveratrol	320 mg/kg day	14 weeks	Sirt1 upregulation, FOX1 downregulation, ↑ SERCA2a	↑ E/A ratio, improves LV relaxation	Das SK. et al. 2015 [134]
Doxorubicin-induced cardiomyopathy, male mice	Resveratrol	15 mg/kg/day	3 weeks	Sirt1 upregulation, ↓ p53 acetylation	↓ myocardial apoptosis, improves LV relaxation and contractility	Zhang C. et al. 2011 [135]
Pressure overload model, male mice	Resveratrol	10mg/kg/day	4 weeks	↑SOD ↓ HIF-1α	↓HW/BW, ↑ LVEF, ↑ FS, ↓ cardiac fibrosis	Gupta PK.et al. 2014 [136]
I/R injury, male rats	Curcumin	150 mg/kg	6 weeks	↓ MDA, ↓ TGFβ/ Smad pathway	↓ cardiac fibrosis, ↑ LVEF, FS, SV	Wang NP. et al. 2012 [139]
I/R injury, male rats	Curcumin	300 mg/kg	1 week	↓ TLR2	↑ myocardial contractility	Kim YS. et al. 2012 [140]
I/R injury, male rats	Curcumin	0.25, 0.5, 1 μM	Before reperfusion	Sirt1 upregulation, ↑ SOD, ↓ MDA	↓ infarct size, improves LV contractility	Duan W. et al. 2012 [141]

Table 1: Continued.

Experimental model	Phytochemical class	Dose	Treatment	Molecular pathway	Cardiovascular effect	References
Angiotensin II-induced cardiac fibrosis, male rats	Curcumin	150 mg/kg	2-4 weeks	↓ TGFβ/Smad pathway	↓ SBP, ↓ cardiac fibrosis	Pang XF. et al. 2015 [142]
Surgical-induced myocardial infarction, male and female rats	Curcumin	150 mg/kg	4 weeks	↓ NF-κB, ↑ PPAR-γ	↓ cardiac fibrosis, ↓ cardiac apoptosis	Lv FH et al. 2016 [143]
Surgical-induced MI, male rats	Curcumin	50 mg/kg/day	7 weeks	↓ p300 HAT activity	↑ FS	Morimoto T. et al. 2008 [144]
Surgical-induced myocardial infarction, male mice	Curcumin	100 mg/kg/day	1 week	Sirt1 upregulation	↓ cardiac necrosis	Xiao J. et al. 2016 [145]
ISO-induced myocardial infarction, male rats	Curcumin nanoparticles	100, 150, 200 mg/kg/day	15 days	↓ TNF-α, ↓ IL-6, IL-1α, IL-1β	↓ cardiac necrosis	Boarescu PM. et al. 2019 [148]

I/R: ischemia reperfusion; ISO: isoproterenol; TNF-α: tumor necrosis factor alpha; eNOS: nitric oxide synthase; NADPH: nicotinamide adenine dinucleotide phosphate; MDA: malondialdehyde; SOD: superoxide dismutase; TGFβ1: transforming growth factor beta 1; NF-κB: nuclear factor kappa beta; GSH/GSSS ratio: reduced glutathione/oxidized glutathione ratio; MMP2: matrix metalloproteinase-2; HMGB1: high mobility group box 1 protein; PPAR-γ: peroxisome proliferator-activated receptor gamma; MPO: myeloperoxidase; TLR: toll-like receptor, Sirt1: sirtuin 1; HIF-1α : hypoxia-inducible factor 1-alpha; HAT: hystone acetyl transferase; IL-6: interleukin-6; IL-1α: interleukin 1 alpha; IL-1β: Interleukin 1-beta; SBP: systolic blood pressure; LVEF: left ventricular ejection fraction; HW/BW: heart weight/body weight; FS: fractional shortening; SV: stroke volume.

Table 2: Phytochemical effects on human heart failure models.

Overall population	Study	Setting	Phytochemical class	Dose	Treatment	Molecular effects	Cardiovascular effects	References
26 M 15 F	RDBPC	Prehypertension and stage 1 hypertension in overweight or obese subjects	Quercetin	325 mg twice day	4 weeks	No effect on oxidative stress	↓ SBP ↓ DBP	Edwards RL. et al. 2007 [149]
34 M 34 F	RDBPC	Prehypertension and stage 1 hypertension	Quercetin	162 mg/day	6 weeks	No effect on oxidative stress and endothelial function	↓ SBP	Brull V. et al. 2015 [150]
36 M 49 F	RCT	Stable CAD	Quercetin	121 mg twice per day	9 weeks	↓ TNF-α, ↓ IL-1β, ↓ IL-10	↑ LVEF, ↑ E/A	Chekalina N.et al. 2018 [153]
69 M 61 F	RDBPC	CABG patients	Quercetin	4 g/day	8 days	↓ CRP, MDA, NT-proBNP	↑ LVEF, ↓ post-MI CABG	Wongcharoen W. et al. 2012 [154]
64 M 9 F	RTBPC	Stable CAD	Resveratrol	350 mg/day; 700 mg/day	12 months	↓ PAI-1, ↑ adiponectin	Not mentioned	Tome-Carniero J. et al. 2013 [156]
71 M 45 F	RDBPC	Stable angina pectoris	Resveratrol/ calcium fructoborate	20 mg/ 112 mg/day	6 months	↓ hsCRP	↓ NT-proBNP	Militaru C. et al. 2013 [157]
26 M 4 F	RDBPC	Stable CAD	Resveratrol	10 mg/day	3 months	No effect on inflammation	↑ FMD, ↑ E/A	Magyar K. et al. 2012 [158]
17 M 3 F	RCT	Chronic HFrEF	Flavonol-rich chocolate	40 g/day	4 weeks	No effect on oxidative stress	↑ FMD	Flammer EJ. et al. 2012 [159]

M: males; F: females; RDBPC: randomized double-blinded placebo controlled study; RCT: randomized controlled trial; CAD: coronary artery disease; MI: myocardial infarction; CAGB: coronary artery graft bypass; HFrEF: heart failure reduced ejection fraction; TNF-α . tumor necrosis factor alpha; CRP: C-reactive protein; hsCRP: high-sensitivity C-reactive protein; MDA: malondialdehyde; PAI-1: plasminogen activator inhibitor-1; NT-proBNP: N-terminal pro b-type natriuretic peptide; SBP: systolic blood pressure; DBP: diastolic blood pressure; LVEF: left ventricular ejection fraction; FMD: flow-mediated dilatation.

While examples of plant stanols are campestanol and sitostanol. About 0.5 % of dietary plant stanols and 5% of dietary plant sterols are systemically absorbed [161]. In brief, the absorption process includes their incorporation into mixed micelles, transportation from the intestinal lumen to enterocytes mediated by Niemann Pick C1 Like 1 (NPC1L) protein, and phytosterols secretion into the intestinal lumen mediated by efflux transporters as ATP-binding cassette (ABC) proteins known as ABCG5 and ABCG8 [162].

The speculation with regard to a potential deleterious effect of phytosterols has been largely motivated by the fact that phytosterolemia, a rare autosomal recessive disease, is characterized by a 50-fold increased circulating concentration of plant sterols and may be associated with early atherosclerosis [163]. Several studies have evaluated the association between plasma phytosterol concentration and CVD; however, the results are conflicting. Dietary phytosterol intake increases plasma levels, but increased plasma phytosterols are believed to be a coronary heart disease risk factor. Epidemiological studies have suggested either a direct association between plasma phytosterols and coronary heart disease risk [164] or a null [165, 166] and even inverse association [167]. In the prospective cohort of the Spanish EPIC study [168], plasma concentrations of the main phytosterols, sitosterol, and campesterol appear to be markers of a lower cardiometabolic risk. The study suggests that moderately elevated plasma sitosterol, but not campesterol, might signal individuals with a reduced risk for CHD. However, the authors concluded that they cannot answer the important question of whether circulating phytosterols are proatherogenic, antiatherogenic, or neutral.

Genser et al. [169] published a systematic review and meta-analysis based on 17 studies involving 11,182 individuals and found no evidence of an association between serum concentration of phytosterols and the development of CVD. The authors of this meta-analysis attributed the great divergence in the results of the studies to the different designs of studies and adjustments for potential confounding variables. The results in the study were conflicting because most of them do not take into account potential confounding variables and are provided in different study designs.

Different studies [170–174] have investigated the role of phytosterols on endothelial function and inflammatory profile. Similarly, the arterial stiffness and the flow-mediated dilatation were not modified in hypercholesterolemia or hypercholesterolemia and diabetes [170, 171]. Nonetheless, Gylling et al. [172] have reported beneficial effects on endothelial function and arterial stiffness. Other authors relate the restore of endothelial function to the modification of biomarkers such as E-selectin and plasminogen activator inhibitor 1 (PAI-1) [143, 173]. However, in a setting of dyslipidemic patients, either modification of inflammatory profile or endothelial function was not observed. Again, a meta-analysis study failed to show a modification of the inflammatory biomarkers as mainly C-reactive protein (CRP), after regular intake of phytosterols [174]. Limited data investigated the role of phytosterols on oxidative stress and modification of ROS release after phytosterol consumption. A recently published meta-analysis [175] evaluated the effects of phytosterol consumption in plasma concentrations of liposoluble vitamins and carotenoids. It included 41 randomized clinical trials ($n = 3{,}306$) with a mean phytosterol intake of 2.5 g/day. In the analyses adjusted for total cholesterol, there was a significant reduction in the concentration of hydrocarbon carotenoids (β-carotene, α-carotene, and lycopene) and some oxygenated carotenoids (zeaxanthin and cryptoxanthin). In contrast, there was no significant reduction in the concentration of tocopherol, vitamin D, or retinol. A very important finding of this meta-analysis was that the concentration of these substances remained within the normal range, not indicating that the observed reductions could have negative health implications [175]. Yoshida et al. [176] investigated the antioxidant effects of phytosterol and its components, beta-sitosterol, stigmasterol, and campesterol, against lipid peroxidation. It was found that these compounds exerted antioxidant effects on the oxidation of methyl linoleate in solution. Taken together, the findings of the present study showed that phytosterol chemically acts as an antioxidant, a modest radical scavenger, and physically as a stabilizer in the membranes [176]. It is rational to think that lowering the LDL cholesterol level, as one of the major cardiovascular risk factors, may directly influence the risk of developing coronary heart disease and, as a consequence, may reduce the risk from cardiovascular events. However, it should be underlined that studies evaluating the impact of phytosterols and phytostanols on cardiovascular outcome and possible relationship with HF pathophysiology are lacking.

Prospective cohort studies support the beneficial impact of plant-based dietary patterns on incident HF [177–179]. In a study of 38,075 Finnish people over a median of 14.1 years, higher consumption of vegetables was associated with a lower incidence of HF in men, but not in women [180]. Similarly, among 20,900 healthy male physicians in the Physicians' Health Study I, a greater consumption of fruits and vegetables was associated with a decreased risk of HF [181]. In a subset of the Reasons for Geographic and Racial Differences in Stroke (REGARDS) Cohort of 15,569 persons with no coronary artery disease or HF diagnosis patients with closer adherence to the plant-based dietary pattern had a lower risk of incident HF [179]. In a prospective cohort from Sweden of 34,319 women without cardiovascular disease and cancer at initial assessment, after 12.9 years, greater fruit and vegetable consumption was associated with a lower rate of HF [178]. It is hypothesized that HFpEF may be secondary, in part, to diffuse endothelial dysfunction, including that of the myocardial microvasculature, due partly, to increased inflammation [182]. Many plant-based foods are anti-inflammatory and increase NO bioavailability [183], thereby improving vascular health and potentially ameliorating this microvascular dysfunction. The Dietary Approach to Stop Hypertension in "Diastolic" Heart Failure (DASH—DHF) pilot study evaluated the impact of a DASH diet on 13 postmenopausal women with diastolic HF. After 3 weeks, consuming the DASH diet was associated with significant improvements in blood pressure, arterial elasticity, and oxidative stress [184].

4. Dietary Phytochemicals and Sex-Gender

As discussed in the previous paragraphs, the redox state and oxidative stress response vary between female and male individuals. It is therefore not surprising that such variability involves also the effects produced by the phytochemicals in them.

This largely depends on the differences existing between women and men in the adsorption, distribution, metabolism, and elimination (i.e., pharmacokinetics) and in the pharmacodynamics of the xenobiotics [185].

In particular, phenolic compounds undergo important processes of storage, transport, and biotransformation [186]. The latter is very important considering that female and male subjects have a different amount of CYP450 isoenzymes and molecules controlling their activity (e.g., constitutive androstane receptor (CAR) expression is greater in women than in men). Also, polymorphisms in some CYP450 genes are associated with variable levels of their products [186]. The sex-gender-based dissimilarities regard also the enzymes belonging to the phase II of metabolism, and this is reasonable for the phytochemicals, largely metabolized by such proteins including UDP-glucuronosyltransferases (UGTs) and sulfatases (SULTs). Then, the renal elimination of the conjugated phenolic compounds is lower in women compared to men [185].

The differences in the kinetics processes might lead to variability in the effects of all xenobiotics, including dietary phytochemicals. However, the data are still scarce in humans in whom the awareness of the method of action of the drugs, as well as of the natural products, is very important given the potential consequences in the treatment and management of several chronic diseases.

Analyzing the results of the Rotterdam study on the protective effects of quercetin against atherosclerosis, some authors [187] proposed that the better response showed by women could be dependent on a better adsorption of quercetin from rutin. This hypothesis was different from that of the Rotterdam study authors who suggested that the higher benefits could be dependent on the women's estrogen activity [188]. Erlund et al. [189] performed a diet-controlled, double-blind, cross-over study to assess the pharmacokinetics of quercetin in healthy volunteers using doses similar to those derivable from the diet. The evaluation in seven women and nine men revealed that quercetin from rutin but not from aglycone was much more bioavailable in women than in men, particularly in those assuming oral contraceptives.

Not only quercetin but also other (poly)phenolic compounds, such as curcumin and resveratrol, seem to have cardiovascular beneficial effects. However, the strongest evidence has been produced in animal models, while in humans the data are still inconclusive [190].

Curcumin has been suggested to improve vascular endothelial function. In this regard, Santos-Parker et al. [191] recently showed that a 12-week curcumin supplementation is able to increase NO bioavailability and decrease oxidative stress thereby improving both resistance and conduit artery endothelial function in healthy middle-aged and older adults. Notably, the authors reported improvements in both sex-genders but at a greater extent in men compared to women [191].

Resveratrol is one of the most studied phytochemicals because of its potential beneficial effects on several pathologies, including CVD. However, contrasting results have been found. As for other molecules, this could be explained by the numerous factors that potentially influence the resveratrol efficacy and tolerability in humans, such as age, lifestyle, dose, administration medium, gut microbiota, and gender. The latter, as well as the other variables, have not yet been sufficiently investigated [192].

A recent meta-analysis, including 18 randomized trials performed in humans, aimed to clarify whether flavonol supplementation could be useful to reduce biomarkers of CVD risk. The main result was that flavonol consumption improved lipid profile, plasma glucose, and blood pressure but in a variable manner, is strongly dependent on individuals' genetic background and health status. Notably, 9 out of 18 trials included both women and men but most of them did not make a sex-gender-based distinction of the results [193].

In women affected by diabetes mellitus type II, chronic supplementation with quercetin significantly reduced systolic blood pressure [194]. Soy product intake was associated with a reduction of diastolic blood pressure in peri- and postmenopausal women and men [195]. Although both in men and women with mild to moderate hypertension soy products reduced blood pressure [196], the incidence of hypertension was lower among men consuming olive oil [197]. Globally, the above data suggest a plausible sex-gender polyphenol effect on endothelial function.

Ostertag et al. investigated the effects of an acute administration of flavan-3-oil-enriched dark chocolate, one of the bioactive compounds contained in the dark chocolate. By analyzing blood and urine samples of both women and men, the authors found that this flavonol exerted beneficial effects in both sex-genders in a different way. In men, flavan-3-oil-enriched dark chocolate significantly decreased P-selectin expression and adenosine diphosphate-induced platelet aggregation, while, in women, decreased thrombin receptor-activating peptide-induced platelet aggregation and increased thrombin receptor-activating peptide-induced fibrinogen binding. Increased collagen/epinephrine-induced ex vivo bleeding time was observed in both men and women. White chocolate significantly decreased adenosine diphosphate-induced platelet P-selectin expression and increased collagen/epinephrine-induced ex vivo bleeding time only in men [198]. In a prospective cohort study, aimed at assessing the CVD mortality in the US population with a different intake of flavonoids, no significant sex-gender-based heterogeneity in the results was observed. However, when the authors analyzed the data separately in men and women, they found that flavone consumption was associated with a lower risk of fatal ischemic heart disease especially among women and with a lower risk of fatal stroke in men [199].

The impact of sex-gender in the cholesterol-lowering effects exerted by phytosterols also represents a debated issue. Some studies found no differences, while others [200]

suggested a possible effect of such phytochemicals in reducing LDL-C levels in men but not in women.

It is important to note that, until now, the clinical studies aimed at investigating the effects of phytochemicals by sex-gender are small-scale studies; thus, they are not powered enough to give a conclusive response to a so complex question.

5. Dietary Phytochemicals, Sex-Gender, and HF

As previously discussed, the different promising studies suggest a protective role of different phytochemical on heart function. In isolated guinea pig myocytes, polyphenols seem to act differently on intracellular Ca2+ signaling in male and female cells. Lew et al. [201] found fundamental sex differences in the acute actions of the widely consumed isoflavone genistein in guinea pig ventricular myocytes. These differences result in an overall increase in contraction of male myocytes, but little or no change in females. Although genistein inhibited L-type Ca2+ currents in cardiac myocytes from both male and female guinea pigs, a greater percentage inhibition in females was found, suggesting consequent greater cardioprotection of this phytochemical in females than in males.

Stauffer et al. [202] reported that male mice with hypertrophic cardiomyopathy that were fed the traditional soy-based diet deteriorate to severe, dilated cardiomyopathy and more fibrosis, induction of beta-myosin heavy chain, inactivation of glycogen synthase kinase-3beta, and activation of caspase-3. However, simply changing the diet to a milk-based (no soy) diet prevents these phenotypes [202]. Female mice with hypertrophic cardiomyopathy did not exhibit clinical signs of severe cardiac disease on the soy diet, and they were not significantly affected by the dietary change, supporting the hypothesis that in HF some phytochemicals can act in a different sex-oriented way.

Another in vivo study [203] performed on transgenic alpha-myosin heavy chain gene usually fed with polyphenols showed that while female mice increased their cardiac mass and preserved cardiac contractile function; male mice developed thin ventricular walls and had poorly contractile hearts, suggesting a possible role in HF prevention.

However, in all clinical studies, the influence of sex-gender in HF prevention and therapy was not fully studied. In a randomized control trial [157] performed on patients with stable angina undergone to administration with calcium-fructoborate and resveratrol, after 2 months, a significant reduction in BNP levels and inflammatory markers, like PCR, was observed. Of interest, males and females were included in this study but an interaction between gender and BNP or inflammatory response to resveratrol level was not performed. Similarly, in other studies [158, 159], although resveratrol improved the endothelial function measured by brachial artery flow dilatation and the inflammatory profile and the E/A ratio in HF patients, the sex-gender influence was not taken into account as a confounding variable [159].

6. Conclusions

While a large body of evidence supports an association between oxidative stress and HF, and phytochemicals are characterized by important antioxidant properties, until now only a few studies were able to demonstrate some beneficial effects of phytochemicals in HF patients. Scavenging of ROS with antioxidants has proved to not affect in modifying patients' prognosis. Surely one of the main problems in the definition of the phytochemicals' efficacy is related to the sex-gender influence. The still unknown different response to the oxidative stress in women and men surely condition the response to phytochemicals administration, especially in HF subjects. Therefore, further studies are needed to better clarify the possible effects of phytochemicals in HF subjects, taking into account the different sex-gender antioxidant response.

Conflicts of Interest

The authors declare that there is no conflict of interest regarding the publication of this paper.

Authors' Contributions

Klara Komici and Valeria Conti equally contributed to this work.

References

[1] D. Mozaffarian, E. J. Benjamin, A. S. Go et al., "Heart disease and stroke statistics–2015 update: a report from the American Heart Association," *Circulation*, vol. 131, no. 4, pp. e29–322, 2015.

[2] A. Cannavo, K. Komici, L. Bencivenga et al., "GRK2 as a therapeutic target for heart failure," *Expert Opinion on Therapeutic Targets*, vol. 22, no. 1, pp. 75–83, 2018.

[3] K. Komici, G. D. Femminella, C. de Lucia et al., "Predisposing factors to heart failure in diabetic nephropathy: a look at the sympathetic nervous system hyperactivity," *Aging Clinical and Experimental Research*, vol. 31, no. 3, pp. 321–330, 2019.

[4] N. Ferrara, P. Abete, G. Corbi et al., "Insulin-induced changes in beta-adrenergic response: an experimental study in the isolated rat papillary muscle," *American Journal of Hypertension*, vol. 18, no. 3, pp. 348–353, 2005.

[5] G. Russomanno, G. Corbi, V. Manzo et al., "The anti-ageing molecule sirt1 mediates beneficial effects of cardiac rehabilitation," *Immunity & Ageing*, vol. 14, no. 1, p. 7, 2017.

[6] A. Sharma, G. C. Fonarow, J. Butler, J. A. Ezekowitz, and G. M. Felker, "Coenzyme Q10 and heart failure: a state-of-the-art review," *Circulation: Heart Failure*, vol. 9, no. 4, article e002639, 2016.

[7] G. Corbi, G. Gambassi, G. Pagano et al., "Impact of an innovative educational strategy on medication appropriate use and length of stay in elderly patients," *Medicine*, vol. 94, no. 24, article e918, 2015.

[8] F. Franconi, I. Campesi, D. Colombo, and P. Antonini, "Sex-gender variable: methodological recommendations for increasing scientific value of clinical studies," *Cells*, vol. 8, no. 5, p. 476, 2019.

[9] A. L. Bui, T. B. Horwich, and G. C. Fonarow, "Epidemiology and risk profile of heart failure," *Nature Reviews Cardiology*, vol. 8, no. 1, pp. 30–41, 2011.

[10] J. P. Hellermann, S. J. Jacobsen, G. S. Reeder, F. Lopez-Jimenez, S. A. Weston, and V. L. Roger, "Heart failure after myocardial infarction: prevalence of preserved left ventricular systolic function in the community," *American Heart Journal*, vol. 145, no. 4, pp. 742–748, 2003.

[11] C. de Lucia, G. D. Femminella, G. Rengo et al., "Risk of acute myocardial infarction after transurethral resection of prostate in elderly," *BMC Surgery*, vol. 13, Supplement 2, p. S35, 2013.

[12] A. A. Merz and S. Cheng, "Sex differences in cardiovascular ageing," *Heart*, vol. 102, pp. 825–831, 2016.

[13] C. Gebhard, B. E. Stahli, C. E. Gebhard et al., "Age- and gender dependent left ventricular remodeling," *Echocardiography*, vol. 30, no. 10, pp. 1143–1150, 2013.

[14] C. F. Deschepper and B. Llamas, "Hypertensive cardiac remodeling in males and females," *Hypertension*, vol. 49, no. 3, pp. 401–407, 2007.

[15] A. Levinsson, M. P. Dubé, J. C. Tardif, and S. de Denus, "Sex, drugs, and heart failure: a sex-sensitive review of the evidence base behind current heart failure clinical guidelines," *ESC Heart Failure*, vol. 5, no. 5, pp. 745–754, 2018.

[16] G. Corbi, I. Ambrosino, K. Komici, M. Cellurale, A. Lombardi, and N. Ferrara, "Gender differences in response to therapy for cardiovascular diseases," *Current Pharmacogenomics and Personalized Medicine*, vol. 15, no. 1, 2017.

[17] J. Ballard-Hernandez and D. Itchhaporia, "Heart failure in women due to hypertensive heart disease," *Heart Failure Clinics*, vol. 15, no. 4, pp. 497–507, 2019.

[18] A. Deswal and B. Bozkurt, "Comparison of morbidity in women versus men with heart failure and preserved ejection fraction," *The American Journal of Cardiology*, vol. 97, no. 8, pp. 1228–1231, 2006.

[19] F. S. Loffredo, A. P. Nikolova, J. R. Pancoast, and R. T. Lee, "Heart failure with preserved ejection fraction: molecular pathways of the aging myocardium," *Circulation Research*, vol. 115, no. 1, pp. 97–107, 2014.

[20] G. De Simone, R. B. Devereux, M. Chinali et al., "Sex differences in obesity-related changes in left ventricular morphology: the Strong Heart Study," *Journal of Hypertension*, vol. 29, no. 7, pp. 1431–1438, 2011.

[21] S. Meyer, P. van der Meer, B. M. Massie et al., "Sex-specific acute heart failure phenotypes and outcomes from PROTECT," *European Journal of Heart Failure*, vol. 15, no. 12, pp. 1374–1381, 2013.

[22] C. Franssen, S. Chen, A. Unger et al., "Myocardial microvascular inflammatory endothelial activation in heart failure with preserved ejection fraction," *JACC: Heart Failure*, vol. 4, no. 4, pp. 312–324, 2016.

[23] S. F. Mohammed, S. Hussain, S. A. Mirzoyev, W. D. Edwards, J. J. Maleszewski, and M. M. Redfield, "Coronary microvascular rarefaction and myocardial fibrosis in heart failure with preserved ejection fraction," *Circulation*, vol. 131, no. 6, pp. 550–559, 2015.

[24] D. Westermann, D. Lindner, M. Kasner et al., "Cardiac inflammation contributes to changes in the extracellular matrix in patients with heart failure and normal ejection fraction," *Circulation: Heart Failure*, vol. 4, no. 1, pp. 44–52, 2011.

[25] B. W. Florijn, R. Bijkerk, E. P. van der Veer, and A. J. van Zonneveld, "Gender and cardiovascular disease: are sex-biased microRNA networks a driving force behind heart failure with preserved ejection fraction in women?," *Cardiovascular Research*, vol. 114, no. 2, pp. 210–225, 2018.

[26] F. J. Giordano, "Oxygen, oxidative stress, hypoxia, and heart failure," *The Journal of Clinical Investigation*, vol. 115, no. 3, pp. 500–508, 2005.

[27] V. Conti, M. Forte, G. Corbi et al., "Sirtuins: possible clinical implications in cardio and cerebrovascular diseases," *Current Drug Targets*, vol. 18, no. 4, pp. 473–484, 2017.

[28] H. Tsutsui, S. Kinugawa, and S. Matsushima, "Oxidative stress and heart failure," *American Journal of Physiology Heart and Circulatory Physiology*, vol. 301, no. 6, pp. H2181–H2190, 2011.

[29] V. Conti, G. Corbi, V. Manzo, G. Pelaia, A. Filippelli, and A. Vatrella, "Sirtuin 1 and aging theory for chronic obstructive pulmonary disease," *Analytical Cellular Pathology*, vol. 2015, Article ID 897327, 8 pages, 2015.

[30] S. G. Rhee, "Redox signaling: hydrogen peroxide as intracellular messenger," *Experimental & Molecular Medicine*, vol. 31, no. 2, pp. 53–59, 1999.

[31] T. Ide, H. Tsutsui, S. Kinugawa et al., "Mitochondrial electron transport complex i is a potential source of oxygen free radicals in the failing myocardium," *Circulation Research*, vol. 85, no. 4, pp. 357–363, 1999.

[32] T. Ide, H. Tsutsui, S. Kinugawa et al., "Direct evidence for increased hydroxyl radicals originating from superoxide in the failing myocardium," *Circulation Research*, vol. 86, no. 2, pp. 152–157, 2000.

[33] M. F. Hill and P. K. Singal, "Antioxidant and oxidative stress changes during heart failure subsequent to myocardial infarction in rats," *The American Journal of Pathology*, vol. 148, no. 1, pp. 291–300, 1996.

[34] Z. Mallat, I. Philip, M. Lebret, D. Chatel, J. Maclouf, and A. Tedgui, "Elevated levels of 8-iso-prostaglandin $F_{2\alpha}$ in pericardial fluid of patients with heart failure: a potential role for in vivo oxidant stress in ventricular dilatation and progression to heart failure," *Circulation*, vol. 97, no. 16, pp. 1536–1539, 1998.

[35] S. S. Signorelli, M. Anzaldi, M. Libra et al., "Plasma levels of inflammatory biomarkers in peripheral arterial disease: results of a cohort study," *Angiology*, vol. 67, no. 9, pp. 870–874, 2016.

[36] T. Ide, H. Tsutsui, S. Hayashidani et al., "Mitochondrial DNA damage and dysfunction Associated with oxidative stress in failing hearts after myocardial infarction," *Circulation Research*, vol. 88, no. 5, pp. 529–535, 2001.

[37] I. A. Hobai and B. O'Rourke, "Enhanced Ca^{2+}-activated Na^{+}-Ca^{2+} exchange activity in canine pacing-induced heart failure," *Circulation Research*, vol. 87, no. 8, pp. 690–698, 2000.

[38] M. Kohlhaas, T. Liu, A. Knopp et al., "Elevated cytosolic Na^{+} increases mitochondrial formation of reactive oxygen species in failing cardiac myocytes," *Circulation*, vol. 121, pp. 1606–1613, 2010.

[39] J. M. Li, N. P. Gall, D. J. Grieve, M. Chen, and A. M. Shah, "Activation of NADPH oxidase during progression of cardiac hypertrophy to failure," *Hypertension*, vol. 40, no. 4, pp. 477–484, 2002.

[40] C. Doerries, K. Grote, D. Hilfiker-Kleiner et al., "Critical role of the NAD(P)H oxidase subunit $p47^{phox}$ for left ventricular

remodeling/dysfunction and survival after myocardial infarction," *Circulation Research*, vol. 100, no. 6, pp. 894–903, 2007.

[41] J. Kuroda, T. Ago, S. Matsushima, P. Zhai, M. D. Schneider, and J. Sadoshima, "NADPH oxidase 4 (Nox4) is a major source of oxidative stress in the failing heart," *Proceedings of the National Academy of Sciences of the United States of America*, vol. 107, no. 35, pp. 15565–15570, 2010.

[42] E. Takimoto, H. C. Champion, M. Li et al., "Oxidant stress from nitric oxide synthase-3 uncoupling stimulates cardiac pathologic remodeling from chronic pressure load," *The Journal of Clinical Investigation*, vol. 115, no. 5, pp. 1221–1231, 2005.

[43] A. K. Doughan, D. G. Harrison, and S. I. Dikalov, "Molecular mechanisms of angiotensin II-mediated mitochondrial dysfunction: linking mitochondrial oxidative damage and vascular endothelial dysfunction," *Circulation Research*, vol. 102, no. 4, pp. 488–496, 2008.

[44] N. Khaper, K. Kaur, T. Li, F. Farahmand, and P. K. Singal, "Antioxidant enzyme gene expression in congestive heart failure following mycardial infarction," *Molecular and Cellular Biochemistry*, vol. 251, no. 1-2, pp. 9–15, 2003.

[45] T. Shiomi, H. Tsutsui, H. Matsusaka et al., "Overexpression of glutathione peroxidase prevents left ventricular Remodeling and failure after myocardial infarction in mice," *Circulation*, vol. 109, no. 4, pp. 544–549, 2004.

[46] T. Yoshida, M. Watanabe, D. T. Engelman et al., "Transgenic mice overexpressing glutathione peroxidase are resistant to myocardial ischemia reperfusion injury," *Journal of Molecular and Cellular Cardiology*, vol. 28, no. 8, pp. 1759–1767, 1996.

[47] N. Khaper and P. K. Singal, "Effects of afterload-reducing drugs on pathogenesis of antioxidant changes and congestive heart failure in rats," *Journal of the American College of Cardiology*, vol. 29, no. 4, pp. 856–861, 1997.

[48] N. Khaper, K. Kaur, T. Li, F. Farahmand, and P. K. Singal, "Antioxidant enzyme gene expression in congestive heart failure following myocardial infarction," *Molecular and Cellular Biochemistry*, vol. 251, no. 1-2, pp. 9–15, 2003.

[49] J. B. Pillai, A. Isbatan, S. Imai, and M. P. Gupta, "Poly(ADP-ribose) polymerase-1-dependent cardiac myocyte cell death during heart failure is mediated by NAD^+ Depletion and reduced Sir2α deacetylase activity," *The Journal of Biological Chemistry*, vol. 280, no. 52, pp. 43121–43130, 2005.

[50] C. P. Hsu, S. Oka, D. Shao, N. Hariharan, and J. Sadoshima, "Nicotinamide Phosphoribosyltransferase regulates cell survival through NAD^+ Synthesis in cardiac myocytes," *Circulation Research*, vol. 105, no. 5, pp. 481–491, 2009.

[51] T. Damy, M. Kirsch, L. Khouzami et al., "Glutathione deficiency in cardiac patients is related to the functional status and structural cardiac abnormalities," *PLoS One*, vol. 4, no. 3, article e4871, 2009.

[52] H. Tsutsui, T. Ide, S. Hayashidani et al., "Greater susceptibility of failing cardiac myocytes to oxygen free radical-mediated injury," *Cardiovascular Research*, vol. 49, no. 1, pp. 103–109, 2001.

[53] H. Mollnau, M. Oelze, M. August et al., "Mechanisms of increased vascular superoxide production in an experimental model of idiopathic dilated cardiomyopathy," *Arteriosclerosis, Thrombosis, and Vascular Biology*, vol. 25, no. 12, pp. 2554–2559, 2005.

[54] A. Schafer, D. Fraccarollo, P. Tas, I. Schmidt, G. Ertl, and J. Bauersachs, "Endothelial dysfunction in congestive heart failure: ACE inhibition vs. angiotensin II antagonism," *European Journal of Heart Failure*, vol. 6, no. 2, pp. 151–159, 2004.

[55] G. A. Silberman, T. H. Fan, H. Liu et al., "Uncoupled cardiac nitric oxide synthase mediates diastolic dysfunction," *Circulation*, vol. 121, no. 4, pp. 519–528, 2010.

[56] K. Bhatia, A. A. Elmarakby, A. B. El-Remessey, and J. C. Sullivan, "Oxidative-stress contributes to sex differences in angiotensin II-mediated hypertension in spontaneously hypertensive rats," *American Journal of Physiology Regulatory, Integrative and Comparative Physiology*, vol. 302, no. 2, pp. R274–R282, 2012.

[57] P. Matarrese, T. Colasanti, B. Ascione et al., "Gender disparity in susceptibility to oxidative stress and Apoptosis Induced by autoantibodies specific to RLIP76 in vascular cells," *Antioxidants & Redox Signaling*, vol. 15, no. 11, pp. 2825–2836, 2011.

[58] H. S. Marinho, C. Real, L. Cyrne, H. Soares, and F. Antunes, "Hydrogen peroxide sensing, signaling and regulation of transcription factors," *Redox Biology*, vol. 2, pp. 535–562, 2014.

[59] R. P. Brandes and A. Mügge, "Gender differences in the generation of superoxide anions in the rat aorta," *Life Sciences*, vol. 60, pp. 391–396, 1997.

[60] C. Vassalle, R. Sciarrino, S. Bianchi, D. Battaglia, A. Mercuri, and S. Maffei, "Sex-related differences in association of oxidative stress status with coronary artery disease," *Fertility and Sterility*, vol. 97, no. 2, pp. 414–419.e2, 2012.

[61] Y. Chen, L. L. Ji, T. Y. Liu, and Z. T. Wang, "Evaluation of gender-related differences in various oxidative stress enzymes in mice," *The Chinese Journal of Physiology*, vol. 54, no. 6, pp. 385–390, 2011.

[62] J. Barp, A. S. Araújo, T. R. G. Fernandes et al., "Myocardial antioxidant and oxidative stress changes due to sex hormones," *Brazilian Journal of Medical and Biological Research*, vol. 35, no. 9, pp. 1075–1081, 2002.

[63] A. A. Miller, G. R. Drummond, A. E. Mast, H. H. H. W. Schmidt, and C. G. Sobey, "Effect of gender on NADPH-oxidase activity, expression, and function in the cerebral circulation: role of estrogen," *Stroke*, vol. 38, no. 7, pp. 2142–2149, 2007.

[64] S. Matsushima, J. Kuroda, T. Ago et al., "Broad suppression of NADPH oxidase activity exacerbates ischemia/reperfusion injury through inadvertent downregulation of hypoxia-inducible Factor-1α and upregulation of peroxisome proliferator-activated Receptor-α," *Circulation Research*, vol. 112, no. 8, pp. 1135–1149, 2013.

[65] T. Münzel, T. Gori, J. F. Keaney Jr., C. Maack, and A. Daiber, "Pathophysiological role of oxidative stress in systolic and diastolic heart failure and its therapeutic implications," *European Heart Journal*, vol. 36, no. 38, pp. 2555–2564, 2015.

[66] P. S. Wong, M. D. Randall, and R. E. Roberts, "Sex differences in the role of NADPH oxidases in endothelium-dependent vasorelaxation in porcine isolated coronary arteries," *Vascular Pharmacology*, vol. 72, pp. 83–92, 2015.

[67] M. E. Mendelsohn, "Protective effects of estrogen on the cardiovascular system," *The American Journal of Cardiology*, vol. 89, Supplement 1, pp. 12E–17E, 2002.

[68] A. H. Wagner, M. R. Schroeter, and M. Hecker, "17β-estradiol inhibition of NADPH oxidase expression in human endothelial cells," *The FASEB Journal*, vol. 15, no. 12, pp. 2121–2130, 2001.

[69] J. R. Nofer, "Estrogens and atherosclerosis: insights from animal models and cell systems," *Journal of Molecular Endocrinology*, vol. 48, no. 2, pp. R13–R29, 2012.

[70] D. Camper-Kirby, S. Welch, A. Walker et al., "Myocardial Akt activation and gender: increased nuclear activity in females versus males," *Circulation Research*, vol. 88, no. 10, pp. 1020–1027, 2001.

[71] R. D. Patten, I. Pourati, M. J. Aronovitz et al., "17β-estradiol reduces cardiomyocyte apoptosis in vivo and in vitro via activation of phospho-inositide-3 kinase/Akt signaling," *Circulation Research*, vol. 95, no. 7, pp. 692–699, 2004.

[72] M. Skavdahl, C. Steenbergen, J. Clark et al., "Estrogen receptor-β mediates male-female differences in the development of pressure overload hypertrophy," *American Journal of Physiology Heart and Circulatory Physiology*, vol. 288, no. 2, pp. H469–H476, 2005.

[73] A. Iorga, J. Li, S. Sharma et al., "Rescue of pressure overload-induced heart failure by estrogen therapy," *Journal of the American Heart Association*, vol. 5, article e002482, 2016.

[74] T. M. De Silva, B. R. Broughton, G. R. Drummond, C. G. Sobey, and A. A. Miller, "Gender influences cerebral vascular responses to angiotensin II through Nox2-derived reactive oxygen species," *Stroke*, vol. 40, no. 4, pp. 1091–1097, 2009.

[75] J. P. Pierce, J. Kievits, B. Graustein, R. C. Speth, C. Iadecola, and T. A. Milner, "Sex differences in the subcellular distribution of angiotensin type 1 receptors and NADPH oxidase subunits in the dendrites of C1 neurons in the rat rostral ventrolateral medulla," *Neuroscience*, vol. 163, no. 1, pp. 329–338, 2009.

[76] A. P. Dantas, M. C. Franco, M. M. Silva-Antonialli et al., "Gender differences in superoxide generation in microvessels of hypertensive rats: role of NAD(P)H-oxidase," *Cardiovascular Research*, vol. 61, no. 1, pp. 22–29, 2004.

[77] R. P. Goncalves, K. L. Guarido, J. Assreuy, and J. E. da Silva-Santos, "Gender-specific differences in the *in situ* cardiac function of endotoxemic rats detected by pressure-volume catheter," *Shock*, vol. 42, no. 5, pp. 415–423, 2014.

[78] J. Sun, E. Picht, K. S. Ginsburg, D. M. Bers, C. Steenbergen, and E. Murphy, "Hypercontractile female hearts exhibit increased S-nitrosylation of the L-type Ca^{2+} channel α1 subunit and reduced ischemia/reperfusion injury," *Circulation Research*, vol. 98, no. 3, pp. 403–411, 2006.

[79] C. Steenbergen, E. Murphy, L. Levy, and R. E. London, "Elevation in cytosolic free calcium concentration early in myocardial ischemia in perfused rat heart," *Circulation Research*, vol. 60, no. 5, pp. 700–707, 1987.

[80] H. M. Piper, K. Meuter, and C. Schafer, "Cellular mechanisms of ischemia–reperfusion injury," *The Annals of Thoracic Surgery*, vol. 75, pp. S644–S648, 2003.

[81] E. Murphy and C. Steenbergen, "Gender-based differences in mechanisms of protection in myocardial ischemia–reperfusion injury," *Cardiovascular Research*, vol. 75, no. 3, pp. 478–486, 2007.

[82] M. C. Kander, Y. Cui, and Z. Liu, "Gender difference in oxidative stress: a new look at the mechanisms for cardiovascular diseases," *Journal of Cellular and Molecular Medicine*, vol. 21, no. 5, pp. 1024–1032, 2017.

[83] C. Chen, L. X. Hu, T. Dong et al., "Apoptosis and autophagy contribute to gender difference in cardiac ischemia- reperfusion induced injury in rats," *Life Sciences*, vol. 93, no. 7, pp. 265–270, 2013.

[84] S. Muralimanoharan, C. Li, E. S. Nakayasu et al., "Sexual dimorphism in the fetal cardiac response to maternal nutrient restriction," *Journal of Molecular and Cellular Cardiology*, vol. 108, pp. 181–193, 2017.

[85] L. Du, R. W. Hickey, H. Bayir et al., "Starving neurons show sex difference in autophagy," *Journal of Biological Chemistry*, vol. 284, no. 4, pp. 2383–2396, 2009.

[86] P. Matarrese, P. Tieri, S. Anticoli et al., "X-chromosome-linked miR548am-5p is a key regulator of sex disparity in the susceptibility to mitochondria-mediated apoptosis," *Cell Death & Disease*, vol. 10, no. 9, p. 673, 2019.

[87] R. H. Liu, "Potential synergy of phytochemicals in cancer prevention: mechanism of action," *The Journal of Nutrition*, vol. 134, no. 12, pp. 3479S–3485S, 2004.

[88] G. Corbi, V. Conti, S. Davinelli, G. Scapagnini, A. Filippelli, and N. Ferrara, "Dietary phytochemicals in neuroimmunoaging: a new therapeutic possibility for humans?," *Frontiers in Pharmacology*, vol. 7, p. 364, 2016.

[89] V. Conti, V. Izzo, G. Corbi et al., "Antioxidant supplementation in the treatment of aging-associated diseases," *Frontiers in Pharmacology*, vol. 7, p. 24, 2016.

[90] S. Davinelli, A. Trichopoulou, G. Corbi, I. De Vivo, and G. Scapagnini, "The potential nutrigeroprotective role of Mediterranean diet and its functional components on telomere length dynamics," *Ageing Research Reviews*, vol. 49, pp. 1–10, 2019.

[91] D. Vauzour, A. Rodriguez-Mateos, G. Corona, M. J. Oruna-Concha, and J. P. Spencer, "Polyphenols and human health: prevention of disease and mechanisms of action," *Nutrients*, vol. 2, no. 11, pp. 1106–1131, 2010.

[92] R. Mattera, M. Benvenuto, M. G. Giganti et al., "Effects of polyphenols on oxidative stress-mediated injury in cardiomyocytes," *Nutrients*, vol. 9, no. 5, p. 523, 2017.

[93] H. Cory, S. Passarelli, J. Szeto, M. Tamez, and J. Mattei, "The role of polyphenols in human health and food systems: a mini-review," *Frontiers in Nutrition*, vol. 5, p. 87, 2018.

[94] M. Fantini, M. Benvenuto, L. Masuelli et al., "*In vitro* and *in vivo* antitumoral effects of combinations of polyphenols, or polyphenols and anticancer drugs: perspectives on cancer treatment," *International Journal of Molecular Sciences*, vol. 16, no. 12, pp. 9236–9282, 2015.

[95] C. Manach, A. Scalbert, C. Morand, C. Rémésy, and L. Jiménez, "Polyphenols: food sources and bioavailability," *The American Journal of Clinical Nutrition*, vol. 79, no. 5, pp. 727–747, 2004.

[96] S. Quideau, D. Deffieux, C. Douat-Casassus, and L. Pouysegu, "Plant polyphenols: chemical properties, biological activities, and synthesis," *Angewandte Chemie International Edition*, vol. 50, no. 3, pp. 586–621, 2011.

[97] S. Davinelli, G. Corbi, S. Righetti et al., "Cardioprotection by cocoa polyphenols and ω-3 fatty acids: a disease-prevention perspective on aging-associated cardiovascular risk," *Journal of Medicinal Food*, vol. 21, no. 10, pp. 1060–1069, 2018.

[98] K. B. Pandey and S. I. Rizvi, "Plant polyphenols as dietary antioxidants in human health and disease," *Oxidative Medicine and Cellular Longevity*, vol. 2, no. 5, 278 pages, 2009.

[99] T. Walle, F. Hsieh, M. H. DeLegge, J. E. Oatis Jr., and U. K. Walle, "High absorption but very low bioavailability of oral resveratrol in humans," *Drug Metabolism and Disposition*, vol. 32, no. 12, pp. 1377–1382, 2004.

[100] H. Doostdar, M. D. Burke, and R. T. Mayer, "Bioflavonoids: selective substrates and inhibitors for cytochrome P450 CYP1A and CYP1B1," *Toxicology*, vol. 144, no. 1-3, pp. 31–38, 2000.

[101] J. B. Vaidyanathan and T. Walle, "Glucuronidation and sulfation of the tea flavonoid (−)-epicatechin by the human and rat enzymes," *Drug Metabolism and Disposition*, vol. 30, no. 8, pp. 897–903, 2002.

[102] F. Qian, D. Wei, and Q. Zhang, "Modulation of P-glycoprotein function and reversal of multidrug resistance by (−)-epigallocatechin gallate in human cancer cells," *Biomedicine & Pharmacotherapy*, vol. 59, no. 3, pp. 64–69, 2005.

[103] H. M. Wortelboer, M. Usta, A. E. van der Velde et al., "Interplay between MRP inhibition and metabolism of MRP inhibitors: the case of curcumin," *Chemical Research in Toxicology*, vol. 16, no. 12, pp. 1642–1651, 2003.

[104] A. C. Whitley, D. H. Sweet, and T. Walle, "The dietary polyphenol ellagic acid is a potent inhibitor of hOAT1," *Drug Metabolism and Disposition*, vol. 33, no. 8, pp. 1097–1100, 2005.

[105] R. J. Nijveldt, E. van Nood, D. E. van Hoorn, P. G. Boelens, K. van Norren, and P. A. van Leeuwen, "Flavonoids: a review of probable mechanisms of action and potential applications," *The American Journal of Clinical Nutrition*, vol. 74, no. 4, pp. 418–425, 2001.

[106] P. I. Oteiza, A. G. Erlejman, S. V. Verstraeten, C. L. Keen, and C. G. Fraga, "Flavonoid-membrane interactions: a protective role of flavonoids at the membrane surface?," *Clinical & Developmental Immunology*, vol. 12, no. 1, pp. 19–25, 2005.

[107] B. S. Cheon, Y. H. Kim, K. S. Son, H. W. Chang, S. S. Kang, and H. P. Kim, "Effects of prenylated flavonoids and biflavonoids on lipopolysaccharide-induced nitric oxide production from the mouse macrophage cell line RAW 264.7," *Planta Medica*, vol. 66, no. 7, pp. 596–600, 2000.

[108] M. P. Mattson and A. Cheng, "Neurohormetic phytochemicals: low-dose toxins that induce adaptive neuronal stress responses," *Trends in Neurosciences*, vol. 29, no. 11, pp. 632–639, 2006.

[109] S. Davinelli, G. Corbi, A. Zarrelli et al., "Short-term supplementation with flavanol-rich cocoa improves lipid profile, antioxidant status and positively influences the AA/EPA ratio in healthy subjects," *The Journal of Nutritional Biochemistry*, vol. 61, pp. 33–39, 2018.

[110] G. Corbi, V. Conti, K. Komici et al., "Phenolic Plant Extracts Induce Sirt1 Activity and Increase Antioxidant Levels in the Rabbit's Heart and Liver," *Oxidative Medicine and Cellular Longevity*, vol. 2018, Article ID 2731289, 10 pages, 2018.

[111] M. Karim, K. McCormick, and C. T. Kappagoda, "Effects of cocoa extracts on endothelium-dependent relaxation," *The Journal of Nutrition*, vol. 130, no. 8, pp. 2105S–2108S, 2000.

[112] L. Rivera, R. Morón, M. Sánchez, A. Zarzuelo, and M. Galisteo, "Quercetin ameliorates metabolic syndrome and improves the inflammatory status in obese Zucker rats," *Obesity*, vol. 16, no. 9, pp. 2081–2087, 2008.

[113] J. Duarte, R. Pérez-Palencia, F. Vargas et al., "Antihypertensive effects of the flavonoid quercetin in spontaneously hypertensive rats," *British Journal of Pharmacology*, vol. 133, no. 1, pp. 117–124, 2001.

[114] M. Sanchez, M. Galisteo, R. Vera et al., "Quercetin downregulates NADPH oxidase, increases eNOS activity and prevents endothelial dysfunction in spontaneously hypertensive rats," *Journal of Hypertension*, vol. 24, no. 1, pp. 75–84, 2006.

[115] J. J. Han, J. Hao, C. H. Kim, J. S. Hong, H. Y. Ahn, and Y. S. Lee, "Quercetin prevents cardiac hypertrophy induced by pressure overload in rats," *The Journal of Veterinary Medical Science*, vol. 71, no. 6, pp. 737–743, 2009.

[116] M. Li, Y. Jiang, W. Jing, B. Sun, C. Miao, and L. Ren, "Quercetin provides greater cardioprotective effect than its glycoside derivative rutin on isoproterenol-induced cardiac fibrosis in the rat," *Canadian Journal of Physiology and Pharmacology*, vol. 91, no. 11, pp. 951–959, 2013.

[117] S. K. Panchal, H. Poudyal, and L. Brown, "Quercetin ameliorates cardiovascular, hepatic, and metabolic changes in diet-induced metabolic syndrome in rats," *The Journal of Nutrition*, vol. 142, no. 6, pp. 1026–1032, 2012.

[118] R. L. Castillo, E. A. Herrera, A. Gonzalez-Candia et al., "Quercetin prevents diastolic dysfunction induced by a high-cholesterol diet: role of oxidative stress and bioenergetics in hyperglycemic rats," *Oxidative Medicine and Cellular Longevity*, vol. 2018, Article ID 7239123, 14 pages, 2018.

[119] M. Barteková, P. Šimončíková, M. Fogarassyová et al., "Quercetin improves postischemic recovery of heart function in doxorubicin-treated rats and prevents doxorubicin-induced matrix metalloproteinase-2 activation and apoptosis induction," *International Journal of Molecular Sciences*, vol. 16, no. 12, pp. 8168–8185, 2015.

[120] L. Y. Dong, F. Chen, M. Xu, L. P. Yao, Y. J. Zhang, and Y. Zhuang, "Quercetin attenuates myocardial ischemia-reperfusion injury via downregulation of the HMGB1-TLR4-NF-κB signaling pathway," *American Journal of Translational Research*, vol. 10, no. 5, pp. 1273–1283, 2018.

[121] X. Liu, Z. Yu, X. Huang et al., "Peroxisome proliferator-activated receptor γ (PPARγ) mediates the protective effect of quercetin against myocardial ischemia-reperfusion injury via suppressing the NF-κB pathway," *American Journal of Translational Research*, vol. 8, no. 12, pp. 5169–5186, 2016.

[122] H. Guo, X. Zhang, Y. Cui et al., "Taxifolin protects against cardiac hypertrophy and fibrosis during biomechanical stress of pressure overload," *Toxicology and Applied Pharmacology*, vol. 287, no. 2, pp. 168–177, 2015.

[123] X. Sun, R. C. Chen, Z. H. Yang et al., "Taxifolin prevents diabetic cardiomyopathy in vivo and in vitro by inhibition of oxidative stress and cell apoptosis," *Food and Chemical Toxicology*, vol. 63, pp. 221–232, 2014.

[124] K. Rivera, F. Salas-Pérez, G. Echeverría et al., "Red wine grape pomace attenuates atherosclerosis and myocardial damage and increases survival in association with improved plasma antioxidant activity in a murine model of lethal ischemic heart disease," *Nutrients*, vol. 11, no. 9, article 2135, 2019.

[125] S. Haseeb, B. Alexander, and A. Baranchuk, "Wine and cardiovascular health: a comprehensive review," *Circulation*, vol. 136, no. 15, pp. 1434–1448, 2017.

[126] A. Riba, L. Deres, B. Sumegi, K. Toth, E. Szabados, and R. Halmosi, "Cardioprotective effect of resveratrol in a post-infarction heart failure model," *Oxidative Medicine and Cellular Longevity*, vol. 2017, Article ID 6819281, 10 pages, 2017.

[127] S. Martin, E. Andriambeloson, K. Takeda, and R. Andriantsitohaina, "Red wine polyphenols increase calcium in bovine aortic endothelial cells: a basis to elucidate signalling pathways leading to nitric oxide production," *British Journal of Pharmacology*, vol. 135, no. 6, pp. 1579–1587, 2002.

[128] M. Ndiaye, T. Chataigneau, M. Chataigneau, and V. B. Schini-Kerth, "Red wine polyphenols induce EDHF-mediated relaxations in porcine coronary arteries through the redox-sensitive activation of the PI3-kinase/Akt pathway," *British Journal of Pharmacology*, vol. 142, no. 7, pp. 1131–1136, 2004.

[129] Y. Tang, J. Xu, W. Qu et al., "Resveratrol reduces vascular cell senescence through attenuation of oxidative stress by SIRT1/-NADPH oxidase-dependent mechanisms," *The Journal of Nutritional Biochemistry*, vol. 23, no. 11, pp. 1410–1416, 2012.

[130] C. L. Kao, L. K. Chen, Y. L. Chang et al., "Resveratrol protects human endothelium from H2O2-induced oxidative stress and senescence via SirT1 activation," *Journal of Atherosclerosis and Thrombosis*, vol. 17, no. 9, pp. 970–979, 2010.

[131] L. Cheng, Z. Jin, R. Zhao, K. Ren, C. Deng, and S. Yu, "Resveratrol attenuates inflammation and oxidative stress induced by myocardial ischemia-reperfusion injury: role of Nrf2/ARE pathway," *International Journal of Clinical and Experimental Medicine*, vol. 8, no. 7, pp. 10420–10428, 2015.

[132] J. Li, C. Xie, J. Zhuang et al., "Resveratrol attenuates inflammation in the rat heart subjected to ischemia-reperfusion: role of the TLR4/NF-κB signaling pathway," *Molecular Medicine Reports*, vol. 11, no. 2, pp. 1120–1126, 2014.

[133] Z. J. Mao, H. Lin, J. W. Hou, Q. Zhou, Q. Wang, and Y. H. Chen, "A Meta-Analysis of Resveratrol Protects against Myocardial Ischemia/Reperfusion Injury: Evidence from Small Animal Studies and Insight into Molecular Mechanisms," *Oxidative Medicine and Cellular Longevity*, vol. 2019, Article ID 5793867, 11 pages, 2019.

[134] S. K. Das, W. Wang, P. Zhabyeyev et al., "Iron-overload injury and cardiomyopathy in acquired and genetic models is attenuated by resveratrol therapy," *Scientific Reports*, vol. 5, no. 1, article 18132, 2015.

[135] C. Zhang, Y. Feng, S. Qu et al., "Resveratrol attenuates doxorubicin-induced cardiomyocyte apoptosis in mice through SIRT1-mediated deacetylation of p53," *Cardiovascular Research*, vol. 90, no. 3, pp. 538–545, 2011.

[136] P. K. Gupta, D. J. DiPette, and S. C. Supowit, "Protective effect of resveratrol against pressure overload-induced heart failure," *Food Science & Nutrition*, vol. 2, no. 3, pp. 218–229, 2014.

[137] Q. Q. Wu, Y. Xiao, X. H. Jiang et al., "Evodiamine attenuates TGF-β1-induced fibroblast activation and endothelial to mesenchymal transition," *Molecular and Cellular Biochemistry*, vol. 430, no. 1-2, pp. 81–90, 2017.

[138] S. Miriyala, M. Panchatcharam, and P. Rengarajulu, "Cardioprotective effects of curcumin," *Advances in Experimental Medicine and Biology*, vol. 595, pp. 359–377, 2007.

[139] N. P. Wang, Z. F. Wang, S. Tootle, T. Philip, and Z. Q. Zhao, "Curcumin promotes cardiac repair and ameliorates cardiac dysfunction following myocardial infarction," *British Journal of Pharmacology*, vol. 167, no. 7, pp. 1550–1562, 2012.

[140] Y. S. Kim, J. S. Kwon, Y. K. Cho et al., "Curcumin reduces the cardiac ischemia-reperfusion injury: involvement of the toll-like receptor 2 in cardiomyocytes," *The Journal of Nutritional Biochemistry*, vol. 23, no. 11, pp. 1514–1523, 2012.

[141] W. Duan, Y. Yang, J. Yan et al., "The effects of curcumin post-treatment against myocardial ischemia and reperfusion by activation of the JAK2/STAT3 signaling pathway," *Basic Research in Cardiology*, vol. 107, no. 3, p. 263, 2012.

[142] X. F. Pang, L. H. Zhang, F. Bai et al., "Attenuation of myocardial fibrosis with curcumin is mediated by modulating expression of angiotensin II AT1/AT2 receptors and ACE2 in rats," *Drug Design, Development and Therapy*, vol. 9, pp. 6043–6054, 2015.

[143] F. H. Lv, H. L. Yin, Y. Q. He et al., "Effects of curcumin on the apoptosis of cardiomyocytes and the expression of NF-κB, PPAR-γ and Bcl-2 in rats with myocardial infarction injury," *Experimental and Therapeutic Medicine*, vol. 12, no. 6, pp. 3877–3884, 2016.

[144] T. Morimoto, Y. Sunagawa, T. Kawamura et al., "The dietary compound curcumin inhibits p300 histone acetyltransferase activity and prevents heart failure in rats," *The Journal of Clinical Investigation*, vol. 118, no. 3, pp. 868–878, 2008.

[145] J. Xiao, X. Sheng, X. Zhang, M. Guo, and X. Ji, "Curcumin protects against myocardial infarction-induced cardiac fibrosis via SIRT1 activation in vivo and in vitro," *Drug Design, Development and Therapy*, vol. 10, pp. 1267–1277, 2016.

[146] Y. Sun, X. Hu, G. Hu, C. Xu, and H. Jiang, "Curcumin attenuates hydrogen peroxide-induced premature senescence via the activation of SIRT1 in human umbilical vein endothelial cells," *Biological & Pharmaceutical Bulletin*, vol. 38, no. 8, pp. 1134–1141, 2015.

[147] Y. Sunagawa, S. Sono, Y. Katanasaka et al., "Optimal dose-setting study of curcumin for improvement of left ventricular systolic function after myocardial infarction in rats," *Journal of Pharmacological Sciences*, vol. 126, no. 4, pp. 329–336, 2014.

[148] P. M. Boarescu, I. Chirilă, A. E. Bulboacă et al., "Effects of curcumin nanoparticles in isoproterenol-induced myocardial infarction," *Oxidative Medicine and Cellular Longevity*, vol. 2019, Article ID 7847142, 13 pages, 2019.

[149] R. L. Edwards, T. Lyon, S. E. Litwin, A. Rabovsky, J. D. Symons, and T. Jalili, "Quercetin reduces blood pressure in hypertensive subjects," *The Journal of Nutrition*, vol. 137, no. 11, pp. 2405–2411, 2007.

[150] V. Brüll, C. Burak, B. Stoffel-Wagner et al., "Effects of a quercetin-rich onion skin extract on 24 h ambulatory blood pressure and endothelial function in overweight-to-obese patients with (pre-)hypertension: a randomised double-blinded placebo-controlled cross-over trial," *British Journal of Nutrition*, vol. 114, no. 8, pp. 1263–1277, 2015.

[151] V. E. Kondratiuk and Y. P. Synytsia, "Effect of quercetin on the echocardiographic parameters of left ventricular diastolic function in patients with gout and essential hypertension," *Wiadomości Lekarskie*, vol. 71, no. 8, pp. 1554–1559, 2018.

[152] N. I. Chekalina, S. V. Shut, T. A. Trybrat et al., "Effect of quercetin on parameters of central hemodynamics and myocardial ischemia in patients with stable coronary heart disease," *Wiadomości Lekarskie*, vol. 70, no. 4, pp. 707–711, 2017.

[153] N. Chekalina, Y. Burmak, Y. Petrov et al., "Quercetin reduces the transcriptional activity of NF-kB in stable coronary artery disease," *Indian Heart Journal*, vol. 70, no. 5, pp. 593–597, 2018.

[154] W. Wongcharoen, S. Jai-Aue, A. Phrommintikul et al., "Effects of curcuminoids on frequency of acute myocardial infarction after coronary artery bypass grafting," *The American Journal of Cardiology*, vol. 110, no. 1, pp. 40–44, 2012.

[155] K. Fujitaka, H. Otani, F. Jo et al., "Modified resveratrol Longevinex improves endothelial function in adults with

metabolic syndrome receiving standard treatment," *Nutrition Research*, vol. 31, no. 11, pp. 842–847, 2011.

[156] J. Tome-Carneiro, M. Gonzalvez, M. Larrosa et al., "Grape resveratrol increases serum adiponectin and downregulates inflammatory genes in peripheral blood mononuclear cells: a triple-blind, placebo-controlled, one-year clinical trial in patients with stable coronary artery disease," *Cardiovascular Drugs and Therapy*, vol. 27, no. 1, pp. 37–48, 2013.

[157] C. Militaru, I. Donoiu, A. Craciun, I. D. Scorei, A. M. Bulearca, and R. I. Scorei, "Oral resveratrol and calcium fructoborate supplementation in subjects with stable angina pectoris: effects on lipid profiles, inflammation markers, and quality of life," *Nutrition*, vol. 29, no. 1, pp. 178–183, 2013.

[158] K. Magyar, R. Halmosi, A. Palfi et al., "Cardioprotection by resveratrol: a human clinical trial in patients with stable coronary artery disease," *Clinical Hemorheology and Microcirculation*, vol. 50, no. 3, pp. 179–187, 2012.

[159] A. J. Flammer, I. Sudano, M. Wolfrum et al., "Cardiovascular effects of flavanol-rich chocolate in patients with heart failure," *European Heart Journal*, vol. 33, no. 17, pp. 2172–2180, 2012.

[160] F. Potì, D. Santi, G. Spaggiari, F. Zimetti, and I. Zanotti, "Polyphenol health effects on cardiovascular and neurodegenerative disorders: a review and meta-analysis," *International Journal of Molecular Sciences*, vol. 20, no. 2, p. 351, 2019.

[161] R. E. Ostlund Jr., J. B. McGill, C. M. Zeng et al., "Gastrointestinal absorption and plasma kinetics of soy Δ^5-phytosterols and phytostanols in humans," *American Journal of Physiology Endocrinology and Metabolism*, vol. 282, no. 4, pp. E911–E916, 2002.

[162] M. Rocha, C. Banuls, L. Bellod, A. Jover, V. M. Victor, and A. Hernandez-Mijares, "A review on the role of phytosterols: new insights into cardiovascular risk," *Current Pharmaceutical Design*, vol. 17, no. 36, pp. 4061–4075, 2011.

[163] C. E. Cabral, "Phytosterols in the treatment of hypercholesterolemia and prevention of cardiovascular diseases," *Arquivos Brasileiros de Cardiologia*, vol. 109, no. 5, pp. 475–482, 2017.

[164] T. Sudhop, B. M. Gottwald, and K. von Bergmann, "Serum plant sterols as a potential risk factor for coronary heart disease," *Metabolism*, vol. 51, no. 12, pp. 1519–1521, 2002.

[165] S. Pinedo, M. N. Vissers, K. von Bergmann et al., "Plasma levels of plant sterols and the risk of coronary artery disease: the prospective EPIC-Norfolk Population Study," *Journal of Lipid Research*, vol. 48, no. 1, pp. 139–144, 2007.

[166] E. Windler, B. C. Zyriax, F. Kuipers, J. Linseisen, and H. Boeing, "Association of plasma phytosterol concentrations with incident coronary heart disease: Data from the CORA study, a case-control study of coronary artery disease in women," *Atherosclerosis*, vol. 203, no. 1, pp. 284–290, 2009.

[167] K. Fassbender, D. Lütjohann, M. G. Dik et al., "Moderately elevated plant sterol levels are associated with reduced cardiovascular risk—The LASA study," *Atherosclerosis*, vol. 196, no. 1, pp. 283–288, 2008.

[168] V. Escurriol, M. Cofán, C. Moreno-Iribas et al., "Phytosterol plasma concentrations and coronary heart disease in the prospective Spanish EPIC cohort," *Journal of Lipid Research*, vol. 51, no. 3, pp. 618–624, 2010.

[169] B. Genser, G. Silbernagel, G. De Backer et al., "Plant sterols and cardiovascular disease: a systematic review and meta-analysis," *European Heart Journal*, vol. 33, no. 4, pp. 444–451, 2012.

[170] O. T. Raitakari, P. Salo, H. Gylling, and T. A. Miettinen, "Plant stanol ester consumption and arterial elasticity and endothelial function," *British Journal of Nutrition*, vol. 100, no. 3, pp. 603–608, 2008.

[171] M. Hallikainen, T. Lyyra-Laitinen, T. Laitinen, L. Moilanen, T. A. Miettinen, and H. Gylling, "Effects of plant stanol esters on serum cholesterol concentrations, relative markers of cholesterol metabolism and endothelial function in type 1 diabetes," *Atherosclerosis*, vol. 199, no. 2, pp. 432–439, 2008.

[172] H. Gylling, J. Halonen, H. Lindholm et al., "The effects of plant stanol ester consumption on arterial stiffness and endothelial function in adults: a randomised controlled clinical trial," *BMC Cardiovascular Disorders*, vol. 13, no. 1, pp. 50–50, 2013.

[173] R. T. Ras, D. Fuchs, W. P. Koppenol et al., "The effect of a low-fat spread with added plant sterols on vascular function markers: results of the Investigating Vascular Function Effects of Plant Sterols (INVEST) study," *The American Journal of Clinical Nutrition*, vol. 101, no. 4, pp. 733–741, 2015.

[174] V. Z. Rocha, R. T. Ras, A. C. Gagliardi, L. C. Mangili, E. A. Trautwein, and R. D. Santos, "Effects of phytosterols on markers of inflammation: a systematic review and meta-analysis," *Atherosclerosis*, vol. 248, pp. 76–83, 2016.

[175] S. Baumgartner, R. T. Ras, E. A. Trautwein, R. P. Mensink, and J. Plat, "Plasma fat-soluble vitamin and carotenoid concentrations after plant sterol and plant stanol consumption: a meta-analysis of randomized controlled trials," *European Journal of Nutrition*, vol. 56, no. 3, pp. 909–923, 2017.

[176] Y. Yoshida and E. Niki, "Antioxidant effects of phytosterol and its components," *Journal of Nutritional Science and Vitaminology*, vol. 49, no. 4, pp. 277–280, 2003.

[177] R. Pfister, S. J. Sharp, R. Luben, N. J. Wareham, and K. T. Khaw, "Plasma vitamin C predicts incident heart failure in men and women in European Prospective Investigation into Cancer and Nutrition-Norfolk prospective study," *American Heart Journal*, vol. 162, no. 2, pp. 246–253, 2011.

[178] S. Rautiainen, E. B. Levitan, M. A. Mittleman, and A. Wolk, "Fruit and vegetable intake and rate of heart failure: a population-based prospective cohort of women," *European Journal of Heart Failure*, vol. 17, no. 1, pp. 20–26, 2015.

[179] K. M. Lara, E. B. Levitan, O. M. Gutierrez et al., "Dietary patterns and incident heart failure in U.S. Adults without known coronary disease," *Journal of the American College of Cardiology*, vol. 73, no. 16, pp. 2036–2045, 2019.

[180] Y. Wang, J. Tuomilehto, P. Jousilahti et al., "Lifestyle factors in relation to heart failure among Finnish men and women," *Circulation: Heart Failure*, vol. 4, no. 5, pp. 607–612, 2011.

[181] L. Djousse, J. A. Driver, and J. M. Gaziano, "Relation between modifiable lifestyle factors and lifetime risk of heart failure," *Journal of the American Medical Association*, vol. 302, no. 4, pp. 394–400, 2009.

[182] K. Sharma and D. A. Kass, "Heart failure with preserved ejection fraction: mechanisms, clinical features, and therapies," *Circulation*, vol. 115, no. 1, pp. 79–96, 2014.

[183] J. Kobayashi, K. Ohtake, and H. Uchida, "NO-rich diet for lifestyle-related diseases," *Nutrients*, vol. 7, no. 6, pp. 4911–4937, 2015.

[184] S. L. Hummel, E. M. Seymour, R. D. Brook et al., "Low-sodium dietary approaches to stop hypertension diet reduces

blood pressure, arterial stiffness, and oxidative stress in hypertensive heart failure with preserved ejection fraction," *Hypertension*, vol. 60, no. 5, pp. 1200–1206, 2012.

[185] O. P. Soldin and D. R. Mattison, "Sex differences in pharmacokinetics and pharmacodynamics," *Clinical Pharmacokinetics*, vol. 48, no. 3, pp. 143–157, 2009.

[186] I. Campesi, M. Marino, M. Cipolletti, A. Romani, and F. Franconi, "Put "gender glasses" on the effects of phenolic compounds on cardiovascular function and diseases," *European Journal of Nutrition*, vol. 57, no. 8, pp. 2677–2691, 2018.

[187] J. M. Geleijnse, L. J. Launer, A. Hofman, H. A. Pols, and J. C. Witteman, "Tea flavonoids may protect against atherosclerosis: the Rotterdam Study," *Archives of Internal Medicine*, vol. 159, no. 18, pp. 2170–2174, 1999.

[188] J. M. Geleijnse, J. C. Witteman, L. J. Launer, S. W. Lamberts, and H. A. Pols, "Tea and coronary heart disease: protection through estrogen-like activity?," *Archives of Internal Medicine*, vol. 160, no. 21, pp. 3328-3329, 2000.

[189] I. Erlund, T. Kosonen, G. Alfthan et al., "Pharmacokinetics of quercetin from quercetin aglycone and rutin in healthy volunteers," *European Journal of Clinical Pharmacology*, vol. 56, no. 8, pp. 545–553, 2000.

[190] M. Forte, V. Conti, A. Damato et al., "Targeting nitric oxide with natural derived compounds as a therapeutic strategy in vascular diseases," *Oxidative Medicine and Cellular Longevity*, vol. 2016, Article ID 7364138, 20 pages, 2016.

[191] J. R. Santos-Parker, T. R. Strahler, C. J. Bassett, N. Z. Bispham, M. B. Chonchol, and D. R. Seals, "Curcumin supplementation improves vascular endothelial function in healthy middle-aged and older adults by increasing nitric oxide bioavailability and reducing oxidative stress," *Aging*, vol. 9, no. 1, pp. 187–208, 2017.

[192] S. L. Ramírez-Garza, E. P. Laveriano-Santos, M. Marhuenda-Muñoz et al., "Health effects of resveratrol: results from human intervention trials," *Nutrients*, vol. 10, no. 12, article 1892, 2018.

[193] R. Menezes, A. Rodriguez-Mateos, A. Kaltsatou et al., "Impact of Flavonols on cardiometabolic biomarkers: a meta-analysis of randomized controlled human trials to explore the role of Inter-Individual variability," *Nutrients*, vol. 9, no. 2, p. 117, 2017.

[194] M. Zahedi, R. Ghiasvand, A. Feizi, G. Asgari, and L. Darvish, "Does quercetin improve cardiovascular risk factors and Inflammatory biomarkers in women with type 2 diabetes: a Double-blind randomized controlled clinical trial," *International Journal of Preventive Medicine*, vol. 4, no. 7, pp. 777–785, 2013.

[195] C. Nagata, H. Shimizu, R. Takami, M. Hayashi, N. Takeda, and K. Yasuda, "Association of blood pressure with intake of soy products and other food groups in Japanese men and women," *Preventive Medicine*, vol. 36, no. 6, pp. 692–697, 2003.

[196] M. Rivas, R. P. Garay, J. F. Escanero, P. Cia Jr., P. Cia, and J. O. Alda, "Soy milk lowers blood pressure in men and women with mild to moderate essential hypertension," *The Journal of Nutrition*, vol. 132, no. 7, pp. 1900–1902, 2002.

[197] A. Alonso and M. A. Martinez-Gonzalez, "Olive oil consumption and reduced incidence of hypertension: the SUN study," *Lipids*, vol. 39, no. 12, pp. 1233–1238, 2004.

[198] L. M. Ostertag, P. A. Kroon, S. Wood et al., "Flavan-3-ol-enriched dark chocolate and white chocolate improve acute measures of platelet function in a gender-specific way–a randomized-controlled human intervention trial," *Molecular Nutrition & Food Research*, vol. 57, no. 2, pp. 191–202, 2013.

[199] M. L. McCullough, J. J. Peterson, R. Patel, P. F. Jacques, R. Shah, and J. T. Dwyer, "Flavonoid intake and cardiovascular disease mortality in a prospective cohort of US adults," *The American Journal of Clinical Nutrition*, vol. 95, no. 2, pp. 454–464, 2012.

[200] E. A. Trautwein, M. A. Vermeer, H. Hiemstra, and R. T. Ras, "LDL-cholesterol lowering of plant sterols and stanols-which factors influence their efficacy?," *Nutrients*, vol. 10, no. 9, article 1262, 2018.

[201] R. Liew, M. A. Stagg, J. Chan, P. Collins, and K. T. MacLeod, "Gender determines the acute actions of genistein on intracellular calcium regulation in the guinea-pig heart," *Cardiovascular Research*, vol. 61, no. 1, pp. 66–76, 2004.

[202] B. L. Stauffer, J. P. Konhilas, E. D. Luczak, and L. A. Leinwand, "Soy diet worsens heart disease in mice," *The Journal of Clinical Investigation*, vol. 116, no. 1, pp. 209–216, 2006.

[203] M. C. Olsson, B. M. Palmer, L. A. Leinwand, and R. L. Moore, "Gender and aging in a transgenic mouse model of hypertrophic cardiomyopathy," *American Journal of Physiology Heart and Circulatory Physiology*, vol. 280, no. 3, pp. H1136–H1144, 2001.

Hindawi
Oxidative Medicine and Cellular Longevity
Volume 2019, Article ID 6304058, 14 pages
https://doi.org/10.1155/2019/6304058

Research Article

Myricetin Alleviates Pathological Cardiac Hypertrophy via TRAF6/TAK1/MAPK and Nrf2 Signaling Pathway

Hai-han Liao,[1,2] Nan Zhang,[1,2] Yan-yan Meng,[1,2] Hong Feng,[3] Jing-jing Yang,[1,2] Wen-jin Li,[1,2] Si Chen,[2] Hai-ming Wu,[2] Wei Deng,[1,2] and Qi-zhu Tang[1,2]

[1]*Department of Cardiology, Renmin Hospital of Wuhan University, Wuhan, Hubei 430060, China*
[2]*Hubei Key Laboratory of Metabolic and Chronic Diseases, Wuhan, Hubei 430060, China*
[3]*Department of Geriatrics, Renmin Hospital of Wuhan University, Wuhan, Hubei 430060, China*

Correspondence should be addressed to Wei Deng; vivideng1982@whu.edu.cn and Qi-zhu Tang; qztang@whu.edu.cn

Received 31 May 2019; Revised 25 September 2019; Accepted 18 November 2019; Published 6 December 2019

Academic Editor: Paola Rizzo

Myricetin (Myr) is a common plant-derived polyphenol and is well recognized for its multiple activities including antioxidant, anti-inflammation, anticancer, and antidiabetes. Our previous studies indicated that Myr protected mouse heart from lipopolysaccharide and streptozocin-induced injuries. However, it remained to be unclear whether Myr could prevent mouse heart from pressure overload-induced pathological hypertrophy. Wild type (WT) and cardiac Nrf2 knockdown (Nrf2-KD) mice were subjected to aortic banding (AB) surgery and then administered with Myr (200 mg/kg/d) for 6 weeks. Myr significantly alleviated AB-induced cardiac hypertrophy, fibrosis, and cardiac dysfunction in both WT and Nrf2-KD mice. Myr also inhibited phenylephrine- (PE-) induced neonatal rat cardiomyocyte (NRCM) hypertrophy and hypertrophic markers' expression *in vitro*. Mechanically, Myr markedly increased Nrf2 activity, decreased NF-κB activity, and inhibited TAK1/p38/JNK1/2 MAPK signaling in WT mouse hearts. We further demonstrated that Myr could inhibit TAK1/p38/JNK1/2 signaling via inhibiting Traf6 ubiquitination and its interaction with TAK1 after Nrf2 knockdown in NRCM. These results strongly suggested that Myr could attenuate pressure overload-induced pathological hypertrophy *in vivo* and PE-induced NRCM hypertrophy via enhancing Nrf2 activity and inhibiting TAK1/P38/JNK1/2 phosphorylation by regulating Traf6 ubiquitination. Thus, Myr might be a potential strategy for therapy or adjuvant therapy for malignant cardiac hypertrophy.

1. Introduction

Pathological cardiac hypertrophy plays a central role in a variety of cardiovascular diseases and is an independent predictor for heart failure, arrhythmia, and sudden death [1, 2]. Many pathological stimuli, such as chronic hypertension, myocardial infarction, and aortic stenosis, could inevitably induce pathological hypertrophy [1, 2]. A series of malignant remodeling occurred in pathological hypertrophy, including enlarged cardiomyocyte, accelerated protein synthesis, cell death, aggravated fibrosis, dysregulated Ca^{2+}-handling, disturbed mitochondrial function, and reactivated fetal gene expression [1, 2]. Multiple signaling pathways, such as mitogen-activated protein kinase (MAPK), NF-κB, and Nrf2/HO-1, were dysregulated and were demonstrated to involve in promoting malignant remodeling. Targeting at these dysregulated signaling might find out strategies for protesting against pathological hypertrophy.

Myricetin (Myr) is a well-known polyphenol and possesses a similar molecular structure with kaempferol, quercetin, morin, and fisetin [3]. Scientific investigations had revealed that Myr possessed multiple pharmacological activities including antioxidant, antiphotoaging, anti-inflammation, antidiabetes, and anticancer [3]. Myr has also been demonstrated to protest against cardiovascular disease in both clinical and basic researches. Myr intake from daily diet was inversely associated with the incidence of cardiovascular diseases [4, 5]. In basic researches, Myr treatment protected isoproterenol- (ISO-) induced myocardial infarction via increasing superoxide dismutase (SOD) and catalase (CAT) [6]. Myr exerted a more pronounced capacity than quercetin for preventing STAT1 activation in ischemia/reperfusion [7]

and consequently showed more cardiovascular benefits. Myr treatment could also promote coronary dilation via increasing intracellular cGMP without affecting cardiomyocyte systolic and diastolic function [8]. These investigations implied that Myr might be a potential drug for therapy or adjuvant therapy in various cardiovascular diseases, but the underling mechanisms remain to be further explored.

In our laboratory, we have demonstrated that Myr attenuated LPS-induced mouse heart injuries by inhibiting oxidative stress and NF-κB/p65 activity [9]. We further demonstrated that the antioxidant activity of Myr might be associated with enhancing Nrf2/HO-1 pathway in diabetic mouse heart. However, Myr remained to inhibit NF-κB activity after Nrf2 silence in neonatal rat cardiomyocytes (NRCMs) [10]. Thus, some mechanisms independent of Nrf2/HO-1 remain to be investigated in mouse heart. Also, none published studies have investigated the roles and mechanisms of Myr in pressure overload-induced pathological hypertrophy. In this study, we intended to investigate whether Myr could protect mouse heart from pressure overload-induced hypertrophy and clarify the underlying mechanisms.

2. Methods

2.1. Reagents. Myr (>99% purity) was purchased from Shanghai Winherb Medical Science Co., Ltd. (Shanghai, China). BCA protein assay kit was purchased from Pierce (Rockford, IL, USA). The following primary antibodies were used in this study: T-ERK (CST, 4695), p-JNK (T183/Y185) (CST, 4668P), T-JNK (CST, 9258S), T-TAK1 (CST, 4060), p-P38 (CST, 4511P), T-p38 (CST, 9212P), p-TAK1 (CST, 4508), p-P65 (s276) (BIOWORLD, BS4135), T-P65 (CST, 8242), GAPDH (CST, 2118), p-ERK1/2 (Thr202/Tyr 204) (CST, 4370P), Histone-3 (Abcam, ab5176), TRAF6 (Santa Cruz, sc-8409), ubiquitin (Proteintech, 10201-2-AP), Nrf2 (Proteintech, 16396-1-AP), 4-hydroxynonenal (Abcam, ab46545), SOD1 (Abcam, ab16831), and catalase (Proteintech, 19792-1-AP). Lip 6000 (C0528) and protein A+G Agarose were purchased from Beyotime (Jiangsu, China). Peroxidase-conjugated secondary antibodies were from Jackson ImmunoResearch Laboratories (1 : 10000); fetal calf serum was from HyClone (Waltham, MA, USA).

2.2. Animal Models. All experimental protocols used for animal experiments in this study were approved by the Animal Care and Use Committee of Renmin Hospital of Wuhan University. All surgery procedures were performed according to the National Institutes of Health (NIH) Guide for the Care and Use of Laboratory Animals.

2.2.1. Generation of Cardiac-Specific Nrf2 Knockdown (Nrf2-KD) Mice. Nrf2 shRNA Lentiviral Particles (for mouse) were purchased from Santa Cruz Biotechnology (sc-37049-v). Intramyocardial injection of lentiviral particles was performed according to our previous study [11]. Briefly, mice were anaesthetized with pentobarbital sodium and mechanically ventilated. A horizontal skin incision was made at the 3-4 intercostal space. The heart was smoothly and gently "popped out." Lentiviral particles were injected into the left ventricle with a syringe equipped with a 31-gauge needle. The sham group was injected with scram shRNA Lentiviral Particles. Three different injection points were selected around the left ventricle. After injection, mouse heart was immediately put back and then close muscle and suture the skin. All mice were allowed for shRNA expression for 2 weeks and then were prepared for following experiments.

2.2.2. Pressure Overload-Induced Hypertrophy Model. Aortic banding (AB) surgery was performed to establish pathological hypertrophy models according to previous depict [11]. Briefly, male mice (C57/BL6, age 8-10 weeks and weight 23.5-27.5 g) were anaesthetized with pentobarbital sodium (50 mg/kg, Sigma) by intraperitoneal injection. After losing toe pinch reflex, open the left chest at the 2-3 intercostal space to expose the aorta with blunting dissection. The aorta was tied with a 27-gauge or 26-gauge needle using a 7-0 silk suture. After ligation, the needle was removed gently to cause aortic constriction. Sham mice went through a similar procedure without aorta ligation.

2.2.3. Animal Groups and Myr Administration. After three days of AB surgery or sham operation, mice were allocated into different experimental groups randomly. In this study, two independent animal experiments were performed. Firstly, animals were allocated into four groups: sham+normal saline (NS) group (control group, CON), sham+Myr treatment group (Myr), AB+NS (AB) group, and AB+Myr (AB+M) group. Secondly, animals were allocated into scram shRNA+sham+vehicle (NS) (sham+scram+Veh), scram shRNA+sham+Myr (sham+scram+Myr), shRNA+AB+Veh (shRNA+Veh+AB), and shRNA+AB+Myr. Myr were dissolved in NS and were administrated by gastric needle for consecutive 6 weeks with a dose of 200 mg/kg/d, which have been performed according to our previous studies [9, 10]. The control groups were treated with NS.

2.3. Echocardiographic Analysis. Cardiac function was measured by echocardiography before mouse sacrifice. Mice were anesthetized by 1.5% isoflurane. Mylab 30CV (ESAOTE S. P. A) equipped with a 15 MHZ linear-array ultrasound transducer was used to assess the left ventricle (LV) dimension at the parasternal short axis. M-mode tracing was used to detect and calculate the following parameters: interventricular septal thickness (IVS) at diastole (IVSd), IVS at systole (IVSs), LV end-diastolic diameter (LVEDd), LV end-systolic diameter (LVEDs), LV end-diastolic posterior wall thickness (LVPWd), LV end-systolic posterior wall thickness (LVPWs), LV ejection fraction (LVEF), and fractional shortening (FS). End-diastole or systole was defined as the phase of the largest or smallest area of the LV, respectively.

2.4. Histology Analysis. After echocardiography measurement, mice were sacrificed by cervical dislocation. Heart weight (HW), lung weight (LW), and tibia length (TB) were recorded to calculate the HW/BW, LW/BW, and HW/TL. Then, mouse hearts were arrested in diastole in 10% KCl and fixed by 10% formalin for 12 h. After dehydration, hearts were embedded in paraffin and cut transversely close to the apex with 4-5 μm thickness. Hematoxylin-eosin (HE) and

Table 1: Primers used for RT-PCR.

Gene symbol	Genus	Sense-forward primer	Antisense-reverse primer
ANP	Mouse	ACCTGCTAGACCACCTGGAG	CCTTGGCTGTTATCTTCGGTACCGG
BNP	Mouse	GAGGTCACTCCTATCCTCTGG	GCCATTTCCTCCGACTTTTCTC
α-MHC	Mouse	GTCCAAGTTCCGCAAGGT	AGGGTCTGCTGGAGAGGTTA
β-MHC	Mouse	CCGAGTCCCAGGTCAACAA	CTTCACGGGCACCCTTGGA
TGF-β	Mouse	TGCGCTTGCAGAGATTAAAA	CGTCAAAAGACAGCCACTCA
Collagen I	Mouse	AGGCTTCAGTGGTTTGGATG	CACCAACAGCACCATCGTTA
Collagen III	Mouse	CCCAACCCAGAGATCCCATT	GAAGCACAGGAGCAGGTGTAGA
GAPDH	Mouse	ACTCCACTCACGGCAAATTC	TCTCCATGGTGGTGAAGACA
ANP	Rat	AAAGCAAACTGAGGGCTCTGCTCG	TTCGGTACCGGAAGCTGTTGCA
BNP	Rat	TTCCTTAATCTGTCGCCGCTGG	CAGCAGCTTCTGCATCGTGGAT
β-MHC	Rat	TCTGGACAGCTCCCCATTCT	CAAGGCTAACCTGGAGAAGATG
GAPHD	Rat	GACATGCCGCCTGGAGAAAC	AGCCCAGGATGCCCTTTAGT

picrosirius red (PSR) staining were performed to assess the cardiomyocyte cross-sectional area (CSA) and collagen volume in the LV. A digital image analysis system (Image-Pro Plus, version 6.0) was used for image capture and analysis.

2.5. Neonatal Rat Cardiomyocyte (NRCM) Culture and Treatment. Neonatal rat cardiomyocytes (NRCMs) were isolated from 1-3 day old Sprague-Dawley rats according to published protocol [11]. Briefly, NRCMs were isolated in D-hanks buffer containing 0.125% trypsin for repeated digestion with 15 min × 5 times. The harvested cells were resuspended in DMEM/F12 medium supplemented with 15% fetal bovine serum (FBS). A differential attachment method was used to remove cardiac fibroblasts from NRCMs, and then, NRCMs were seeded at a density of 2×10^5 cells per well in 6-well plates for protein or mRNA extraction and 1×10^4 cells per well in 24-well plates for immunofluorescence staining. NRCMs were incubated with 0.1 mmol/L bromodeoxyuridine (BrdU) in DMEM/F12 medium with 15% FBS for 36 h before the following experiments.

NRCMs were transfected with gene-specific siRNA for Nrf2 silence (SANTACRUZ, SC-156128) or plasmid for TAK1 overexpression using Lipo 6000 transfection reagent according to the manufacturer's instructions. After another 24 h incubation, NRCMs were cultured in serum-free DMEM/F12 for 12 h and then were stimulated with PE (50 μM) or Myr (20 μM). The treatment dosage of Myr was determined according to our previous publication [9].

Immunofluorescence staining was performed to evaluate NRCM hypertrophy. NRCMs were fixed with 4% paraformaldehyde solution for 10 min at room temperature and then washed with PBS for 3 min × 5 times. After permeabilization with 0.1% Triton X-100 in PBS for 15 min, NRCMs were stained with anti-cardiac Troponin T antibody (1 : 100) overnight. In the next day, the secondary antibody, Alexa Fluor 488 anti-mouse IgG, was used to label cTnT in green. The NRCMs were mounted on glass slides with SlowFade Gold antifade reagent with DAPI.

To demonstrate that Myr treatment could cause antioxidative stress via partly regulating Nrf2, NRCMs were transfected with specific siRNA for Nrf2 knockdown. After transfection of siRNA for 24 h, NRCMs were incubated with Myr or H_2O_2 for another 48 hours. And then, NRCMs were harvested for detecting the expression of Nrf2-regulated genes by RT-PCR and antioxidative enzymes by western blots.

2.6. Western Blot Analysis. Mouse heart tissue or NRCMs were lysed in RIPA buffer. To examine NF-κB/P65 and Nrf2 nucleus translocation, nucleus protein was extracted by a commercial kit purchased from Jiancheng Bioengineering Institute (Nanjing, China). Protein concentration was determined by a BCA protein assay kit. 50 μg protein was used for electrophoresis on 10% SDS-PAGE gels and transferred to a polyvinylidene fluoride membrane (Millipore). After blocking with 5% BSA for 1 h, the blots were incubated with corresponding primary antibodies overnight at 4°C. The peroxidase-conjugated secondary antibodies were used to incubate with the blots for 1 h in the next day. The blots were visualized using Bio-Rad ChemiDocTX XRS+. All expressions of proteins were normalized to corresponding GAPDH before relative quantitative calculation.

2.7. Quantitative Real-Time PCR (rt-PCR). Total mRNA was extracted from snap-frozen heart tissue or NRCMs using the TRIzol reagent according to the manufacturer's instructions. Harvested mRNA was spectrophotometrically estimated by A260/A280 and A230/260 relying on the Smartspec Plus Spectrophotometer (Bio-Rad). Total mRNA (2 μg/sample) was converted into cDNA using the Transcriptor First Strand cDNA Synthesis Kit. RT-PCR amplification of target genes in this study was performed using LightCycler 480 SYBR Green 1 Master Mix. All expression levels of genes were normalized to GAPDH before relative quantitative calculation. Primers used in this study are shown in Table 1.

2.8. Measured Reactive Oxygen Species. Reactive Oxygen Species (ROS) Assay Kit (Beyotime, Shanghai, China) was purchased for ROS measurement according to the manufacturer's instruction. Briefly, NRCMs were transfected with siRNA for 24 h and then were treated with or without Myr (20 μM) overnight. NRCMs were incubated with 50 μM

Table 2: Effects of myricetin on mouse cardiac hypertrophy.

	CON	Myr	AB	AB+Myr
N	12	12	16	16
BW	28.89 ± 1.04	28.17 ± 0.0.97	28.96 ± 1.35	28.52 ± 1.37
HW	122.5 ± 5	120.25 ± 5.08	187.69±14.78**	160.56 ± 20.33##
LW	132.08 ± 7.91	135.33 ± 8.59	162.25±15.04**	148.56 ± 9.8#
TB	19.04 ± 0.5	18.92 ± 0.51	19.19 ± 0.36	19.22 ± 0.36
HW/BW	4.25 ± 0.28	4.27 ± 0.13	6.49±0.58**	5.85 ± 0.83##
LW/BW	4.58 ± 0.36	4.81 ± 0.31	5.61±0.49**	5.18 ± 0.39#
HW/TB	6.44 ± 0.37	6.36 ± 0.38	9.78±0.79**	8.35 ± 1.20##

N: number; BW: body weight; HW: heart weight; LW: lung weight; TB: tibia length, $^{*}p < 0.05$ versus the CON group or the Myr group, $^{\#}p < 0.05$ versus the AB +Myr group.

dichlorofluorescein diacetate (DCFDA) at 37°C in the dark for 30 min. DCFDA in cells could be cleaved into nonfluorescent 2,7-dichlorofluorescin, which could be oxidized by intracellular ROS to product fluorescent dichlorofluorescein (DCF). NRCMs were then incubated with H_2O_2 (30 μM) for 30 min in the dark. Finally, NRCMs were trypsinized and counted for fluorescence quantification in a fluorescence plate reader (BioTek) ($\lambda_{Ex} = 488$, $\lambda_{Em} = 525$).

2.9. HEK 293T Culture and Plasmid Transfections. Plasmid of Prk5-HA-Ubiquitin-K63 (K63-Ub) was obtained from addgene, which only expressed ubiquitin with K63, and other lysines were mutated to arginines [12]. The cDNA of TAK1 (NM 145331) was purchased from Vigene Biosciences (China) and cloned into pc-DNA 3.1 system (Invitrogen, USA) for TAK1 overexpression. HEK393T cells were purchased from China Center for Type Culture Collection (Wuhan, China) and prepared according to published protocol [13]. Briefly, HEK293T cells were seeded in 6-well plates with culture medium supplemented with 10% FBS. Cells were transfected with plasmid (2 μg) by Lipo 6000™ transfection reagent when cell density reached the 60-70% area of the culture dish. After 24 h transfection, cells were treated with 50 μM PE or 20 μM Myr for another 30 min. Finally, the cells were washed twice with 4 ml ice-cold PBS and lysed on ice with 70 μl lysis buffer in each well. Six-well plates were swirled on ice for 15 min, and the cell debris was collected with a cell scraper for following experiments.

2.10. Immunoprecipitation and Ubiquitination Assay. Protein lysate from NRCMs or HEK293T cells was immunoprecipitated with anti-Traf6 coupled to protein A+G Agarose (Beyotime, Shanghai, China). Briefly, protein concentration was determined by BCA assay. Sufficient primary monoclonal antibody of Traf6 was added into 200 μg proteins and incubated at 4°C overnight with gentle rotation. The next day, the beads containing complexes were collected by centrifugation at 2500 rpm for 5 min. The containing complexes were washed and boiled in SDS-PAGE loading buffer. The immunoprecipitated proteins were electrophoresed on 10% SDS-PAGE gels and transferred to a polyvinylidene fluoride membrane (Millipore). Blots were incubated with anti-TAK1 and antiubiquitin to determine the Traf6 ubiquitination and interaction between Traf6 and TAK1.

2.11. Statistical Analysis. All data were presented with mean ± s.d. One-way analysis of variance (ANOVA) was used to compare means among groups followed by least significant difference (LSD, equal variances) or Tamhane' s T2 (none equal variances) tests. Image-Pro 6.0 was used for quantitative analysis of western blots and pictures. SPSS 19.0 was used for statistical analysis in this study. $p < 0.05$ was considered significant.

3. Results

3.1. Myr Treatment Attenuated Pathological Cardiac Hypertrophy and Fibrosis. As presented in Table 2, pressure overload induced obvious cardiac hypertrophy evidenced by increased HW, HW/BW, and HW/TB ratios compared with CON and Myr groups. However, Myr treatment significantly alleviated cardiac hypertrophy evidenced by decreased HW, HW/BW, and HW/TB. HE staining showed significant enlargement of cardiomyocyte (Figures 1(a) and 1(b)) and overproduction of ANP and BNP after AB surgery (Figure 1(c)). Besides, the adult α-MHC was downregulated in mouse heart whereas the fetal β-MHC was significantly upregulated compared with CON and Myr groups (Figures 1(c) and 1(d)). Myr treatment significantly blunted these pathological changes induced by pressure overload (Figures 1(a)–1(d)).

Cardiac fibrosis is an integrate process in the development of pathological cardiac hypertrophy. In this study, AB induced significant interstitial and perivascular fibrosis compared with CON and Myr groups (Figures 1(e) and 1(f)); however, Myr treatment significantly attenuated cardiac fibrosis and inhibited fibrosis-associated markers' expression compared with the AB group (Figures 1(e)–1(g)). Persistent cardiac hypertrophy and fibrosis directly contributed to cardiac dysfunction and heart failure. After 6 weeks of pressure overload, IVSd, LVEDd, LVEPWd, and LVEDs were significantly increased while EF and FS were markedly decreased compared with the CON group or the Myr group (Table 3). Myr treatment significantly improved cardiac function evidenced by decreased IVSd, LVEDd, LVEPWd, and LVEDs,

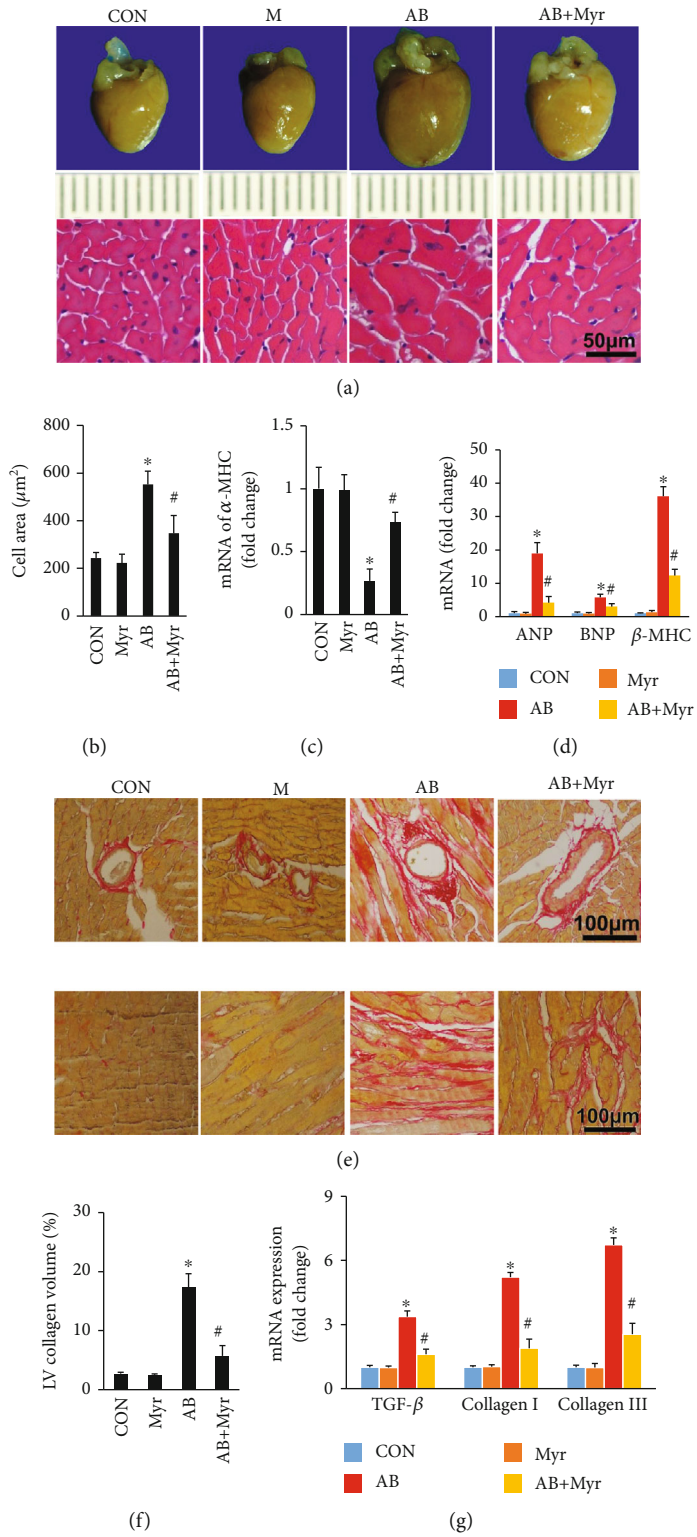

Figure 1: Myr treatment attenuated cardiac hypertrophy and fibrosis. (a) Gross image of the heart; (b) calculated cardiomyocyte across the area of HE staining; (c) Myr prevented the downregulation of α-MHC; (d) Myr inhibited the expression of ANP, BNP, and β-MHC; (e) Myr inhibited interstitial and perivascular fibrosis in mouse heart; (f) calculated LV collagen volume of PSR staining; (g) Myr inhibited the expression of fibrosis-associated markers, $n \geq 6$ for staining experiments, $n = 4$ for mRNA determination, $^{*}p < 0.05$ versus the CON group or the Myr group, $^{\#}p < 0.05$ versus the AB+Myr group.

Table 3: Effects of myricetin on echocardiographic parameters.

	CON	Myr	AB	AB+Myr
N	10	10	10	10
HR (bpm)	496 ± 15	487 ± 27	492 ± 33	478 ± 34
IVSd (mm)	0.79 ± 0.05	0.78 ± 0.05	0.86 ± 0.03*	0.81 ± 0.06#
LVEDd (mm)	3.88 ± 0.23	3.73 ± 0.14	4.56 ± 0.40*	3.97 ± 0.33#
LVEPWd (mm)	0.77 ± 0.05	0.79 ± 0.05	0.89 ± 0.05*	0.83 ± 0.05#
IVDs (mm)	1.12 ± 0.04	1.15 ± 0.08	1.2 ± 0.07	1.19 ± 0.12
LVEDs (mm)	2.05 ± 0.18	1.98 ± 0.09	3.1 ± 0.34*	2.4 ± 0.49#
LVEPWs (mm)	1.13 ± 0.05	1.2 ± 0.06	1.16 ± 0.05	1.16 ± 0.12
EF (%)	81.5 ± 1.87	80.83 ± 2.4	63.08 ± 2.71*	71.45 ± 3#
FS (%)	45 ± 4.38	46.77 ± 2.15	31.67 ± 2.42*	37.8 ± 2.54#

HR: heart rate; IVSd: interventricular septal thickness (IVS) at diastole; IVSs: IVS at systole; LVEDd: LV end-diastolic diameter; LVEDs: LV end-systolic diameter; LVPWd: LV end-diastolic posterior wall thickness; LVPWs: LV end-systolic posterior wall thickness; LVEF: LV ejection fraction; FS: fractional shortening. *$p < 0.05$ versus the CON group or the Myr group, #$p < 0.05$ versus the AB+Myr group.

as well as increased EF and FS compared with the AB group (Table 3).

3.2. Myr Enhanced the Nrf2/HO-1 and Inhibited MAPK/NF-κB. In our previous study, we have showed that Myr treatment could significantly enhance the Nrf2/HO-1 pathway and block NF-κB nuclei translocation [9, 10]. In this study, we also detected the enhanced expression and nuclei translocation of Nrf2 resulted in the activation of the Nrf2/HO-1 pathway (Figures 2(a) and 2(b)), which was downregulated under chronic pressure overload (Figures 2(a) and 2(b)). In addition, chronic pressure overload induced hyperphosphorylation and translocation of NF-κB/p65 (Figures 2(c) and 2(d)), which was also prevented by Myr treatment (Figures 2(c) and 2(d)). Moreover, MAPK signaling (JNK1/2, P38, and ERK1/2) was significantly activated under pressure overload (Figures 2(e) and 2(f)); Myr treatment significantly blocked JNK1/2 and P38 overactivation compared with the AB group (Figures 2(e) and 2(f)), but no significant difference of ERK1/2 phosphorylation was found between the AB group and the AB+Myr group (Figures 2(e) and 2(f)).

3.3. Myr Partly Alleviated Pathological Cardiac Hypertrophy after Nrf2 Knockdown. Based on previous result that enhanced Nrf2 expression could contribute to MAPK and NF-κB pathway inhibition, we investigated here whether Myr could still prevent cardiac hypertrophy after Nrf2 knockdown (Nrf2-KD). To address this question, mouse hearts were firstly injected with lentivirus-wrapped shRNA or scram RNA for Nrf2-KD or negative control, respectively. After lentivirus injection for 3 weeks, mice were subjected to AB surgery and then treated with Myr for another 6 weeks. Unexpectedly, Myr treatment still obviously reversed pressure overload-induced cardiac hypertrophy (Table 4) and dysfunction (Table 5) after Nrf2-KD, as evidenced by decreased HW/BW, LW/BW, HW/TL, IVSd LVEDd, LVEPWd, LVEDs, and LEPWs compared with the shRNA+AB group (Tables 4 and 5). The EF and FS were also significantly improved in the shRNA+AB+Myr group compared to the shRNA+AB group (Table 5). HE and PSR staining presented consistent results that Myr treatment significantly attenuated cardiomyocyte hypertrophy and fibrosis compared with the shRNA+AB group (Figures 3(a), 3(b), 3(d), and 3(e)). Similarly, hypertrophic-associated markers (ANP, BNP, and β-MHC) and fibrosis-associated markers (TGF-β and collagen I/III) were also significantly inhibited by Myr treatment compared with the shRNA+AB group (Figures 3(c) and 3(e)). Obviously, Myr remained to be partly beneficial for protecting against pressure overload-induced cardiac hypertrophy after Nrf2-KD.

3.4. Myr Treatment Inhibited the TAK1/MAPK Pathway Independent of Nrf2. Nrf2 was significantly downregulated in mouse heart after shRNA injection compared with the scram group or the scram+Myr group (Figures 4(a) and 4(b)). Myr treatment remained to inhibit NF-κB/p65 hyperphosphorylation and Nrf2 nucleus translocation after Nrf2 knockdown (Figures 4(a) and 4(b)). Meanwhile, Myr treatment could inhibit pressure overload-induced JNK and p38 hyperphosphorylation (Figures 4(c) and 4(d)) but showed none significant effects for ERK1/2 hyperphosphorylation (Figures 4(c) and 4(d)). Further investigations indicated that Myr treatment markedly blocked TAK1 excessive phosphorylation, which was the common upstream regulator of p-JNK and p-p38 (Figures 4(c) and 4(d)). According to these results, it was reasonable to deduce that Myr treatment prevented cardiac hypertrophy at least partly through inhibiting the TAK1/MAPK pathway.

3.5. Myr Prevented PE-Induced NRCM Hypertrophy and H_2O_2-Induced Oxidative Stress. In *in vitro* experiment, PE treatment induced significant NRCM hypertrophy, which could be markedly inhibited by Myr treatment (Figures 5(a) and 5(b)). After Nrf2 knockdown, Myr could also partly prevent NRCM from PE-induced hypertrophy (Figures 5(a) and 5(b)). However, after Nrf2 knockdown and TAK1 overexpression in NRCM, Myr could not protect NRCMs from PE-induced hypertrophy (Figures 5(a) and 5(b)). RT-PCR was also performed to examine hypertrophy-associated biomarkers in vitro. Myr treatment could significantly prevent

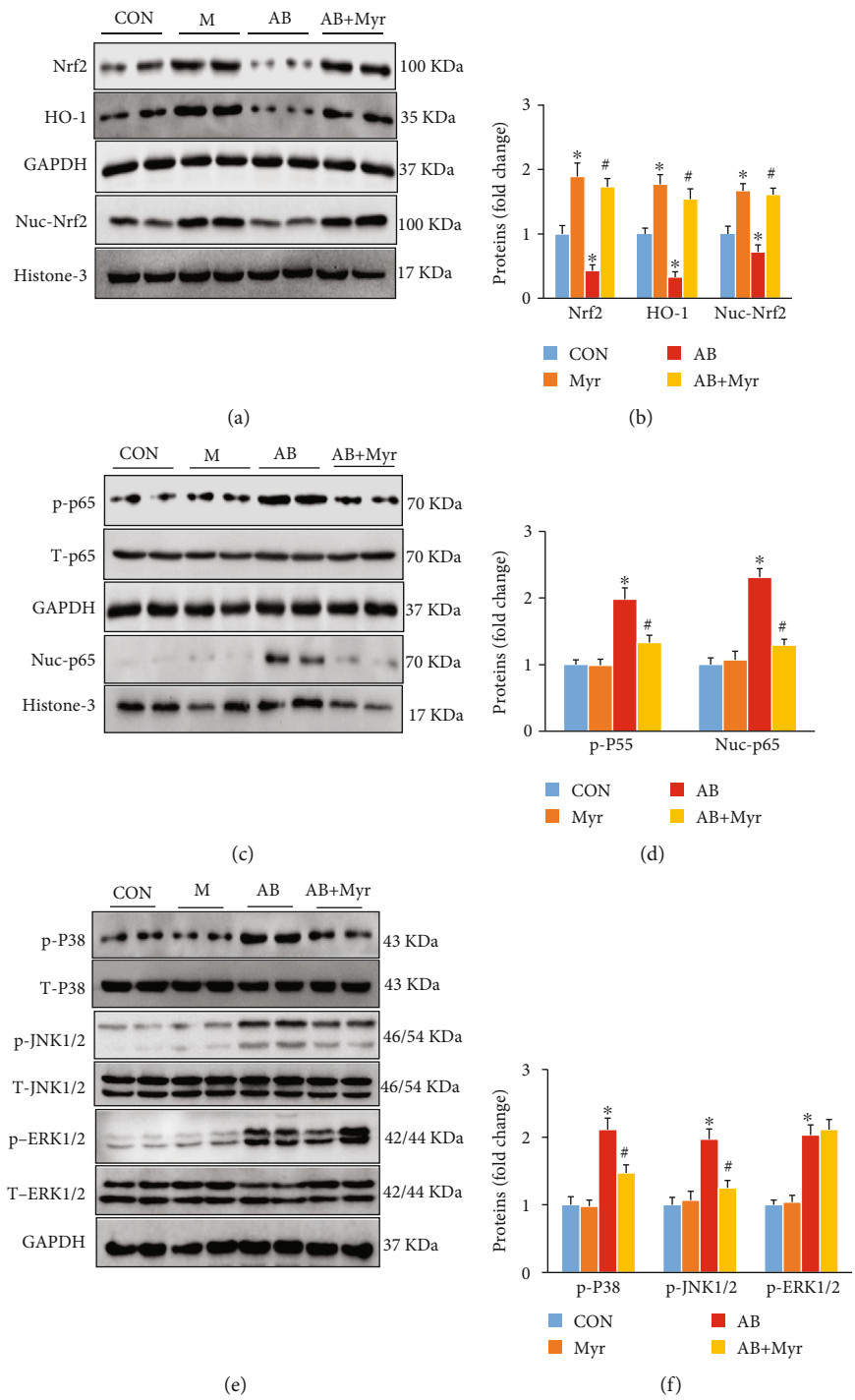

Figure 2: Protein levels of signaling pathways after Myr treatment. (a, b) Myr inhibited the Nrf2/HO-1 pathway; (c, d) Myr inhibited the phosphorylation and nuclei translocation of p65; (d, e) Myr inhibited the phosphorylation of p38 and JNK1.2 MAPK kinase. $n = 6$, $^{*}p < 0.05$ versus the CON group or the Myr group, $^{\#}p < 0.05$ versus the AB+Myr group.

overexpression of ANP, BNP, and β-MHC in both the PE group and the PE+siNrf2 group (Figures 5(c) and 5(d)); however, after overexpression of TAK1 in Nrf2 knockdown cells, Myr could no longer attenuate PE-induced hypertrophic biomarkers' expression (Figure 5(c) and 5(d)).

To further demonstrate that Myr might possess antioxidant stress via regulating Nrf2, NRCMs were treated with H_2O_2 or Myr with or without Nrf2 knockdown. Nrf2 downstream genes including HO-1, NQO1, and GCLC were significantly downregulated in the siNrf2+H_2O_2+Myr group compared to the H_2O_2 treatment group (Figures 5(f)–5(i)). Myr treatment could not upregulate the expression of HO-1, NQO1, and GCLC compared to control groups after Nrf2 knockdown (Figures 5(f)–5(i)); however, Myr treatment could significantly upregulate these Nrf2-associated downstream genes in none Nrf2 knockdown NRCMs

Table 4: Effects of myricetin on cardiac hypertrophy after Nrf2 knockdown.

	Scram	Scram+M	shRAN+AB	shRNA+AB+M
N	12	12	13	13
BW	25.85 ± 0.62	25.77 ± 0.72	24.76 ± 0.48	25.01 ± 0.58
HW	114.42 ± 5.2	119 ± 6.84	214.21 ± 21.9*	185.67 ± 17.97#
LW	136.63 ± 11.55	139.84 ± 13.94	212.36 ± 28.04*	177.75 ± 23.53#
TB	19.08 ± 0.36	19.2 ± 0.33	19.29 ± 0.25	19.17 ± 0.33
HW/BW	4.42 ± 0.24	4.61 ± 0.23	8.66 ± 0.97*	7.42 ± 0.70#
LW/BW	5.29 ± 0.52	5.42 ± 0.56	8.59 ± 1.22*	7.1 ± 0.90#
HW/TB	6.0 ± 0.32	6.1 ± 0.3	11.11 ± 1.19*	9.69 ± 0.95#

N: number; BW: body weight; HW: heart weight; LW: lung weight; TB: tibia length; *$p < 0.05$ versus the scram group or the scram+Myr group, #$p < 0.05$ versus the shRNA+AB group.

Table 5: Effects of myricetin on echocardiographic parameters after Nrf2 knockdown.

	Scram	Scram+Myr	shRNA+AB	shRNA+AB+Myr
N	10	10	10	10
HR (bpm)	487 ± 15	496 ± 15	491 ± 14	486 ± 14
IVSd (mm)	0.79 ± 0.05	0.78 ± 0.04	0.88 ± 0.02*	0.80 ± 0.04#
LVEDd (mm)	3.88 ± 0.15	3.75 ± 0.11	5.08 ± 0.35*	4.58 ± 0.16#
LVEPWd (mm)	0.78 ± 0.03	0.77 ± 0.04	0.91 ± 0.04*	0.81 ± 0.07#
IVDs (mm)	1.13 ± 0.05	1.15 ± 0.05	1.15 ± 0.05	1.11 ± 0.13
LVEDs (mm)	2.23 ± 0.18	2.18 ± 0.15	4.13 ± 0.32*	3.43 ± 0.14#
LVEPWs (mm)	1.12 ± 0.08	1.1 ± 0.09	0.94 ± 0.12*	1.06 ± 0.15#
EF (%)	78.83 ± 4.54	78.5 ± 3.21	43.75 ± 5.9*	53.63 ± 3.8#
FS (%)	42.67 ± 3.83	41.83 ± 2.93	19.25 ± 2.25*	25.31 ± 2.97#

HR: heart rate; IVSd: interventricular septal thickness (IVS) at diastole; IVSs: IVS at systole; LVEDd: LV end-diastolic diameter; LVEDs: LV end-systolic diameter; LVPWd: LV end-diastolic posterior wall thickness; LVPWs: LV end-systolic posterior wall thickness; LVEF: LV ejection fraction; FS: fractional shortening. *$p < 0.05$ versus the scram group or the scram+Myr group, #$p < 0.05$ versus the shRNA+AB group.

(Figures 5(f)–5(i)). DCF measurement demonstrated that Myr could attenuate H_2O_2-induced ROS accumulation in Nrf2 none knockdown NRCMs not in Nrf2 knockdown NRCMs (Figure 5(j)). H_2O_2 treatment 24 h induced significant upregulation of 4-HEN and downregulation of SOD1 and CAT compared to the control group (Figures 5(k) and 5(l)). Importantly, Myr treatment could inhibit 4-HEN expression and restore SOD1 and CAT expressions (Figures 5(k) and 5(l)); however, Myr could not inhibit 4-HEN expression and restore SOD1 and CAT expressions in Nrf2 knockdown NRCMs (Figures 5(k) and 5(l)). These results suggested that Myr-mediated Nrf2 expression prevented H_2O_2-induced oxidative stress in NRCMs.

3.6. Myr Prevented TRAF6/TAK1 Interaction via Regulating Traf6 Ubiquitin. Finally, we intended to investigate the exact mechanism from which Myr regulated the TAK1/MAPK pathway. Previous studies suggested that polyphenols could regulate protein ubiquitination [14, 15]. Here, we investigated whether Myr could regulate Traf6 ubiquitination. PE treatment induced Traf6 ubiquitination, while Myr treatment significantly inhibited Traf6 ubiquitination in NRCM (Figure 6(a)). It was also observed that Myr treatment prevented hyperphosphorylation of TAK1, P38 and JNK1/2 but not ERK1/2 phosphorylation in PE-treated NRCMs (Figure 6(a)). To further investigate the ubiquitination regulation manner, K63-only ubiquitin (K63-Ub) and Traf6 were cloned into plasmid and then were cotransfected into HEK293 cell. After PE treatment, Traf6 was obviously ubiquitinated by K63 ubiquitin, and Myr treatment significantly prevented this ubiquitin (Figure 6(b)). Finally, TAK-1 and Traf6 were cotransfected into HEK293 cell (Figure 6(c)). PE treatment caused significant interaction between TAK-1 and Traf6 (Figure 6(c)), but Myr treatment obviously disturbed the interaction between TAK1 and Traf6 (Figure 6(c)).

4. Discussion

This study demonstrated for the first time that Myr protected mouse heart and NRCM from pressure overload or PE-induced hypertrophy, respectively. Hypertrophic stimuli caused Nrf2/HO-1 downregulation and TRAF6 unregulation and its ubiquitination. Ubiquitinated TRAF6 could interact with TAK1 promoting TAK1/JNK1/2/P38 phosphorylation. Myr treatment significantly inhibited the TRAF6/TAK1/-MAPK pathway and restored Nrf2/HO-1 activity. Moreover,

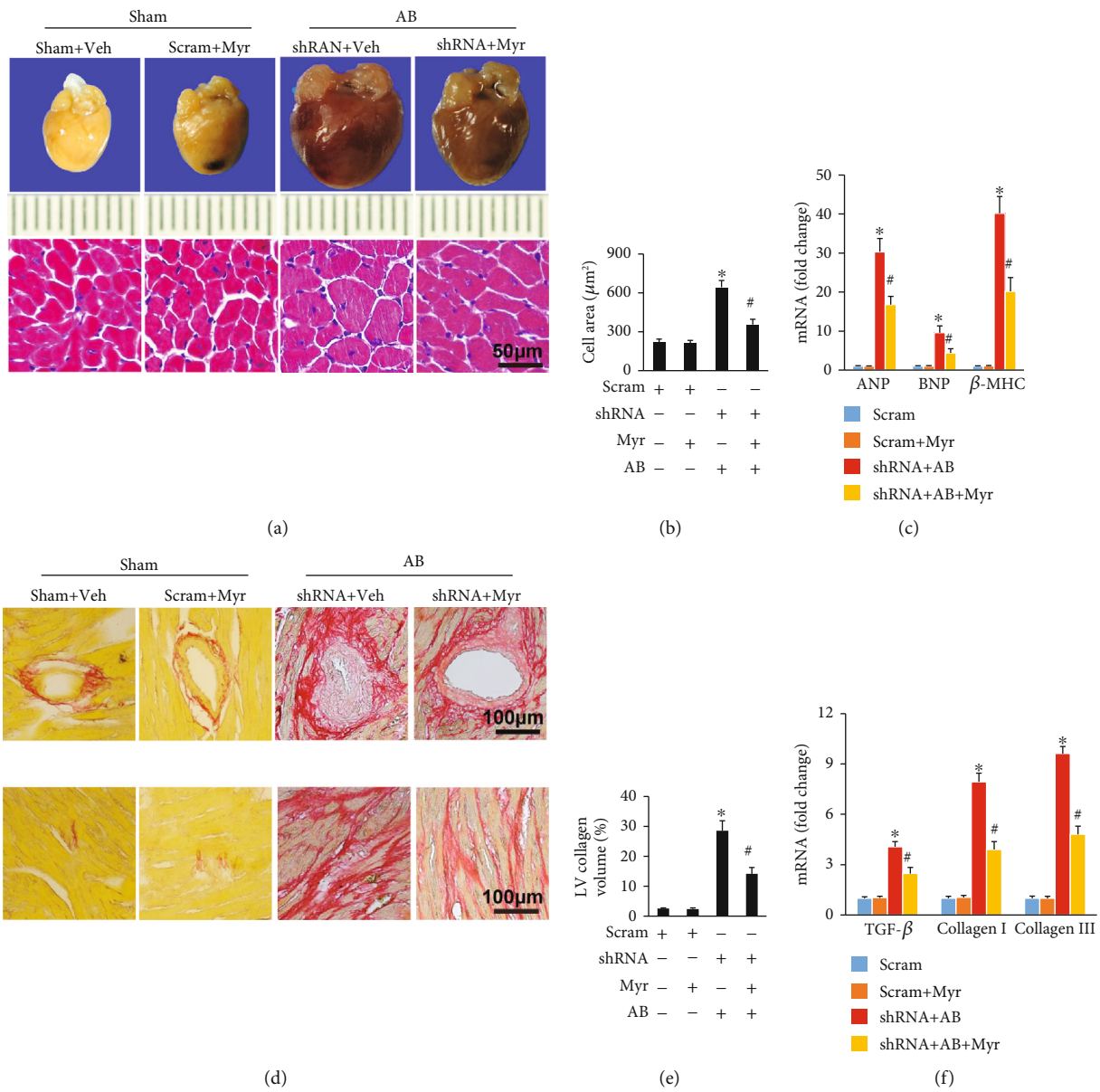

Figure 3: Myr inhibited cardiac hypertrophy and fibrosis after Nrf2 knockdown. (a) Myr inhibited mouse heart and cardiomyocyte hypertrophy; (b) calculated cardiomyocyte across the area of HE staining; (c) Myr inhibited the expression of ANP, BNP, and β-MHC; (d) Myr inhibited interstitial and perivascular fibrosis in mouse heart; (e) calculated LV collagen volume of PSR staining; (f) Myr inhibited the expression of fibrosis-associated markers, $n \geq 6$ for staining experiments, $n = 4$ for mRNA determination, $^{*}p < 0.05$ versus the scram group or the scram+Myr group, $^{\#}p < 0.05$ versus the shRNA+AB group.

Traf6/TAK1/MAPK cascade inhibition was independent of Nrf2/HO-1 activity. In addition, Myr treatment prevented Traf6 expression and ubiquitination and also prevented the TRAF6-TAK1 interaction.

Previous investigations have presented that Myr was a powerful antioxidant in various cells and diseases [3]. Myr could increase the activity and protein expression of many antioxidases including SOD, GSH/GSSG ratio, catalase, and glutathione. These antioxidases were markedly downregulated in ischemia/reperfusion-induced myocardial injury and deoxycorticosterone acetate- (DOCA-) salt-hypertensive rats [16, 17]. Myr reacted with oxygen-centered galvinoxyl radicals 28 times faster than vitamin E [18]. Gene microarray analysis in HepG2 cells suggested that Myr might involve in promoting Nrf2-mediated antioxidant response element (ARE) activation for exerting its antioxidant roles [19]. Further investigations revealed that Myr treatment prevented Nrf2 ubiquitination and protein turnover, promoting Nrf2 expression and kelch-like erythroid cell-derived protein with CNC homology-associated protein 1 modification [19]. Our previous study also demonstrated that Myr treatment attenuated diabetes-associated cardiomyocyte hypertrophy, apoptosis, and interstitial fibrosis via restoring Nrf2/HO-1 pathway activity [10]. Nrf2 has been demonstrated to play important roles in regulating cardiac pathophysiology. Published data have showed that deficiency

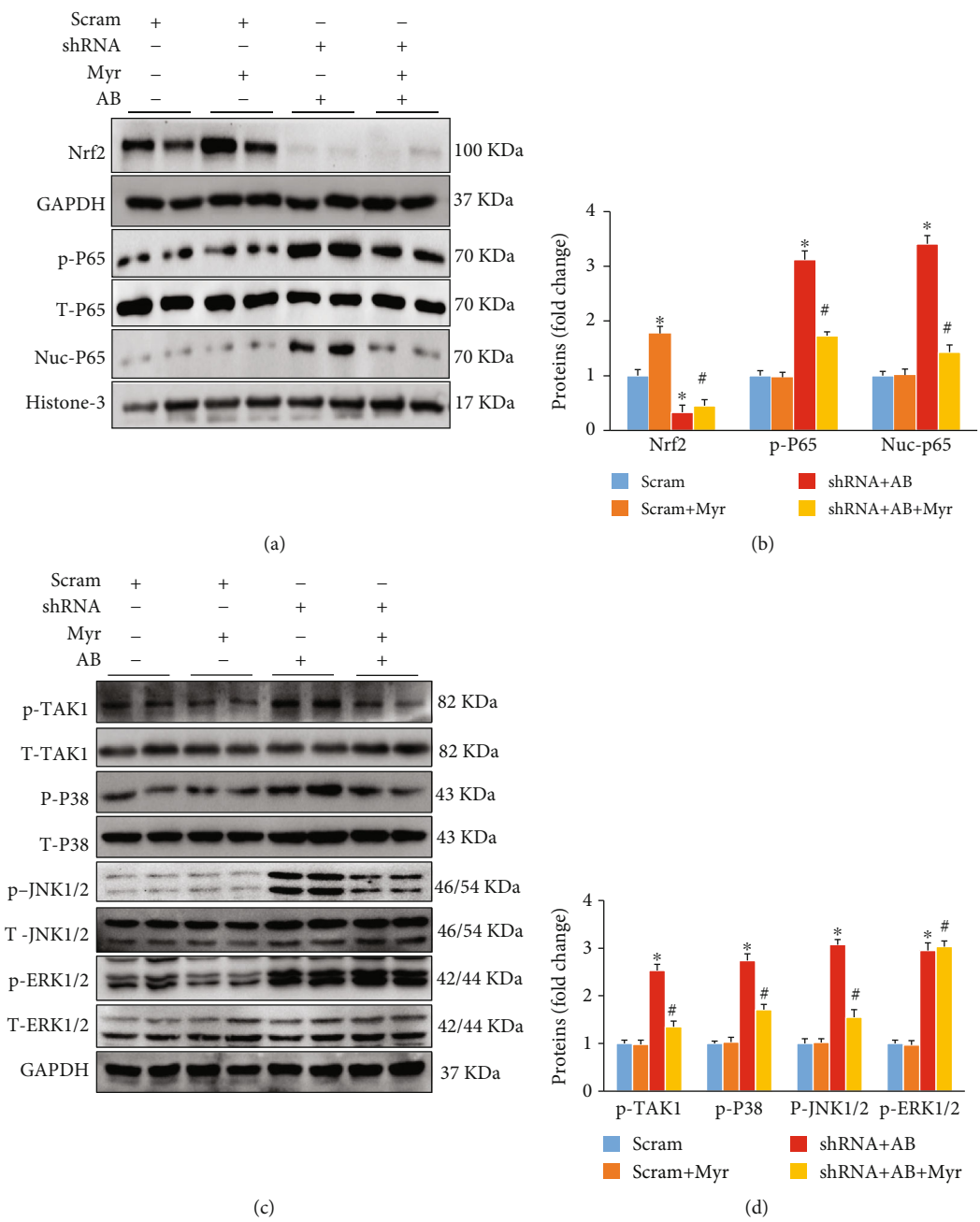

Figure 4: Determination of signaling pathways after Nrf2 knockdown in mouse heart. (a, b) Myr treatment inhibited the phosphorylation and nuclei translocation of p65; (c, d) Myr treatment inhibited the phosphorylation of TAK1/p38/JNK1/2 after Nrf2 knockdown, $n = 6$, $^{*}p < 0.05$ versus the scram group or the scram+Myr group, $^{\#}p < 0.05$ versus the shRNA+AB group.

or downregulation of Nrf2 exacerbated pathological cardiac hypertrophy [20, 21], while stimulating Nrf2 expression by genetic or drug treatment strategies could significantly attenuate pathological remodeling [22, 23]. Taken together these evidences, Myr-mediated Nrf2 regulation was undoubtedly one of the most important mechanisms for preventing pathological cardiac remodeling. Some clinical investigations have figured out that Myr intake was inversely associated with the morbidity of myocardial infarction or coronary heart disease, but the underlying mechanisms remained to be unclear [4, 24].

Our previous investigation showed that Myr treatment could improve LPS-induced cardiac injury by inhibiting IκB/NF-κB (p65) signaling and inflammatory cytokine secretion [9]. In a high glucose-induced NRCM injury model, we further demonstrated that Myr-mediated IκB/NF-κB (p65) inhibition was independent of Nrf2 enhancement [10]. In this study, we observed that Myr treatment inhibited p65 phosphorylation and nuclei translocation in both wild type and Nrf2-knockdown mouse hearts. These studies intensively displayed that Myr possessed potent anti-inflammatory activity. In lipoteichoic acid- (LTA-) treated human gingival

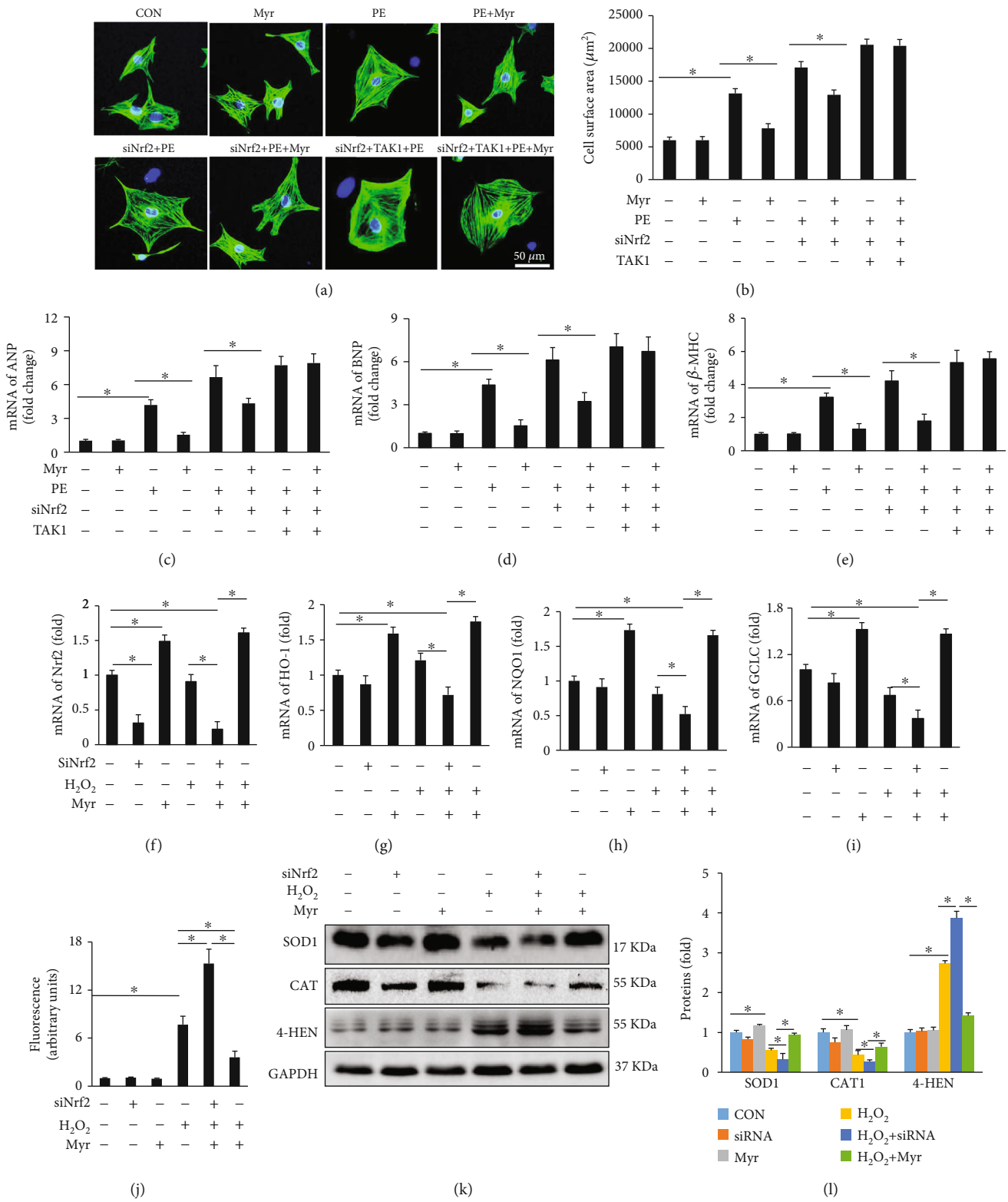

Figure 5: Myr prevented NRCM hypertrophy *in vitro*. (a) Immunofluorescence (IF) staining of NRCM in different groups; (b) calculated cell surface area (>100 cells per group); (c–e) mRNA expression levels of ANP, BNP, and β-MHC, respectively; Nrf2 knockdown (f) and its downstream genes including HO-1 (g), NQQ-1 (h), and GCLC (i), respectively. All mRNA expressions of target genes were normalized to GAPDH; (j) DCF fluorescence was quantified to present the reactive oxygen species after different treatments indicated in the pictures; (k) representative western blots for SOD1, CAT, and 4-HEN after different treatments indicated in the pictures; (l) quantified SOD1, CAT1, and 4-HEN after normalized to GAPDH. Cellular experiments were repeated three times independently. $^{*}p < 0.05$ versus the group indicated in the picture.

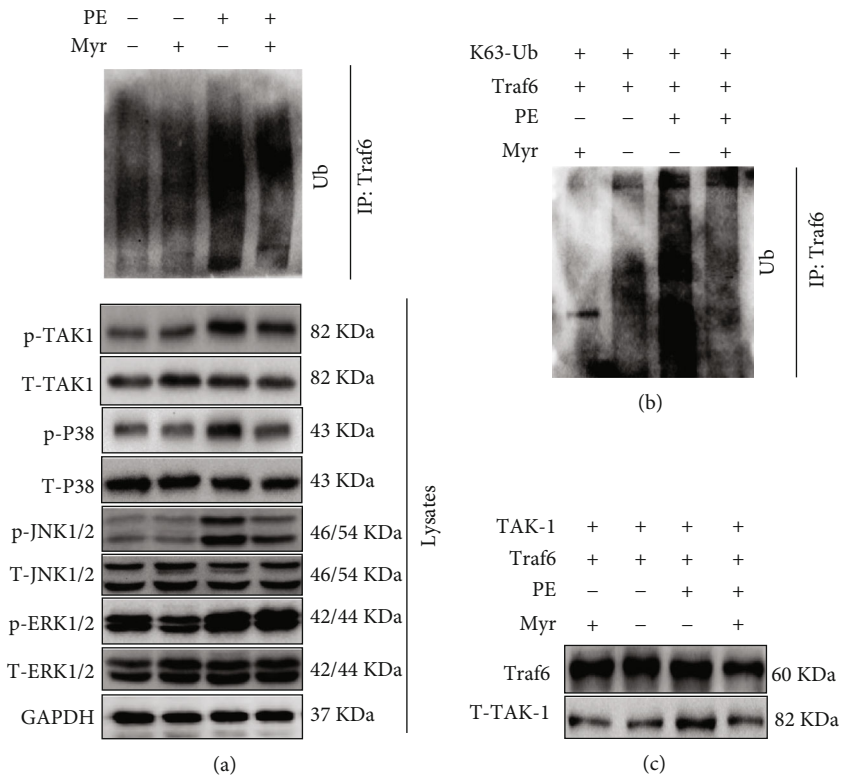

Figure 6: Myr treatment prevented Traf6 ubiquitination *in vitro*. (a) Myr (20 μM, preincubation with NRCM for 1 h) treatment prevented PE (50 μM, 30 min) induced TRAF6 ubiquitination and the phosphorylation of p38 and JNK1/2; (b) Myr treatment inhibited K63-Ub-induced TRAF6 ubiquitination in HEK293 cell; (c) Myr inhibited the interaction between Traf6 and TAK1, and TAK1phosphorylation. All experiments were repeated three times independently.

fibroblasts (HGFs), Myr treatment depressed p38 and ERK1/2 activation and also inhibited IκBα degradation [23, 25]. In IL-1β-stimulated SW982 synovial cells, Myr significantly reduced JNK and p38 phosphorylation [26]. These results implied that Myr-mediated inflammation reduction might be associated with MAPK signaling regulation. Based on these previous studies, this study detected MAPK signaling and figured out that Myr treatment significantly inhibited p38 and JNK1/2 phosphorylation but showed none significant effects for ERK1/2 phosphorylation.

TAK1 is an upstream regulatory protein of p38 and JNK1/2 MAPK [27, 28]. TAK1 phosphorylation could contribute to p38 and JNK1/2 MAPK hyperphosphorylation resulted in aggravated pathological cardiac hypertrophy [27, 28]. In this study, Myr treatment significantly depressed TAK1 phosphorylation after Nrf2 knockdown in *in vivo* experiment. Accordingly, we deduced that Myr alleviated cardiac hypertrophy through inhibiting TAK1 activation, which could be regulated by TRAF6 ubiquitination. Ji et al. [29] demonstrated that Traf6 autoubiquitination promoted the interaction of TRAF6 and TAK1 in the process of pressure overload-induced cardiac hypertrophy, and Traf6 deletion or inhibiting Traf6 ubiquitin effectively attenuated pressure overload-induced cardiac hypertrophy [29]. In previous studies, polyphenols have been demonstrated to suppress NF-κB activation through decreasing Traf6 ubiquitination in Hela-T6RZC stable cells and to disrupt the polyubiquitin synthesis in *in vitro* kinase assay system [15]. Resveratrol, another well-known polyphenolic compound, has also been demonstrated to inhibit LPS-induced p38 and JNK1/2 activation via diminishing TRAF6 ubiquitination [14].

Based on these studies, we investigated whether Myr would show similar function with other polyphenolic compounds to regulate Traf6 ubiquitination. PE induced Traf6 ubiquitination in NRCM accompanied with increased phosphorylation of TAK1, p38, JNK1/2, and ERK1/2. Myr treatment significantly inhibited the TRAF6 expression and its ubiquitination and decreased the activity of TAK1, p38, and JNK1/2. Previous studies have indicated that the TRAF6-associated ubiquitination activation was largely determined by a site-specific nondegradative Lys-63-linked autoubiquitination (K63-Ub) [29–31]. So, K63-Ub and TRAF6 plasmids were cotransfected into HEK-293-cells. PE treatment obviously promoted TRAF6 ubiquitination, which was significantly inhibited by Myr treatment. TRAF6 autoubiquitination promoted TRAF6 and TAK1 interaction. TRAF6 and TAK1 plasmids were cotransfected into HEK-293 cells to detect the TRAF6 and TAK1 interaction. Our results showed that PE treatment significantly promoted TRAF6 and TAK1 interaction, which could be markedly blocked by Myr treatment.

Taken together, Myr possessed potent capacity to restore Nrf2/HO-1 activity and to inhibit TAK1/p38/JNK1/2 MAPK signaling via inhibiting TRAF6 autoubiquitination. Thus, Myr might be a potential drug with multiple targets for

therapy or adjunct therapy of pathological cardiac hypertrophy. However, some questions remain to be addressed in following studies. For example, a previous study suggested that Myr promoted Nrf2 expression and nuclear translocation via regulating KEAP1 ubiquitination, but this study presented that Myr regulated TRAF6 autoubiquitination. How does Myr regulate the TRAF6 and KEAP ubiquitination at the same time? What is the exact mechanism of ubiquitination regulation?

Data Availability

If someone or any research requests data or any details of the experiment about this article, please contact the first author (Hai-han Liao, email address: liaohaihan@whu.edu.cn or Nan Zhang, email address: zhangnan0609@whu.edu.cn) or corresponding author (Qi-zhu Tang, email address: qztang@whu.edu.cn).

Conflicts of Interest

The authors declare that they have no conflicts of interest.

Authors' Contributions

Hai-han Liao and Nan Zhang contributed equally to this work.

References

[1] M. Nakamura and J. Sadoshima, "Mechanisms of physiological and pathological cardiac hypertrophy," *Nature Reviews Cardiology*, vol. 15, no. 7, pp. 387–407, 2018.

[2] I. Shimizu and T. Minamino, "Physiological and pathological cardiac hypertrophy," *Journal of Molecular and Cellular Cardiology*, vol. 97, pp. 245–262, 2016.

[3] D. Semwal, R. Semwal, S. Combrinck, and A. Viljoen, "Myricetin: a dietary molecule with diverse biological activities," *Nutrients*, vol. 8, no. 2, p. 90, 2016.

[4] J. M. Geleijnse, L. J. Launer, D. A. Van der Kuip, A. Hofman, and J. C. Witteman, "Inverse association of tea and flavonoid intakes with incident myocardial infarction: the Rotterdam Study," *The American Journal of Clinical Nutrition*, vol. 75, no. 5, pp. 880–886, 2002.

[5] M. G. Hertog, E. J. Feskens, P. C. Hollman, M. B. Katan, and D. Kromhout, "Dietary antioxidant flavonoids and risk of coronary heart disease: the Zutphen Elderly Study," *The Lancet*, vol. 342, no. 8878, pp. 1007–1011, 1993.

[6] R. Tiwari, M. Mohan, S. Kasture, A. Maxia, and M. Ballero, "Cardioprotective potential of myricetin in isoproterenol-induced myocardial infarction in Wistar rats," *Phytotherapy Research*, vol. 23, no. 10, pp. 1361–1366, 2009.

[7] T. M. Scarabelli, S. Mariotto, S. Abdel-Azeim et al., "Targeting STAT1 by myricetin and delphinidin provides efficient protection of the heart from ischemia/reperfusion-induced injury," *FEBS Letters*, vol. 583, no. 3, pp. 531–541, 2009.

[8] T. Angelone, T. Pasqua, D. Di Majo et al., "Distinct signalling mechanisms are involved in the dissimilar myocardial and coronary effects elicited by quercetin and myricetin, two red wine flavonols," *Nutrition, Metabolism, and Cardiovascular Diseases*, vol. 21, no. 5, pp. 362–371, 2011.

[9] N. Zhang, H. Feng, H. H. Liao et al., "Myricetin attenuated LPS induced cardiac injury in vivo and in vitro," *Phytotherapy Research*, vol. 32, no. 3, pp. 459–470, 2018.

[10] H.-h. Liao, J.-x. Zhu, H. Feng et al., "Myricetin Possesses Potential Protective Effects on Diabetic Cardiomyopathy through Inhibiting I κ B α /NF κ B and Enhancing Nrf2/HO-1," *Oxidative Medicine and Cellular Longevity*, vol. 2017, Article ID 8370593, 14 pages, 2017.

[11] Y. Yuan, L. Yan, Q. Q. Wu et al., "Mnk1 (mitogen-activated protein kinase-interacting kinase 1) deficiency aggravates cardiac remodeling in mice," *Hypertension*, vol. 68, no. 6, pp. 1393–1399, 2016.

[12] K. L. Lim, K. C. Chew, J. M. Tan et al., "Parkin mediates nonclassical, proteasomal-independent ubiquitination of synphilin-1: implications for Lewy body formation," *The Journal of Neuroscience*, vol. 25, no. 8, pp. 2002–2009, 2005.

[13] A. Gupta, H. Maccario, N. Kriplani, and N. R. Leslie, "In cell and in vitro assays to measure PTEN ubiquitination," *Methods in Molecular Biology*, vol. 1388, pp. 155–165, 2016.

[14] P. B. Jakus, N. Kalman, C. Antus et al., "TRAF6 is functional in inhibition of TLR4-mediated NF-κB activation by resveratrol," *The Journal of Nutritional Biochemistry*, vol. 24, no. 5, pp. 819–823, 2013.

[15] K. Wang, A. C. H. F. Sawaya, L. Hu et al., "Polyphenol-rich propolis extracts from China and Brazil exert anti- inflammatory effects by modulating ubiquitination of TRAF6 during the activation of NF-κB," *Journal of Functional Foods*, vol. 19, pp. 464–478, 2015.

[16] P. Borde, M. Mohan, and S. Kasture, "Effect of myricetin on deoxycorticosterone acetate (DOCA)-salt-hypertensive rats," *Natural Product Research*, vol. 25, no. 16, pp. 1549–1559, 2011.

[17] Y. Qiu, N. Cong, M. Liang, Y. Wang, and J. Wang, "Systems pharmacology dissection of the protective effect of myricetin against acute ischemia/reperfusion-induced myocardial injury in isolated rat heart," *Cardiovascular Toxicology*, vol. 17, no. 3, pp. 277–286, 2017.

[18] C. J. Bennett, S. T. Caldwell, D. B. McPhail, P. C. Morrice, G. G. Duthie, and R. C. Hartley, "Potential therapeutic antioxidants that combine the radical scavenging ability of myricetin and the lipophilic chain of vitamin E to effectively inhibit microsomal lipid peroxidation," *Bioorganic & Medicinal Chemistry*, vol. 12, no. 9, pp. 2079–2098, 2004.

[19] S. Qin, J. Chen, S. Tanigawa, and D. X. Hou, "Microarray and pathway analysis highlight Nrf2/ARE-mediated expression profiling by polyphenolic myricetin," *Molecular Nutrition & Food Research*, vol. 57, no. 3, pp. 435–446, 2013.

[20] R. Erkens, C. M. Kramer, W. Lückstädt et al., "Left ventricular diastolic dysfunction in Nrf2 knock out mice is associated with cardiac hypertrophy, decreased expression of SERCA2a, and preserved endothelial function," *Free Radical Biology & Medicine*, vol. 89, pp. 906–917, 2015.

[21] C. Tian, L. Gao, M. C. Zimmerman, and I. H. Zucker, "Myocardial infarction-induced microRNA-enriched exosomes contribute to cardiac Nrf2 dysregulation in chronic heart failure," *American Journal of Physiology. Heart and Circulatory Physiology*, vol. 314, no. 5, pp. H928–H939, 2018.

[22] I. Smyrnias, X. Zhang, M. Zhang et al., "Nicotinamide adenine dinucleotide phosphate oxidase-4-dependent upregulation of nuclear factor erythroid-derived 2-like 2 protects the heart during chronic pressure overload," *Hypertension*, vol. 65, no. 3, pp. 547–553, 2015.

[23] C. Zeng, P. Zhong, Y. Zhao et al., "Curcumin protects hearts from FFA-induced injury by activating Nrf2 and inactivating NF-κB both in vitro and in vivo," *Journal of Molecular and Cellular Cardiology*, vol. 79, pp. 1–12, 2015.

[24] P. C. H. Hollman and M. B. Katan, "Health effects and bioavailability of dietary flavonols," *Free Radical Research*, vol. 31, Supplement 1, pp. 75–80, 1999.

[25] G. Gutiérrez-Venegas, O. Luna, J. Arreguín-Cano, and C. Hernández-Bermúdez, "Myricetin blocks lipoteichoic acid-induced COX-2 expression in human gingival fibroblasts," *Cellular & Molecular Biology Letters*, vol. 19, no. 1, pp. 126–139, 2014.

[26] Y. S. Lee and E. M. Choi, "Myricetin inhibits IL-1β-induced inflammatory mediators in SW982 human synovial sarcoma cells," *International Immunopharmacology*, vol. 10, no. 7, pp. 812–814, 2010.

[27] L. Chen, J. Huang, Y. X. Ji et al., "Tripartite motif 8 contributes to pathological cardiac hypertrophy through enhancing transforming growth factor β-activated kinase 1-dependent signaling pathways," *Hypertension*, vol. 69, no. 2, pp. 249–258, 2017.

[28] C. Y. Li, Q. Zhou, L. C. Yang et al., "Dual-specificity phosphatase 14 protects the heart from aortic banding-induced cardiac hypertrophy and dysfunction through inactivation of TAK1-P38MAPK/-JNK1/2 signaling pathway," *Basic Research in Cardiology*, vol. 111, no. 2, p. 19, 2016.

[29] Y. X. Ji, P. Zhang, X. J. Zhang et al., "The ubiquitin E3 ligase TRAF6 exacerbates pathological cardiac hypertrophy via TAK1-dependent signalling," *Nature Communications*, vol. 7, no. 1, article 11267, 2016.

[30] B. Lamothe, A. Besse, A. D. Campos, W. K. Webster, H. Wu, and B. G. Darnay, "Site-specific Lys-63-linked tumor necrosis factor receptor-associated factor 6 auto-ubiquitination is a critical determinant of I kappa B kinase activation," *The Journal of Biological Chemistry*, vol. 282, no. 6, pp. 4102–4112, 2007.

[31] Q. Yin, S. C. Lin, B. Lamothe et al., "E2 interaction and dimerization in the crystal structure of TRAF6," *Nature Structural & Molecular Biology*, vol. 16, no. 6, pp. 658–666, 2009.

Hindawi
Oxidative Medicine and Cellular Longevity
Volume 2019, Article ID 7049237, 10 pages
https://doi.org/10.1155/2019/7049237

Research Article

Cardiac Rehabilitation Increases SIRT1 Activity and β-Hydroxybutyrate Levels and Decreases Oxidative Stress in Patients with HF with Preserved Ejection Fraction

Graziamaria Corbi,[1] Valeria Conti,[2] Jacopo Troisi,[2,3,4] Angelo Colucci,[2,3] Valentina Manzo,[2] Paola Di Pietro,[2] Maria Consiglia Calabrese,[2] Albino Carrizzo,[5] Carmine Vecchione,[2,5] Nicola Ferrara,[6,7] and Amelia Filippelli[2]

[1]*Department of Medicine and Health Sciences, University of Molise, Campobasso, Italy*
[2]*Department of Medicine, Surgery and Dentistry, University of Salerno, Baronissi, Italy*
[3]*Theoreo srl, Via degli Ulivi 3 84090 Montecorvino Pugliano, Italy*
[4]*European Biomedical Research Institute of Salerno (EBRIS), Via S. de Renzi 3, 84125 Salerno, Italy*
[5]*IRCCS Neuromed, Department of Vascular Physiopathology, Pozzilli, Italy*
[6]*Department of Translational Medical Sciences, Federico II University of Naples, Naples, Italy*
[7]*Istituti Clinici Scientifici Maugeri SpA Società Benefit (ICS Maugeri SpA SB), Telese Terme, Italy*

Correspondence should be addressed to Valeria Conti; vconti@unisa.it

Received 31 May 2019; Revised 14 September 2019; Accepted 22 October 2019; Published 27 November 2019

Academic Editor: Massimo Collino

Purpose. Exercise training induces beneficial effects also by increasing levels of Sirtuin 1 (Sirt1) and β-hydroxybutyrate (βOHB). Up to date, no studies investigated the role of exercise training-based cardiac rehabilitation (ET-CR) programs on βOHB levels. Therefore, the present study is aimed at investigating whether a supervised 4-week ET-CR program was able to induce changes in Sirt1 activity and βOHB levels and to evaluate the possible relationship between such parameters, in Heart Failure with preserved Ejection Fraction (HFpEF) patients. *Methods*. A prospective longitudinal observational study was conducted on patients consecutively admitted to the Cardiology and Cardiac Rehabilitation Units of "San Gennaro dei Poveri" Hospital in Naples, Italy. In fifty elderly patients affected by HFpEF, in NYHA II and III class, Sirt1 activity, Trolox Equivalent Antioxidant Capacity (TEAC), βOHB, and Oxidized Low-Density Lipoprotein (Ox-LDL) levels were measured before and at the end of the ET-CR program. A control group of 20 HFpEF patients was also recruited, and the same parameters were evaluated 4 weeks after the beginning of the study. *Results*. ET-CR induced an increase of Sirt1 activity, βOHB levels, and antioxidant capacity. Moreover, it was associated with a rise in NAD^+ and NAD^+/NADH ratio levels and a reduction in Ox-LDL. No changes affected the controls. *Conclusion*. The characterization of the ET-CR effects from a metabolic viewpoint might represent an important step to improve the HFpEF management.

1. Introduction

Despite recent advances in both pharmacological and nonpharmacological therapies, heart failure (HF) is still a prevalent cause of death or permanent invalidity worldwide [1]. The exercise training-based cardiac rehabilitation (ET-CR) surely represents a valid nonpharmacological therapeutic approach against HF; nevertheless, it is still underprescribed in aged patients. The reason for this behavior could be ascribed to their comorbidity and polytherapy that complicate the participation in the ET-CR programs.

In HF, tissue hypoxia, caused either by low cardiac output or by sympathetic vasoconstriction, may also trigger a significant increase in the production of free radicals [2]. In fact, oxidative stress, which occurs when reactive oxygen species (ROS) are produced in excess and overcome the action of

the endogenous antioxidants mechanisms, is implicated in the pathophysiology of HF. This is proved by a correlation between oxidative stress markers and HF in human and animal studies [3, 4] and by direct molecular evidence about an etiological role of ROS [5] in cardiovascular diseases, including HF.

During life, the cardiovascular system is constantly exposed to oxidative stress; hence, the balance between the production of ROS and activation of the antioxidant defence system is crucial for the human physiology and control of the cellular homeostasis [6].

Several *in vitro* and *in vivo* studies have demonstrated that ROS activation might occur in HF as a response to various stressors [7]; animal studies have also suggested that antioxidants and ROS defence pathways can ameliorate ROS-mediated cardiac abnormalities [8].

Up to date, no effective therapies for reducing morbidity or mortality in HF with preserved ejection fraction (HFpEF) are available, limiting the treatment for symptom relief and comorbidity management in such a category of patients [9, 10]. A key barrier to therapeutic development is a significant lack of knowledge about HFpEF pathogenesis and pathophysiology [11, 12]. Thus, elucidating molecular mechanisms and identifying novel therapeutic targets in the HFpEF phenotype are essential needs to improve the management of these patients [13].

A recent meta-analysis demonstrated that ET-CR is associated with improvements in cardiorespiratory fitness and quality of life of the patients with HFpEF [14]. ET, as part of CR, is effective in inducing beneficial effects at cardiac level via the reduction of the oxidant amount and stimulation of the antioxidant capacity [15, 16].

An important mechanism, involved in the cellular response to exogenous stressors, is represented by the sirtuins, NAD^+-dependent deacetylases, now recognized as oxidative stress sensors and modulators of cellular redox state [17, 18].

A supervised ET-CR program increases the activity of the best-characterized member of sirtuins, Sirt1. As a consequence, a systemic antioxidant defence in elderly HFpEF patients is stimulated by inducing the activation of Sirt1's molecular targets, such as the antioxidants superoxide dismutases (SODs) and catalase [19]. Interestingly, Nagao et al. [20] have demonstrated that myocardial βOHB has the potential to exert compensatory antioxidant effects under pathological conditions. In particular, the authors found that βOHB was elevated in failing mouse hearts, attenuated ROS production, and alleviated apoptosis induced by oxidative stress, suggesting that a build-up of βOHB might occur as a compensatory response against oxidative stress in failing hearts. Besides, ketone bodies have been proposed as agents mimicking the effects of caloric restriction which is considered a valid therapeutic approach linked to the beneficial effects of Sirt1 [21]. So far, no studies have been performed to investigate the role of an ET-CR program on βOHB levels. Therefore, the main aims of the present study were to investigate whether a supervised 4-week ET-CR program was able to induce changes in Sirt1 activity and βOHB levels and to evaluate the possible relationship between these two parameters in HFpEF patients.

2. Methods

2.1. Study Design and Population. A prospective longitudinal observational study was conducted in patients consecutively admitted to the Cardiology and Cardiac Rehabilitation Units of "San Gennaro dei Poveri" Hospital of Naples, Italy. Patients' written informed consent forms were collected; the study was approved by the local Medical Research Ethics Committee and was performed in accordance with the Declaration of Helsinki Fifth Revision (2013) and its amendments. This report adheres to the standards for the reporting of observational trials and was written according to the STROBE guidelines for Observational Studies in Epidemiology-Molecular Epidemiology (STROBE-ME) [22].

Male elderly subjects with HF in clinically stable condition, classified as in NYHA II and III class and with a preserved ejection fraction (EF) (70 with HF preserved EF), were enrolled. All definitions were based on the ESC and ACCF/AHA criteria, in which the term "stable" defines treated patients with symptoms and signs remained generally unchanged for at least a month [23, 24].

Of the study population, 50 patients underwent a well-structured ET-CR program of 4 weeks, while 20 patients represented the control group. The reasons why the control group did not undergo ET-CR program were related to individual circumstances that have made unpractical the participation in an outpatient program (e.g., patients who lived in a long-term care facility or no cardiac rehabilitation program available within 60 minutes of travel time from the patient's home).

The exclusion criteria included unstable angina pectoris, use of nitrates, uncompensated HF, complex ventricular arrhythmias, pacemaker implantation, and orthopedic or neurological limitations to exercise. No sex-based or racial/ethnic-based differences were present between the groups.

All enrolled patients underwent a physical examination, collection of demographic and routine blood chemistry tests, chest X-ray, blood pressure measurement, electrocardiographic and echocardiographic examinations, and a cardiopulmonary stress test at baseline.

After 4 weeks, both groups underwent physical examination and blood chemistry tests.

None of the patients had experienced a myocardial infarction in the 12 months preceding the study, and based on body mass index, none were cachectic (Table 1).

2.2. Training Protocol. Patients underwent a 4-week structured exercise training, on a hospital ambulatory-based regimen. At an initial stage, on a cycle ergometer, the progression of aerobic exercise training provided an intensity set at 50% VO2 max, based on the performance achieved in the cardiopulmonary stress test. The exercise duration was increased from 15 to 30 min, according to perceived symptoms and clinical status, for the first 1–2 weeks. A gradual increase of intensity (60–70% of peak VO2, if tolerated) was achieved within 2 weeks [25]. The target of 60–70% VO2 peak was

Table 1: Main characteristics of total population and ET-CR group at baseline.

Variables	Total population	Ctr	ET-CR	p
Age (years), mean ± SD	69.5 ± 4.3	70.25 ± 4.7	69.20 ± 4.1	0.357
BMI (kg/m^2), mean ± SD	27.6 ± 3.2	26.7 ± 3.3	27.9 ± 3.1	0.154
SBP (mmHg), mean ± SD	120.9 ± 11.0	119.3 ± 11.0	121.5 ± 11.0	0.443
DBP (mmHg), mean ± SD	71.7 ± 5.7	71.0 ± 5.3	72.0 ± 5.9	0.511
EF (%), mean ± SD	56.7 ± 4.0	57.9 ± 3.8	56.2 ± 4.0	0.117
LVEDD (mm)	52.27 ± 4.27	52.95 ± 4.19	52.00 ± 4.35	0.404
CAD, n (%)	14 (71.4)	14 (70)	36 (72)	0.542
PTCA, n (%)	37 (52.9)	11 (55)	26 (52)	0.516
CABG, n (%)	10 (14.3)	3 (15)	7 (14)	0.59
Previous IMA, n (%)	47 (67.1)	13 (65)	(68)	0.51
Valvular substitution, n (%)	3 (4.3)	1 (5)	2 (4)	0.642
Smoking, n (%)	37 (52.9)	9 (45)	28 (56)	0.285
Hypertension, n (%)	30 (42.9)	8 (40)	22 (44)	0.487
Dislipidemia, n (%)	31 (44.3)	9 (45)	22 (44)	0.574
Diabetes, n (%)	14 (20)	4 (20)	10 (20)	0.619
COPD, n (%)	13 (18.6)	4 (20)	9 (18)	0.545
Beta blockers	64 (91.4)	18 (90)	46 (92)	0.556
ACE inhibitors	32 (45.7)	9 (45)	23 (46)	0.576
ARBs	9 (12.9)	2 (10)	7 (14)	0.495
Diuretics	20 (28.6)	5 (25)	15 (30)	0.458
Ca2 antagonists	7 (10)	2 (10)	5 (10)	0.652
Aspirin	56 (80)	15 (75)	41 (82)	0.361
Anticoagulants	33 (47.1)	9 (45)	24 (48)	0.516
Oral hypoglycemics	11 (15.7)	4 (20)	7 (14)	0.385
Insulin	5 (7.1)	1 (5)	4 (8)	0.556
Statin	53 (75.7)	15 (75)	38 (76)	0.578

Data are expressed as the mean ± SD or number of subjects (%). BMI: body mass index; SBP: systolic blood pressure; DPB: diastolic blood pressure; EF: ejection fraction; LVEDD: left end diastolic diameter; CAD: coronary artery disease; PTCA: percutaneous transluminal coronary angioplasty; CABG: coronary artery bypass graft; COPD: chronic obstructive pulmonary disease; ARBs: angiotensin II receptor blockers.

then utilized to schedule each exercise session at the beginning of the 4-week training program. The exercise workload was gradually increased until the achievement of the predefined target. Each session was forerun by a 10 min unloaded warm-up phase and followed by a 5 min unloaded cool-down [26]. The training sessions were performed 5 times per week, under continuous electrocardiographic monitoring, and supervised by a cardiologist, a physiotherapist, and a graduate nurse.

2.3. Blood Sample Collection. Overnight fasting blood samples were obtained at baseline and after 4 weeks in both the groups. After centrifugation at $1500 \times g$ for 10 min, plasma samples were transferred to new tubes and stored at -80°C until analysis. Peripheral blood mononuclear cells (PBMCs) were isolated from whole blood by Ficoll-Paque PLUS (GE Healthcare, Munich, Germany), according to the manufacturer's procedures.

2.4. Sirt1 Activity. Sirt1 activity was determined, in nuclei extracted by PBMCs of all recruited subjects, using a SIRT1/Sir2 Deacetylase Fluorometric Assay (CycLex, Ina, Nagano, Japan) and 96 flat bottom transparent polystyrene plates (Thermo Fisher Scientific, USA), following the manufacturer's instructions. Values were reported as relative fluorescence/μg of protein (AU). All data are expressed as the mean ± SD of three independent experiments. Replicated sample analysis showed a coefficient of variation (CV) < 5%.

2.5. β-Hydroxybutyrate Plasma Levels. β-Hydroxybutyrate (βOHB) extraction, purification, and derivatization were carried by the MetaboPrep GC kit (Theoreo, Montecorvino Pugliano, Italy). According to the protocol by Troisi et al. [27], 50 μL of sample was added to 200 μL of extraction mix solution containing the internal standard. The sample and extraction mixture were vortexing at 1250 rpm for 30 seconds. The extract was centrifuged for 5 minutes at 16000 rpm, keeping the temperature below 4°C. Two hundred microliters of the upper liquid phase was removed and transferred into a microcentrifuge tube containing the purification mixture (200 μL). This was vortexed at 1250 rpm for

Table 2: Changes in some hemodynamic variables in HFpEF controls and HFpEF patients who underwent ET-CR.

Variables	Ctr		p	ET-CR		p
	Baseline	After 4 weeks		Baseline	After 4 weeks	
SBP (mmHg), mean ± SD	119.3 ± 11.0	119.75 ± 10.6	0.163	121.5 ± 11.0	120.26 ± 8.8	**0.026**
DBP (mmHg), mean ± SD	71.0 ± 5.3	71.5 ± 5.2	0.163	72.0 ± 5.9	71.8 ± 5.3	0.159
EF (%), mean ± SD	57.9 ± 3.8	57.6 ± 3.5	0.110	56.2 ± 4.0	57.22 ± 3.19	**0.001**
LVEDD (mm)	52.95 ± 4.19	53.15 ± 4.23	0.428	52.0 ± 4.35	51.86 ± 3.96	0.442

SBP: systolic blood pressure; DPB: diastolic blood pressure; EF: ejection fraction; LVEDD: left end diastolic diameter.

30 seconds. A rapid centrifuge of the sample (to prevent the sediment suspension) at 16000 rpm was performed keeping the temperature below 4°C. One hundred seventy-five microliters of liquid upper phase was transferred into the glass vial and freeze-dried overnight.

After the derivatization, the extract was transferred in a 100 μL insert for the autosampler injection. This was centrifuged for 5 minutes at 16000 rpm keeping the temperature below 4°C before injecting. The sample (2 μL) was analyzed using a gas chromatography-mass spectrometry (GC-MS) system (GC-2010 Plus gas chromatography coupled to a 2010 Plus single quadrupole mass spectrometer; Shimadzu Corp., Kyoto, Japan). Chromatographic separation was achieved with a 30 m 0.25 mm CP-Sil 8 CB fused silica capillary GC column with 1.00 μm film thickness from Agilent (Agilent, J&W), with helium as the carrier gas.

βOHB was evaluated quantitatively by the use of external calibration. The analytical standard was purchased from Sigma-Aldrich (Milan, Italy). Five calibration standards were prepared, freeze-dried overnight to eliminate the solvent, and derivatized with the same procedure of the samples. GC-MS βOHB calibration curve showed an $R^2 = 0.997$, while replicated samples analysis showed a coefficient of variation (CV) < 10% and the analytical standard was analyzed in triplicate.

2.6. Oxidative Stress Markers. Total antioxidant capacity (Trolox Equivalent Antioxidant Capacity (TEAC)) and Oxidized Low-Density Lipoproteins (Ox-LDL) were measured in plasma samples isolated from the patients who underwent the ET-CR and the controls. The TEAC assay was performed according to the protocol already described in the authors' previous study [28].

The levels of Ox-LDL were determined, by using a human Ox-LDL ELISA Kit (MyBiosource, Inc., USA) and 96 flat bottom transparent polystyrene plates (Thermo Fisher Scientific, USA), following the manufacturer's instructions.

2.7. NAD^+/NADH Ratio. NAD^+/NADH ratio was quantified using the EnzyCromTM NAD^+/NADH Assay Kit with a detection limit of 0.05 microM and linearity up to 10 microM (BioAssay Systems, Hayward, CA) and 96 flat bottom transparent polystyrene plates (Thermo Fisher Scientific, USA), following the manufacturer's instructions. The optical density was read at 565 nm at time zero (OD0) and, after incubation (15 min), at room temperature (OD15). OD values were used to determine the NAD^+/NADH concentration of each sample from a standard curve. All data are expressed as the mean ± SD of three independent experiments.

2.8. Statistical Analysis. Continuous variables are expressed as the mean ± standard deviation compared with paired or unpaired Student's t-test (normally distributed variables), or as median ± interquartile range value compared with the Mann-Whitney U test (not normally distributed). Normality of data distribution was evaluated using the Kolmogorov-Smirnov test. Nonnormally distributed continuous variables were converted to their natural log functions. Categorical variables are expressed as a proportion and compared with the χ^2 test.

Correlation between variables were assessed by linear regression analysis, and variables, which demonstrated statistical significance in a univariate model, were then included in a multivariate analysis. All data were analyzed using SPSS version 23.0 (SPSS, Inc., Chicago, Illinois, USA). Statistical significance was accepted at $p < 0.05$.

3. Results

The study population consisted of 70 male subjects (mean age 69.5 ± 4.27 years) affected by HFpEF. All patients completed the study. At baseline, no differences in medical therapy were found between the groups, and no therapeutic changes occurred during the study period (Table 1).

Table 1 shows the main demographic, hemodynamic, and chemical characteristics of the group who underwent a 4-week ET-CR program and the control group. Changes in some hemodynamic variables after 4 weeks are reported in Table 2. The ET-CR was able to induce a significant reduction in systolic blood pressure and an increase in ejection fraction. No changes were observed in the controls (Table 2).

Table 3 and Figure 1 show the changes in Sirt1 activity, βOHB, and oxidant and antioxidant parameters, at baseline and after 4 weeks. No differences were found between the groups at baseline, while significant differences were found between groups and intragroup (see above). The ET-CR induced a significant increase in Sirt1 activity, βOHB, and antioxidant capacity measured by TEAC assay, as shown by the raised levels of such parameters in the ET-CR group but not in the controls (Table 3 and Figures 1(a), 1(b), and 1(d)) and decreased levels of Ox-LDL in the ET-CR group but not in the controls (Figure 1(c)).

Moreover, the ET-CR was effective in inducing a significant increase in NAD^+ and NAD^+/NADH ratio and a

Table 3: Changes in oxidant/antioxidant parameters in HFpEF controls and HFpEF patients who underwent ET-CR.

Variables	Ctr		p	ET-CR		p
	Baseline	After 4 weeks		Baseline	After 4 weeks	
SIRT1 activity (AU)	1941.80 ± 149.35	1942.16 ± 149.67	0.560	1953.14 ± 125.06	2082.44 ± 108.68*	<0.0001
βOHB (μmol/L)	47.96 ± 4.84	49.35 ± 5.21	0.280	48.76 ± 3.27	61.58 ± 6.91*	<0.0001
Ox-LDL (pg/mL)	3227.62 ± 281.13	3255.33 ± 388.57	0.492	3286.49 ± 527.08	2380.47 ± 608.30*	<0.0001
TEAC (mmol Trolox Equiv/L)	0.295 ± 0.084	0.286 ± 0.722	0.075	0.290 ± 0.723	0.425 ± 0.061*	<0.0001
NAD^+	19.74 ± 2.03	18.41 ± 2.49	0.136	19.50 ± 1.48	21.64 ± 1.27*	<0.0001
NADH	12.26 ± 1.43	13.25 ± 1.67	0.090	12.16 ± 0.97	11.15 ± 1.09*	<0.001
NAD^+/NADH	1.64 ± 0.32	1.44 ± 0.40	0.115	1.62 ± 0.24	1.96 ± 0.28*	<0.0001

ET-CR: exercise training-based cardiac rehabilitation; βOHB: β-hydroxybutyrate; Ox-LDL: Oxidized Low-Density Lipoprotein. *CR vs. Ctr after 4 weeks, $p < 0.0001$.

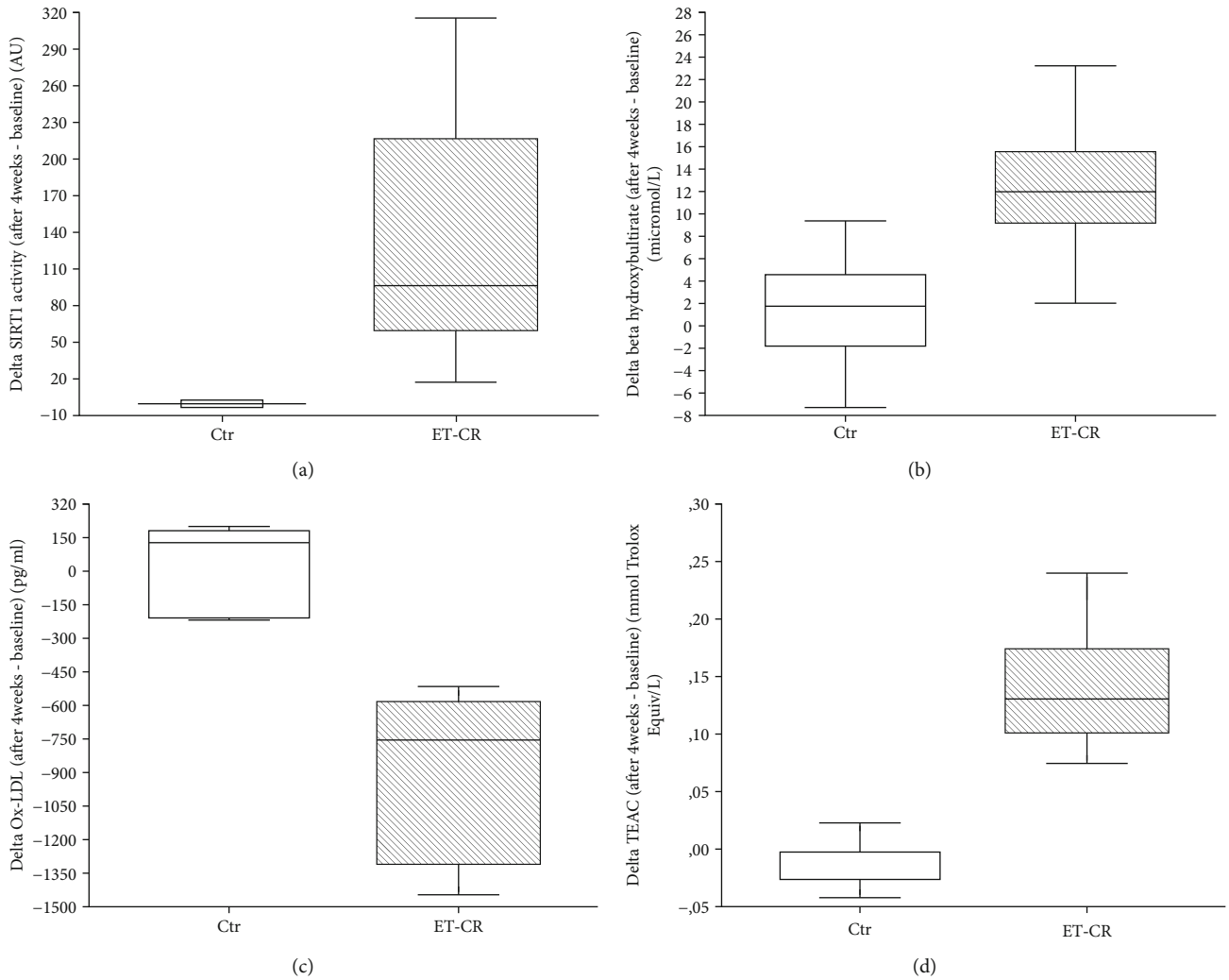

Figure 1: Changes in control and ET-CR groups of Sirt1 activity, β-hydroxybutyrate, Ox-LDL levels, and TEAC from baseline to 4 weeks after the study start. The ET-CR was able to induce a significant increase in Sirt1 activity (a) and β-hydroxybutyrate (βOHB) (b) (both, $p < 0.0001$); a reduction in Ox-LDL (c) ($p < 0.001$) and increased levels of antioxidant response measured by TEAC assay (d) ($p < 0.0001$), as showed by the difference between the levels after 4 weeks minus the levels at baseline.

decrease in NADH (all $p < 0.0001$, Table 3 and Figures 2(a), 2(c), and 2(d)), while no changes were found in the controls.

All these findings were confirmed when all the parameters were expressed as differences between levels after 4 weeks minus baseline levels (delta, Figures 1–3). Notably, the

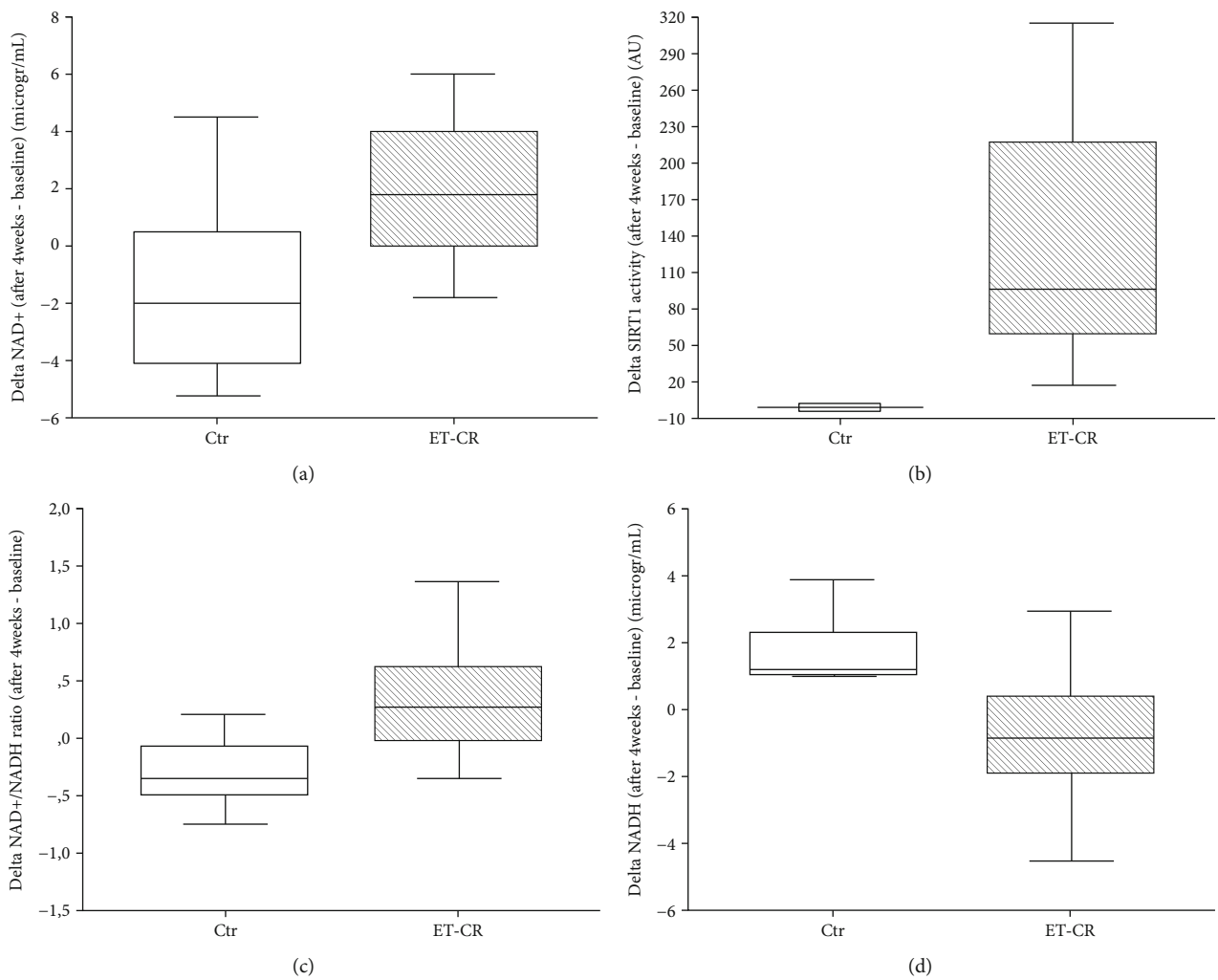

Figure 2: Changes in the control and ET-CR groups of Sirt1 activity, NAD^+, NADH levels, and NAD^+/NADH ratio from baseline to 4 weeks after the study start. The ET-CR was able to induce a significant increase in NAD^+ (a), Sirt1 activity (b), and NAD^+/NADH ratio (c) (all $p < 0.0001$), associated with a reduction in NADH levels (d) ($p < 0.001$), expressed as the difference between the levels after 4 weeks minus the levels at baseline.

increasing delta levels of NAD^+ and NAD^+/NADH ratio were associated with increasing levels of delta Sirt1 activity (Figures 2(a)–2(c)), as expected by the requirement of NAD^+ for Sirt1 activity.

By a multivariate linear regression analysis, introducing the delta TEAC as a dependent variable, we found that the best predictors of the changes in antioxidant levels were represented by the delta Sirt1 activity ($p < 0.0001$, $r^2 = 0.845$; $\beta = 0.000$; 95% CI 0.000–0.001; Figure 3(a)) and the ET-CR group ($p < 0.0001$, $\beta = 0.061$; 95% CI 0.045–0.076) followed by the delta βOHB levels ($p = 0.032$, $r^2 = 0.840$; $\beta = 0.002$; 95% CI 0.000–0.004; Figure 3(b)). Moreover, introducing the delta Ox-LDL as dependent variable, we found that the best predictors of the oxidant levels changes were represented by the delta Sirt1 activity ($p < 0.0001$, $r^2 = 0.812$; $\beta = -5.639$; 95% CI -6.839 to -4.438; Figure 3(c)) and the ET-CR group ($p < 0.0001$, $\beta = -510.5$; 95% CI -614.3 to -406.7). In particular, higher changes in TEAC and Ox-LDL were associated with higher changes in SIRT1 activity in a direct ($r^2 = 0.845$, Figure 3(a)) and inverse relationship ($r^2 = 0.812$, Figure 3(c)), respectively.

Finally, introducing in a multivariate linear regression analysis the delta NAD^+ as a dependent variable, we found that the best predictors were the delta Sirt1 activity ($p < 0.0001$, $r^2 = 0.915$; $\beta = 0.051$; 95% CI 0.037–0.065; Figure 3(d)), followed by the ET-CR group ($p = 0.004$, $\beta = 2.71$; 95% CI 0.920–4.494).

A strong direct association was found between the delta Sirt1 activity and the delta of NAD^+ levels ($r^2 = 0.915$, Figure 3(d)) and between the delta of βOHB levels and the delta of Sirt1 activity ($r^2 = 0.901$, Figure 3(e)).

4. Discussion

In the present study, we have demonstrated that a well-structured 4-week ET-CR program was able to increase the levels of Sirt1 activity and β-hydroxybutyrate, and these

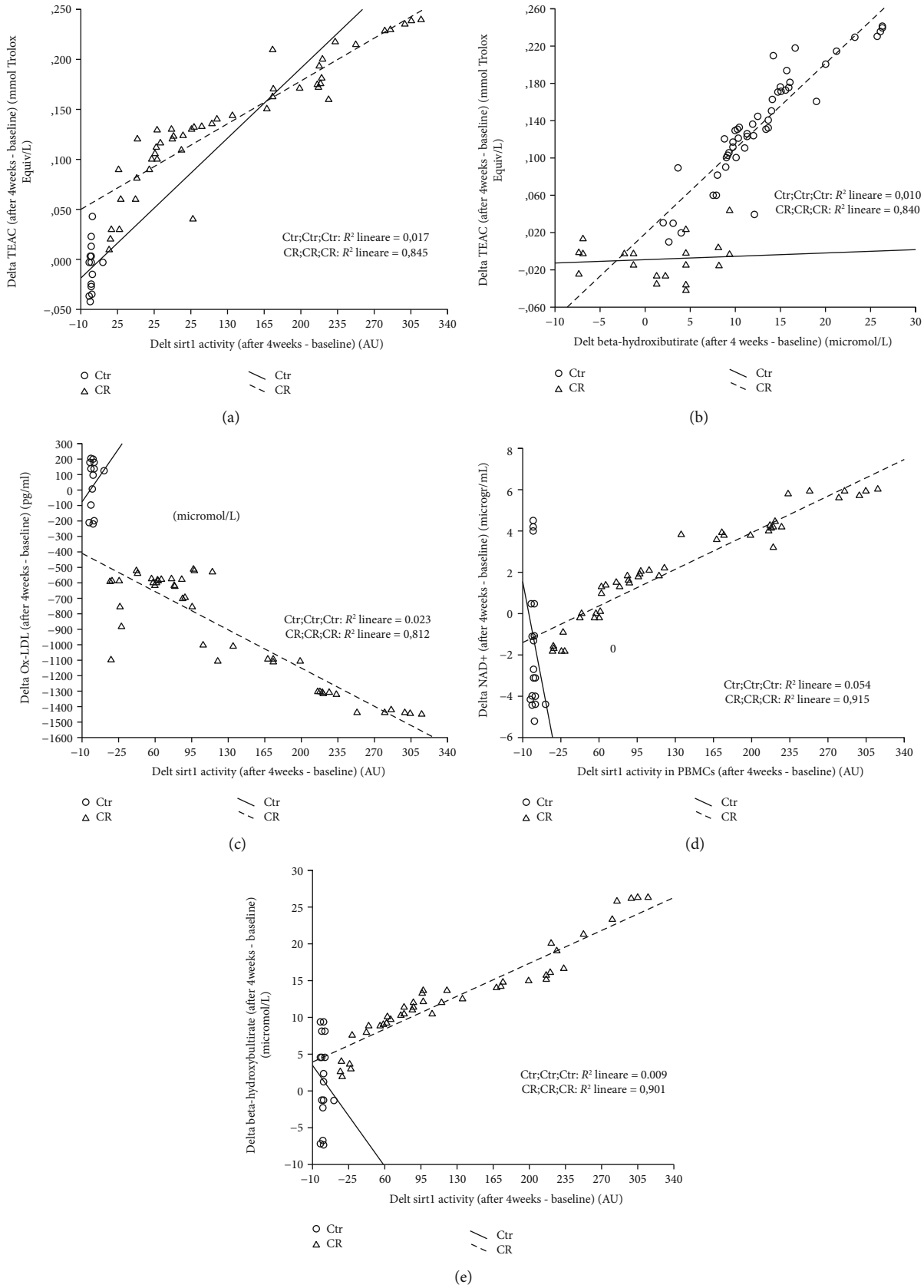

Figure 3: Linear regression correlation among delta Sirt1 activity and delta oxidants and antioxidants. (a) Linear regression correlation between TEAC and delta Sirt1 activity. (b) Linear regression correlation between delta TEAC and delta βOHB levels. (c) Linear regression correlation between delta Ox-LDL and delta Sirt1 activity. (d) Linear regression correlation between delta NAD+ and delta Sirt1 activity. (e) Linear regression correlation between delta βOHB levels and delta Sirt1 activity.

findings were associated with an improvement of TEAC and a reduction of Ox-LDL.

To treat and especially manage the patients with HFpEF can be very challenging. This is mostly caused by a significant lack of knowledge in this field. For this reason, there is now high interest to elucidate the pathophysiology of the different HF phenotypes.

From a molecular point of view, the ET-CR might represent not only a valuable complementary therapeutic approach but also a study model to expose the molecular actors involved in HFpEF.

Previously, we demonstrated that Sirt1 was able to mediate the ET-CR effects at a molecular level inducing activation of its target catalase [19].

Several studies have demonstrated that both Sirt1 and βOHB are involved in the antioxidant cellular response. In particular, increased circulating levels of βOHB were linked to a reduction in oxidative stress [29], increased AMPK activity [30], and autophagy [31].

Moreover, βOHB was found to be an endogenous inhibitor of class I and IIa histone deacetylases (HDACs) [32] but not of the sirtuins (class III HDACs) representing a structurally distinct group of NAD-dependent deacetylases, in which βOHB is not known to directly regulate [33].

βOHB seems to work as a mimetic of caloric restriction that is the most known natural activator of some sirtuins [21]. Edwards et al. [34] have demonstrated that a βOHB administration in *C. elegans* delayed glucose toxicity and extended the worm's lifespan in a Sir2- (the homolog of the human Sirt1) dependent manner. Therefore, these authors have proposed βOHB as a valuable treatment against aging-associated disorders [34].

Similar to the caloric restriction, the exercise training (ET) is recognized as a helpful tool against cardiovascular diseases. Indeed, ET is widely recommended in HF for its beneficial effects on the exercise tolerance [35].

Noteworthy, both caloric restriction and ET are associated with a significant increase of ketone bodies, such as βOHB [36–38].

Although the metabolic profiles differ in dependence on the timing and duration of physical activity, both short-term and long-term studies have sought to characterize the biochemical response to exercise [36]. Interestingly, Matoulek et al. showed that βOHB increased after exercise in patients who underwent a three-month fitness program [39].

Moreover, an acute bout of aerobic exercise increases class IIa HDAC phosphorylation and subsequent nuclear exclusion, thus inhibiting HDAC-mediated repression of specific exercise-responsive genes such as GLUT4 and PGC-1α [40, 41]. This suggests that compounds such as βOHB could be used to mimic or enhance adaptations to a physical exercise [36].

In our study, an ET-CR program was able to induce, in patients affected by HFpEF, an increase of both Sirt1 and βOHB, in association to a better antioxidant activity, as showed by higher levels of TEAC and NAD^+.

Notably, it has been proposed that the relative sparing of cytoplasmic NAD levels with the utilization of βOHB, rather than glucose, can alter the activity of NAD-dependent enzymes such as sirtuins [42]. Recent studies observed an increase in the mitochondrial β-hydroxybutyrate dehydrogenase (BDH1), which coincided with elevated plasma levels of βOHB in both rodent and human models of heart failure [43, 44]. Increased amount of βOHB oxidation in isolated perfused hearts was also found [43]. These studies suggested that the increase of ketone body metabolism could represent an additional strategy leading to a metabolic remodeling in the failing heart. However, whether this is an adaptive or maladaptive response remains uncertain [45]. In this context, to better characterize the ET-CR effects from the metabolic point of view can represent an important step to improve the HFpEF management.

4.1. Limitations. A possible limitation of this study is the lack of cell sorting useful to identify what cells compose the PBMCs that could be mainly involved in the observed molecular modifications. However, Sirt1 is a ubiquitous molecule and several studies have shown changes in Sirt1 activity in PBMCs without a distinction of the PBMC cell types [28, 46].

Another limitation could be the lack of women in the study population. We did recruit only three women and then decided to exclude them because of the small number. This is in line with the fact that women are less inclined to take part in exercise training-based cardiac rehabilitation programs [47, 48]. Therefore, further studies are necessary to better clarify the molecular effects of ET-CR also in female patients.

5. Conclusions

The ability of exercise training to regulate metabolic and oxidative stress response can explain why ET-CR can be considered a sort of pharmacological tool in CVD management. In particular, ET-CR is a helpful medical practice in which several molecular factors mutually influence each other. The exercise training included in CR programs acts as a nonpharmacological inductor of antioxidant response. The HFpEF represents a peculiar phenotype of HF whose pathophysiological aspects have yet to be clarified.

Further studies should be addressed to evaluate the role of ET-CR in influencing the evolution of HFpEF considering the molecular changes induced by this tool to better clarify the mechanism and the pathway involved in the genesis and progression of the disease.

Data Availability

The data used to support the findings of this study are available from the corresponding author upon request.

Conflicts of Interest

The authors have no conflicts of interest to report.

Authors' Contributions

All authors read and met the Oxidative Medicine and Cellular Longevity criteria for authorship. Valeria Conti, Graziamaria Corbi, and Amelia Filippelli conceived and designed the experiments. Jacopo Troisi, Angelo Colucci, Valentina

Manzo, and Albino Carrizzo performed the experiments. Carmine Vecchione, Maria Consiglia Calabrese, and Paola Di Pietro contributed with acquisition of clinical data and human samples. Graziamaria Corbi and Valeria Conti performed the analysis and interpretation of the data and wrote the first draft of the paper. Nicola Ferrara and Amelia Filippelli critically revised the paper. All authors read and approved the final paper. Graziamaria Corbi and Valeria Conti contributed equally to this work.

Acknowledgments

We thank Jan Festa who revised and edited the English language of the manuscript. This work was supported by the Department of Medicine and Health Sciences of the University of Molise (R-DIPA_20112013300118CORBI-GR to G.C.) and the Department of Medicine, Surgery and Dentistry of the University of Salerno (ORSA153180).

References

[1] D. Mozaffarian, E. J. Benjamin, A. S. Go et al., "Heart disease and stroke statistics—2016 Update," *Circulation*, vol. 133, no. 4, pp. e38–e360, 2016.

[2] M. A. H. Witman, J. McDaniel, A. S. Fjeldstad et al., "A differing role of oxidative stress in the regulation of central and peripheral hemodynamics during exercise in heart failure," *American Journal of Physiology-Heart and Circulatory Physiology*, vol. 303, pp. H1237–H1244, 2012.

[3] T. Ide, H. Tsutsui, S. Kinugawa et al., "Direct evidence for increased hydroxyl radicals originating from superoxide in the failing myocardium," *Circulation Research*, vol. 86, no. 2, pp. 152–157, 2000.

[4] G. Corbi, V. Conti, K. Komici et al., "Phenolic plant extracts induce Sirt1 activity and increase antioxidant levels in the rabbit's heart and liver," *Oxidative Medicine and Cellular Longevity*, vol. 2018, Article ID 2731289, 10 pages, 2018.

[5] N. Anilkumar, A. Sirker, and A. M. Shah, "Redox sensitive signaling pathways in cardiac remodeling, hypertrophy and failure," *Frontiers in Bioscience*, no. 14, pp. 3168–3187, 2009.

[6] V. Conti, G. Corbi, V. Simeon et al., "Aging-related changes in oxidative stress response of human endothelial cells," *Aging Clinical and Experimental Research*, vol. 27, no. 4, pp. 547–553, 2015.

[7] D. B. Sawyer, "Oxidative stress in heart failure: what are we missing?," *The American Journal of the Medical Sciences*, vol. 342, no. 2, pp. 120–124, 2011.

[8] F. J. Giordano, "Oxygen, oxidative stress, hypoxia, and heart failure," *The Journal of Clinical Investigation*, vol. 115, no. 3, pp. 500–508, 2005.

[9] C. W. Yancy, M. Jessup, B. Bozkurt et al., "2017 ACC/AHA/HFSA Focused Update of the 2013 ACCF/AHA Guideline for the Management of Heart Failure: a report of the American College of Cardiology/American Heart Association Task Force on Clinical Practice Guidelines and the Heart Failure Society of America," *Journal of Cardiac Failure*, vol. 23, no. 8, pp. 628–651, 2017.

[10] G. Corbi, G. Gambassi, G. Pagano et al., "Impact of an innovative educational strategy on medication appropriate use and length of stay in elderly patients," *Medicine*, vol. 94, no. 24, p. e918, 2015.

[11] D. W. Kitzman, B. Upadhya, and S. Vasu, "What the dead can teach the living: systemic nature of heart failure with preserved ejection fraction," *Circulation*, vol. 131, no. 6, pp. 522–524, 2015.

[12] K. Sharma and D. A. Kass, "Heart failure with preserved ejection fraction: mechanisms, clinical features, and therapies," *Circulation Research*, vol. 115, no. 1, pp. 79–96, 2014.

[13] W. G. Hunter, J. P. Kelly, R. W. McGarrah III et al., "Metabolomic profiling identifies novel circulating biomarkers of mitochondrial dysfunction differentially elevated in heart failure with preserved versus reduced ejection fraction: evidence for shared metabolic impairments in clinical heart failure," *Journal of the American Heart Association*, vol. 5, no. 8, 2016.

[14] A. Pandey, A. Parashar, D. J. Kumbhani et al., "Exercise training in patients with heart failure and preserved ejection fraction: meta-analysis of randomized control trials," *Circulation: Heart Failure*, vol. 8, no. 1, pp. 33–40, 2015.

[15] G. Corbi, V. Conti, G. Russomanno et al., "Is physical activity able to modify oxidative damage in cardiovascular aging?," *Oxidative Medicine and Cellular Longevity*, vol. 2012, Article ID 728547, 6 pages, 2012.

[16] P. Meyer, M. Gayda, M. Juneau, and A. Nigam, "High-intensity aerobic interval exercise in chronic heart failure," *Current Heart Failure Reports*, vol. 10, no. 2, pp. 130–138, 2013.

[17] V. Conti, M. Forte, G. Corbi et al., "Sirtuins: possible clinical implications in cardio and cerebrovascular diseases," *Current Drug Targets*, vol. 18, no. 4, pp. 473–484, 2017.

[18] C.-H. Peng, Y.-L. Chang, C.-L. Kao et al., "SirT1—a sensor for monitoring self-renewal and aging process in retinal stem cells," *Sensors*, vol. 10, no. 6, pp. 6172–6194, 2010.

[19] G. Russomanno, G. Corbi, V. Manzo et al., "The anti-ageing molecule sirt1 mediates beneficial effects of cardiac rehabilitation," *Immunity & Ageing*, vol. 14, p. 7, 2017.

[20] M. Nagao, R. Toh, Y. Irino et al., "β-Hydroxybutyrate elevation as a compensatory response against oxidative stress in cardiomyocytes," *Biochemical and Biophysical Research Communications*, vol. 475, no. 4, pp. 322–328, 2016.

[21] R. L. Veech, P. C. Bradshaw, K. Clarke, W. Curtis, R. Pawlosky, and M. T. King, "Ketone bodies mimic the life span extending properties of caloric restriction," *IUBMB Life*, vol. 69, no. 5, pp. 305–314, 2017.

[22] V. Gallo, M. Egger, V. McCormack et al., "Strengthening the reporting of observational studies in Epidemiology – Molecular Epidemiology (STROBE-ME): an extension of the STROBE statement," *PLoS Medicine*, vol. 8, no. 10, article e1001117, 2011.

[23] J. J. V. McMurray, S. Adamopoulos, S. D. Anker et al., "ESC guidelines for the diagnosis and treatment of acute and chronic heart failure 2012: the Task Force for the Diagnosis and Treatment of Acute and Chronic Heart Failure 2012 of the European Society of Cardiology. Developed in collaboration with the Heart Failure Association (HFA) of the ESC," *European Heart Journal*, vol. 33, no. 14, pp. 1787–1847, 2012.

[24] C. W. Yancy, M. Jessup, B. Bozkurt et al., "2013 ACCF/AHA guideline for the management of heart failure: Executive Summary," *Circulation*, vol. 128, no. 16, pp. 1810–1852, 2013.

[25] M. F. Piepoli, U. Corrà, W. Benzer et al., "Secondary prevention through cardiac rehabilitation: from knowledge to implementation. A position paper from the Cardiac Rehabilitation Section of the European Association of Cardiovascular Prevention and Rehabilitation," *European Journal of*

Cardiovascular Prevention and Rehabilitation, vol. 17, no. 1, pp. 1–17, 2010.

[26] K. Wasserman, J. E. Hansen, D. Y. Sue, W. W. Stringer, and B. J. Whipp, *Principles of Exercise Testing and Interpretation*, Lippincott Williams & Wilkins, Philadelphia, 5th edition, 2012.

[27] J. Troisi, L. Sarno, A. Landolfi et al., "Metabolomic signature of endometrial cancer," *Journal of Proteome Research*, vol. 17, no. 2, pp. 804–812, 2018.

[28] V. Conti, G. Corbi, V. Manzo et al., "SIRT1 activity in peripheral blood mononuclear cells correlates with altered lung function in patients with chronic obstructive pulmonary disease," *Oxidative Medicine and Cellular Longevity*, vol. 2018, Article ID 9391261, 8 pages, 2018.

[29] T. Shimazu, M. D. Hirschey, J. Newman et al., "Suppression of oxidative stress by β-hydroxybutyrate, an endogenous histone deacetylase inhibitor," *Science*, vol. 339, no. 6116, pp. 211–214, 2013.

[30] T. Laeger, R. Pöhland, C. C. Metges, and B. Kuhla, "The ketone body β-hydroxybutyric acid influences agouti-related peptide expression via AMP-activated protein kinase in hypothalamic GT1-7 cells," *The Journal of Endocrinology*, vol. 213, no. 2, pp. 193–203, 2012.

[31] P. F. Finn and J. F. Dice, "Ketone bodies stimulate chaperone-mediated autophagy," *Journal of Biological Chemistry*, vol. 280, no. 27, pp. 25864–25870, 2005.

[32] I. V. Gregoretti, Y. M. Lee, and H. V. Goodson, "Molecular evolution of the histone deacetylase family: functional implications of phylogenetic analysis," *Journal of Molecular Biology*, vol. 338, no. 1, pp. 17–31, 2004.

[33] X. J. Yang and E. Seto, "The Rpd3/Hda1 family of lysine deacetylases: from bacteria and yeast to mice and men," *Nature Reviews Molecular Cell Biology*, vol. 9, no. 3, pp. 206–218, 2008.

[34] C. Edwards, J. Canfield, N. Copes, M. Rehan, D. Lipps, and P. C. Bradshaw, "D-beta-hydroxybutyrate extends lifespan in C. *elegans*," *Aging*, vol. 6, no. 8, pp. 621–644, 2014.

[35] F. Edelmann, G. Gelbrich, H. D. Düngen et al., "Exercise training improves exercise capacity and diastolic function in patients with heart failure with preserved ejection fraction: results of the Ex-DHF (Exercise training in Diastolic Heart Failure) pilot study," *Journal of the American College of Cardiology*, vol. 58, no. 17, pp. 1780–1791, 2011.

[36] M. Evans, K. E. Cogan, and B. Egan, "Metabolism of ketone bodies during exercise and training: physiological basis for exogenous supplementation," *The Journal of Physiology*, vol. 595, no. 9, pp. 2857–2871, 2017.

[37] J. C. Newman and E. Verdin, "β-Hydroxybutyrate: a signaling metabolite," *Annual Review of Nutrition*, vol. 37, no. 1, pp. 51–76, 2017.

[38] E. F. Sutton, R. Beyl, K. S. Early, W. T. Cefalu, E. Ravussin, and C. M. Peterson, "Early time-restricted feeding improves insulin sensitivity, blood pressure, and oxidative stress even without weight loss in men with prediabetes," *Cell Metabolism*, vol. 27, no. 6, pp. 1212–1221.e3, 2018.

[39] M. Matoulek, S. Svobodova, R. Vetrovska, Z. Stranska, and S. Svacina, "Post-exercise changes of beta hydroxybutyrate as a predictor of weight changes," *Physiological Research*, vol. 63, Supplement 2, pp. S321–S325, 2014.

[40] S. L. McGee, E. Fairlie, A. P. Garnham, and M. Hargreaves, "Exercise-induced histone modifications in human skeletal muscle," *The Journal of Physiology*, vol. 587, Part 24, pp. 5951–5958, 2009.

[41] B. Egan, B. P. Carson, P. M. Garcia-Roves et al., "Exercise intensity-dependent regulation of peroxisome proliferator-activated receptor coactivator-1 mRNA abundance is associated with differential activation of upstream signalling kinases in human skeletal muscle," *The Journal of Physiology*, vol. 588, no. 10, pp. 1779–1790, 2010.

[42] J. C. Newman and E. Verdin, "β-hydroxybutyrate: much more than a metabolite," *Diabetes Research and Clinical Practice*, vol. 106, no. 2, pp. 173–181, 2014.

[43] G. Aubert, O. J. Martin, J. L. Horton et al., "The failing heart relies on ketone bodies as a fuel," *Circulation*, vol. 133, no. 8, pp. 698–705, 2016.

[44] K. C. Bedi Jr., N. W. Snyder, J. Brandimarto et al., "Evidence for intramyocardial disruption of lipid metabolism and increased myocardial ketone utilization in advanced human heart failure," *Circulation*, vol. 133, no. 8, pp. 706–716, 2016.

[45] S. C. Kolwicz Jr., S. Airhart, and R. Tian, "Ketones step to the plate: a game changer for metabolic remodeling in heart failure?," *Circulation*, vol. 133, no. 8, pp. 689–691, 2016.

[46] D. Wendling, W. Abbas, M. Godfrin-Valnet et al., "Dysregulated serum IL-23 and SIRT1 activity in peripheral blood mononuclear cells of patients with rheumatoid arthritis," *PLoS One*, vol. 10, no. 3, article e0119981, 2015.

[47] P. O'Farrell, J. Murray, P. Huston, C. LeGrand, and K. Adamo, "Sex differences in cardiac rehabilitation," *The Canadian Journal of Cardiology*, vol. 16, no. 3, pp. 319–325, 2000.

[48] S. L. Grace, C. Racco, C. Chessex, T. Rivera, and P. Oh, "A narrative review on women and cardiac rehabilitation: program adherence and preferences for alternative models of care," *Maturitas*, vol. 67, no. 3, pp. 203–208, 2010.

Hindawi
Oxidative Medicine and Cellular Longevity
Volume 2019, Article ID 1616239, 13 pages
https://doi.org/10.1155/2019/1616239

Research Article

β-Lactoglobulin Heptapeptide Reduces Oxidative Stress in Intestinal Epithelial Cells and Angiotensin II-Induced Vasoconstriction on Mouse Mesenteric Arteries by Induction of Nuclear Factor Erythroid 2-Related Factor 2 (Nrf2) Translocation

Giacomo Pepe,[1] Manuela Giovanna Basilicata,[1,2] Albino Carrizzo,[3] Simona Adesso,[1] Carmine Ostacolo,[4] Marina Sala,[1] Eduardo Sommella,[1] Marco Ruocco,[1] Stella Cascioferro,[5] Mariateresa Ambrosio,[3] Simona Pisanti,[6] Veronica Di Sarno,[1] Alessia Bertamino,[1] Stefania Marzocco,[1] Carmine Vecchione,[3,6] and Pietro Campiglia[1,7]

[1]*Department of Pharmacy, University of Salerno, Fisciano, Italy*
[2]*PhD Program in Drug Discovery and Development, University of Salerno, Fisciano, Italy*
[3]*IRCCS Neuromed, Loc. Camerelle, Pozzilli, Italy*
[4]*Department of Pharmacy, University of Naples Federico II, NA, Italy*
[5]*Dipartimento di Scienze e Tecnologie Biologiche, Chimiche e Farmaceutiche (STEBICEF), University of Palermo, PA, Italy*
[6]*Department of Medicine and Surgery, University of Salerno, Baronissi, Italy*
[7]*European Biomedical Research Institute of Salerno, SA, Italy*

Correspondence should be addressed to Pietro Campiglia; pcampigl@unisa.it

Received 5 December 2018; Revised 18 March 2019; Accepted 8 October 2019; Published 12 November 2019

Academic Editor: Maria U. Moreno

Peptides derived from buffalo dairy products possess multiple healthy properties that cannot be exerted as long as they are encrypted in parent proteins. To evaluate the biological activities of encrypted peptide sequences from buffalo ricotta cheese, we performed a simulated gastrointestinal (GI) digestion. Chemical and pharmacological characterization of the digest led to the identification of a novel peptide endowed with antioxidant and antihypertensive action. The GI digest was fractionated by Semiprep-HPLC, and fractions were tested against reactive oxygen species (ROS) release in an H_2O_2-treated intestinal epithelial cell line. UHPLC-PDA-MS/MS analysis revealed the presence of an abundant β-lactoglobulin peptide (BRP2) in the most active fraction. Pharmacological characterization of BRP2 highlighted its antioxidant activity, involving ROS reduction, nuclear factor erythroid 2-related factor 2 (Nrf2) activation, and cytoprotective enzyme expression. The bioavailability of BRP2 was evaluated in intestinal transport studies through a Caco-2 cell monolayer. Equal bidirectional transport and linear permeability indicate that BRP2 was absorbed mainly through passive diffusion. In addition to its local effects, the BRP2 administration on mouse mesenteric arteries was able to reduce the angiotensin II-induced vasoconstriction by the Nrf2 nuclear translocation, the reduction of the active form of Ras-related C3 botulinum toxin substrate 1 (Rac1), and the NADPH oxidase activity. These data further highlight the role of buffalo ricotta cheese-derived peptides against oxidative stress-related diseases and suggest their health-promoting potential.

1. Introduction

Food proteins are an important source of bioactive peptides. These are inactive, since encrypted in their parent sequences, but turn active when released by fermentation or ripening during food processing or by digestive enzymes during gastrointestinal transit [1, 2]. Once released, the bioactive peptides are able to exert various physiological effects

beneficial for human health [3]. In particular, bioactive peptides can either have local effects on the digestive tract or be absorbed through the intestine, playing a physiological role in tissues [4]. These peptides can exhibit various biological activities, such as antioxidant, antimicrobial, immunomodulatory, antithrombotic, and antihypertensive, depending on their amino acid sequence [5]. The size of active sequences may vary from two to twenty amino acid residues, and several peptides are known to reveal multifunctional properties since some regions in the primary structure of parent protein, considered "strategic zones," contain overlapping sequences [6].

The effect of natural antioxidant peptides on health by treatment and prevention of numerous diseases is of great interest nowadays due to their safety, small size, low toxicity, and high activity in addition to the negative consumer perception about synthetic drugs [7]. This is why food-derived antioxidant peptides have become an interesting target in food chemistry. Enhancement of the body's antioxidant defense mechanism through dietary supplementation would seem to be a practical approach to reduce the level of reactive oxygen species (ROS) [8–10].

ROS are produced in a well-regulated manner to help maintain homeostasis at the cellular level in the normal healthy tissues, play an important role as second messengers, and regulate cellular function by modulating signaling pathways [11]. An imbalance in the equilibration of prooxidant/antioxidant status determines oxidative stress, characterized by damage to cellular macromolecules such as DNA, proteins, and membrane lipids, by human aging, and by diseases, such as gastrointestinal (GI) and cardiovascular pathologies [12].

The GI tract is prone to ROS attack as it is accessed by the outside environment with dietary factors that, together with resident immune cells and intestinal flora, are potential sources of ROS.

ROS have been linked with various inflammatory GI disorders such gastroesophageal reflux disease, gastritis, enteritis, colitis, and associated cancers as well as pancreatitis and liver cirrhosis [13]. Several studies demonstrate that oxidative stress also plays an important role in the pathogenesis and development of cardiovascular diseases, including hypertension, dyslipidemia, diabetes mellitus, atherosclerosis, myocardial infraction, angina pectoris, and heart failure [14]. In fact, oxidative stress is considered to be the main cause of endothelial dysfunction leading to cardiovascular complications, mostly through the reduction of nitric oxide (NO) bioavailability, which is one of the most important mediators of the physiological properties of endothelial cells. The increased production of ROS and decreased NO bioavailability promote endothelial dysfunction, leading to remodeling, platelet aggregation, loss of vasodilation, inflammation, and smooth muscle cell growth [15]. An imbalance between NO and ROS has been observed in patients with hypertension [16].

In order to prevent and counteract some GI pathologies and cardiovascular diseases, the employment of natural antioxidant molecules is crucial. Dairy products and their fractions can be considered carriers for the delivery of antioxidant peptides. We recently evidenced the antioxidant properties of buffalo milk dairy products and in particular buffalo ricotta cheese [17, 18].

In addition, several studies showed the antihypertensive effect of whey protein as renin-angiotensin-converting enzyme inhibitors, direct stimulators of endothelial NO, opioid receptor agonists, or direct inhibitors of endothelin-1 production, but no studies were described concerning the hypotensive activity of buffalo whey protein-derived peptides [19–22].

In this regard, the aim of the present work was to investigate the release, the intestinal absorption, and the biological activities of potential antioxidant peptides after simulated oral intake of buffalo ricotta cheese. After *in vitro* gastrointestinal digestion, the sample was separated into two fractions that were challenged for its antioxidant properties. The peptidomic workflow led to the identification of an abundant β-lactoglobulin peptide in the most active fraction. The effect of this peptide on oxidative stress induced by H_2O_2 in the intestinal epithelial cells (IEC-6) and by angiotensin II in mouse mesenteric arteries was evaluated, together with its bioavailability.

2. Materials and Methods

2.1. Preparation and Fractionation of Buffalo Ricotta Gastrointestinal Digest by Semiprep-RP-HPLC. The simulated gastrointestinal digestion of buffalo ricotta cheese was performed according to Pepe et al. [23]. Briefly, the lyophilized sample was incubated with pepsin at 37°C for 2 h to pH = 2, and the reaction was stopped by heating the solution at 95°C for 15 min. Then, the gastric digest was incubated with pancreatin, chymotrypsin, and bile salts at 37°C for 2 h to pH 7.5, and the reaction was stopped bringing the solution to pH 2.

The peptides released after gastrointestinal digestion of buffalo ricotta cheese were fractionated by semipreparative reversed-phase liquid chromatography. For the separation, a Shimadzu Semiprep-HPLC was employed consisting of two LC-20 AP pumps, a SIL-20 AP autosampler, a fraction collector FRC-10 A, a UV detector SPD-20 A equipped with a preparative cell, and a system controller CBM-20 A.

The separation was carried out on a Kinetex™ C18 column (150×21.2 mm $\times$ 5 μm (100 Å)), and flow rate (20 mL min^{-1}), injection volume (5 mL (2 mg mL^{-1})), detection UV (214 and 220 nm), and the collection were based on UV-triggering signal. The optimal mobile phase consisted of (A) H_2O and (B) ACN both acidified by trifluoroacetic acid 0.1% (v/v). Analysis was performed in gradient elution as follows: 0.01-5.00 min, isocratic to 1% B; 5-40.00 min, 1-35% B; 40-43.00 min, 35-95% B; and 43-46.00 min, isocratic to 95% B, and then five minutes for column reequilibration. The fractions were collected on the basis of their elution times and thus hydrophobicity. In detail, the fractionation of peptide digesta led to the collection of two different aliquots: fraction I (BRF1), from 10.00 min to 20.00 min, and fraction II (BRF2), from 20.00 to 30.00 min.

2.2. Peptide Identification in the BRF2. Analyses of the bioactive peptides contained in the BRF2 were performed on a Shimadzu Nexera UHPLC system coupled online to an LCMS-IT-TOF mass spectrometer through an ESI source

(Shimadzu, Kyoto, Japan). Separation of BRF2 was carried out on an Aeris™ Peptide XB-C18 column (100×2.1 mm $\times$ 1.7 μm) (Phenomenex, Bologna, Italy). The flow rate and the column oven temperature were set to 0.5 mL min^{-1} and 60°C, respectively. The chromatograms were monitored at 214 and 220 nm. The mobile phase for the analysis of BRF2 consisted of 0.1% (*v*/*v*) HCOOH/H_2O (A) and 0.1% (*v*/*v*) HCOOH/ACN (B). Analysis was performed in gradient elution as follows: 0.01-45.0 min, 0-30% B; 45-47.00 min, 30-95% B; and 47-49.00 min, isocratic to 95% B, and then five minutes for column reequilibration.

MS detection was operated in ESI$^+$ mode, and MS/MS experiments were conducted in data-dependent acquisition; precursor ions were acquired in the range 300-2000 *m*/*z*.

A free trial of PEAKS 7.5 software (Bioinformatics Solutions Inc., Waterloo, Canada) was employed for sequence determination. A search was performed using a database search tool, by searching against the SwissProt/UniProt database (database *Bubalus bubalis* release 2017).

2.3. Synthesis and Quantification of Buffalo Ricotta Peptide 2 (BRP2). Synthesis of the analogue peptide was performed according to the solid phase approach using standard Fmoc methodology, with a Biotage Initiator+Alstra (Uppsala, Sweden) automated microwave synthesizer (for detailed conditions, see Supporting Information Appendix S1).

The quantification of BRP2 in buffalo ricotta digesta and BRF2 was performed on a Nexera UHPLC system coupled online to an LCMS-8050 mass spectrometer (Shimadzu, Kyoto, Japan), equipped with an ESI source operated in positive mode. MS/MS analysis was conducted in selected reaction monitoring (SRM), employing the synthetic peptide as an external standard. Stock solution was prepared in water, the calibration curve was obtained in a concentration range of 0.1-125 μg L^{-1} with eight concentration levels, and triplicate injection of each level was run. Peak areas of BRP2 were plotted against the corresponding concentrations. Linear regression was used to generate the calibration curve ($y = 0.0004x - 1.5321$) with R^2 values being $\geq$0.9998 (see Supporting Information Appendix S2).

2.4. IEC-6 Cells: Culture, Treatment, and Viability Assay. The IEC-6 cell line (CRL-1592), derived from normal rat intestinal crypt cells, was purchased from the American Type Culture Collection (ATCC, Rockville, MD, USA).

These cells were cultured by using Dulbecco's modified Eagle's medium (DMEM) (4 g/L glucose), supplemented with 10% (*v*/*v*) heat-inactivated foetal bovine serum, 1.5 g/L $NaHCO_3$, 2 mM L-glutamine, and 0.1 unit mL^{-1} bovine insulin. Cells were used, for the experiments, between the 17th and 21st passages.

The IEC-6 cells (2×10^4) were plated into 96-multiwell plates and allowed to adhere. After 24 h, cells were exposed to BRF1 and BRF2 (50-1.25 μg mL^{-1}) and BRP2 (100-1 μM), for 24 h. Cell viability was then assessed using the MTT assay, as previously reported [24].

2.4.1. Measurement of Intracellular ROS Release. ROS levels were evaluated by means of the probe 2′,7′-dichlorofluorescin-diacetate (H_2DCF-DA) [25]. For this experiment, IEC-6 cells were plated into 24-well plates (8×10^4 cells /well). After adhesion time of 24 h, cells were then treated with BRF1 and BRF2 (50-1.25 μg mL^{-1}) and with BRP2 (100-1 μM), for 1 h, either alone or in the presence of H_2O_2 (1 mM) for further 1 h.

IEC-6 cells were then collected, and a PBS buffer was used in order to wash them. Subsequently, cells were incubated in PBS containing H_2DCF-DA (10 μM), for 15 min at 37°C. A fluorescence-activated cell sorter (FACSscan; Becton Dickinson, Franklin Lakes, NJ, USA) was used for the purpose of measuring cell fluorescence, and CellQuest software (Becton Dickinson, Milan, Italy) was employed in order to analyze it.

2.4.2. Immunofluorescence Analysis for Nuclear Factor-Like 2 Activation. IEC-6 cells (2×10^5 cells/well) were seeded on coverslips in a 12-well plate and treated with BRP2 at concentration of 50 μM for 1 h, both alone and in the presence of H_2O_2 (1 mM) for further 1 h in order to evaluate nuclear factor- (erythroid-derived 2) like 2 (Nrf2) activation. After the cellular treatment, 4% paraformaldehyde in PBS was used to fix the cells. Then, IEC-6 cells were permeabilized with 0.1% saponin in PBS. After the blocking made with BSA and PBS, cells were incubated with a rabbit anti-Nrf2 antibody (Santa Cruz Biotechnology, Dallas, TX, USA) for 1 h at 37°C. The slides were then washed three times with PBS. After that, a fluorescein-conjugated secondary antibody (FITC) was added for further 1 h. 4′,6-diamidine-2′-phenylindole dihydrochloride (DAPI) was used for the counterstaining of nuclei. At the end, coverslips were mounted in mounting medium. Fluorescent images were taken under the laser confocal microscope (Leica TCS SP5, Leica, Wetzlar, Germany) as previously reported [26].

2.4.3. Measurement of Heme Oxygenase 1 (HO-1), NAD(P)H Quinone Dehydrogenase 1 (NQO1), and Superoxide Dismutase (SOD) Expression. IEC-6 cells were plated into 96-well plates (1×10^4 cells/well) and allowed to adhere. After 24 h, cells were treated with BRP2 (100-1 μM) for 1 h, either alone or in the presence of H_2O_2 (1 mM) for further 1 h. After cellular treatment, IEC-6 cells were collected, washed with PBS, and incubated in fixing solution for 20 min and then in Fix Perm Solution for further 30 min. Anti-heme oxygenase 1 (Santa Cruz Biotechnology, Dallas, TX, USA), anti-NAD(P)H quinone dehydrogenase 1 (Santa Cruz Biotechnology, Dallas, TX, USA), or anti-superoxide dismutase (Santa Cruz Biotechnology, Dallas, TX, USA) antibodies were then added. The cells were then treated with the secondary antibody. A fluorescence-activated cell sorter (FACSscan; Becton Dickinson, Franklin Lakes, NJ, USA) was used for the purpose of measuring cell fluorescence, and CellQuest software (Becton Dickinson, Milan, Italy) was employed in order to analyze it.

2.5. In Vitro Intestinal Transepithelial Transport Studies

2.5.1. Caco-2 Cell Monolayer Permeation Experiments. The colorectal adenocarcinoma (Caco-2) cell line was purchased from ATCC (Rockville, MD, USA). Cells were maintained

in high-glucose DMEM (4.5 g/L) supplemented with 2 mM L-glutamine and 10% (*v*/*v*) heat-inactivated foetal bovine serum. Cells were cultured at 37°C in a humidified 5% CO_2 atmosphere. To induce enterocytic Caco-2 differentiation, cells were seeded in a 12-well multiwell in transwell inserts (PET membrane, 0.4 μm pore size, 1.12 cm^2 surface area) at 2.6×10^5 cells/cm^2 and maintained for 21 days in complete medium. The medium was changed every second day. By 21 days, the monolayers become completely differentiated.

The integrity of the monolayers was evaluated by measurement of the transepithelial electrical resistance (TEER) using an EVOM2 epithelial voltohmmeter (World Precision Instruments, Sarasota, FL, USA). Only monolayers showing TEER higher than $300\,\Omega \times cm^2$ were then used for transport experiments. The integrity of the monolayers was checked before, during, and after the experiment. The filters were washed for 15-20 min at 37°C adding prewarmed Hank's balanced salt solution buffered with 25 mM HEPES and $NaHCO_3$ (0.35 g/L) at pH 7.4 to the apical (0.4 mL) and to the basolateral (1.2 mL) transwell compartments, as previously described [27]. For transport experiments, donor solution containing BRP2 peptide at the desired concentration (100-1 μM) was added to the apical compartment for the apical to basolateral (absorptive) direction. Samples from the receiving compartment were collected at different time points up to 120 min (15, 30, 60, 90, and 120 min). Samples from the donor compartment were collected at time 0 and at the end of the experiment (120 min) for the calculation of the mass balance.

Samples were stored at −20°C until UHPLC-MS/MS analyses to measure the concentration of BRP2 in both compartments (for detailed conditions, see Supporting Information Appendix S2).

The apparent permeability coefficient (P_{app}) was calculated as described according to

$$P_{app} = \frac{dM_{R(t)}}{dt} \times \frac{1}{A \times C_{D0}}, \quad (1)$$

where M_R is the amount of substance in the receiver chamber, A (cm^2) is the surface area of the barrier, and C_{D0} (μM) is the initial donor concentration. The reduction in donor concentration was also taken after every sampling (see Supporting Information Appendix S3) [28].

2.5.2. Immunofluorescence Analysis on Caco-2 Cell Monolayers. The transwell membranes from TEER experiments were washed with PBS and fixed with 4% paraformaldehyde (PFA) for 15 min. Membranes were then washed in PBS and blocked with blocking solution (0.1% Triton, 1% BSA, 0.02% sodium azide, and 50 mM ammonium chloride) for 20 min at room temperature in the dark. Afterwards, they were incubated with an anti-zonulin 1 antibody (#402200, Invitrogen, Thermo Fisher Scientific, Waltham, MA, USA) at the final concentration of 2 μg mL^{-1} at room temperature for 2 hours. Immunofluorescence staining was obtained by incubating the membranes for 90 min with Alexa Fluor 488 donkey anti-rabbit IgG (#A31573) at the final concentration of 4 μg mL^{-1} (Invitrogen). The nuclei were counterstained with DAPI (1 : 2000). Membranes were cut down with an operating knife blade along the margin of the chamber and were mounted on slides using VectaMount solution (AQ Vector Laboratories, Burlingame, CA, USA). Slides were examined under a Nikon fluorescence inverted microscope (Nikon Instruments Europe, Firenze, Italy) and then analyzed through ImageJ software as previously described [29].

2.6. Vascular Reactivity Studies. Second-order branches of the mesenteric arterial tree (internal diameter between 150 and 250 μm) were dissected and mounted on a wire myograph as previously described [30]. Briefly, vessels were equilibrated for 60 min at 45 mmHg intraluminal pressure in warmed oxygenated (95 : 5%, air : CO_2) Krebs solution (pH 7.4) containing the following (mmol L^{-1}): 120 NaCl, 25 $NaHCO_3$, 4.7 KCl, 1.18 KH_2PO_4, 1.18 $MgSO_4$, 2.5 $CaCl_2$, 0.026 EDTA, and 5.5 glucose. Media and lumen diameters were measured with a computer-based video imaging system (Danish Myo Technology). Endothelium-dependent and endothelium-independent relaxation was assessed by measuring the dilatory responses to cumulative doses of acetylcholine (Ach, 10^{-9} to 10^{-5} mol L^{-1}) or nitroglycerine (Nitro, 10^{-9} to 10^{-5} mol L^{-1}), respectively, in vessels precontracted with phenylephrine (10^{-9} to 10^{-5} mol L^{-1}). After evaluation of basal vascular function, we have tested the effect of peptide on angiotensin II-induced vasoconstriction (Ang II, 10^{-9} to 10^{-5} mol L^{-1}), preincubating the vessels with different dosages of BRP2 (100-1 μmol L^{-1}).

2.6.1. Dihydroethidium (DHE) Staining. DHE was used to evaluate the levels of oxidative stress in mouse mesenteric arteries as previously described [31]. Briefly, vessels were stained with 5 mol L^{-1} DHE for 20 min, then mounted and observed under a fluorescence microscope (Zeiss, Oberkochen, Germany). Images were acquired by a digital camera system.

2.6.2. NADPH Oxidase Activity Measurement. NADPH oxidase (NOX) activity in a pool of mesenteric arteries was measured in untreated cells and cells treated with angiotensin II and preincubated with BRP2 plus Ang II as previously described [31]. In another experimental set, we measure NADPH oxidase activity in IEC-6 cells following the same protocol but using 150 μg of protein extract. Vessels were placed in a chilled modified Krebs/HEPES buffer. Periadventitial tissue was carefully removed, and the vessels were repeatedly washed to remove adherent blood cells. A 10% vessel homogenate was prepared in 50 mmol L^{-1} phosphate buffer containing 0.01 mmol L^{-1} EDTA. The homogenate was then subjected to low-speed centrifugation (1000 g) for 10 min to remove unbroken cells and debris. 20 μL was added to glass scintillation vials containing 5 μmol L^{-1} lucigenin in 1 mL phosphate buffer. The chemiluminescence that occurred over the ensuing 5 min in response to the addition of 100 μmol L^{-1} NADPH was recorded (Beckman LS6500 Multipurpose Scintillation Counter; Beckman Coulter, Fullerton, CA). In preliminary experiments, homogenates alone without the addition of NADPH gave only minimal

signals. Furthermore, NADPH did not evoke lucigenin chemiluminescence in the absence of homogenate.

2.6.3. Immunoblotting and Nuclear/Cytoplasmic Fractionation. Immunoblots were performed as previously described [32]. Briefly, 30 μg tissue extract for each sample was separated by SDS-PAGE and transferred onto a nitrocellulose membrane. Blocked membranes were incubated with primary antibodies in TBS-Tween and 5% milk overnight. Blocked membranes were then incubated with anti-MnSOD (1 : 1500) and anti-β-actin (1 : 1000).

Nuclear and cytoplasmic fractions, obtained as previously described [32], were separated by SDS-PAGE and transferred onto nitrocellulose membranes [32]. Blocked membranes were incubated with anti-Nrf2 (1 : 2000), anti-GAPDH (glyceraldehyde 3-phosphate dehydrogenase, 1 : 3000), and anti-HDAC2 (histone deacetylase 2, 1 : 2000) overnight and then detected using an appropriate horseradish peroxidase-coupled secondary antibody (Millipore, Milan, Italy) and visualized with enhanced chemiluminescence. The purity of nuclear and cytoplasmic fractions was confirmed using anti-HDAC2 and anti-GAPDH, respectively. Immunoblotting data were analyzed using ImageJ software (developed by Wayne Rasband, National Institutes of Health, USA) to determine OD of the bands. The OD reading was normalized to account for variations in loading.

2.6.4. Ras-Related C3 Botulinum Toxin Substrate 1- (Rac1-) GTP Pull-Down Experiments. Mesenteric arteries were lysed in a buffer containing NP-40 equipped with kit STA-401-1 (Cell Biolabs Inc., San Diego, CA). The p21-binding domain of p21-activated protein kinase bound to agarose beads was added, and active Rac1, binding to PAK1, was separated by repetitive centrifugation and washing. Then, the specimens were boiled in Laemmli buffer and subjected to SDS-PAGE, and Rac1 was quantified by immunoblot analysis. In detail, Rac1-GTP was detected with the monoclonal antibody anti-Rac1-GTP c (1 : 800; STA-401-1, Cell Biolabs Inc.) and total Rac1 with monoclonal anti-Rac1 (1 : 1000; Abcam). The amount of Rac1-GTP was normalized to the total amount of Rac1 in tissue lysates for the comparison of Rac1 activity (GTP-bound Rac1) among different samples.

2.7. Data Analysis. Data were reported as mean ± standard error mean values, of at least three independent experiments, each in triplicate. In order to analyze the effects of our treatments on increasing doses of acetylcholine, we performed a 2-way repeated measures ANOVA with the Bonferroni post hoc test for multiple comparisons. Statistical analysis was performed by analysis of the variance test, and multiple comparisons were made by the Bonferroni test. A p value less than 0.05 was considered significant.

3. Results

3.1. Antioxidant Effect of BRP2 on ROS Release in IEC-6 Cells Treated with H_2O_2. With the aim of investigating the potential of buffalo ricotta cheese against oxidative stress induced by H_2O_2 in IEC-6 cells, the intracellular ROS production was measured. The GI digest of buffalo ricotta cheese was separated into two different fractions BRF1 and BRF2 by Semiprep-RPLC (Figure 1(a)).

No cytotoxic effect was observed when IEC-6 cells were treated with BRF1 and BRF2 fractions (data not shown). On the other hand, both tested fractions significantly reduced ROS release in a concentration-dependent manner ($p < 0.05$ vs. H_2O_2; Figure 1(b)), with BRF2 fraction showing higher efficacy ($p < 0.01$ vs. BRF1; Figure 1(b)).

Thus, we focused on the identification of most abundant peptides of this fraction by UHPLC-PDA-MS/MS analysis. An intense peak in BRF2 was selected and identified as BRP2 (Figure 2(a)), namely, Ser-Phe-Asn-Pro-Thr-Gln-Leu (β-LG, f168-174, and SFNPTQL, Figure 2(b)). The relative amount of the peptide was calculated by MS/MS in 1 mg of BR digest and BRF2 (14.73 ± 0.38% μM and 33.48 ± 0.56 μM, respectively).

To investigate its biological properties, the peptide was synthesized by an Fmoc solid-phase approach (see Supporting Information Figure S1). Finally, the antioxidant potential of BRP2 was tested in IEC-6 cells treated with H_2O_2. Our results showed that BRP2 caused, at all tested concentrations (100-1 μM), a significant decrement of ROS release induced by H_2O_2 (1 mM; $p < 0.01$ vs. H_2O_2, Figure 2(c)), thus exerting a cytoprotective effect against induced oxidative stress.

3.2. Evaluation of BRP2 Bioavailability. To assess BRP2 bioavailability, its transmembrane permeability was evaluated through Caco-2 fully differentiated cell monolayers [28]. As shown in Figure S2 (see Supporting Information), the transport amounts of BRP2 increased approximately linearly, in a time- (0-120 min) and concentration-dependent (1-100 μM) manner.

BRP2 showed moderate transport due to P_{app} values, ranging from 0.20 to 0.53×10^{-6} cm/s (see Supporting Information Table S1). Finally, the P_{app} of BRP2 in the apical to basolateral direction (A-B), as well as that in the basolateral to apical direction (B-A), was compared to explore the possible transport mechanism. In particular, the efflux ratio, defined as the quotient of the secretory permeability and the absorptive permeability (B-A/A-B), was less than 1 suggesting that passive diffusion could be the main intestinal transport mechanism of BRP2 [33]. Moreover, in order to evaluate the effects of BRP2 on Caco-2 monolayer integrity and cell vitality, we performed immunofluorescence analysis on transwell inserts at the end of transport studies. As shown in Figure S3 (see Supporting Information), Caco-2 cell monolayer integrity was preserved upon BRP2 treatment at all the concentrations tested as confirmed by tight junction protein zonulin-1 expression (green) and cell vitality.

3.3. BRP2 Reduces Angiotensin II-Induced Vasoconstriction and Oxidative Stress in the Mouse Mesenteric Artery. In order to investigate the antioxidant capability of BRP2 also in *ex vivo* model able to reproduce the cardiovascular condition of the vascular system, we performed experiments on the mouse mesenteric artery that is considered the prototype of resistance vessels involved in the modulation of systemic

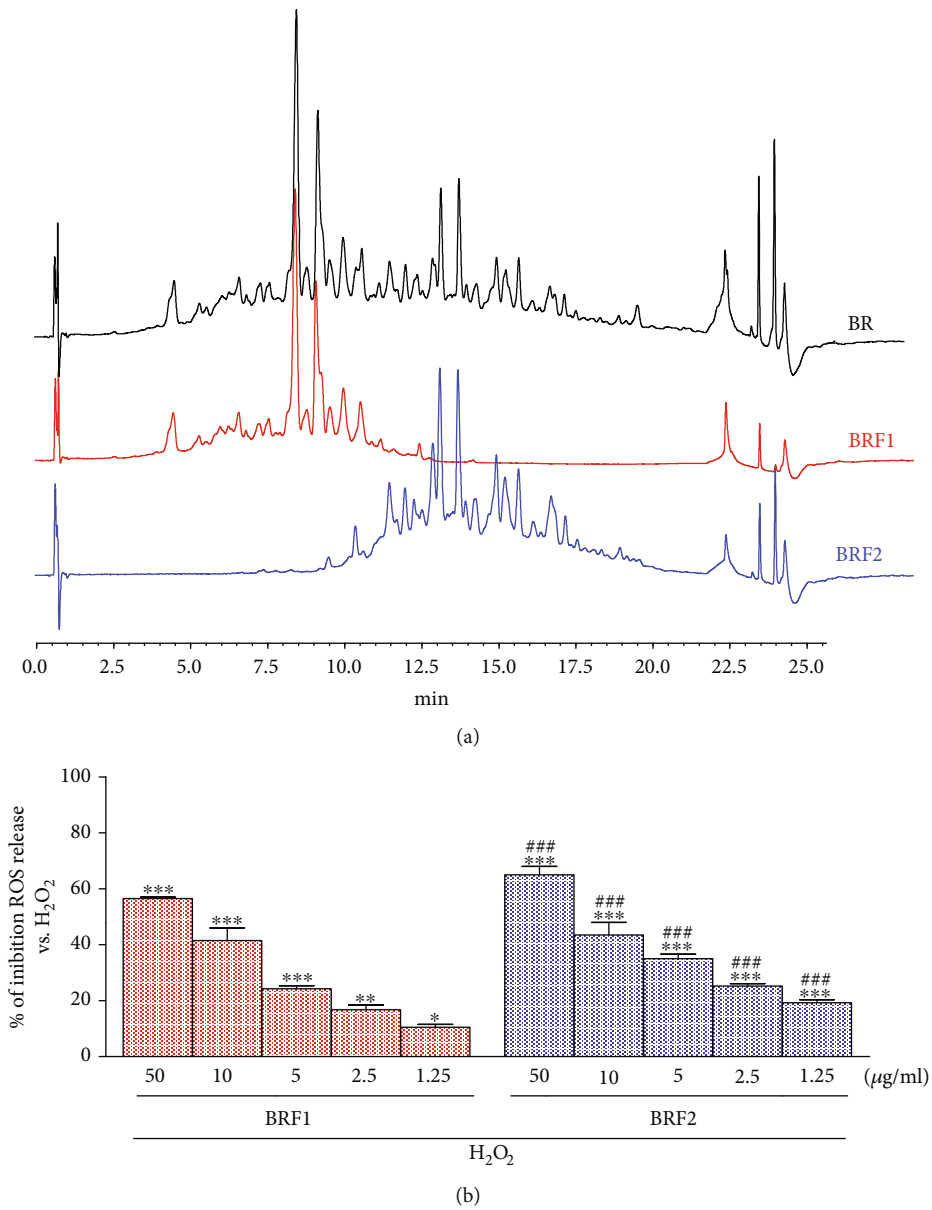

Figure 1: (a) Chromatographic profiles (λ: 214 nm) of the gastrointestinal digest of BR (black line), BRF1 (red line), and BRF2 (blue line). (b) Effect of BRF1 and BRF2 fractions on ROS formation, in IEC-6 cells, evaluated by H_2DCF-DA. Values, mean ± s.e.m., are expressed as % of inhibition of ROS release vs. H_2O_2. ∗∗∗, ∗∗, and ∗ denote $p < 0.001$, $p < 0.01$, and $p < 0.05$ vs. H_2O_2, respectively. ### and ## denote $p < 0.001$ and $p < 0.01$ vs. BRF1+H_2O_2, respectively.

hemodynamic parameter. Interestingly, the preincubation of mesenteric arteries with increasing doses of BRP2 showed a progressive dose-dependent reduction of Ang II-induced vasoconstriction (Figure 3(a)), with maximal effects at 100 μM, with a reduction of the Ang II-vasoconstrictive response of about 92.0 ± 4.0% (Figure 3(b)). This functional effect drove us to explore its action on the oxidative stress status, since oxygen-derived free radicals are selectively involved in the vascular response to Ang II. By DHE staining, we showed that BRP2 specifically reduces the Ang II-induced ROS production (Figure 3(c)). To support this effect, the measurement of NOX activity revealed that BRP2 is capable of markedly attenuating the lucigenin signal in a dose-dependent manner (Figure 3(d)).

3.4. Antioxidant and Hypotensive Effects of BRP2. The endogenous antioxidant system mainly consists of intracellular enzymatic antioxidants that are responsible for redox homeostasis balance. Nrf2 is an intracellular transcription factor that regulates the expression of several genes to activate antioxidative enzymes and detoxifying factors [34]. For these reasons, in order to give an insight into the molecular mechanisms underlying the antioxidant effects of BRP2, its influence on this specific antioxidant pathway was studied.

As shown in Figure 4(a), nuclear Nrf2 levels are increased in IEC-6 cells treated with BRP2 (50 μM)+H_2O_2 (1 mM), with respect to H_2O_2 alone. It is known that Nrf2 activation leads to the expression of cytoprotective enzymes. In our experimental model, the effect of BRP2

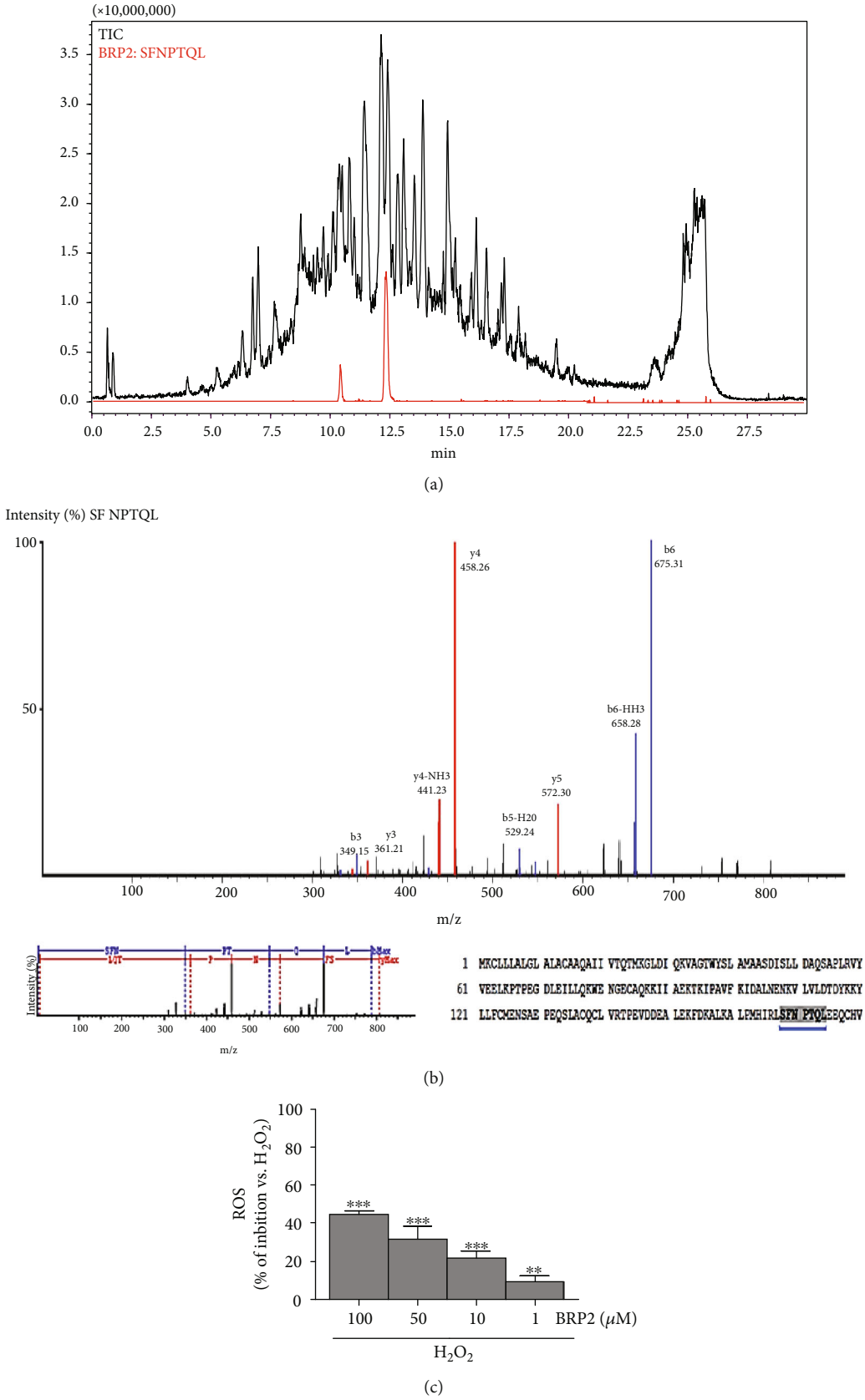

Figure 2: (a) Total ion chromatogram of BRF2 and (b) MS/MS fragmentation pattern of identified BRP2 (SFNPTQL) in BRF2 fraction. (c) Effect of BRP2 on ROS formation in H_2O_2-treated IEC-6 cells. Values, mean ± s.e.m., are expressed as % of inhibition of ROS vs. H_2O_2. ∗∗∗ and ∗∗ denote $p < 0.001$ and $p < 0.01$ vs. H_2O_2.

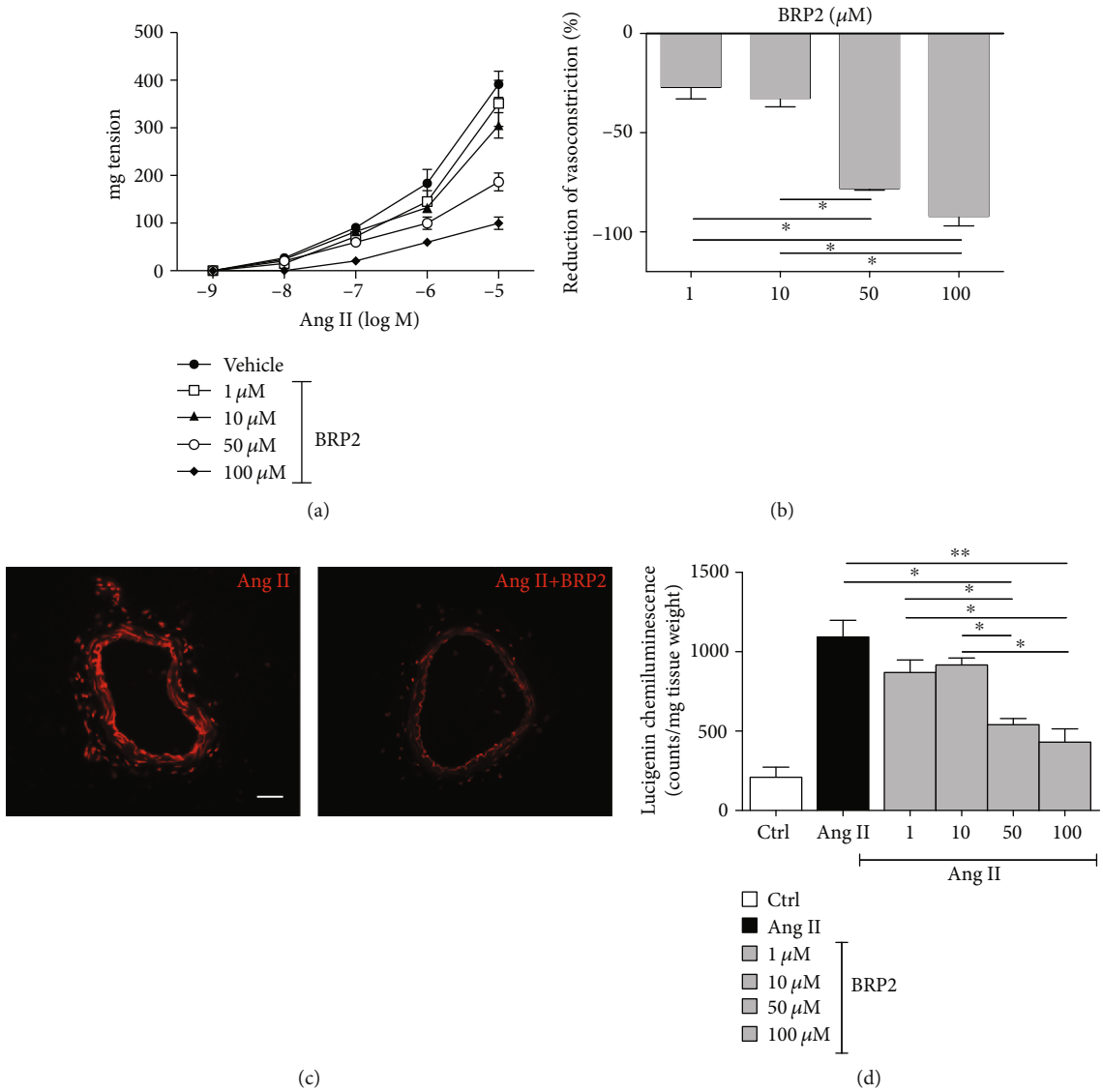

Figure 3: (a) Vascular responses to increasing doses of angiotensin II (10^{-9} to 10^{-5}) of mouse mesenteric arteries preincubated with increasing doses of BRP2 (1, 10, 50, and 100 μM). (b) Bar graph of the last time point of dose-response curve to angiotensin II (10^{-5} M). (c) In situ detection of superoxide generation with DHE staining in segments of mesenteric arteries treated with Ang II (10^{-5} M) alone or plus BRP2 (100 μM). Scale bar: 50 μm. (d) Graphs of superoxide production in mesenteric arteries measured continuously in the presence or absence of BRP2 by using 5 μmol L^{-1} lucigenin-enhanced chemiluminescence. Values are mean ± s.e.m., expressed as RLU/(s·mg dry weight) ($n = 4$).

on HO-1, NQO1, and SOD enzymatic expression was assessed. We observed that the expression of cytoprotective enzymes was significantly enhanced in the presence of H_2O_2 (1 mM; $p < 0.001$ vs. control). Administration of BRP2 (100-1 μM) further increased HO-1 ($p < 0.001$ vs. H_2O_2; Figure 4(b)), NQO1 ($p < 0.001$ vs. H_2O_2; Figure 4(c)), and SOD expression ($p < 0.001$ vs. H_2O_2; Figure 4(d)). Nrf2 is generally held in the cytoplasm as an inactive complex bound to a repressor molecule and sensor of intracellular redox state. We found that in a time-dependent manner, BRP2 is able to induce Nrf2 translocation to the nucleus, where it turns active. Already starting from 1 hour of treatment, it is possible to appreciate the translocation of this factor that becomes maximal after 6 hours from BRP2 treatment (Figure 5(a)). Moreover, associated with the Nrf2 translocation, it was possible to note that at 1 hour there was an increase in MnSOD expression (Figure 5(b)).

It is well known that Ang II-induced ROS production is mainly mediated by NADPH oxidase activation, a multimeric complex that requires the small GTPase Rac1 to become active. Some studies have reported the functional and mechanistic connection between Rac1 and the transcription factor Nrf2. Based on these evidences, using the pull-down assay, we found a 50% reduction of Rac1-GTP after 1 hour of BRP2 treatment that further reduces up to six hours, thus supporting the capability of BRP2 to inhibit the angiotensin II-induced ROS production through NADPH oxidase recruitment inhibiting Rac1 activation (Figure 5(c)).

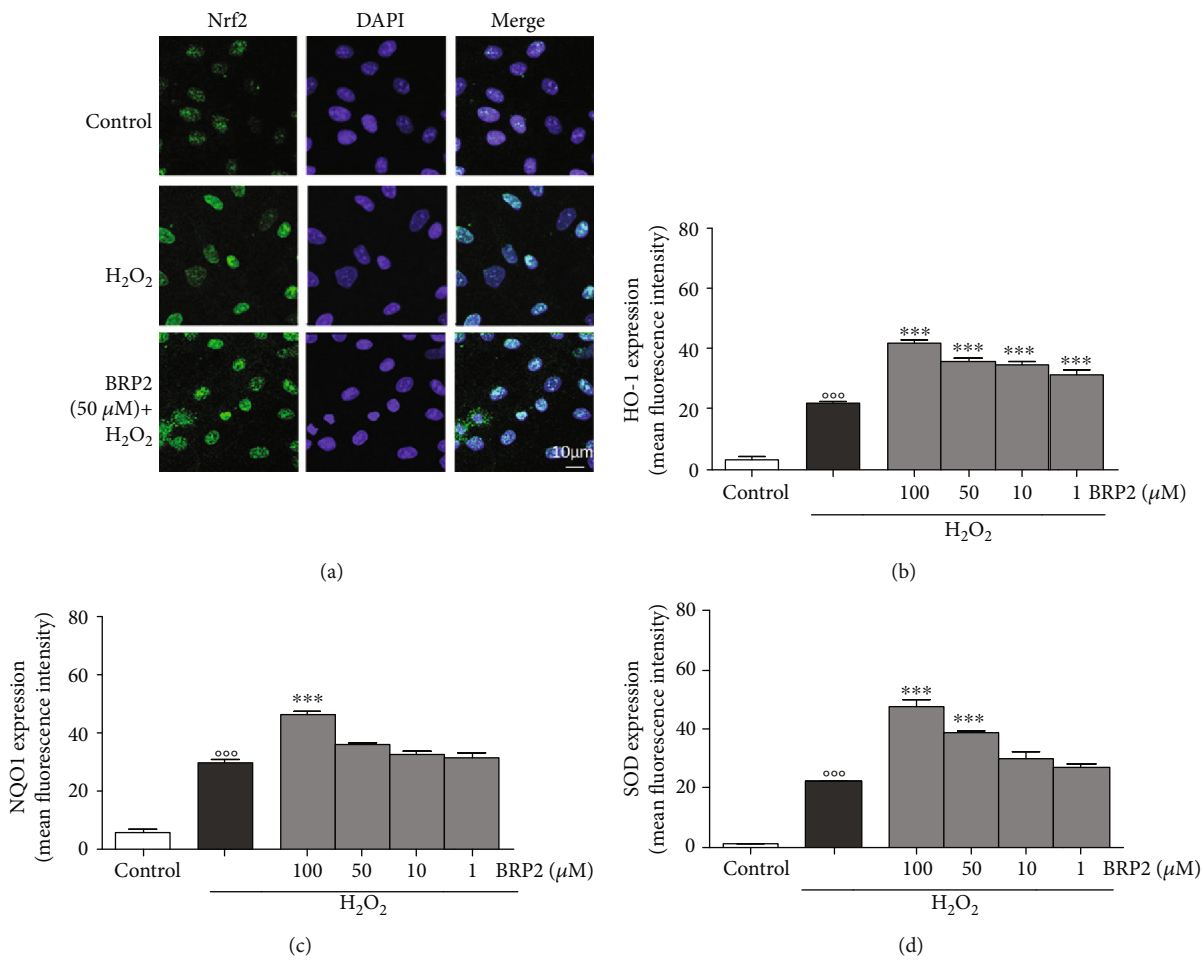

Figure 4: (a) Effect of BRP2 on Nrf2 nuclear translocation (scale bar: 10 μm). Blue fluorescence and green fluorescence indicate localization of the nucleus (DAPI) and Nrf2, respectively. Effect of BRP2 on (b) HO-1, (c) NQO1, and (d) SOD expression in the IEC-6 cells, evaluated by the cytofluorimetric technique. Values, mean ± s.e.m., are expressed as % of inhibition of HO-1, NQO1, and SOD expression vs. H_2O_2. $^{\circ\circ\circ}$ denotes $p < 0.001$ vs. control. $***$ denotes $p < 0.001$ vs. H_2O_2.

4. Discussion

In our previous study, the peptidomic profile of six different commercial dairy products based on buffalo milk was highlighted, revealing the presence of numerous peptides with immunomodulatory, antihypertensive, antioxidant, antimicrobial, anticancer, and antidiabetic properties [17]. However, only one-third of the identified peptides showed a recognized biological activity. Based on this data, we started a rational biological characterization of the six selected commercial products [18]. Buffalo ricotta cheese showed the highest antioxidant activity, compared to the other investigated buffalo dairy products. The peptidomic approach led to the identification of an abundant peptide, corresponding to the fragment 60-72 of β-lactoglobulin, namely, BRP, with interesting antioxidant activity [18]. With respect to the previous study, based on ultrafiltration with different cut-off membranes, in the present study, we fractionated the entire buffalo ricotta cheese digest by semipreparative liquid chromatography. Two main fractions were obtained in the most active fraction, and abundant β-lactoglobulin peptides (f168-174, SFNPTQL, and BRP2) were detected. The antioxidant potential of this peptide was not reported so far (see Supporting Information Appendix S4); thus, we focused on its possible potential against oxidative stress, in particular on its ability to decrease ROS release. The intestine is the main organ of exposure and/or absorption of nutrients, toxic food contaminants, and metabolic products coming from the intestinal bacteria. The alteration of the integrity and function of the intestinal epithelium produces a negative impact on the rest of the body [35]. In many cases, the intestine responds adequately against the oxidative stress, but aging or disequilibrium in the redox state of the gut can induce intestinal pathologies such as inflammatory bowel disease, gastroduodenal ulcers, and colon cancer [36].

Our results showed that β-lactoglobulin-derived peptide BRP2 reduced ROS release induced by H_2O_2 in IEC-6 cells. Interestingly, BRP2 possessed a discrete bioavailability, showing a moderate absorption through a fully differentiated Caco-2 intestinal monolayer, without affecting its integrity and tight junction zonulin-1 protein expression.

To understand the antioxidant effect of BRP2 peptide, its molecular basis was investigated.

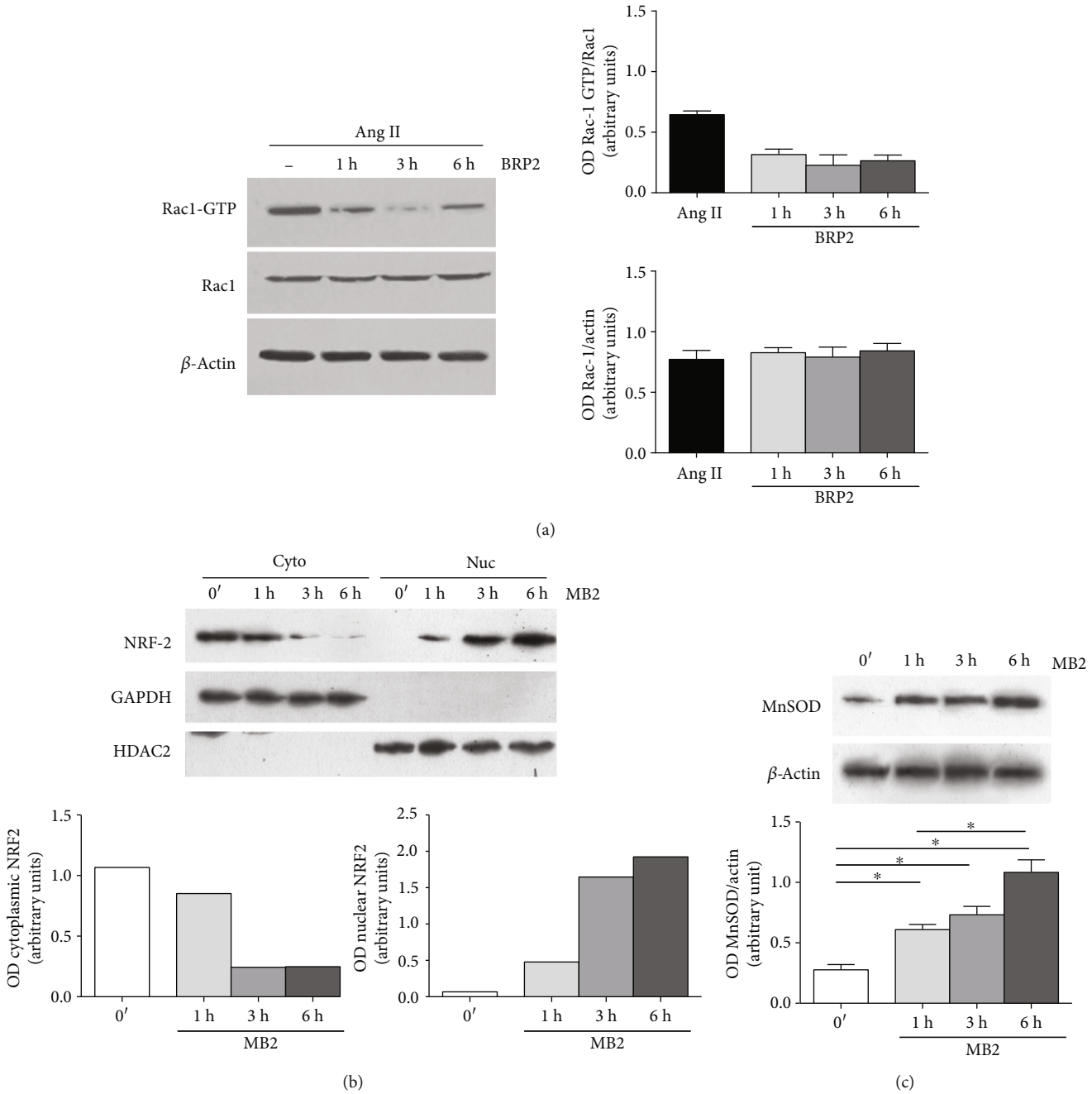

Figure 5: (a) Representative immunoblot from the pull-down assay of mouse mesenteric arteries for active Rac1 (Rac1-GTP). (b) Immunoblot analysis for Nrf2. Cytoplasmic (Cyto) and nuclear (Nuc) fractions were prepared from untreated mouse mesenteric arteries or treated with BRP2. GAPDH and HDAC2 were used as cytoplasmic and nuclear markers, respectively. Right: nuclear/cytoplasmic ratios for Nrf2 are plotted from densitometry ($n = 3$). (c) Representative immunoblot for MnSOD in mouse mesenteric arteries treated with BRP2 (100 μM) and Ang II (10^{-5} M) ($n = 3$).

Nrf2 is a transcription factor that plays a central role in the regulation of antioxidant and phase 2 detoxifying enzymes and related proteins [37]. An increase in intracellular ROS enhances nuclear translocation of Nrf2 and expression of its target genes such as HO-1, NQO1, and SOD [38, 39]. Our results indicated that BRP2 protects intestinal epithelial cells from oxidative stress by ROS release inhibition and by upregulation of cytoprotective enzymes via the Nrf2/ARE pathway.

An oxidant mechanism of BRP2 could be related to the presence of amino acidic residues such as proline and threonine in its primary sequence as previously reported for β-lactoglobulin and β-casein peptides [18, 40].

A growing body of evidence indicates that an imbalance between endogenous reactive oxygen species and antioxidants in favor of the former contributes markedly to vascular dysfunction [41]. Based on the local antioxidant properties and on the moderate intestinal permeation of BRP2, we

decided to investigate its potential systemic effects in an *ex vivo* mouse model of vascular reactivity. The most important endogenous bioactive octapeptide that exerts a potent vasoconstrictor through ROS production, modulating systemic hemodynamic parameters, is represented by Ang II. Our studies clearly demonstrated that pretreatment with BRP2 inhibits the Ang II-derived vasoconstrictive responses of mouse mesenteric arteries, in a dose-dependent manner. The 90% of inhibition after the exposure to the maximal dose of the peptide was obtained. This potent effect evoked by BRP2 is strictly related to its antioxidant properties, counteracting the oxidative stress induced by Ang II. In this regard, several evidences suggest that NAD(P)H oxidase is a major source recruited by Ang II to induce ROS generation in the vascular wall [42]. The evaluation of NADPH oxidase activity revealed a significant reduction of enzymatic activity after pretreatment with BRP2.

NOX is a multisubunit enzyme complex that requires specific interactions with a plethora of molecules. In this regard, the small GTPase Rac1 is essential for the correct assembly of NADPH subunits and their activation [43]. The treatment of mesenteric arteries with BRP2 significantly reduces Rac1 activation, supporting the effect of the peptide on the reduction of NADPH oxidase activity and the reduction of vasoconstrictive responses to Ang II. These *ex vivo* results demonstrate that BRP2 is able to act on two concomitant mechanisms, the reduction of the active form of Rac1 with a consequent reduction of NOX activity and the induction of nuclear translocation of Nrf2 that is pivotal in cellular defense against oxidative stress [44].

5. Conclusions

In conclusion, the results obtained highlight the important role of BRP2 in intestinal and cardiovascular protection, both inhibiting ROS release and enhancing an important antioxidant response consisting of Nrf2 pathway activation and cytoprotective enzyme expression. The antioxidant effects evoked in mice mesenteric arteries suggest BRP2 as a novel peptide candidate with promising cardiovascular effects and pave the way to its *in vivo* characterization in a model of cardiovascular disease.

Abbreviations

Ang II:	Angiotensin II
BR:	Buffalo ricotta
BRF:	Buffalo ricotta fraction
BRP:	Buffalo ricotta peptide
Caco-2:	Colorectal adenocarcinoma
DAPI:	4′,6-diamidine-2′-phenylindole dihydrochloride
DHE:	Dihydroethidium
GI:	Gastrointestinal
GAPDH:	Glyceraldehyde 3-phosphate dehydrogenase
H_2DCF-DA:	2′,7′-dichlorofluorescin-diacetate
HDAC2:	Histone deacetylase 2
HO-1:	Heme oxygenase-1
IEC-6:	Intestinal epithelial cell line
NO:	Nitric oxide
NOX:	NADPH oxidase
NQO1:	NAD(P)H quinone oxidoreductase 1
Nrf2:	Nuclear factor erythroid 2-related factor 2
Rac1:	Ras-related C3 botulinum toxin substrate 1
ROS:	Reactive oxygen species
P_{app}:	Apparent permeability coefficient
SOD:	Superoxide dismutase.

Data Availability

The data used to support the findings of this study are included within the article and the supplementary information files.

Conflicts of Interest

The authors declare no conflict of interest.

Acknowledgments

The authors would like to thank San Salvatore Dairy Factory (Capaccio, SA, Italy) which kindly gifted the buffalo ricotta cheese. This project was supported by the project Progetto PON Ricerca e Innovazione 2014-2020 titolo: "PROGEMA - Processi Green per l'Estrazione di principi attivi e la depurazione di Matrici di scarto e non" (ARS01_00432).

Supplementary Materials

Figure S1: (A) chromatographic profile acquired by RP-UHPLC-UV and (B) mass spectrum of synthetic BRP2 obtained by direct infusion Fourier-transform ion cyclotron resonance MS. Figure S2: transport of BRP2 across Caco-2 cell monolayer. Table S1: the apparent permeability coefficient (P_{app}) values of BRP2 with different concentrations. Figure S3: fluorescence micrograph of the Caco-2 cell monolayers. Caco-2 cell monolayers treated with BRP2 (50 μM, 2 h) from TEER experiments were stained for tight junction protein expression of zonulin-1 (FITC, green). Nuclei were counterstained with DAPI (blue). Pictures are representative of two independent experiments. Original magnification, 200x. Figure S4: (A) graphs of NADPH superoxide production in IEC-6 cells measured continuously in the presence or absence of BRP2 by using 5 μmol L^{-1} lucigenin-enhanced chemiluminescence. Values are mean ± s.e.m., expressed as counts/mg proteins ($n = 4$). (B) Representative immunoblot of three independent experiments from the pull-down assay of IEC-6 cells for active Rac1 (Rac1-GTP), Ang II (10-5 M), and BRP2 (100 μM) ($n = 4$). *(Supplementary Materials)*

References

[1] G. Pierri, D. Kotoni, P. Simone et al., "Analysis of bovine milk caseins on organic monolithic columns: an integrated capillary liquid chromatography-high resolution mass spectrometry approach for the study of time-dependent casein degradation," *Journal of Chromatography A*, vol. 1313, pp. 259–269, 2013.

[2] G. C. Tenore, A. Ritieni, P. Campiglia et al., "Antioxidant peptides from "Mozzarella di Bufala Campana DOP" after simulated gastrointestinal digestion: _In vitro_ intestinal protection, bioavailability, and anti-haemolytic capacity," *Journal of Functional Foods*, vol. 15, pp. 365–375, 2015.

[3] E. Sommella, G. Pepe, G. Ventre et al., "Detailed peptide profiling of "Scotta": from a dairy waste to a source of potential health-promoting compounds," *Dairy Science & Technology*, vol. 96, no. 5, pp. 763–771, 2016.

[4] T. Sayd, C. Dufour, C. Chambon, C. Buffière, D. Remond, and V. Santé-Lhoutellier, "Combined _in vivo_ and _in silico_ approaches for predicting the release of bioactive peptides from meat digestion," *Food Chemistry*, vol. 249, pp. 111–118, 2018.

[5] M. Chalamaiah, B. Dinesh kumar, R. Hemalatha, and T. Jyothirmayi, "Fish protein hydrolysates: proximate composition, amino acid composition, antioxidant activities and applications: a review," *Food Chemistry*, vol. 135, no. 4, pp. 3020–3038, 2012.

[6] A. M. Fiat, D. Migliore-Samour, P. Jollès, L. Drouet, C. Bal dit Sollier, and J. Caen, "Biologically active peptides from milk proteins with emphasis on two examples concerning antithrombotic and immunomodulating activities," *Journal of Dairy Science*, vol. 76, no. 1, pp. 301–310, 1993.

[7] S. Sakanaka, Y. Tachibana, N. Ishihara, and L. Raj Juneja, "Antioxidant activity of egg-yolk protein hydrolysates in a linoleic acid oxidation system," *Food Chemistry*, vol. 86, no. 1, pp. 99–103, 2004.

[8] F. Sansone, T. Mencherini, P. Picerno et al., "Microencapsulation by spray drying of Lannea microcarpa extract: Technological characteristics and antioxidant activity," *Journal of Pharmacy & Pharmacognosy Research*, vol. 2, no. 4, pp. 100–109, 2014.

[9] A. Sofo, B. Lundegårdh, A. Mårtensson et al., "Different agronomic and fertilization systems affect polyphenolic profile, antioxidant capacity and mineral composition of lettuce," *Scientia Horticulturae*, vol. 204, pp. 106–115, 2016.

[10] S. Adesso, G. Pepe, E. Sommella et al., "Anti-inflammatory and antioxidant activity of polyphenolic extracts from Lactuca sativa (var. Maravilla de Verano) under different farming methods," *Journal of the Science of Food and Agriculture*, vol. 96, no. 12, pp. 4194–4206, 2016.

[11] W. Dröge, "Free radicals in the physiological control of cell function," *Physiological Reviews*, vol. 82, no. 1, pp. 47–95, 2002.

[12] Y. H. Wei, C. Y. Lu, C. Y. Wei, Y. S. Ma, and H. C. Lee, "Oxidative stress in human aging and mitochondrial disease-consequences of defective mitochondrial respiration and impaired antioxidant enzyme system," *The Chinese Journal of Physiology*, vol. 44, no. 1, pp. 1–11, 2001.

[13] Y. J. Kim, E. H. Kim, and K. B. Hahm, "Oxidative stress in inflammation-based gastrointestinal tract diseases: challenges and opportunities," *Journal of Gastroenterology and Hepatology*, vol. 27, no. 6, pp. 1004–1010, 2012.

[14] T. Heitzer, T. Schlinzig, K. Krohn, T. Meinertz, and T. Münzel, "Endothelial dysfunction, oxidative stress, and risk of cardiovascular events in patients with coronary artery disease," *Circulation*, vol. 104, no. 22, pp. 2673–2678, 2001.

[15] R. M. Touyz, "Reactive oxygen species, vascular oxidative stress, and redox signaling in hypertension: what is the clinical significance?," *Hypertension*, vol. 44, no. 3, pp. 248–252, 2004.

[16] E. H. Tang and P. M. Vanhoutte, "Endothelial dysfunction: a strategic target in the treatment of hypertension?," *Pflügers Archiv - European Journal of Physiology*, vol. 459, no. 6, pp. 995–1004, 2010.

[17] M. G. Basilicata, G. Pepe, E. Sommella et al., "Peptidome profiles and bioactivity elucidation of buffalo-milk dairy products after gastrointestinal digestion," *Food Research International*, vol. 105, pp. 1003–1010, 2018.

[18] M. Basilicata, G. Pepe, S. Adesso et al., "Antioxidant properties of buffalo-milk dairy products: a β-Lg peptide released after gastrointestinal digestion of buffalo ricotta cheese reduces oxidative stress in intestinal epithelial cells," *International Journal of Molecular Sciences*, vol. 19, no. 7, p. 1955, 2018.

[19] T. Tavares, M.-Á. Sevilla, M.-J. Montero, R. Carrón, and F. X. Malcata, "Acute effect of whey peptides upon blood pressure of hypertensive rats, and relationship with their angiotensin-converting enzyme inhibitory activity," *Molecular Nutrition & Food Research*, vol. 56, no. 2, pp. 316–324, 2012.

[20] K. D. Ballard, R. S. Bruno, R. L. Seip et al., "Acute ingestion of a novel whey-derived peptide improves vascular endothelial responses in healthy individuals: a randomized, placebo controlled trial," *Nutrition Journal*, vol. 8, no. 1, 2009.

[21] H. Ijäs, M. Collin, P. Finckenberg et al., "Antihypertensive opioid-like milk peptide α-lactorphin: lack of effect on behavioural tests in mice," *International Dairy Journal*, vol. 14, no. 3, pp. 201–205, 2004.

[22] W. Maes, J. van Camp, V. Vermeirssen et al., "Influence of the lactokinin Ala-Leu-Pro-Met-His-Ile-Arg (ALPMHIR) on the release of endothelin-1 by endothelial cells," *Regulatory Peptides*, vol. 118, no. 1-2, pp. 105–109, 2004.

[23] G. Pepe, F. Pagano, S. Adesso et al., "Bioavailable Citrus sinensis extract: polyphenolic composition and biological activity," *Molecules*, vol. 22, no. 4, p. 623, 2017.

[24] G. Bianco, B. Fontanella, L. Severino, A. Quaroni, G. Autore, and S. Marzocco, "Nivalenol and deoxynivalenol affect rat intestinal epithelial cells: a concentration related study," *PLoS One*, vol. 7, no. 12, p. e52051, 2012.

[25] S. Marzocco, S. Adesso, M. Alilou, H. Stuppner, and S. Schwaiger, "Anti-inflammatory and anti-oxidant potential of the root extract and constituents of Doronicum austriacum," *Molecules*, vol. 22, no. 6, p. 1003, 2017.

[26] S. Marzocco, L. Calabrone, S. Adesso et al., "Anti-inflammatory activity of horseradish (Armoracia rusticana) root extracts in LPS-stimulated macrophages," *Food & Function*, vol. 6, no. 12, pp. 3778–3788, 2015.

[27] I. Hubatsch, E. G. Ragnarsson, and P. Artursson, "Determination of drug permeability and prediction of drug absorption in Caco-2 monolayers," *Nature Protocols*, vol. 2, no. 9, pp. 2111–2119, 2007.

[28] S. Tavelin, J. Grasjo, J. Taipalensuu, G. Ocklind, and P. Artursson, *Methods in Molecular Biology*, C. Wise, Ed., vol. 188, Humana Press, Totowa, New Jersey, 2002.

[29] R. Ranieri, E. Ciaglia, G. Amodio et al., "N6-isopentenyladenosine dual targeting of AMPK and Rab7 prenylation inhibits melanoma growth through the impairment of autophagic flux," *Cell Death and Differentiation*, vol. 25, no. 2, pp. 353–367, 2018.

[30] A. Carrizzo, M. Ambrosio, A. Damato et al., "Morus alba extract modulates blood pressure homeostasis through eNOS signaling," *Molecular Nutrition & Food Research*, vol. 60, no. 10, pp. 2304–2311, 2016.

[31] A. Carrizzo, C. Vecchione, A. Damato et al., "Rac1 pharmacological inhibition rescues human endothelial dysfunction," *Journal of the American Heart Association*, vol. 6, no. 3, 2017.

[32] A. Carrizzo, A. Puca, A. Damato et al., "Resveratrol improves vascular function in patients with hypertension and dyslipidemia by modulating NO metabolism," *Hypertension*, vol. 62, no. 2, pp. 359–366, 2013.

[33] C. O. Chan, J. Jing, W. Xiao et al., "Enhanced intestinal permeability of bufalin by a novel bufalin-peptide-dendrimer inclusion through Caco-2 cell monolayer," *Molecules*, vol. 22, no. 12, p. 2088, 2017.

[34] Q. Ma, "Role of nrf2 in oxidative stress and toxicity," *Annual Review of Pharmacology and Toxicology*, vol. 53, pp. 401–426, 2013.

[35] A. S. Londero, M. R. Arana, V. G. Perdomo et al., "Intestinal multidrug resistance-associated protein 2 is down-regulated in fructose-fed rats," *The Journal of Nutritional Biochemistry*, vol. 40, pp. 178–186, 2017.

[36] I. Moret, E. Cerrillo, A. Navarro-Puche et al., "Oxidative stress in Crohn's disease," *Gastroenterología y Hepatología*, vol. 37, no. 1, pp. 28–34, 2014.

[37] H. Zhu, K. Itoh, M. Yamamoto, J. L. Zweier, and Y. Li, "Role of Nrf2 signaling in regulation of antioxidants and phase 2 enzymes in cardiac fibroblasts: protection against reactive oxygen and nitrogen species-induced cell injury," *FEBS Letters*, vol. 579, no. 14, pp. 3029–3036, 2005.

[38] V. Afonso, R. Champy, D. Mitrovic, P. Collin, and A. Lomri, "Reactive oxygen species and superoxide dismutases: role in joint diseases," *Joint, Bone, Spine*, vol. 74, no. 4, pp. 324–329, 2007.

[39] Y. Wang, R. Branicky, A. Noë, and S. Hekimi, "Superoxide dismutases: dual roles in controlling ROS damage and regulating ROS signaling," *The Journal of Cell Biology*, vol. 217, no. 6, pp. 1915–1928, 2018.

[40] G. Pepe, E. Sommella, G. Ventre et al., "Antioxidant peptides released from gastrointestinal digestion of "Stracchino" soft cheese: Characterization, in vitro intestinal protection and bioavailability," *Journal of Functional Foods*, vol. 26, pp. 494–505, 2016.

[41] U. Förstermann, "Oxidative stress in vascular disease: causes, defense mechanisms and potential therapies," *Nature Clinical Practice. Cardiovascular Medicine*, vol. 5, no. 6, pp. 338–349, 2008.

[42] D. Sorescu and K. K. Griendling, "Reactive oxygen species, mitochondria, and NAD(P)H oxidases in the development and progression of heart failure," *Congestive Heart Failure*, vol. 8, no. 3, pp. 132–140, 2002.

[43] A. Carrizzo, M. Forte, M. Lembo, L. Formisano, A. A. Puca, and C. Vecchione, "Rac-1 as a new therapeutic target in cerebro- and cardio-vascular diseases," *Current Drug Targets*, vol. 15, no. 13, pp. 1231–1246, 2014.

[44] T. Ashino, M. Yamamoto, T. Yoshida, and S. Numazawa, "Redox-sensitive transcription factor Nrf2 regulates vascular smooth muscle cell migration and neointimal hyperplasia," *Arteriosclerosis, Thrombosis, and Vascular Biology*, vol. 33, no. 4, pp. 760–768, 2013.

Hindawi
Oxidative Medicine and Cellular Longevity
Volume 2019, Article ID 7838149, 12 pages
https://doi.org/10.1155/2019/7838149

Research Article

Supplementation with *Spirulina platensis* Modulates Aortic Vascular Reactivity through Nitric Oxide and Antioxidant Activity

Aline de Freitas Brito,[1,2] Alexandre Sérgio Silva,[2,3,4] Alesandra Araújo de Souza,[5] Paula Benvindo Ferreira,[6] Iara Leão Luna de Souza,[7] Layanne Cabral da Cunha Araujo,[8] Gustavo da Silva Félix,[2,4] Renata de Souza Sampaio,[6] Maria da Conceição Correia Silva,[6] Renata Leite Tavares,[9] Reabias de Andrade Pereira,[2,4] Manoel Miranda Neto,[9] and Bagnólia Araújo Silva[6,10]

[1]*School of Physical Education, University of Pernambuco, Recife, Pernambuco, Brazil*
[2]*Post-Graduation Program in Physical Education UPE/UFPB, Brazil*
[3]*Physical Education Department, Health Sciences Center, Federal University of Paraiba, João Pessoa, Paraíba, Brazil*
[4]*Laboratory of Studies of Physical Training Applied to the Performance and the Health, Health Sciences Center/Federal University of Paraiba, João Pessoa, Paraíba, Brazil*
[5]*Federal University of Tocantins, Tocantinópolis, Tocantins, Brazil*
[6]*Postgraduate Program in Natural and Synthetic Products Bioactive/Health Sciences Center, Federal University of Paraiba, João Pessoa, Paraíba, Brazil*
[7]*Department of Biological Sciences and Health, State University of Roraima, Boa Vista, Roraima, Brazil*
[8]*Department of Biophysics and Physiology, University of Sao Paulo, Institute of Biomedical Sciences, Sao Paulo, Sao Paulo, Brazil*
[9]*Postgraduate Program in Nutrition Science/Health Sciences Center, Federal University of Paraiba, João Pessoa, Paraíba, Brazil*
[10]*Pharmaceutical Sciences Department/Health Sciences Center, Federal University of Paraiba, João Pessoa, Paraíba, Brazil*

Correspondence should be addressed to Aline de Freitas Brito; alineebritoo@gmail.com

Received 1 June 2019; Accepted 9 August 2019; Published 24 October 2019

Guest Editor: Albino Carrizzo

The possible mechanism is involved in the effects of *Spirulina platensis* on vascular reactivity. Animals were divided into sedentary group (SG) and sedentary groups supplemented with *S. platensis* at doses of 50 (SG50), 150 (SG150), and 500 mg/kg (SG500). To evaluate reactivity, cumulative concentration-response curves were constructed for phenylephrine and acetylcholine. To evaluate the involvement of the nitric oxide (NO) pathway, aorta tissue was preincubated with L-NAME and a new curve was then obtained for phenylephrine. Biochemical analyses were performed to evaluate nitrite levels, lipid peroxidation, and antioxidant activity. To contractile reactivity, only SG500 ($pD_2 = 5.6 \pm 0.04$ vs. 6.1 ± 0.06, 6.2 ± 0.02, and 6.2 ± 0.04) showed reduction in phenylephrine contractile potency. L-NAME caused a higher contractile response to phenylephrine in SG150 and SG500. To relaxation, curves for SG150 ($pD_2 = 7.0 \pm 0.08$ vs. 6.4 ± 0.06) and SG500 ($pD_2 = 7.3 \pm 0.02$ vs. 6.4 ± 0.06) were shifted to the left, more so in SG500. Nitrite was increased in SG150 and SG500. Lipid peroxidation was reduced, and oxidation inhibition was increased in all supplemented groups, indicating enhanced antioxidant activity. Chronic supplementation with *S. platensis* (150/500 mg/kg) caused a decrease in contractile response and increase in relaxation and nitrite levels, indicating greater NO production, due to decreased oxidative stress and increased antioxidant activity.

1. Introduction

Nowadays, the practice of herbal medicine involves the use of more than 53,000 species of natural products for primary health care [1]. Several of these species are of aquatic origin and have drawn the attention of pharmaceutical research, considering that the aquatic environment is rich in natural resources and many biologically active compounds [2]. One group of aquatic organisms that has been highlighted due to its diverse biological activities is the blue-green algae. They belong to the phylum Cyanobacteria and family Spirulinaceae and are among the photosynthetic prokaryotes found in aquatic ecosystems. Certain species, including *Aphanizomenon flos-aquae*, *Spirulina platensis*, *S. maxima*, *S. fusiformis*, *Spirulina* sp, and *Nostoc comuna* var. sphaeroids Kutzing, have been consumed for centuries by humans [3]. Over time, these microalgae were used as traditional food by some Mexican, African, Native American, and Oriental people [3].

Clement [4] added that *S. platensis* and *S. maxima* have some advantages over other algae, such as pleasant taste, and do not present problems in your digestion and even apparent toxicity to humans, justifying the high consumption of *Spirulina* species by people. But populations of *S. platensis* are mostly found in waters with higher salt concentrations, such as a temporary nursery just before a drought, which makes this alga capable of adapting to different habitats and colonizing certain environments where other microorganisms would find it very difficult or even impossible to live [3], and such conditions characterize northeastern Brazil. *S. platensis* has a high reproduction rate, dividing three times a day, and in the same area, its cultivation can produce 125 times more protein than growing corn or 70 times more than raising cattle [5].

S. platensis, also known as *Arthrospira platensis*, is a blue-green alga with a helical shape and length of 0.2 to 0.5 mm. *S. platensis* has a high protein content (65 to 70% of its dry weight), contains all the essential amino acids, and represents a rich source of vitamin B_{12}, minerals, essential fatty acids, and 15% complex carbohydrates [6, 7], plus photosynthetic pigments that display a variety of pharmacological properties [6, 8, 9].

Because of the above properties, there have been preclinical and clinical studies on the intake of *S. platensis*, showing that it can promote a decrease in serum triglycerides and low-density lipoproteins [10, 11], glycemic control [12, 13], reduction in allergic rhinitis [14, 15], growth of favorable intestinal microflora [16], anticancer [17], anti-inflammatory [13, 18, 19], antihypertensive [20, 21], and antioxidant [19, 21, 22] actions and reduction in endothelial dysfunction [20, 23, 24].

Among the effects attributed to *S. platensis*, antioxidant effects and regulation of endothelial function are important, considering that physiological changes characterized by an increase in vasoconstrictor response, decrease in vasodilator capacity, and increase in the production of reactive oxygen species due to decreased antioxidant enzyme activity are associated with cardiovascular risk factors such as hypertension [25–27].

Accordingly, various studies have investigated the pharmacological effects of a species of *Spirulina* and S. *maxima* and have demonstrated that it improves vascular tone [28, 29], while studies on *S. platensis* are still scarce. Huang et al. [30] reported the effect of supplementation with polysaccharides from *S. platensis* in diabetic rats and found that the contractile response was significantly reduced, while the relaxation response was increased in the aortic rings of these animals. Therefore, we tested the hypothesis that chronic dietary supplementation with freeze-dried powder of *Spirulin platensis* be able to improve the vascular reactivity, antioxidant activity, and endothelial function in the aorta of Wistar rats. Therefore, the objective of this research was to determine the effects of *S. platensis* on vascular reactivity in the isolated aorta of Wistar rats and the possible mechanisms involved in this response.

2. Materials and Methods

2.1. Drugs. Calcium chloride dihydrate ($CaCl_2{\cdot}2H_2O$), potassium chloride (KCl), and sodium bicarbonate ($NaHCO_3$) were purchased from Vetec (Rio de Janeiro, RJ, Brazil). Glucose ($C_6H_{12}O_6$), magnesium sulfate heptahydrate ($MgSO_4{\cdot}7H_2O$), hydrochloric acid (HCl), and monobasic potassium phosphate (KH_2PO_4) were from Nuclear (Porto Alegre, RS, Brazil). Sodium chloride (NaCl) was purchased from Dinâmica (Diadema, SP, Brazil) and acetylcholine chloride (ACh) from Merck (Brazil). Phenylephrine (PHE) was obtained from Pfizer (USA), and Nω-nitro-L-arginine methyl ester (L-NAME) was purchased from Sigma-Aldrich (Brazil). Ethylenediamine tetraacetic acid (EDTA) (1 : 250) came from BioTécnica-Advanced Biotechnology (Brazil), and carbogen mixture (95% O_2 and 5% CO_2) was obtained from White Martins (Brazil). All substances were weighed on an analytical balance, GEHAKA model AG 200 (Sao Paulo, SP, Brazil).

2.2. Animals. Wistar rats (*Rattus norvegicus*), weighing between 250 and 300 g, 2 months old, were obtained from the Professor Thomas George Bioterium from Universidade Federal da Paraíba (UFPB). The animals were maintained under controlled ventilation and temperature (21 ± 1°C) with water ad libitum in a 12 h light-dark cycle (light on from 6 to 18 h). Male Wistar rats (*Rattus norvegicus)* were used, weighing between 250 and 300 g; the animals were obtained from the Prof. Thomas George Bioterium of the Biotechnology Center of the Federal University of Paraiba (UFPB). All experiments were performed between 8 am and 8 pm, according to the guidelines for the ethical use of animals [31]. The experimental protocol was previously approved by Ethics Committee in Animal Use from CBiotec (CEUA/CBiotec) with certificate number 0511/13.

2.3. Preparation of and Supplementation with Spirulina platensis. S. platensis in powder form was obtained from Bio-engineering Dongtai Top Co., Ltd. (Nanjing, China) (lot no. 20130320). A sample was analyzed by the Pharma Nostra Quality Control Laboratory (Anapolis, GO) (lot no. 1308771A) to certify that the extract was obtained from *S. platensis* and was then prepared by Dilecta Manipulation

Drugstore (Joao Pessoa, PB) (lot no. 20121025) for the preparation of the lyophilized powder.

The *S. platensis*-lyophilized powder was dissolved in saline solution (NaCl 0.9%) at doses of 50, 150, and 500 mg/kg. These values were based on the results of the experiments from other studies conducted with spirulina that investigated the anti-inflammatory, antioxidant, and relaxing effect [12, 22, 30, 32]. The supplements were administered for eight weeks for all doses (adapted, [19, 33]). Oral administration was daily between 12:00 pm and 14:00 pm, using stainless steel needles for gavage (BD-12, Insight, Ribeirão Preto, SP) and 5 ml syringes with an accuracy of 0.2 ml (BD, HIGILAB, Joao Pessoa, PB).

2.4. Groups and Supplementation. Animals were divided into sedentary saline (0.9% NaCl, control) and sedentary supplemented with *S. platensis* (50, 150, or 500 mg/kg) groups, using oral administration. Thus, the study was composed of the following groups with 20 rats randomly divided into 4 groups: sedentary saline group (SG, control) and sedentary groups supplemented with *S. platensis* at 50 mg/kg (SG50), 150 mg/kg (SG150), and 500 mg/kg (SG500). After eight weeks of intervention, the animals were anesthetized with thiopental sodium (100 mg/kg body weight) mixed with lidocaine (10 mg/ml) and then decapitated and after euthanized by cervical dislocation followed by exsanguination.

2.5. Aortic Ring Isolation. Animals were euthanized by guillotine, and the aorta was removed, cleaned of connective tissue and fat, immersed in physiological solution at room temperature, and bubbled with carbogen mixture (95% O_2 and 5% CO_2). In order to record the isometric contractions, aortic rings (3-5 mm) were individually suspended in organ baths (6 ml) by strap of stainless steel clips and isometric tension was evaluated by isometric force transducers (TIM-05 model), coupled to an AECAD04F model amplifier and connected to a digital acquisition system with AQCAD version 2.1.6 software to obtain the data and ANCAD software for analysis with a thermostatic pump model Polystat 12002 Cole-Parmer (Vernon Hills) that controlled the organ bath temperature.

The physiological solution of Krebs's solution was used and has the composition (in mM) as follows: NaCl 118.0, KCl 4.6, KH_2PO_4 1.1, $MgSO_4$ 5.7, $CaCl_2$ 2.5, $NaHCO_3$ 25.0, and glucose 11.0. The pH was adjusted to 7.4, and the ileum was stabilized for 1 h under a resting tension of 1 g at 37°C and bubbled with a carbogen mixture [34].

2.6. Concentration-Response Curves. The preparations were equilibrated for one hour, maintained under a rest tension of 1 g, and after the equilibration period, a contraction was induced with 3×10^{-7} M PHE, and during the tonic component, 10^{-6} M ACh was added to verify endothelium integrity [35]. The vascular endothelium was considered intact when the aortic rings showed relaxation equal to or greater than 50% [36]. In some aortic rings, the luminal surface was low rubbed with Krebs wet cotton to remove the endothelial layer. If the relaxation was equal to or less than 10%, the rings were considered devoid of functional endothelium.

To evaluate the contractile response of the rat aorta, after the verification of endothelium integrity, the preparations were washed, and after 30 min, cumulative concentration-response curves to PHE (10^{-10}-10^{-4} M) in aortic rings were constructed for all groups, and to assess the relaxation response of the rat aorta, a new contraction with 3×10^{-7} M PHE was induced, during the tonic component of the contraction ACh (10^{-11}–10^{-4} M) was added cumulatively to the aortic rings of all groups [33, 37].

To assess of the nitric oxide pathway, after the verification of endothelium integrity, preparations were washed, and after 30 min, the organ was preincubated with L-NAME (10^{-4} M), a competitive inhibitor of nitric oxide synthase (NOS) [33, 38, 39], and for 30 min, a cumulative concentration-response curve to PHE (10^{-11}–10^{-3} M) was then induced in the aortic preparations of all groups.

The reactivity was evaluated based on the values of the maximum effect (E_{max}) and the negative logarithm of the molar concentration of a substance that produced 50% of its maximal effect (pCE_{50}) of both contractile agents, calculated from the concentration-response curves obtained.

2.7. Biochemical Measurements. After the animals were euthanized, 2 ml of blood was collected by cardiac puncture [40] and placed in test tubes containing anticoagulant (EDTA) to obtain plasma for determination of nitrite, MDA, and antioxidant activity [29, 40]. The samples were centrifuged at 1207 g for 15 min using a CENTRIBIO 80-2B-15ML centrifuge (Guarulhos, SP, Brazil). The plasma was transferred to Eppendorf tubes and stored at -20°C until analysis, and all analyses were performed within 7 days after blood collection. Nitrite, MDA, and antioxidant activity were measured in aorta fragments 8 mm long; these tissues were quickly removed, cleaned with Krebs solution to remove residual blood, placed in Eppendorf tubes, and stored in a freezer at -80°C until analysis.

2.8. Nitrite Assessment in Plasma and Aorta. Nitrite concentration was determined by the Griess method as described by Green [41]. Accordingly, the Griess reagent was prepared using equal parts of 5% phosphoric acid, 0.1% N-1-naphthyl ethylenediamine (NEED), and 1% sulfanilamide in 5% phosphoric acid and distilled water. A 500 μl volume of plasma or tissue homogenate was added to 500 μl of Griess reagent, and absorbance was read at 532 nm after 10 min. The blank used was 100 μl of the reagent plus 100 μl of 10% potassium phosphate buffer, and sodium nitrite ($NaNO_2$) standards were made by twofold serial dilutions, to obtain 100, 50, 25, 12.5, 6.25, 3.12, and 1.56 mM solutions. Plasma and tissue samples were filtered prior to the assay. A Biospectro SP-220 spectrophotometer (Curitiba, PR, Brazil) was used for absorbance readings.

2.9. Assessment of Lipid Peroxidation. Lipid peroxidation was measured by the chromogenic product of 2-thiobarbituric acid (TBA) reaction with malondialdehyde (MDA) that is a product formed as a result of membrane lipid peroxidation [42]. Tissue samples were homogenized with 10% KCl in 1 : 1 proportions. Tissue homogenate and plasma samples

(250 μl) were incubated in a water bath at 37°C for 60 min. The samples were precipitated with 400 μl of 35% perchloric acid and centrifuged at 26,295 g for 10 min at 4°C. The supernatant was transferred to new Eppendorf tubes, and 400 μl of 0.6% thiobarbituric acid was added, followed by incubation at 95-100°C for 30 min. After cooling, the samples were read at 532 nm. Malondialdehyde concentration in plasma and tissue samples was determined using an MDA standard curve constructed using a standard solution (1 μl of 1,1,3,3-tetramethoxypropane in 70 ml distilled water) diluted in a series of 250, 500, 750, 1000, 1250, 1500, 1750, 2000, 2250, 2500, 2750, and 3000 μl of distilled water. In tissue, the absorbance values obtained were normalized to dry weight present in a given sample volume.

2.10. Evaluation of Antioxidant Activity. The procedure was based on the method described by Brand-Williams et al. [43], where 1.25 mg of DPPH (1,1-diphenyl-2-picrylhydrazyl radical) was dissolved in 100 ml of ethanol, kept under refrigeration, and protected from light (aluminum paper or amber glass). Then, 3.9 ml of DPPH solution was added with 100 μl of the supernatant ileum homogenate on appropriate centrifuge tubes, vortexed, and allowed to stand for 30 min. They were centrifuged at 1207 g for 15 min at 20°C, and the absorbance of the supernatant was read at 515 nm. The results were expressed as percentage of the inhibition of oxidation, where AOA (antioxidant activity) = 100 − ((DPPH · R) T/(DPPH · R) B 100), where (DPPH · R) and (DPPH · R) B correspond to the concentration of DPPH$^{\cdot}$ remaining after 30 min, measured in the sample (T) and blank (B) prepared with distilled water. Tissue samples were homogenized with 10% KCl in 1 : 1 proportions. In tissue, the absorbance values obtained were normalized to dry weight present in a given sample volume.

2.11. Data Analysis. The functional results obtained were expressed as mean and standard error of the mean (S.E.M., $n = 5$), while the biochemical results were expressed as mean and standard deviation (S.D., $n = 10$). These results were statistically analyzed using two-way analysis of variance (ANOVA) followed by Bonferroni's posttest, and the differences between the means were considered significant when $p < 0.05$. pCE_{50} values were calculated by nonlinear regression [44], and E_{max} was obtained by averaging the maximum percentages of contraction or relaxation. All results were analyzed by the GraphPad Prism version 5.01 (GraphPad Software Inc., San Diego CA, USA).

3. Results

3.1. Effect of Supplementation with S. platensis on Contractile Response Induced by PHE in the Presence of Functional Endothelium in Isolated Rat Aorta. Supplementation with *S. platensis* at doses of 50 ($pCE_{50} = 6.2 \pm 0.02$) and 150 mg/kg ($pCE_{50} = 6.2 \pm 0.04$) did not alter the contractile reactivity of the rat aorta to PHE compared with SG ($pCE_{50} = 6.1 \pm 0.06$). However, rat treatment with 500 mg/kg *S. platensis* ($pCE_{50} = 5.6 \pm 0.04$) shifted the cumulative concentration-response curve to PHE to the right, indicating a decrease in the contractile reactivity of the rat aorta with functional endothelium (Figure 1).

3.2. Effect of Supplementation with S. platensis on Contractile Response Induced by PHE in the Absence of Functional Endothelium in Isolated Rat Aorta. Supplementation with *S. platensis* at doses of 50 ($pCE_{50} = 7.0 \pm 0.01$), 150 ($pCE_{50} = 7.1 \pm 0.03$), and 500 mg/kg ($pCE_{50} = 7.0 \pm 0.04$) did not alter contractile reactivity to PHE in the rat aorta without functional endothelium compared to SG ($pCE_{50} = 7.1 \pm 0.04$) (Figure 2).

3.3. Effect of Supplementation with S. platensis on Relaxation Induced by ACh in Isolated Rat Aorta. The relaxation curve induced by cumulative addition of ACh in the rat aorta with functional endothelium and precontracted with 3×10^{-7} M PHE from SG ($pCE_{50} = 6.4 \pm 0.06$) was not altered in SG50 ($pCE_{50} = 6.6 \pm 0.1$) (Figure 3). However, the relaxant potency of ACh was increased when the animals received supplementation with *S. platensis* at doses of 150 ($pCE_{50} = 7.0 \pm 0.08$) and 500 mg/kg ($pCE_{50} = 7.3 \pm 0.02$) (Figure 3), where a greater relaxant potency was found in the aorta of animals supplemented with *S. platensis* at 500 compared to 150 mg/kg. Supplementation with *S. platensis* did not alter the maximum effective relaxation of aortic rings ($E_{max} = 100\%$).

3.4. Effect of Supplementation with S. platensis on Cumulative Contractions Induced by PHE in the Absence and Presence of L-NAME. In the presence of L-NAME, cumulative concentration-response curves to PHE in SG ($pCE_{50} = 7.1 \pm 0.08$) were shifted to the left in rats supplemented with *S. platensis* at doses of 50 ($pCE_{50} = 7.1 \pm 0.03$), 150 ($pCE_{50} = 7.6 \pm 0.07$), and 500 mg/kg ($pCE_{50} = 8.2 \pm 0.03$) compared to SG in the absence of L-NAME ($pCE_{50} = 6.1 \pm 0.06$) (Figure 4). In addition, treatment with 150 and 500 mg/kg *S. platensis* increased the contractile potency of PHE compared to SG and SG50 in the presence of L-NAME or SG in the absence of L-NAME (Figure 4).

3.5. Effect of Supplementation with S. platensis on the Production of Nitrite in Plasma and Rat Aorta. Plasma nitrite level was increased when the animals received supplementation with *S. platensis* at doses of 150 and 500 mg/kg, and the highest level was found in animals supplemented with 500 mg/kg compared to the lower doses (Table 1). The nitrite level in the aorta of animals that received supplementation with 150 mg/kg *S. platensis* increased compared to SG. However, the highest nitrite in the aorta was found in animals supplemented with 500 mg/kg (Table 1).

3.6. Effect of Supplementation with S. platensis on Lipid Peroxidation. Supplementation with *S. platensis* at doses of 150 and 500 mg/kg caused a significant reduction in lipid peroxidation in plasma. But the production of MDA in animals supplemented with 500 mg/kg *S. platensis* was lower than in those in SG, SG50, and SG150. Similarly, the production of MDA in the aorta was significantly reduced when the animals were supplemented with 150 and 500 mg/kg *S. platensis* compared to the lowest dose and control, but

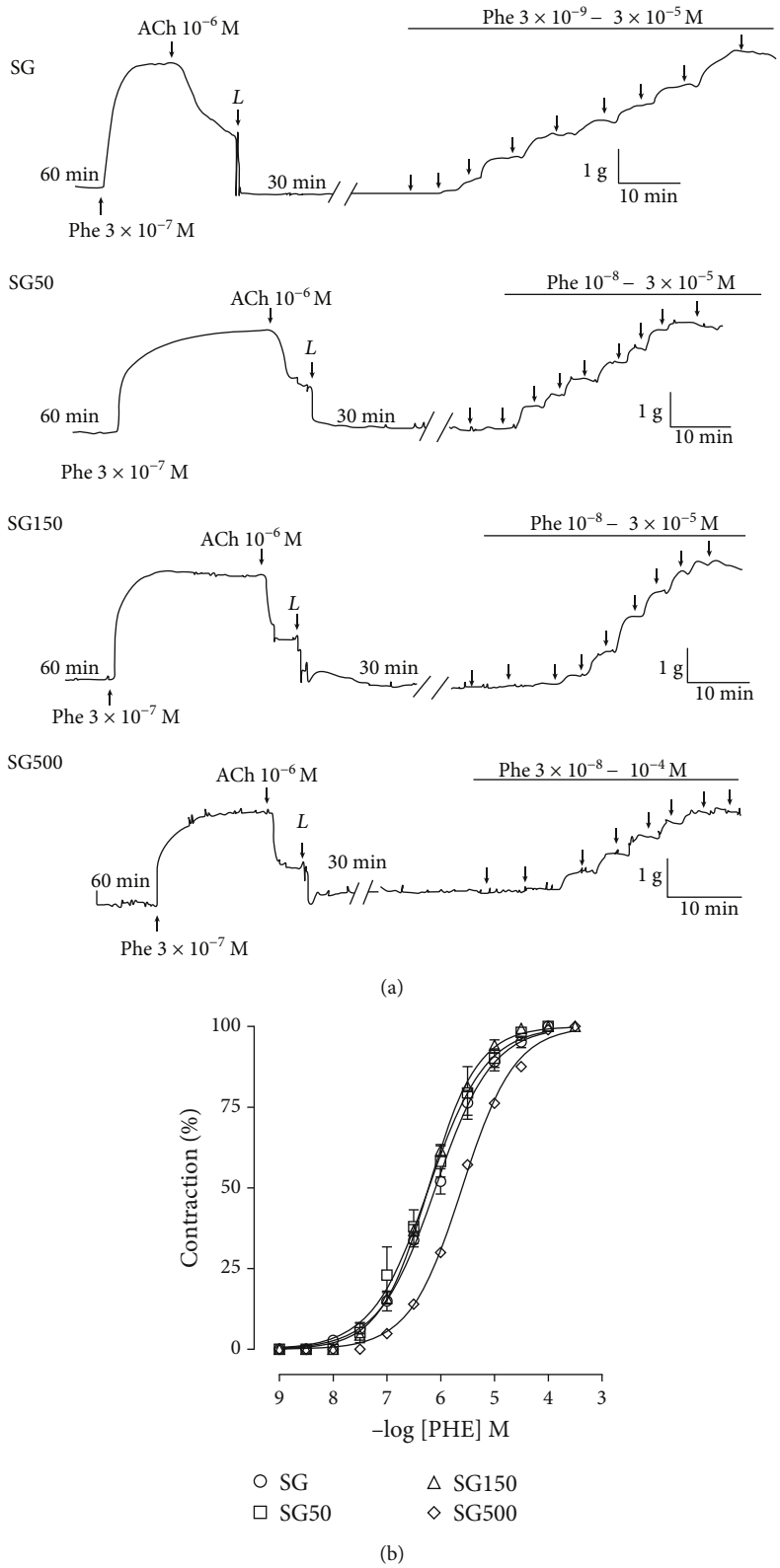

Figure 1: Representative traces (a) and contractile effect (b) of PHE in SG (○), SG50 (□), SG150 (Δ), and SG500 (◊) groups in the rat aorta in the presence of endothelium. The symbols and vertical bars represent the mean and S.E.M., respectively ($n = 05$ indicates the number of samples per treatment). PHE: phenylephrine. Sedentary saline group (SG) and sedentary groups supplemented with *S. platensis* at 50 mg/kg (SG50), 150 mg/kg (SG150), and 500 mg/kg (SG500). Two-way ANOVA followed by Bonferroni's posttest, $^{*}p < 0.01$ (SG vs. SG500), $^{\#}p < 0.01$ (SG50 vs. SG500), $^{\dagger}p < 0.01$ (SG150 vs. SG500).

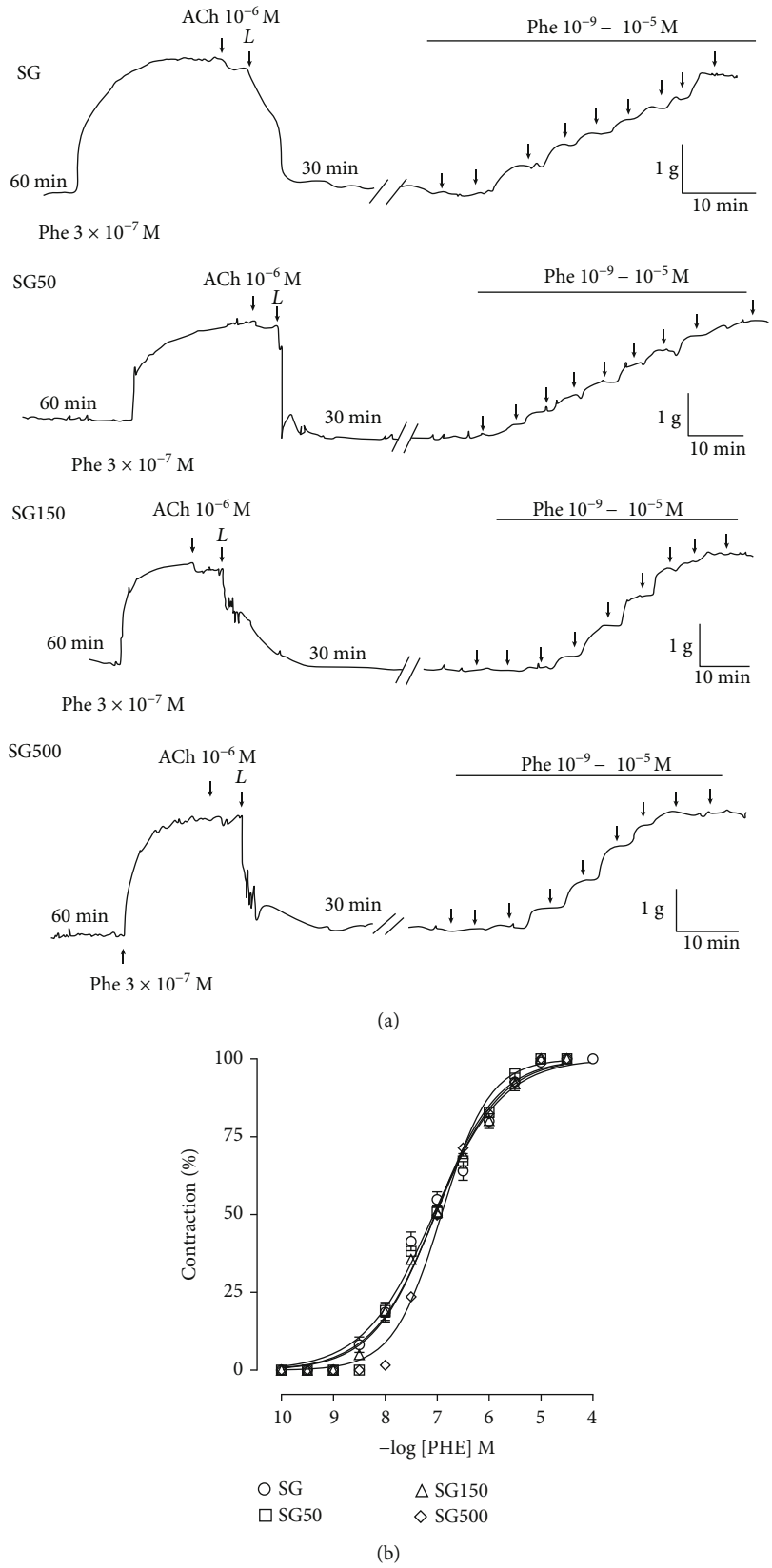

Figure 2: Representative traces (a) and contractile effect (b) of PHE in SG (○), SG50 (□), SG150 (Δ), and SG500 (◊) groups in the rat aorta in the absence of endothelium. The symbols and vertical bars represent the mean and S.E.M., respectively ($n = 05$ indicates the number of samples per treatment). PHE: phenylephrine. Sedentary saline group (SG) and sedentary groups supplemented with *S. platensis* at 50 mg/kg (SG50), 150 mg/kg (SG150), and 500 mg/kg (SG500). Two-way ANOVA followed by Bonferroni's posttest.

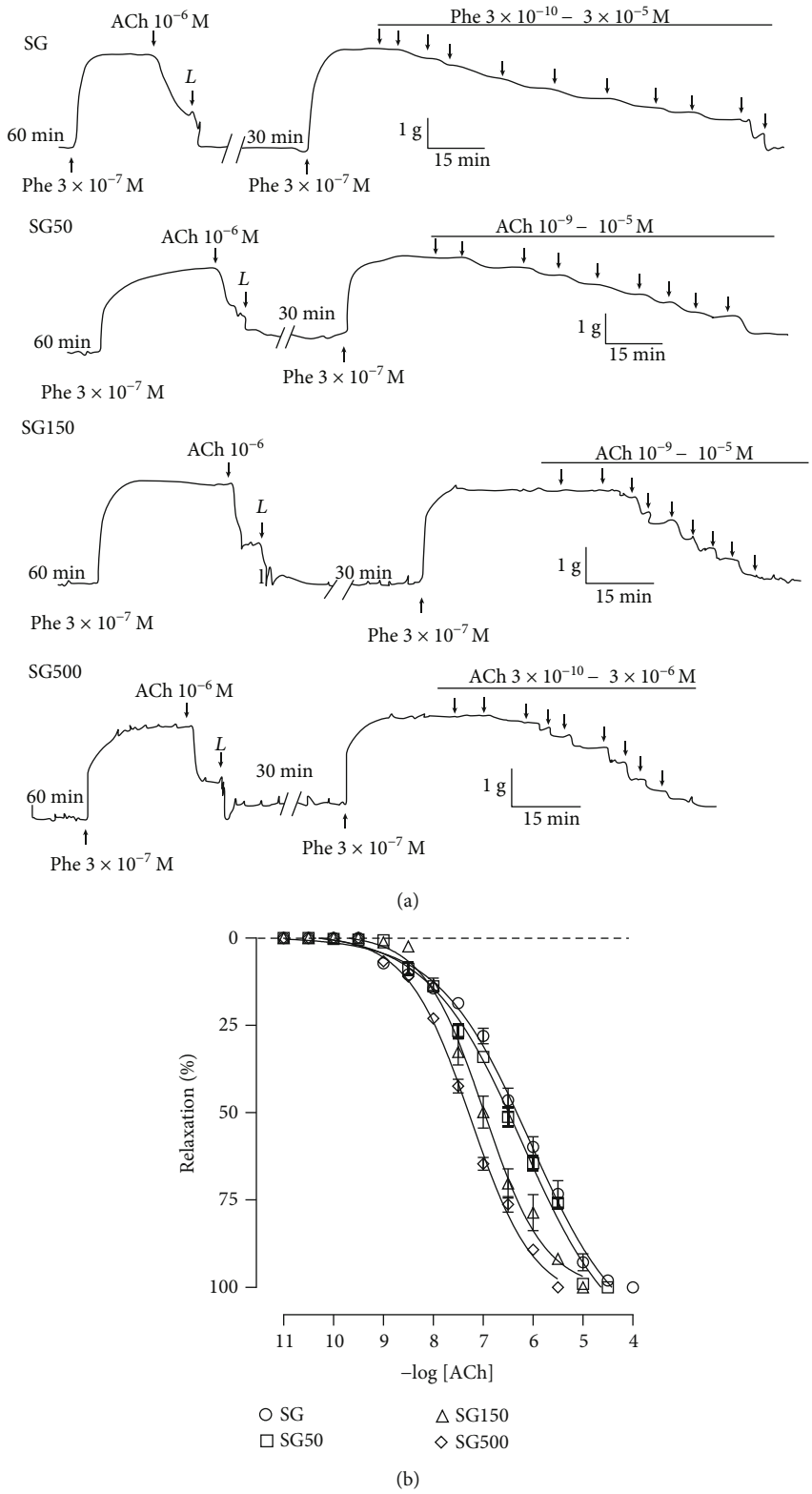

Figure 3: Representative traces (a) and relaxant effect (b) of ACh on the tonic contractions induced by 3×10^{-7} M PHE in SG (○), SG50 (□), SG150 (Δ), and SG500 (◊) groups in the rat aorta in the presence of endothelium. The symbols and vertical bars represent the mean and S.E.M., respectively ($n = 05$ indicates the number of samples per treatment). Ach: acetylcholine. Sedentary saline group (SG) and sedentary groups supplemented with *S. platensis* at 50 mg/kg (SG50), 150 mg/kg (SG150), and 500 mg/kg (SG500). Two-way ANOVA followed by Bonferroni's posttest. $^{*}p < 0.01$ (SG vs. SG150, SG vs. SG500), $^{\#}p < 0.01$ (SG50 vs. SG150, SG50 vs. SG500), $^{\dagger}p < 0.01$ (SG150 vs. SG500).

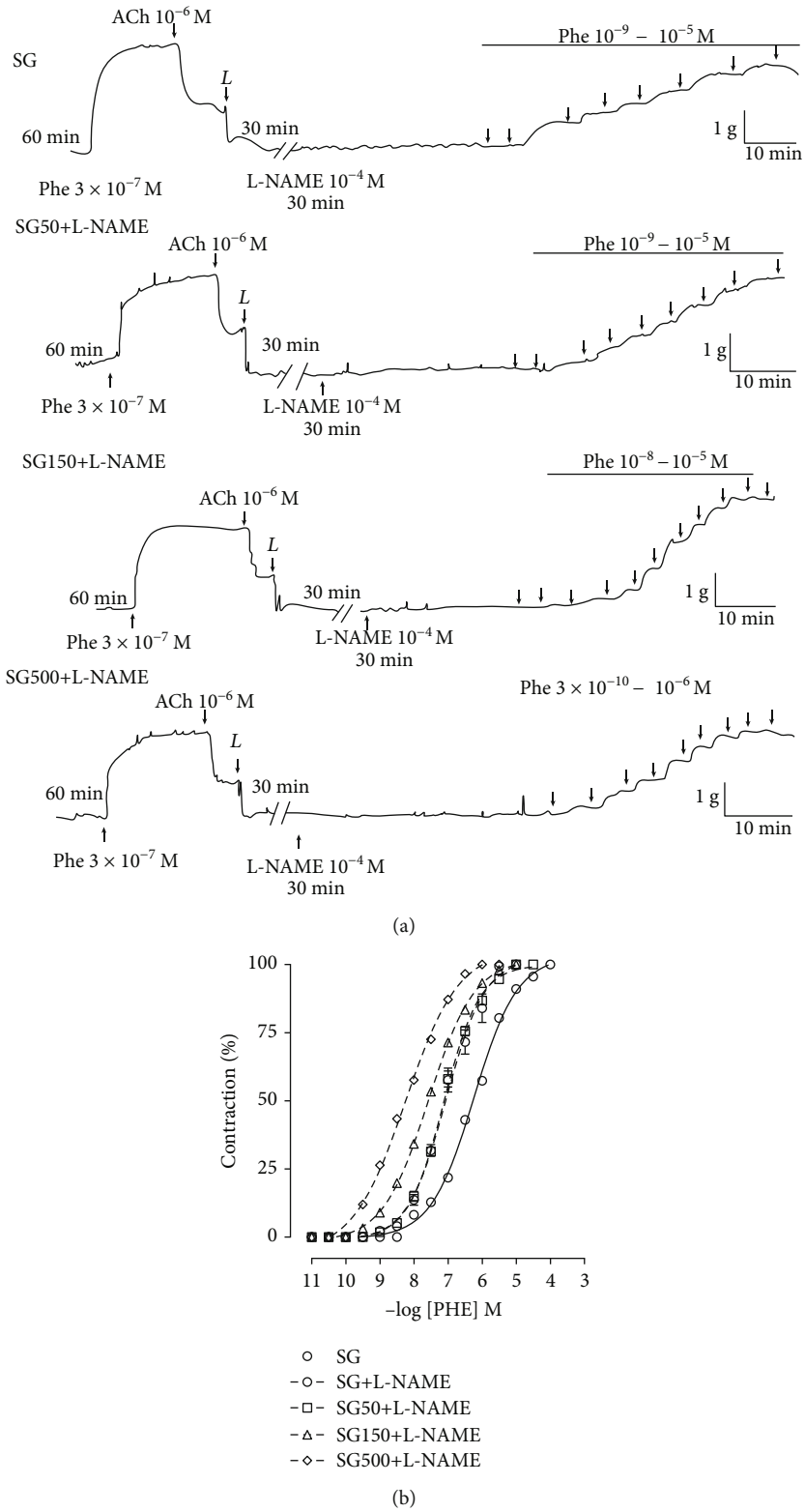

Figure 4: Representative traces (a) and contractile effect (b) of PHE in the presence of L-NAME in SG (○), SG50 (□), SG150 (Δ), and SG500 (◊) groups in the rat aorta. The symbols and vertical bars represent the mean and S.E.M., respectively ($n = 05$ indicates the number of samples per treatment). L-NAME: Nω-nitro-L-arginine methyl ester. Sedentary saline group (SG) and sedentary groups supplemented with *S. platensis* at 50 mg/kg (SG50), 150 mg/kg (SG150), and 500 mg/kg (SG500). Two-way ANOVA followed by Bonferroni's posttest, $^{*}p < 0.001$ (SG vs. SG+L-NAME, SG vs. SG50+L-NAME, SG vs. SG150+L-NAME, SG vs. SG500+L-NAME), $^{\#}p < 0.01$ (SG+L-NAME vs. SG150+L-NAME, SG+L-NAME vs. SG500+L-NAME), $^{\dagger}p < 0.01$ (SG50+L-NAME vs. SG150+L-NAME, SG50+L-NAME vs. SG500 +L-NAME), $^{\S}p < 0.01$ (SG150+L-NAME vs. SG500+L-NAME).

Table 1: Concentration of nitrite in the blood plasma and aorta from the SG, SG50, SG150, and SG500 groups.

Groups	Nitrite (μM)	
	Plasma	Aorta
SG	54 ± 11	28 ± 6
SG50	59 ± 8	31 ± 10
SG150	$70 \pm 7^{*\#}$	$43 \pm 6^{*}$
SG500	$88 \pm 7^{*\#\dagger}$	$71 \pm 7^{*\#\dagger}$

The values represent the mean and S.D., respectively ($n = 5$ indicates the number of samples per treatment). Sedentary saline group (SG) and sedentary groups supplemented with *S. platensis* at 50 mg/kg (SG50), 150 mg/kg (SG150), and 500 mg/kg (SG500). Two-way ANOVA followed by Bonferroni's posttest, $^{*}p < 0.05$ (SG vs. groups), $^{\#}p < 0.05$ (SG50 vs. SG150 and SG500), $^{\dagger}p < 0.01$ (SG150 vs. SG500).

Table 2: Lipid peroxidation in the blood plasma and aorta from the SG, SG50, SG150, and SG500 groups.

Groups	MDA	
	Plasma (nmol/l)	Aorta (μM/g)
SG	8.4 ± 1.0	26 ± 7
SG50	8.2 ± 0.7	24 ± 2
SG150	$6.8 \pm 0.7^{*}$	$18 \pm 2^{*}$
SG500	$5.0 \pm 0.1^{*\#\dagger}$	$10 \pm 3^{*\#\dagger}$

The values represent the mean and S.D., respectively ($n = 10$ indicates the number of samples per treatment). Sedentary saline group (SG) and sedentary groups supplemented with *S. platensis* at 50 mg/kg (SG50), 150 mg/kg (SG150), and 500 mg/kg (SG500). Two-way ANOVA followed by Bonferroni's posttest, $^{*}p < 0.05$ (SG vs. groups), $^{\#}p < 0.05$ (SG50 vs. SG150 and SG500), $^{\dagger}p < 0.01$ (SG150 vs. SG500).

supplementation with the 500 mg/kg dose showed the greatest reduction in MDA production compared to the other groups (Table 2).

3.7. Effect of Supplementation with S. platensis on Antioxidant Activity. Only supplementation with *S. platensis* at the dose of 500 mg/kg increased the percentage of inhibition of the plasma oxidation when compared to SG, SG50, and SG150. Similarly, the percentage of inhibition of oxidation in the aorta was increased only when the animals were supplemented with the 500 mg/kg dose compared to other groups (Table 3).

Table 3: Percentage of oxidation inhibition in the blood plasma and aorta from the SG, SG50, SG150, and SG500 groups.

Groups	Oxidation inhibition (%)	
	Plasma	Aorta
SG	50 ± 5	12 ± 4
SG50	54 ± 4	14 ± 2
SG150	62 ± 3	17 ± 2
SG500	$70 \pm 2^{*\#\dagger}$	$27 \pm 2^{*\#\dagger}$

The values represent the mean and S.D., respectively ($n = 10$ indicates the number of samples per treatment). Sedentary saline group (SG) and sedentary groups supplemented with *S. platensis* at 50 mg/kg (SG50), 150 mg/kg (SG150), and 500 mg/kg (SG500). Two-way ANOVA followed by Bonferroni's posttest, $^{*}p < 0.05$ (SG vs. groups), $^{\#}p < 0.05$ (SG50 vs. SG150 and SG500), $^{\dagger}p < 0.01$ (SG150 vs. SG500).

4. Discussion

The present study demonstrated that chronic supplementation with *Spirulina platensis* at doses of 150 and 500 mg/kg caused an increase in the relaxation response to ACh and a decrease in the contractile reactivity to PHE in the rat aorta, and the mechanism of action seemed to involve the release of nitric oxide, reducing oxidative stress.

We found in the present study the supplementation with a lyophilized powder of *S. platensis*, which is one of the most common forms of this alga in numerous products sold in the market; *S. platensis* has the ability to modulate both in chronic vascular tone and lipid peroxidation in the aorta of Wistar rats.

Previous studies have shown both a reduction in contractile activity and enhanced relaxation in isolated aortic rings. However, most of these previous studies have investigated the *in vitro* effects of the ethanol extract of *S. maxima* in healthy and obese rats [28, 45]. In addition, Huang et al. [30] demonstrated that polysaccharides isolated from *S. platensis* alter vascular response in aortic rings from diabetic rats supplemented for six weeks. Carrizzo et al. [46] demonstrated which the peptidic hydrolyzate of *Spirulina platensis*, and in detail a decapeptide, is able to induce vasorelaxation both on normotensive mice and both on SHR through PI3K/Akt/eNOS-dependent mechanism.

Corroborating these results, our study also found that chronic dietary supplementation with *S. platensis* at doses of 150 and 500 mg/kg increased relaxation response to ACh, and that the 500 mg/kg dose also decreased contractile reactivity to PHE, which was totally dependent on the functional endothelium. The latter finding suggested that *S. platensis* altered the reactivity of the aorta promoting vascular relaxation in a dose-dependent manner that required the presence of factors derived from the vascular endothelium, even in healthy animals. In the study of Huang et al. [30], *S. platensis* polysaccharides were administered orally at doses of 12.261, 36.783, and 110.349 mg/kg in diabetic rats, and the authors reported that improvement in vascular reactivity occurred only with the highest dose. In our study, we also identified an increase in relaxation response and reduction in contractile response at a dose of 150 mg/kg, which was close to that active dose reported by Huang et al. [30], where the diabetic rats showed endothelial dysfunction. Our animals were healthy, and thus, the present results suggest that supplementation with the lyophilized powder of *S. platensis* is quite effective for the prevention of endothelial dysfunction.

In the present study, we also determined whether the reduction of contractile activity would be dependent on the mechanisms modulated by the endothelium. The results showed that the inhibition of contractile activity caused by *S. platensis* was endothelium-dependent, suggesting the participation of the NO pathway. The participation of endothelium in reducing contractile activity was accompanied by a significant increase in nitrite level in both plasma and aorta samples obtained from the animals supplemented with 500 mg/kg *S. platensis*; however, the dose of 150 mg/kg was still insufficient for this behavior to also reflect a reduction

in vasoconstriction, confirming the dose-dependent effect. In addition, these data reinforced the importance of the endothelium in the effects observed with *S. platensis* and showed that these responses in smooth muscle were modulated by an increase in the bioavailability of NO. In view of these results, we can hypothesize that the constituents present in *S. platensis*, such as phycocyanin, can chronically increase the expression of endothelial nitric oxide synthase and consequently promote greater bioavailability of nitric oxide [47].

These results corroborated previous studies that found that *S. maxima* improved relaxant activity and reduced contractile response. Paredes-Carbajal et al. [28] showed that the ethanol extract of *S. maxima*, tested *in vitro*, caused a decrease in the contractile potency of PHE and an increase in relaxation response in rat aortic rings. In the endothelium-intact rings, these effects were blocked by L-NAME, suggesting that *S. maxima* extract increased the synthesis/release of NO [28]. Using the same pharmacological procedures, but in aortic rings of obese rats, Mascher et al. [45] and Juárez-Oropeza et al. [33] found similar results in relation to both relaxing and contractile response, such as the participation of the NO pathway [28, 33, 45]. Despite that possible mechanisms have been investigated in studies of *S. maxima*, in the study using the polysaccharides of *S. platensis*, no mechanism was investigated [30].

Oxidative stress was another mechanism that could also participate in the modulation of the response found in our results. The endothelial dysfunction is mainly a result of impaired NO availability, because a decrease in production and/or increase in degradation of NO leads to an increase in the production of reactive oxygen species such as $O_2^{\cdot-}$, resulting in an increase in contractile response and/or reduced vasodilator response [48]. Accordingly, it was found that a significant decrease in malondialdehyde (MDA) in the plasma and aorta for the groups tested occurred with 150 and 500 mg/kg *S. platensis*. On the other hand, oxidation inhibition was also significantly increased in the plasma and aorta, but this increase occurred only at the dose of 500 mg/kg. Thus, these results reinforced the notion that reduced oxidative stress is essential for decreased contractile reactivity and increased relaxation response, as observed with *S. platensis* supplementation, suggesting that these responses are modulated by an increase in the antioxidant defense of the animals.

Previous data have shown that phycocyanin present in *S. platensis* stands out because of its high antioxidant capacity and scavenging of free radicals due to its stability [49] and inhibiting the formation of superoxide radicals by reducing the expression of the p22phox subunit of nicotinamide adenine dinucleotide phosphate oxidase [50, 51]. As carotenoids are essential for the regulation of superoxide dismutase and catalase and blocking free radicals by chelation of metal ions, they are able to prevent the lipid peroxidation [52]. Furthermore, B and E vitamins also act as antioxidants by capturing radicals and as metal-chelating agents [52].

However, it is important to observe that the techniques used to the determination of lipid peroxidation and antioxidant activity are accepted in the literature, but nonspecifically did not make it possible to understand which antioxidant compounds the *Spirulin platens* influenced.

In view of the changes in vascular reactivity and the benefits provided by dietary supplementation with *S. platensis*, it is worthwhile to investigate the potential of *S. platensis* as a nutraceutical food and dietary supplement to provide an alternative to the region's economy. However, further studies are necessary to extend our data, for example, in animals with certain diseases such as hypertension, diabetes, and/or obesity. Since the results of this study indicated that *S. platensis* could be used as a product with therapeutic targets, the next step proposed is to directly investigate the effect of dietary supplementation with *S. platensis* in humans to confirm that our findings are translatable or directly applicable.

5. Conclusion

This study evaluated the effect of feed supplementation with *S. platensis* on smooth muscle reactivity of the aorta isolated from healthy rats and the participation of the antioxidant system. It can be concluded that chronic supplementation with *S. platensis* at doses of 150 and 500 mg/kg alters the reactivity of the rat aorta resulting in a decrease in contractile response to PHE as well as an increase in relaxation response to Ach. The mechanisms underlying these effects on contractile and relaxation responses of the rat aorta involved presence of factors derived from vascular endothelium, increased bioavailability of NO, reduced lipid peroxidation, and increased antioxidant activity in both the plasma and aorta of healthy rats.

Abbreviations

Ach:	Acetylcholine
DPPH:	1,1-diphenyl-2-picrylhydrazyl radical
EDTA:	Ethylenediamine tetraacetic acid
E_{max}:	Maximum effect
L-NAME:	Nω-nitro-L-arginine methyl ester
MDA:	Malondialdehyde
NO:	Nitric oxide
NOS:	Nitric oxide synthase
PHE:	Phenylephrine
S.E.M.:	Standard error of the mean
SG:	Sedentary saline group
SG150:	Sedentary groups supplemented with *S. platensis* at 150 mg/kg
SG50:	Sedentary groups supplemented with *S. platensis* at 50 mg/kg
SG500:	Sedentary groups supplemented with *S. platensis* at 500 mg/kg
TBARS:	Thiobarbituric acid reactive substances.

Data Availability

The hypothesis and review data used to support the findings of this study are included within the article.

Conflicts of Interest

The authors declare that there is no conflict of interest regarding the publication of this paper.

Acknowledgments

The authors thank the Coordenação de Aperfeiçoamento de Pessoal de Nível Superior (CAPES) for the support to postgraduation activities by the Program of Academic Excellence (PROEX) and Portal of Periodicals, the Conselho Nacional de Desenvolvimento Científico e Tecnológico (CNPq) for the scholarship granted and approved project (protocol 433232/2016-1), and the Fundação de Apoio à Pesquisa do Estado da Paraíba (FAPESQ-PB) for their financial support and Federal University of Paraíba for logistical support.

References

[1] S. Y. Pan, G. Litscher, S. H. Gao et al., "Historical perspective of traditional indigenous medical practices: the current renaissance and conservation of herbal resources," *Evidence-Based Complementary and Alternative Medicine*, vol. 2014, Article ID 525340, 20 pages, 2014.

[2] M. Greque de Morais, E. Greque de Morais, B. da Silva Vaz, C. F. Gonçalves, C. Lisboa, and J. A. V. Costa, "Nanoencapsulation of the bioactive compounds of spirulina with a microalgal biopolymer coating," *Journal of Nanoscience and Nanotechnology*, vol. 16, no. 1, pp. 81–91, 2016.

[3] O. Ciferri, "Spirulina, the edible microorganism," *Microbiological Reviews*, vol. 47, no. 4, pp. 551–578, 1983.

[4] G. Clement, "Une nouvelle algue alimentaire: La Spiruline," *Revist Inst Pasteur Lyon*, vol. 4, pp. 103–114, 1971.

[5] G. P. Rogatto, C. A. M. de Oliveira, J. W. dos Santos et al., "Influência da ingestão de espirulina sobre o metabolismo de ratos exercitados," *Revista Brasileira de Medicina do Esporte*, vol. 10, no. 4, pp. 258–263, 2004.

[6] N. Asmathunisha and K. Kathiresan, "A review on biosynthesis of nanoparticles by marine organisms," *Colloids and Surfaces B: Biointerfaces*, vol. 103, pp. 283–287, 2013.

[7] M. F. de Jesus Raposo, R. M. S. C. de Morais, and A. M. M. B. de Morais, "Health applications of bioactive compounds from marine microalgae," *Life Sciences*, vol. 93, no. 15, pp. 479–486, 2013.

[8] C. S. Ku, Y. Yang, Y. Park, and J. Lee, "Health benefits of blue-green algae: prevention of cardiovascular disease and nonalcoholic fatty liver disease," *Journal of Medicinal Food*, vol. 16, no. 2, pp. 103–111, 2013.

[9] R. J. Marles, M. L. Barrett, J. Barnes et al., "United States pharmacopeia safety evaluation of spirulina," *Critical Reviews in Food Science and Nutrition*, vol. 51, no. 7, pp. 593–604, 2011.

[10] E. E. Mazokopakis, I. K. Starakis, M. G. Papadomanolaki, N. G. Mavroeidi, and E. S. Ganotakis, "The hypolipidaemic effects of spirulina (*Arthrospira platensis*) supplementation in a Cretan population: a prospective study," *Journal of the Science of Food and Agriculture*, vol. 94, no. 3, pp. 432–437, 2014.

[11] S. Nagaoka, K. Shimizu, H. Kaneko et al., "A novel protein C-phycocyanin plays a crucial role in the hypocholesterolemic action of *Spirulina platensis* concentrate in rats," *The Journal of Nutrition*, vol. 135, no. 10, pp. 2425–2430, 2005.

[12] I. P. Joventino, H. G. R. Alves, L. C. Neves et al., "The microalga *Spirulina platensis* presents anti-inflammatory action as well as hypoglycemic and hypolipidemic properties in diabetic rats," *Journal of Complementary and Integrative Medicine*, vol. 9, no. 1, pp. 1553–3840, 2012.

[13] P. Parikh, U. Mani, and U. Iyer, "Role of *Spirulina* in the control of glycemia and lipidemia in type 2 diabetes mellitus," *Journal of Medicinal Food*, vol. 4, no. 4, pp. 193–199, 2001.

[14] A. Kulshreshtha, J. Anish Zacharia, U. Jarouliya, P. Bhadauriya, G. B. K. S. Prasad, and P. S. Bisen, "Spirulina in health care management," *Current Pharmaceutical Biotechnology*, vol. 9, no. 5, pp. 400–405, 2008.

[15] D. Remirez, N. Ledón, and R. González, "Role of histamine in the inhibitory effects of phycocyanin in experimental models of allergic inflammatory response," *Mediators of Inflammation*, vol. 11, no. 2, 85 pages, 2002.

[16] J. Lu, D. F. Ren, Y. L. Xue, Y. Sawano, T. Miyakawa, and M. Tanokura, "Isolation of an antihypertensive peptide from alcalase digest of *Spirulina platensis*," *Journal of Agricultural and Food Chemistry*, vol. 58, no. 12, pp. 7166–7171, 2010.

[17] J. Lu, Y. Sawano, T. Miyakawa et al., "One-week antihypertensive effect of Ile-Gln-Pro in spontaneously hypertensive rats," *Journal of Agricultural and Food Chemistry*, vol. 59, no. 2, pp. 559–563, 2011.

[18] R. Koníčková, K. Vaňková, J. Vaníková et al., "Anti-cancer effects of blue-green alga *Spirulina platensis*, a natural source of bilirubin-like tetrapyrrolic compounds," *Annals of Hepatology*, vol. 13, no. 2, pp. 273–283, 2014.

[19] H. L. Wu, T. F. Chen, X. Yin, and W. J. Zheng, "Spectrometric characteristics and underlying mechanisms of protective effects of selenium on Spirulina platensis against oxidative stress," *Guang Pu Xue Yu Guang Pu Fen Xi*, vol. 32, no. 3, pp. 749–754, 2012.

[20] A. Miczke, M. Szulińska, R. Hansdorfer-Korzon et al., "Effects of spirulina consumption on body weight, blood pressure, and endothelial function in overweight hypertensive Caucasians: a double-blind, placebo-controlled, randomized trial," *European Review for Medical and Pharmacological Sciences*, vol. 20, no. 1, pp. 150–156, 2016.

[21] J. Zheng, T. Inoguchi, S. Sasaki et al., "Phycocyanin and phycocyanobilin from *Spirulina platensis* protect against diabetic nephropathy by inhibiting oxidative stress," *American Journal of Physiology-Regulatory, Integrative and Comparative Physiology*, vol. 304, no. 2, pp. R110–R120, 2013.

[22] J.-H. Hwang, I. T. Lee, K. C. Jeng et al., "*Spirulina* prevents memory dysfunction, reduces oxidative stress damage and augments antioxidant activity in senescence-accelerated mice," *Journal of Nutritional Science and Vitaminology*, vol. 57, no. 2, pp. 186–191, 2011.

[23] T. Kaji, Y. Fujiwara, C. Hamada et al., "Inhibition of cultured bovine aortic endothelial cell proliferation by sodium spirulan, a new sulfated polysaccharide isolated from *Spirulina platensis*," *Planta Medica*, vol. 68, no. 6, pp. 505–509, 2002.

[24] T. Kaji, Y. Fujiwara, Y. Inomata et al., "Repair of wounded monolayers of cultured bovine aortic endothelial cells is inhibited by calcium spirulan, a novel sulfated polysaccharide isolated from *Spirulina platensis*," *Life Sciences*, vol. 70, no. 16, pp. 1841–1848, 2002.

[25] Y. Higashi, Y. Kihara, and K. Noma, "Endothelial dysfunction and hypertension in aging," *Hypertension Research*, vol. 35, no. 11, pp. 1039–1047, 2012.

[26] R. Rodrigo, J. González, and F. Paoletto, "The role of oxidative stress in the pathophysiology of hypertension," *Hypertension Research*, vol. 34, no. 4, pp. 431–440, 2011.

[27] A. Virdis, M. Fritsch Neves, E. Duranti, G. Bernini, and S. Taddei, "Microvascular endothelial dysfunction in obesity and hypertension," *Current Pharmaceutical Design*, vol. 19, no. 13, pp. 2382–2389, 2013.

[28] M. C. Paredes-Carbajal, P. V. Torres-Durán, J. C. Díaz-Zagoya, D. Mascher, and M. A. Juárez-Oropeza, "Effects of the ethanolic extract of *Spirulina maxima* on endothelium dependent vasomotor responses of rat aortic rings," *Journal of Ethnopharmacology*, vol. 75, no. 1, pp. 37–44, 2001.

[29] A. S. Da Silva, F. C. Paim, R. C. V. Santos et al., "Nitric oxide level, protein oxidation and antioxidant enzymes in rats infected by *Trypanosoma evansi*," *Experimental Parasitology*, vol. 132, no. 2, pp. 166–170, 2012.

[30] Z. X. Huang, X. T. Mei, D. H. Xu, S. B. Xu, and J. Y. Lv, "Protective effects of polysacchride of Spirulina platensis and Sargassum thunbeergii on vascular of alloxan induced diabetic rats," *Zhongguo Zhong Yao Za Zhi*, vol. 30, no. 3, pp. 211–215, 2005.

[31] C. M. Sherwin, S. B. Christiansen, I. J. Duncan et al., "Guidelines for the ethical use of animals in applied ethology studies," *Applied Animal Behaviour Science*, vol. 81, no. 3, pp. 291–305, 2003.

[32] D. Banji, O. J. F. Banji, N. G. Pratusha, and A. R. Annamalai, "Investigation on the role of *Spirulina platensis* in ameliorating behavioural changes, thyroid dysfunction and oxidative stress in offspring of pregnant rats exposed to fluoride," *Food Chemistry*, vol. 140, no. 1-2, pp. 321–331, 2013.

[33] M. A. Juárez-Oropeza, D. Mascher, P. V. Torres-Durán, J. M. Farias, and M. C. Paredes-Carbajal, "Effects of dietary *Spirulina* on vascular reactivity," *Journal of Medicinal Food*, vol. 12, no. 1, pp. 15–20, 2009.

[34] B. M. Altura and B. T. Altura, "Differential effects of substrate depletion on drug-induced contractions of rabbit aorta," *American Journal of Physiology-Legacy Content*, vol. 219, no. 6, pp. 1698–1705, 1970.

[35] R. F. Furchgott and J. V. Zawadzki, "The obligatory role of endothelial cells in the relaxation of arterial smooth muscle by acetylcholine," *Nature*, vol. 288, no. 5789, pp. 373–376, 1980.

[36] M. Ajay, A. U. H. Gilani, and M. R. Mustafa, "Effects of flavonoids on vascular smooth muscle of the isolated rat thoracic aorta," *Life Sciences*, vol. 74, no. 5, pp. 603–612, 2003.

[37] E. Heylen, F. Guerrero, J. Mansourati, M. Theron, S. Thioub, and B. Saïag, "Effect of training frequency on endothelium-dependent vasorelaxation in rats," *European Journal of Cardiovascular Prevention and Rehabilitation*, vol. 15, no. 1, pp. 52–58, 2008.

[38] D. Nunes Guedes, D. F. Silva, J. M. Barbosa-Filho, and I. Almeida de Medeiros, "Endothelium-dependent hypotensive and vasorelaxant effects of the essential oil from aerial parts of *Mentha x villosa* in rats," *Phytomedicine*, vol. 11, no. 6, pp. 490–497, 2004.

[39] D. D. Rees, R. M. J. Palmer, R. Schulz, H. F. Hodson, and S. Moncada, "Characterization of three inhibitors of endothelial nitric oxide synthase *in vitro* and *in vivo*," *British Journal of Pharmacology*, vol. 101, no. 3, pp. 746–752, 1990.

[40] O. Okafor, O. Erukainure, J. Ajiboye, R. Adejobi, F. Owolabi, and S. Kosoko, "Modulatory effect of pineapple peel extract on lipid peroxidation, catalase activity and hepatic biomarker levels in blood plasma of alcohol-induced oxidative stressed rats," *Asian Pacific Journal of Tropical Biomedicine*, vol. 1, no. 1, pp. 12–14, 2011.

[41] L. Green, S. R. Tannenbaum, and P. Goldman, "Nitrate synthesis in the germfree and conventional rat," *Science*, vol. 212, no. 4490, pp. 56–58, 1981.

[42] H. Ohkawa, N. Ohishi, and K. Yagi, "Assay for lipid peroxides in animal tissues by thiobarbituric acid reaction," *Analytical Biochemistry*, vol. 95, no. 2, pp. 351–358, 1979.

[43] W. Brand-Williams, M. E. Cuvelier, and C. Berset, "Use of a free radical method to evaluate antioxidant activity," *LWT - Food Science and Technology*, vol. 28, no. 1, pp. 25–30, 1995.

[44] R. R. Neubig, M. Spedding, T. Kenakin, and A. Christopoulos, "International Union of Pharmacology Committee on Receptor Nomenclature and Drug Classification. XXXVIII. Update on terms and symbols in quantitative pharmacology," *Pharmacological Reviews*, vol. 55, no. 4, pp. 597–606, 2003.

[45] D. Mascher, M. C. Paredes-Carbajal, P. V. Torres-Durán, J. Zamora-González, J. C. Díaz-Zagoya, and M. A. Juárez-Oropeza, "Ethanolic extract of *Spirulina maxima* alters the vasomotor reactivity of aortic rings from obese rats," *Archives of Medical Research*, vol. 37, no. 1, pp. 50–57, 2006.

[46] A. Carrizzo, G. M. Conte, E. Sommella et al., "Novel potent decameric peptide of *Spirulina platensis* reduces blood pressure levels through a PI3K/AKT/eNOS-dependent mechanism," *Hypertension*, vol. 73, no. 2, pp. 449–457, 2019.

[47] M. Ichimura, S. Kato, K. Tsuneyama et al., "Phycocyanin prevents hypertension and low serum adiponectin level in a rat model of metabolic syndrome," *Nutrition Research*, vol. 33, no. 5, pp. 397–405, 2013.

[48] E. H. C. Tang and P. M. Vanhoutte, "Endothelial dysfunction: a strategic target in the treatment of hypertension?," *Pflügers Archiv - European Journal of Physiology*, vol. 459, no. 6, pp. 995–1004, 2010.

[49] V. B. Bhat and K. M. Madyastha, "C-phycocyanin: a potent peroxyl radical scavenger *in vivo* and *in vitro*," *Biochemical and Biophysical Research Communications*, vol. 275, no. 1, pp. 20–25, 2000.

[50] M. F. Mccarty, "Clinical potential of *Spirulina* as a source of phycocyanobilin," *Journal of Medicinal Food*, vol. 10, no. 4, pp. 566–570, 2007.

[51] M. Kuddus, P. Singh, G. Thomas, and A. Al-hazimi, "Recent developments in production and biotechnological applications of C-phycocyanin," *BioMed Research International*, vol. 2013, Article ID 742859, 9 pages, 2013.

[52] M. E. Cuvelier, "Antioxidants," in *Functional foods: an introductory course*, R. Morais, Ed., Universidade Católica Portuguesa—Escola Superior de Biotecnologia, Porto, 2001.

Hindawi
Oxidative Medicine and Cellular Longevity
Volume 2019, Article ID 2650429, 9 pages
https://doi.org/10.1155/2019/2650429

Review Article

Circulating Leukocytes and Oxidative Stress in Cardiovascular Diseases: A State of the Art

Speranza Rubattu,[1,2] **Maurizio Forte**,[2] **and Salvatore Raffa**[1,3]

[1]*Department of Clinical and Molecular Medicine, School of Medicine and Psychology, Sapienza University of Rome, Italy*
[2]*IRCCS Neuromed, Pozzilli (Isernia), Italy*
[3]*Ultrastructural Pathology Lab-Medical Genetics and Advanced Cellular Diagnostics Unit, Sant'Andrea University Hospital, Rome, Italy*

Correspondence should be addressed to Speranza Rubattu; rubattu.speranza@neuromed.it

Received 25 May 2019; Accepted 9 September 2019; Published 15 October 2019

Guest Editor: Sabato Sorrentino

Increased oxidative stress from both mitochondrial and cytosolic sources contributes to the development and the progression of cardiovascular diseases (CVDs), and it is a target of therapeutic interventions. The numerous efforts made over the last decades in order to develop tools able to monitor the oxidative stress level in patients affected by CVDs rely on the need to gain information on the disease state. However, this goal has not been satisfactorily accomplished until now. Among others, the isolation of circulating leukocytes to measure their oxidant level offers a valid, noninvasive challenge that has been tested in few pathological contexts, including hypertension, atherosclerosis and its clinical manifestations, and heart failure. Since leukocytes circulate in the blood stream, it is expected that they might reflect quite closely both systemic and cardiovascular oxidative stress and provide useful information on the pathological condition. The results of the studies discussed in the present review article are promising. They highlight the importance of measuring oxidative stress level in circulating mononuclear cells in different CVDs with a consistent correlation between degree of oxidative stress and severity of CVD and of its complications. Importantly, they also point to a double role of leukocytes, both as a marker of disease condition and as a direct contributor to disease progression. Finally, they show that the oxidative stress level of leukocytes reflects the impact of therapeutic interventions. It is likely that the isolation of leukocytes and the measurement of oxidative stress, once adequately developed, may represent an eligible tool for both research and clinical purposes to monitor the role of oxidative stress on the promotion and progression of CVDs, as well as the impact of therapies.

1. Introduction

Oxidative stress is the product of several intracellular sources such as mitochondrial electron transport chain (ETC), nicotinamide adenine dinucleotide phosphate oxidase (NADPH), nitric oxide synthase, and xanthine oxidase [1–4]. Several antioxidant mechanisms also exist within the mitochondrial compartment (uncoupling proteins, thioredoxins, glutathione peroxidase, and superoxide dismutase) and in the cytosol that are able to counteract the excessive accumulation of reactive oxygen species (ROS) [5, 6]. It is known that physiological concentrations of ROS exert beneficial effects. On the other hand, increased oxidative stress, as a result of an imbalance between the production and the clearance of ROS, represents a relevant mechanism responsible of cell damage and death [7, 8]. In fact, proteins, lipids, and nucleic acids are the main target of excess ROS. Moreover, an increased level of inflammatory markers parallels that of oxidative stress, with a consequent state of chronic evolving pathological inflammation. At the organ level, increased ROS accumulation and inflammation are involved in the cardiovascular functional and structural damage underlying all major cardiovascular diseases (CVDs) [9].

Based on the key role that ROS play within the cardiovascular system and in all major CVDs, it would be important to monitor its level in human patients for both diagnostic and

Table 1: Relevant studies highlighting the correlation between the oxidative stress level detected in circulating leukocytes and the cardiovascular phenotypes/outcomes in CVDs.

Disease	Sample	Level of direct and indirect markers of oxidative stress	Cardiovascular phenotypes/outcomes	Reference
Hypertension	PMNs	↑ ROS	↑ BP	[32]
Hypertension	MNCs	↑ ROS	↑ C-reactive protein level	[32]
Hypertension	MNCs	↑ ROS	(i) Extreme dipper-type hypertension (ii) Morning BP surge-type hypertension	[33]
Hypertension	MNCs	↑ ROS	↑ Left ventricular mass, carotid IMT, nocturnal BP, norepinephrine level	[34]
Hypertension	PMNs	↓ ROS ↑ Antioxidant activity	↑ Response to antihypertensive agents ↓ BP	[35–38]
Cardiac syndrome X	MNCs	↑ ROS	↑ Cardiovascular events	[44]
Atherosclerosis	PBMCs	↑ CD36 expression	↑ Cholesterol level and oxLDL	[45]
Diabetes	PBMCs	↑ p66Shc expression	↑ Macroangiopathy	[50]
CAD	PBMCs	↑ ROS ↑ Mitochondrial dysfunction ↓ Antioxidant genes	ACS	[25]
CAD	PBMCs	↑ ROS ↓ Antioxidant defence ↓ LTL	Premature CAD	[56]
CAD	PBMCs	↑ LTL	Response to statin therapy	[57]
Stroke	PMNs	↑ ROS	↑ Ischaemic brain attack	[62]
HF	PBMCs	↑ ROS ↑ oxLDL ↑ DNA damage	↑ Severity of HF	[65]
HF	PBMCs	↑ ROS ↓ Antioxidant defence	SIRS development after CF-LVAD implant surgery	[73]
HF	PBMCs	↓ ROS	Response to vitamin C therapy Improved endothelial function	[66]
CHF	PBMCs	Mitochondrial dysfunction ↑ ROS ↓ Mitophagy	Not evaluated	[27]
HF	PBMCs	↓ SIRT1 ↑ ROS	Reduced cardiac compensation status	[69]
CHF	PBMCs	↑ ROS	↑ Hospital readmission	[71]

ACS: acute coronary syndrome; BP: blood pressure; CAD: coronary artery disease; HF: heart failure; CF-LVAD: continuous flow left ventricular assist device; CVDs: cardiovascular diseases; IMT: intima-media thickening; LTL: leukocyte telomere length; MNCs: mononuclear cells; oxLDL: oxidized low-density lipoprotein; PBMCs: peripheral blood mononuclear cells; PMNs: polymorphonuclear leukocytes; ROS: reactive oxygen species; SIRS: systemic inflammatory response syndrome; SIRT1: sirtuin 1.

therapeutic purposes since changes in oxidative stress level parallel the progression of the pathological condition as well as the response to treatment. In this regard, a major limitation is obviously represented by the limited availability of tissue samples from both heart and blood vessels so that the use of circulating markers able to represent the condition within the cardiovascular system could overcome the problem. Notably, several studies performed over the last 15 years have identified the isolation of circulating leukocytes as a suitable method to represent systemic cardiovascular stress conditions with minimal invasive intervention. Since leukocytes circulate in the blood stream, they might reflect quite closely both systemic and cardiovascular metabolic state [10].

It is likely that this method, once adequately developed, may provide an eligible tool for both research and clinical purposes to examine the role of several oxidative stress-related mechanisms in the promotion and progression of CVDs.

The present review article is aimed at discussing the relevance of studies of circulating leukocytes in all major CVDs, from arterial hypertension to ischaemic heart disease and to the final stage of heart failure (Table 1). We also highlight the role of leukocytes as both bystander and actor in the context of CVDs.

2. Cellular Sources of ROS and of Antioxidants

Mitochondria represent the major source of ROS production inside the cells [4]. ROS are produced physiologically as by-products across mitochondrial complex I and complex III. This occurs during the forward electron transfer, whereas

oxygen is partially reduced to form anion superoxide (O_2^-) [4]. The reverse electron transfer across electron transport chain complexes is another mechanism contributing to mitochondrial ROS production [4]. Nicotinamide adenine dinucleotide phosphate (NADPH) oxidases (NOXs) also represent an important source of ROS in the cardiovascular system [11, 12]. All members of NOXs (NOX1, NOX2, NOX4, and NOX5) generate O_2^- by using NADPH as electron donor. Then, O_2^- can be converted into hydrogen peroxide (H_2O_2) [11, 12]. NOXs are activated by different stimuli, such as cytokines, growth factor, and angiotensin II. NOX-derived ROS act as signaling molecules, regulating different cellular mechanisms, especially in the cardiovascular system [11, 12]. Other important cellular sources of ROS and reactive nitrogen species are those derived from xanthine oxidase and by the uncoupling of nitric oxide (NO) synthase [13, 14].

Different antioxidant mechanisms are able to counteract the excessive accumulation of ROS. These are expressed both within the mitochondrial compartment (uncoupling proteins, thioredoxins, glutathione peroxidase, and superoxide dismutase) and in the cytosol [5, 6]. Superoxide dismutases (SODs) represent an important defence against oxidative stress. SODs catalyze the dismutation of O_2^- into H_2O_2 [15]. SOD2 is the isoform expressed in the mitochondria whereas SOD1 and SOD3 are expressed in the cytoplasm and in the extracellular compartment, respectively [15]. Mutations of SODs are associated with different diseases including CVDs [15]. Catalase, another enzyme able to reduce oxidative stress, is expressed in peroxisome, and it is devoted to the conversion of H_2O_2 into water and molecular oxygen (O_2) [16]. Notably, catalase overexpression was found to reduce atherosclerosis in mice lacking apolipoprotein E [17].

3. Isolation of PBMCs and Detection of Oxidative Stress Level

The human PBMCs isolation procedure is based on widely optimized protocols of cell separation by gradient centrifugation. This method exploits the principle of differential migration of cells in specific density gradient media [18]. Usually, venous blood samples drawn into collection tubes containing EDTA are centrifuged in the presence of polysucrose medium (Ficoll). After centrifugation, the PBMCs layer, separated from the plasma, is collected and the cells are made available for further processing such as the establishment of primary cultures (e.g., for the development of specific experimental models) or the cryopreservation for long-term storage.

For the evaluation of intracellular oxidative stress, the PBMCs are incubated with chemiluminescent, bioluminescent, or fluorescent redox-active probes detecting cytoplasmic (e.g., 2′,7′-dichlorofluorescein diacetate or CellROX Oxidative Stress Reagent) or mitochondrial reactive species (MitoSOX Red mitochondrial superoxide indicator or HE, hydroethidine) [19, 20]. The signals exhibited by oxidized fluorescent probes can be assessed both in cell lysates and in whole cells by quantitative fluorescence microscopy and flow cytometry. This procedure offers some technical advantages when compared to the complex sample preparation processes required by the methods to detect protein carbonyls [21] or isoprostanes in plasma samples [22].

In addition, in experimental conditions where PBMCs primary cultures are available, the quantitation of reactive species metabolites, ROS scavengers, and antioxidant enzymes can be carried out by chromogenic and enzymatic assays from culture supernatants. Moreover, the gene expression analysis of PMBCs allows the evaluation of antioxidant systems and of other molecules involved in the modulation of intracellular oxidative stress, such as the OXPHOS genes [23–25]. Finally, the quantitative assessment of mitochondrial structure and function provide additional information when oxidative stress has a mitochondrial genesis [25–27].

4. Hypertension

The pathophysiology of hypertension is a complex and multifactorial process. Abnormalities of the sympathetic nervous system, of the renin-angiotensin-aldosterone system, of G protein-coupled receptor signaling, and of inflammatory and immunity mechanisms play a contributory role [28]. Of note, these processes lead to excess oxidative stress through increased ROS generation, decreased NO levels, and reduced antioxidant capacity in the cardiovascular system. Notably, the pathophysiological role that excess ROS plays in inflammation, hypertrophy, fibrosis, proliferation, migration, and angiogenesis becomes of key importance for the process of cardiovascular remodeling and ultimately of target organ damage development in hypertension.

Evidence that oxidative stress contributes to hypertension development comes from old studies [29–31]. However, only few investigations have been performed in the attempt to detect the level of ROS in hypertensive patients and their interaction with key parameters of the hypertensive disease. Interestingly, in a cohort of 529 hypertensive subjects, the level of polymorphonuclear leukocyte (PMN) oxidative stress significantly correlated with mean blood pressure (BP) level and also with hemoglobin A(1c) level. In the same cohort, a significant correlation was found between C-reactive protein level and mononuclear cell (MNC) oxidative stress [32]. Furthermore, subjects from this cohort affected by both hypertension and diabetes showed increased PMN and MNC oxidative stress. These findings, while documenting a tight relationship between hypertension and diabetes with oxidative stress and inflammation, had the merit to develop and propose the measurement of oxidative stress in circulating leukocytes as a valid tool to detect the hypertension-related vascular damage.

As a logical follow-up, the same authors investigated whether an increased level of oxidative stress may be detected in circulating leukocytes of extreme dipper and of morning BP surge-type hypertensives [33]. As expected, ROS formation by MNCs was significantly increased in both types of hypertensive patients. Furthermore, the combination of extreme dipper and of morning surge BP types led to an even higher level of ROS formation. These findings indicate that higher ROS formation from leukocytes in extreme dipper and morning surge BP types is a marker of predisposition

to early morning cardiovascular events (CVE). It cannot be excluded that higher ROS level plays also a contributory pathogenic role into the development of CVE in these types of hypertensive patients. This hypothesis is strengthened by the observation that ROS formation by MNCs relates not only to nocturnal BP level but also to other cardiovascular risk factors, such as left ventricular mass, carotid intima-media thickening (IMT), and norepinephrine [34].

The usefulness of measurement of leukocyte oxidant activities may reveal importance not only for the evaluation of the oxidative stress in hypertension but also to monitor the effect of antihypertensive drugs. In this regard, it has been shown that the use of benidipine reduced oxidative stress in PMNs of hypertensive patients, at least in part by reducing BP levels [35], and that angiotensin II type 1 receptor (AT1R) blockers were able to normalize BP and to reduce the oxidative stress produced by leukocytes, thus suggesting that the latter plays an active role in the pathogenesis of hypertension through the production of oxidative stress. In fact, these studies proposed the leukocytes as a target of antihypertensive drugs [36–38].

5. Atherosclerosis and Ischaemic Heart Disease

Signals that regulate cellular proliferation, neointimal formation, and vessel wall thickening underlie the cellular and molecular basis of atherosclerotic plaque development. This process has both systemic oxidative stress and inflammatory components involving endothelial dysfunction, vascular smooth muscle cell proliferation and migration, circulating immune cells, and monocytes/macrophages [39, 40]. The latter has been shown to be involved in the development and progression of coronary artery disease (CAD) [41]. Moreover, it has been demonstrated that neutrophils play a key role in CAD progression and plaque instability through the generation of myeloperoxidase (MPO) [42]. In fact, the MPO deficiency reduced inflammation, oxidative stress, and plaque formation in the apolipoprotein E-deficient mice fed with high-cholesterol diet [42]. PMNs are tightly linked to other cells involved in the inflammatory responses at the vascular level, and they are modulated by lymphocytes and macrophages. Also, the disruption of mitochondrial function can elicit further oxidative stress. In fact, monocyte mitochondrial DNA damage and decreased complex I and IV activities have been identified in mouse models of atherosclerosis [43].

The use of peripheral blood leukocytes may represent a valid tool to determine the oxidative stress in patients affected by atherosclerosis and particularly by CAD. To support this concept, a study by Leu et al. demonstrated that a basal O_2^- generation by MNCs was able to predict CVE in patients with cardiac syndrome X, independently from other risk factors. This observation suggested the potential role of measuring oxidative stress produced by MNCs both for monitoring CAD progression and for risk stratification in syndrome X patients [44]. However, this method has revealed no practical value in clinics so that other parameters of oxidative stress can be determined in circulating leukocytes.

5.1. Oxidative Stress-Related Gene Expression. Several studies have shown that the detection in PBMCs of the expression of genes involved in the atherosclerotic process reveals useful in terms of prediction and monitoring of the atherosclerotic vascular lesions. In a model of hypercholesterolemic rabbit, a significant relationship was observed between the aorta and PBMC CD36 mRNA expression [45]. The latter is a receptor that facilitates the uptake of oxLDL in the arterial wall [46–48]. It is expressed in intraplaque macrophages and mediates phagocytosis of oxLDL leading to foam cells formation [47]. More importantly, a significant correlation was found between PBMC CD36 mRNA expression and higher cholesterol level in humans [45, 49], thus indicating that the CD36 mRNA level of PBMCs could be used as a biomarker for the diagnosis of the atherosclerotic burden.

Consistently, it was reported that the expression of p66Shc, a mitochondrial protein driving the hyperglycemic cell damage, was higher in PBMCs of diabetic patients who lately developed macroangiopathy [50]. At the experimental level, it has been shown that p66Shc deletion prevents diabetic complications [51]. Thus, this marker can be proposed to predict the onset of vascular complications in diabetes.

The gene expression profiling in blood leukocytes has been proposed as a suitable approach to identify subjects at risk for CAD, although with several inconsistencies between different studies [24]. In fact, no definite information still exists on the genes truly predisposing to CAD development.

Apart from the assessment of CAD risk, the determination of gene expression in circulating leukocytes may help to identify changes in response to alterations of a physiological state. Therefore, we could characterize a specific pathological condition. In particular, we may be able to monitor the presence and progression of CAD as well as the effects of therapeutic interventions [24]. Very few studies have been conducted so far with the detection of oxidative stress-related gene expression level in PBMCs of CAD patients. In a study performed in an Italian cohort of patients affected by acute coronary syndrome (ACS), the PBMCs were used to test the gene expression of a mitochondrial complex I subunit (Ndufc2) and to assess the oxidative stress level dependent from mitochondrial dysfunction. In fact, NDUFC2 expression was significantly impaired, along with a significant reduction of the expression of few antioxidant genes and increased ROS level, whereas no relevant changes could be observed in PBMCs of patients affected by stable angina [25]. This study corroborated the role of increased mitochondrial oxidative stress in the pathogenesis of ACS by demonstrating the presence of mitochondrial dysfunction and of ultrastructural damage along with a relevant reduction of ATP level in PBMCs of the ACS patients. Notably, the mitochondrial complex I deficiency derived from NDUFC2 suppression is responsible at the vascular level of increased inflammation, apoptosis, and necrosis, of impaired endothelial integrity and angiogenesis, and of the release of markers of plaque instability [25]. To our knowledge, this is one of the best example supporting the usefulness of circulating PBMCs as a marker of mitochondrial oxidative stress that mirrors the vascular stress condition and is able to differentiate a state of ACS from that of stable chronic angina.

Interestingly, it appears that PBMCs carry and possibly amplify within the bloodstream a mechanism, the mitochondrial dysfunction, which is directly involved in the pathogenesis of ACS. In fact, they might be considered not only as a bystander but also as an actor in the scene. From this point of view, it is even possible to identify PBMCs as a target for CAD treatment.

5.2. Telomere Length Assessment in PBMCs. An additional parameter that has been investigated in leukocytes is their telomere length. The leukocyte telomere length (LTL) is considered as a marker of biological aging [52–55]. In particular, oxidative stress plays a major role in the process of telomeric DNA loss [52–55]. In a study conducted in Chinese patients affected by premature CAD, the LTL was found to be shorter, and this phenomenon was associated with a reduced antioxidant capacity and increased ROS production [56].

An interesting study supports the use of circulating leukocytes to assess LTL as a marker of CAD. In particular, a relation was found between LTL and statin therapy in CAD patients: those under statin treatment had longer LTL as compared to patients without [57].

5.3. Proteomic Approach. It is clear that changes in several proteins involved in the oxidative stress response to heart ischaemia accompany the cardiac damage. In particular, since mitochondrial metabolism is heavily involved, changes in proteins of ETC are expected, particularly those of complex I proteins [58].

Their detection through a proteomic approach in PBMCs could help to detect and monitor the oxidative stress associated to CAD, to monitor the disease state itself and the response to treatment. However, the use of PBMC proteomics is still at its very early stage. Initial evidence of protein changes in PBMCs is emerging only with regard to human stroke [59].

Future studies using this approach in CAD are warranted.

6. Stroke

The pathogenesis of stroke, a common complex cardiovascular trait, is the result of several contributory factors including hypertension, genetics, and lifestyle. Also in the case of stroke, common mechanisms relate to vascular inflammation, proliferation, angiogenesis, apoptosis, and dysfunction. Experimental evidence highlights a key contributory role of increased oxidative stress in the development of stroke [60, 61].

In humans, we previously demonstrated that the rs11237379/NDUFC2 gene variant, associated to reduced mitochondrial complex I activity and increased oxidative stress, was a risk factor of juvenile ischaemic stroke [60]. Then, we showed that circulating leukocytes of healthy subjects carrying this gene variant have an altered mitochondrial function and relevant structural damage with increased mitochondrial oxidative stress in response to stress stimuli [26]. This interesting evidence underscores the potential role of circulating leukocytes as a marker of oxidative stress and of increased cardiovascular risk in genetically predisposed individuals.

Very few studies exploited the use of PBMCs to detect oxidative stress in the clinical context of cerebrovascular disease. In the study by Aizawa et al., the intracellular ROS level of PMNs was found to be higher in patients with ischaemic brain attack as compared to controls [62]. Notably, treatment with a free radical scavenger (edaravone) reduced the PMN ROS level as well as the O_2^- production in these patients. Thus, this study revealed the importance of circulating mononuclear cells to monitor stroke and the response to a suitable therapy [62].

7. Heart Failure

Heart failure (HF) is a common clinical condition that represents the final stage of several cardiac diseases and of the underlying pathophysiological mechanisms. Among all, HF is characterized by excess oxidative stress, due to a relevant mitochondrial component, and by chronic inflammation. The myocardial oxidative stress deteriorates cardiac function by promoting cellular damage and death.

The PBMCs have been frequently used to detect mitochondrial respiratory dysfunction in HF, with evidence of a significant correlation with cardiac disturbances and clinical manifestations, already detectable at an early stage of the disease [63]. In fact, high levels of ROS and of O_2^- are present in the blood of HF patients. Functional alterations of the antioxidant enzymes are detected in parallel in failing myocardium [64]. In addition, excess DNA double-strand breaks and higher level of DNA repair proteins are found in PBMCs of HF patients [65]. Moreover, the neutrophil O_2^--generating capacity contributes to other deleterious phenotypes of HF such as endothelial dysfunction. The latter remained unchanged after short- and long-term therapy with vitamin C [66].

Of note, the spontaneous reaction of O_2^- and NO generates the potent oxidant peroxynitrite. Protein nitration is a consequence of peroxynitrite production and is found to be higher in PBMCs of HF patients. In addition, the oxidative-nitrative stress leads to the activation of several enzymes, including matrix metalloproteinases and poly(ADP-ribose) polymerase-1 (PARP). The latter, once overactivated, consumes NAD+ and ATP, leading to cell apoptosis and death [67].

A recent study from our group has shown that PBMCs of patients with chronic HF produce excess ROS, have reduced mitochondrial functional performance, and present with ultrastructural damage such as disruption of the inner mitochondrial membrane (IMM) and low IMM/outer MM (OMM) index value [27]. These phenomena were paralleled by an impairment of the activation of antioxidant genes and by a reduced mitophagic flux, with a consequent inadequate mitochondrial dynamics. The functional and structural alterations observed in these patients are likely responsible of a further ETC impairment, mitochondrial uncoupling, and O_2^- production.

Sirtuin 1 (SIRT1) is a factor involved in the cell survival mechanism, heart ischaemic injury, and the pathophysiology

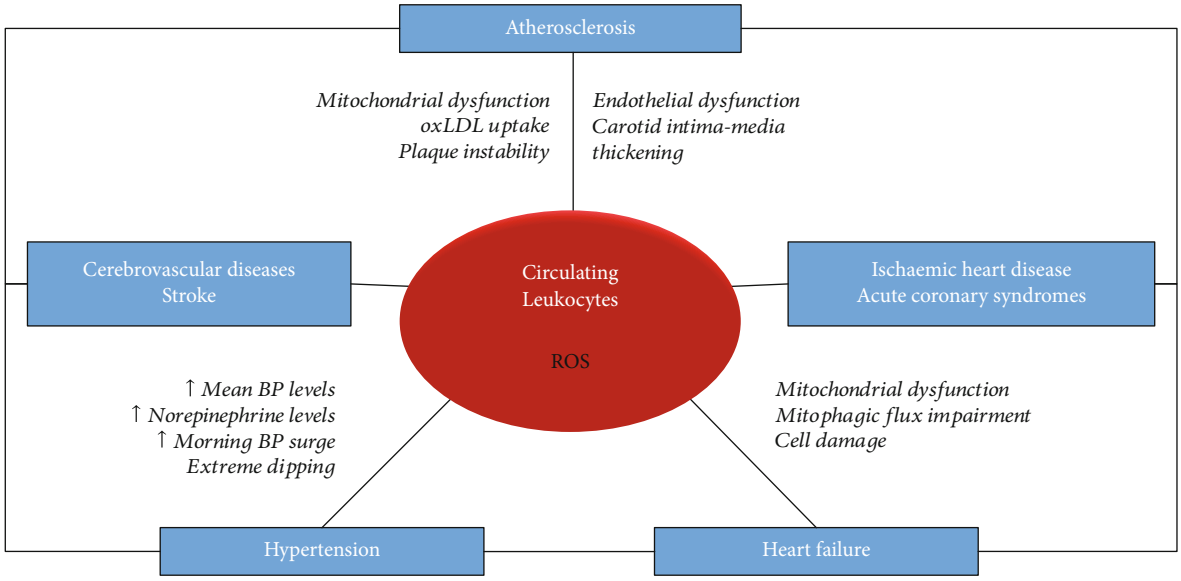

Figure 1: Circulating leukocytes and oxidative stress in cardiovascular diseases (CVDs). Schematic representation of the relationship between circulating leukocytes and reactive oxygen species (ROS) in different CVDs. The evidence collected in the context of the oxidative stress-induced cardiovascular damage points to a double role of leukocytes, both as a marker of disease condition and as an active player of disease progression.

of CVDs [68]. SIRT1 expression in PBMCs was significantly reduced, particularly in decompensated HF, and it was significantly related to the increased oxidant level and decreased antioxidant capacity [69].

Therefore, all studies support the concept that dysfunctional circulating PBMCs can act as an amplifier of oxidative stress and of cell/tissue damage, ultimately contributing to the progression of the HF condition [70]. As a consequence, it is no surprise that PBMC ROS level predicts hospital readmission in chronic HF [71]. Moreover, as outlined above for hypertension and CAD, the PBMCs could become a target also for HF treatment.

The impact of therapies used in HF patients has been evaluated at the cellular level and in circulating leukocytes. Patients with decompensated chronic HF and marked systemic inflammation and increased production of oxygen free radicals improved their functional status and reduced their indices of inflammation and oxidative stress after short-term inotropic support. In particular, short-term inotropic support with milrinone and dobutamine improved clinical status, as assessed by NYHA classification and by the 6 min walk test, and significantly decreased plasma levels of inflammatory and oxidative stress markers at 30 days.

Since oxidative stress is amplified in HF because of absent pulmonary clearance of ROS-loaded circulating leukocytes and platelets, pulmonary removal of ROS and transfer of redox active molecules to the mitochondria can be proposed as targets for chronic HF therapy [70].

A study by Kong et al. evaluated the leukocyte mitochondrial alterations induced by bypass surgery and found that they are part of the systemic immune perturbations related to cardiac surgery [72]. The impact of implantation of the left ventricular assist device on the oxidative stress of circulating leukocytes has been also evaluated. Interestingly, after implantation of the left ventricular assist device (LVAD), an increased production of ROS was observed in the blood leukocytes indicating persistent oxidative stress in these patients [73]. Since the production of ROS and DNA damage relate to high shear stress, the most plausible explanation of the abovementioned phenomenon is that continuous flow LVAD generates high shear stresses, therefore favoring excess ROS production from circulating PBMCs and DNA damage from lymphocytes. Less traumatic devices are warranted to circumvent the problem.

8. Conclusions

A large body of evidence underscores the importance of monitoring oxidative stress in CVDs with the aim of achieving more information on the disease state and on the response to treatment. This observation implies that relevant prognostic information for the patients can be obtained in parallel. At the time being, no definite tool exists in the clinical practice. In particular, although some oxidative stress markers assessing the oxidation of phospholipid and LDL protein components predict increased CV risk, none of them have yet been incorporated into clinical practice [9]. In fact, clinical trials including cross-sectional and retrospective and prospective studies provided conflicting results [74], mostly due to methodological issues.

The choice to study the PBMCs redox state in the CVDs is specifically based on the evidence that these cells play a key role in the modulation of atherogenesis by orchestrating the inflammatory and immune responses [75]. Lymphocytes and monocytes have a tight interaction with intrinsic vascular cells in the atheroma. In this context, cytokines and metabolites of reactive species are the signals that mediate the relationships between different cell types. They also

modulate many key processes such as the induction of endothelial dysfunction, the triggering of coagulation and fibrinolysis, the formation and accumulation of foam cells, the migration and reprogramming of vascular smooth muscle cells, and the activation repair pathways culminating in tissue fibrosis [76–78].

Furthermore, the redox state of PBMCs closely reflect the systemic cardiovascular oxidative stress condition and therefore the presence and progression of CVD. It is likely that an altered redox state of dysfunctional circulating leukocytes can act as an amplifier of oxidative stress at tissue level, worsening the evolution of the disease [63, 70, 79].

Based on the evidence collected over the last few years and summarized in this article (Table 1, Figure 1), it is likely that the use of circulating leukocytes may become a relevant clinical tool. They may also serve to better understand the mechanisms involved in CVD pathogenesis. Nevertheless, more studies are needed to reinforce the current evidence and to identify the advantages, if any, of PBMCs compared to the markers detecting oxidative stress in plasma.

Finally, based on the evidence that PBMCs can directly distribute and amplify oxidative stress in the cardiovascular system, it is tempting to speculate that they may even be proposed as a target for the treatment of CVDs. However, since several difficulties would hamper this achievement in the clinical practice, the isolation of PBMCs to be used as a marker of oxidative stress level in CVDs remains the major and easier goal to pursue.

Conflicts of Interest

The authors declare no conflicts of interest.

Acknowledgments

This work was supported by a grant from the Italian Ministry of Health and by the "5 per mille" grant.

References

[1] M. Y. Lee and K. K. Griendling, "Redox signaling, vascular function, and hypertension," *Antioxidants & Redox Signaling*, vol. 10, no. 6, pp. 1045–1059, 2008.

[2] S. Rubattu, B. Pagliaro, G. Pierelli et al., "Pathogenesis of target organ damage in hypertension: role of mitochondrial oxidative stress," *International Journal of Molecular Sciences*, vol. 16, no. 1, pp. 823–839, 2015.

[3] R. R. Nazarewicz, A. E. Dikalova, A. Bikineyeva, and S. I. Dikalov, "Nox2 as a potential target of mitochondrial superoxide and its role in endothelial oxidative stress," *American Journal of Physiology. Heart and Circulatory Physiology*, vol. 305, no. 8, pp. H1131–H1140, 2013.

[4] M. Forte, S. Palmerio, F. Bianchi, M. Volpe, and S. Rubattu, "Mitochondrial complex I deficiency and cardiovascular diseases: current evidence and future directions," *Journal of Molecular Medicine*, vol. 97, no. 5, pp. 579–591, 2019.

[5] G. Pierelli, R. Stanzione, M. Forte et al., "Uncoupling protein 2: a key player and a potential therapeutic target in vascular diseases," *Oxidative Medicine and Cellular Longevity*, vol. 2017, Article ID 7348372, 11 pages, 2017.

[6] T. Finkel, "Signal transduction by reactive oxygen species," *The Journal of Cell Biology*, vol. 194, no. 1, pp. 7–15, 2011.

[7] K. Hensley, K. A. Robinson, S. P. Gabbita, S. Salsman, and R. A. Floyd, "Reactive oxygen species, cell signaling, and cell injury," *Free Radical Biology & Medicine*, vol. 28, no. 10, pp. 1456–1462, 2000.

[8] N. R. Madamanchi, A. Vendrov, and M. S. Runge, "Oxidative stress and vascular disease," *Arteriosclerosis, Thrombosis, and Vascular Biology*, vol. 25, no. 1, pp. 29–38, 2005.

[9] J. Martin-Ventura, R. Rodrigues-Diez, D. Martinez-Lopez, M. Salaices, L. Blanco-Colio, and A. Briones, "Oxidative stress in human atherothrombosis: sources, markers and therapeutic targets," *International Journal of Molecular Sciences*, vol. 18, no. 11, p. 2315, 2017.

[10] F. K. Swirski and M. Nahrendorf, "Leukocyte behavior in atherosclerosis, myocardial infarction, and heart failure," *Science*, vol. 339, no. 6116, pp. 161–166, 2013.

[11] M. Forte, S. Palmerio, D. Yee, G. Frati, and S. Sciarretta, "Functional role of Nox4 in autophagy," *Advances in Experimental Medicine and Biology*, vol. 982, pp. 307–326, 2017.

[12] M. Forte, C. Nocella, E. De Falco et al., "The pathophysiological role of NOX2 in hypertension and organ damage," *High Blood Pressure & Cardiovascular Prevention*, vol. 23, no. 4, pp. 355–364, 2016.

[13] T. Nishino, K. Okamoto, B. T. Eger, E. F. Pai, and T. Nishino, "Mammalian xanthine oxidoreductase - mechanism of transition from xanthine dehydrogenase to xanthine oxidase," *The FEBS Journal*, vol. 275, no. 13, pp. 3278–3289, 2008.

[14] M. Forte, V. Conti, A. Damato et al., "Targeting nitric oxide with natural derived compounds as a therapeutic strategy in vascular diseases," *Oxidative Medicine and Cellular Longevity*, vol. 2016, Article ID 7364138, 20 pages, 2016.

[15] T. Fukai and M. Ushio-Fukai, "Superoxide dismutases: role in redox signaling, vascular function, and diseases," *Antioxidants & Redox Signaling*, vol. 15, no. 6, pp. 1583–1606, 2011.

[16] H. Li, S. Horke, and U. Forstermann, "Vascular oxidative stress, nitric oxide and atherosclerosis," *Atherosclerosis*, vol. 237, no. 1, pp. 208–219, 2014.

[17] H. Yang, L. J. Roberts, M. J. Shi et al., "Retardation of atherosclerosis by overexpression of catalase or both Cu/Zn-superoxide dismutase and catalase in mice lacking apolipoprotein E," *Circulation Research*, vol. 95, no. 11, pp. 1075–1081, 2004.

[18] H. W. Grievink, T. Luisman, C. Kluft, M. Moerland, and K. E. Malone, "Comparison of three isolation techniques for human peripheral blood mononuclear cells: cell recovery and viability, population composition, and cell functionality," *Biopreservation and Biobanking*, vol. 14, no. 5, pp. 410–415, 2016.

[19] S. Dupré-Crochet, M. Erard, and O. Nüβe, "ROS production in phagocytes: why, when, and where?," *Journal of Leukocyte Biology*, vol. 94, no. 4, pp. 657–670, 2013.

[20] G. Cheng, M. Zielonka, B. Dranka et al., "Detection of mitochondria-generated reactive oxygen species in cells using multiple probes and methods: potentials, pitfalls, and the future," *The Journal of Biological Chemistry*, vol. 293, no. 26, pp. 10363–10380, 2018.

[21] D. Weber, M. J. Davies, and T. Grune, "Determination of protein carbonyls in plasma, cell extracts, tissue homogenates, isolated proteins: focus on sample preparation and derivatization conditions," *Redox Biology*, vol. 5, pp. 367–380, 2015.

[22] Y. Y. Lee, J. M. Galano, C. Oger et al., "Assessment of isoprostanes in human plasma: technical considerations and the use

of mass spectrometry," *Lipids*, vol. 51, no. 11, pp. 1217–1229, 2016.

[23] M. H. Abdullah, Z. Othman, H. M. Noor et al., "Peripheral blood gene expression profile of atherosclerotic coronary artery disease in patients of different ethnicity in Malaysia," *Journal of Cardiology*, vol. 60, no. 3, pp. 192–203, 2012.

[24] B. Rhees and J. A. Wingrove, "Developing peripheral blood gene expression-based diagnostic tests for coronary artery disease: a review," *Journal of Cardiovascular Translational Research*, vol. 8, no. 6, pp. 372–380, 2015.

[25] S. Raffa, X. L. D. Chin, R. Stanzione et al., "The reduction of NDUFC2 expression is associated with mitochondrial impairment in circulating mononuclear cells of patients with acute coronary syndrome," *International Journal of Cardiology*, vol. 286, pp. 127–133, 2019.

[26] S. Raffa, C. Scrofani, S. Valente et al., "*In vitro* characterization of mitochondrial function and structure in rat and human cells with a deficiency of the NADH: ubiquinone oxidoreductase Ndufc2 subunit," *Human Molecular Genetics*, vol. 26, no. 23, pp. 4541–4555, 2017.

[27] R. Coluccia, S. Raffa, D. Ranieri et al., "Chronic heart failure is characterized by altered mitochondrial function and structure in circulating leucocytes," *Oncotarget*, vol. 9, no. 80, pp. 35028–35040, 2018.

[28] A. C. Montezano and R. M. Touyz, "Molecular mechanisms of hypertension–reactive oxygen species and antioxidants: a basic science update for the clinician," *The Canadian Journal of Cardiology*, vol. 28, no. 3, pp. 288–295, 2012.

[29] A. C. Montezano and R. M. Touyz, "Oxidative stress, Noxs, and hypertension: experimental evidence and clinical controversies," *Annals of Medicine*, vol. 44, pp. S2–16, 2012.

[30] R. Rodrigo, J. Gonzalez, and F. Paoletto, "The role of oxidative stress in the pathophysiology of hypertension," *Hypertension Research*, vol. 34, no. 4, pp. 431–440, 2011.

[31] R. M. Touyz, "Reactive oxygen species, vascular oxidative stress, and redox signaling in hypertension: what is the clinical significance?," *Hypertension*, vol. 44, no. 3, pp. 248–252, 2004.

[32] K. Yasunari, K. Maeda, M. Nakamura, and J. Yoshikawa, "Oxidative stress in leukocytes is a possible link between blood pressure, blood glucose, and C-reacting protein," *Hypertension*, vol. 39, no. 3, pp. 777–780, 2002.

[33] K. Maeda, K. Yasunari, T. Watanabe, and M. Nakamura, "Oxidative stress by peripheral blood mononuclear cells is increased in hypertensives with an extreme-dipper pattern and/or morning surge in blood pressure," *Hypertension Research*, vol. 28, no. 9, pp. 755–761, 2005.

[34] K. Yasunari, T. Watanabe, and M. Nakamura, "Reactive oxygen species formation by polymorphonuclear cells and mononuclear cells as a risk factor of cardiovascular diseases," *Current Pharmaceutical Biotechnology*, vol. 7, no. 2, pp. 73–80, 2006.

[35] K. Yasunari, K. Maeda, M. Nakamura, T. Watanabe, and J. Yoshikawa, "Benidipine, a long-acting calcium channel blocker, inhibits oxidative stress in polymorphonuclear cells in patients with essential hypertension," *Hypertension Research*, vol. 28, no. 2, pp. 107–112, 2005.

[36] M. Labios, M. Martinez, F. Gabriel et al., "Superoxide dismutase and catalase anti-oxidant activity in leucocyte lysates from hypertensive patients: effects of eprosartan treatment," *Journal of the Renin-Angiotensin-Aldosterone System*, vol. 10, no. 1, pp. 24–30, 2009.

[37] M. Labios, M. Martinez, F. Gabriel et al., "Effects of eprosartan on mitochondrial membrane potential and H_2O_2 levels in leucocytes in hypertension," *Journal of Human Hypertension*, vol. 22, no. 7, pp. 493–500, 2008.

[38] L. A. Calò, L. D. Maso, P. Caielli et al., "Effect of olmesartan on oxidative stress in hypertensive patients: mechanistic support to clinical trials derived evidence," *Blood Pressure*, vol. 20, no. 6, pp. 376–382, 2011.

[39] X. Yang, Y. Li, Y. Li et al., "Oxidative stress-mediated atherosclerosis: mechanisms and therapies," *Frontiers in Physiology*, vol. 8, p. 600, 2017.

[40] A. J. Kattoor, N. V. K. Pothineni, D. Palagiri, and J. L. Mehta, "Oxidative stress in atherosclerosis," *Current Atherosclerosis Reports*, vol. 19, no. 11, p. 42, 2017.

[41] P. Libby, "Inflammation in atherosclerosis," *Nature*, vol. 420, no. 6917, pp. 868–874, 2002.

[42] V. Tiyerili, B. Camara, M. U. Becher et al., "Neutrophil-derived myeloperoxidase promotes atherogenesis and neointima formation in mice," *International Journal of Cardiology*, vol. 204, pp. 29–36, 2016.

[43] E. Yu, P. A. Calvert, J. R. Mercer et al., "Mitochondrial DNA damage can promote atherosclerosis independently of reactive oxygen species through effects on smooth muscle cells and monocytes and correlates with higher-risk plaques in humans," *Circulation*, vol. 128, no. 7, pp. 702–712, 2013.

[44] H. B. Leu, C. P. Lin, W. T. Lin, T. C. Wu, S. J. Lin, and J. W. Chen, "Circulating mononuclear superoxide production and inflammatory markers for long-term prognosis in patients with cardiac syndrome X," *Free Radical Biology & Medicine*, vol. 40, no. 6, pp. 983–991, 2006.

[45] B. Yazgan, E. Sozen, B. Karademir et al., "CD36 expression in peripheral blood mononuclear cells reflects the onset of atherosclerosis," *BioFactors*, vol. 44, no. 6, pp. 588–596, 2018.

[46] R. F. Thorne, N. M. Mhaidat, K. J. Ralston, and G. F. Burns, "CD36 is a receptor for oxidized high density lipoprotein: implications for the development of atherosclerosis," *FEBS Letters*, vol. 581, no. 6, pp. 1227–1232, 2007.

[47] G. Endemann, L. W. Stanton, K. S. Madden, C. M. Bryant, R. T. White, and A. A. Protter, "CD36 is a receptor for oxidized low density lipoprotein," *The Journal of Biological Chemistry*, vol. 268, no. 16, pp. 11811–11816, 1993.

[48] A. C. Nicholson, S. Frieda, A. Pearce, and R. L. Silverstein, "Oxidized LDL binds to CD36 on human monocyte-derived macrophages and transfected cell lines. Evidence implicating the lipid moiety of the lipoprotein as the binding site," *Arteriosclerosis, Thrombosis, and Vascular Biology*, vol. 15, no. 2, pp. 269–275, 1995.

[49] B. Yazgan, S. Ustunsoy, B. Karademir, and N. Kartal-Ozer, "CD36 as a biomarker of atherosclerosis," *Free Radical Biology and Medicine*, vol. 75, p. S10, 2014.

[50] G. P. Fadini, M. Albiero, B. M. Bonora, N. Poncina, S. Vigili de Kreutzenberg, and A. Avogaro, "p66Shc gene expression in peripheral blood mononuclear cells and progression of diabetic complications," *Cardiovascular Diabetology*, vol. 17, no. 1, p. 16, 2018.

[51] S. Menini, L. Amadio, G. Oddi et al., "Deletion of p66Shc longevity gene protects against experimental diabetic glomerulopathy by preventing diabetes-induced oxidative stress," *Diabetes*, vol. 55, no. 6, pp. 1642–1650, 2006.

[52] T. De Meyer, T. Nawrot, S. Bekaert, M. L. De Buyzere, E. R. Rietzschel, and V. Andres, "Telomere length as cardiovascular

aging biomarker: JACC review topic of the week," *Journal of the American College of Cardiology*, vol. 72, no. 7, pp. 805–813, 2018.

[53] F. N. Ashar, Y. Zhang, R. J. Longchamps et al., "Association of mitochondrial DNA copy number with cardiovascular disease," *JAMA Cardiology*, vol. 2, no. 11, pp. 1247–1255, 2017.

[54] A. Muezzinler, A. K. Zaineddin, and H. Brenner, "A systematic review of leukocyte telomere length and age in adults," *Ageing Research Reviews*, vol. 12, no. 2, pp. 509–519, 2013.

[55] J. L. Sanders and A. B. Newman, "Telomere length in epidemiology: a biomarker of aging, age-related disease, both, or neither?," *Epidemiologic Reviews*, vol. 35, no. 1, pp. 112–131, 2013.

[56] R. Tian, L. N. Zhang, T. T. Zhang et al., "Association between oxidative stress and peripheral leukocyte telomere length in patients with premature coronary artery disease," *Medical Science Monitor*, vol. 23, pp. 4382–4390, 2017.

[57] S. Saliques, J. R. Teyssier, C. Vergely et al., "Circulating leukocyte telomere length and oxidative stress: a new target for statin therapy," *Atherosclerosis*, vol. 219, no. 2, pp. 753–760, 2011.

[58] T. Liu, L. Chen, E. Kim, D. Tran, B. S. Phinney, and A. A. Knowlton, "Mitochondrial proteome remodeling in ischemic heart failure," *Life Sciences*, vol. 101, no. 1-2, pp. 27–36, 2014.

[59] F. Bian, R. P. Simon, Y. Li et al., "Nascent proteomes in peripheral blood mononuclear cells as a novel source for biomarker discovery in human stroke," *Stroke*, vol. 45, no. 4, pp. 1177–1179, 2014.

[60] S. Rubattu, S. Di Castro, H. Schulz et al., "Ndufc2 gene inhibition is associated with mitochondrial dysfunction and increased stroke susceptibility in an animal model of complex human disease," *Journal of the American Heart Association*, vol. 5, no. 2, 2016.

[61] S. Rubattu, R. Stanzione, F. Bianchi et al., "Reduced brain UCP2 expression mediated by microRNA-503 contributes to increased stroke susceptibility in the high-salt fed stroke-prone spontaneously hypertensive rat," *Cell Death & Disease*, vol. 8, no. 6, article e2891, 2017.

[62] H. Aizawa, Y. Makita, K. Sumitomo et al., "Edaravone diminishes free radicals from circulating neutrophils in patients with ischemic brain attack," *Internal Medicine*, vol. 45, no. 1, pp. 1–4, 2006.

[63] P. Li, B. Wang, F. Sun et al., "Mitochondrial respiratory dysfunctions of blood mononuclear cells link with cardiac disturbance in patients with early-stage heart failure," *Scientific Reports*, vol. 5, no. 1, article 10229, 2015.

[64] F. Sam, D. L. Kerstetter, D. R. Pimental et al., "Increased reactive oxygen species production and functional alterations in antioxidant enzymes in human failing myocardium," *Journal of Cardiac Failure*, vol. 11, no. 6, pp. 473–480, 2005.

[65] N. K. Mondal, E. Sorensen, N. Hiivala, E. Feller, B. Griffith, and Z. J. Wu, "Oxidative stress, DNA damage and repair in heart failure patients after implantation of continuous flow left ventricular assist devices," *International Journal of Medical Sciences*, vol. 10, no. 7, pp. 883–893, 2013.

[66] G. R. Ellis, R. A. Anderson, D. Lang et al., "Neutrophil superoxide anion–generating capacity, endothelial function and oxidative stress in chronic heart failure: effects of short- and long-term vitamin C therapy," *Journal of the American College of Cardiology*, vol. 36, no. 5, pp. 1474–1482, 2000.

[67] T. Barany, A. Simon, G. Szabo et al., "Oxidative stress-related parthanatos of circulating mononuclear leukocytes in heart failure," *Oxidative Medicine and Cellular Longevity*, vol. 2017, Article ID 1249614, 12 pages, 2017.

[68] V. Conti, M. Forte, G. Corbi et al., "Sirtuins: possible clinical implications in cardio and cerebrovascular diseases," *Current Drug Targets*, vol. 18, no. 4, pp. 473–484, 2017.

[69] F. Akkafa, I. Halil Altiparmak, M. E. Erkus et al., "Reduced SIRT1 expression correlates with enhanced oxidative stress in compensated and decompensated heart failure," *Redox Biology*, vol. 6, pp. 169–173, 2015.

[70] A. J. J. IJsselmuiden, R. J. P. Musters, G. de Ruiter et al., "Circulating white blood cells and platelets amplify oxidative stress in heart failure," *Nature Clinical Practice. Cardiovascular Medicine*, vol. 5, no. 12, pp. 811–820, 2008.

[71] B. Song, T. Li, S. Chen et al., "Correlations between MTP and ROS levels of peripheral blood lymphocytes and readmission in patients with chronic heart failure," *Heart, Lung & Circulation*, vol. 25, no. 3, pp. 296–302, 2016.

[72] C.-W. Kong, C.-H. Huang, T.-G. Hsu et al., "Leukocyte mitochondrial alterations after cardiac surgery involving cardiopulmonary bypass: clinical correlations," *Shock*, vol. 21, no. 4, pp. 315–319, 2004.

[73] N. K. Mondal, E. N. Sorensen, S. M. Pham et al., "Systemic inflammatory response syndrome in end-stage heart failure patients following continuous-flow left ventricular assist device implantation: differences in plasma redox status and leukocyte activation," *Artificial Organs*, vol. 40, no. 5, pp. 434–443, 2016.

[74] F. Violi and P. Pignatelli, "Clinical application of NOX activity and other oxidative biomarkers in cardiovascular disease: a critical review," *Antioxidants & Redox Signaling*, vol. 23, no. 5, pp. 514–532, 2015.

[75] P. Libby, J. Loscalzo, P. M. Ridker et al., "Inflammation, immunity, and infection in atherothrombosis: JACC review topic of the week," *Journal of the American College of Cardiology*, vol. 72, no. 17, pp. 2071–2081, 2018.

[76] H. Ait-Oufella, S. Taleb, Z. Mallat, and A. Tedgui, "Recent advances on the role of cytokines in atherosclerosis," *Arteriosclerosis, Thrombosis, and Vascular Biology*, vol. 31, no. 5, pp. 969–979, 2011.

[77] T. Kondo, M. Hirose, and K. Kageyama, "Roles of oxidative stress and redox regulation in atherosclerosis," *Journal of Atherosclerosis and Thrombosis*, vol. 16, no. 5, pp. 532–538, 2009.

[78] Y. M. Go and D. P. Jones, "Cysteine/cystine redox signaling in cardiovascular disease," *Free Radical Biology & Medicine*, vol. 50, no. 4, pp. 495–509, 2011.

[79] C. W. Kong, T. G. Hsu, F. J. Lu, W. L. Chan, and K. Tsai, "Leukocyte mitochondria depolarization and apoptosis in advanced heart failure: clinical correlations and effect of therapy," *Journal of the American College of Cardiology*, vol. 38, no. 6, pp. 1693–1700, 2001.

Hindawi
Oxidative Medicine and Cellular Longevity
Volume 2019, Article ID 8742075, 12 pages
https://doi.org/10.1155/2019/8742075

Research Article

Evaluation of the Effect Derived from Silybin with Vitamin D and Vitamin E Administration on Clinical, Metabolic, Endothelial Dysfunction, Oxidative Stress Parameters, and Serological Worsening Markers in Nonalcoholic Fatty Liver Disease Patients

Alessandro Federico,[1] Marcello Dallio,[1] Mario Masarone,[2] Antonietta Gerarda Gravina,[1] Rosa Di Sarno,[1] Concetta Tuccillo,[1] Valentina Cossiga,[3] Stefania Lama,[1] Paola Stiuso,[1] Filomena Morisco,[3] Marcello Persico,[2] and Carmelina Loguercio[1]

[1]*Department of Precision Medicine, University of Campania "Luigi Vanvitelli", Via De Crecchio 7, 80138 Naples, Italy*
[2]*Department of Medicine and Surgery, University of Salerno, "Scuola Medica Salernitana" Internal Medicine and Hepatology Unit, Via Allende, 84081 Baronissi, Salerno, Italy*
[3]*Department of Clinical Medicine and Surgery, University of Naples "Federico II", Naples, Italy*

Correspondence should be addressed to Marcello Dallio; marcello.dallio@gmail.com

Received 30 May 2019; Accepted 10 September 2019; Published 15 October 2019

Academic Editor: Marco Malaguti

Nowadays, the nonalcoholic fatty liver disease represents the main chronic liver disease in the Western countries, and the correct medical therapy remains a big question for the scientific community. The aim of our study was to evaluate the effect derived from the administration for six months of silybin with vitamin D and vitamin E (RealSIL 100D®) on metabolic markers, oxidative stress, endothelial dysfunction, and worsening of disease markers in nonalcoholic fatty liver disease patients. We enrolled 90 consecutive patients with histological diagnosis of nonalcoholic fatty liver disease and 60 patients with diagnosis of reflux disease (not in therapy) as healthy controls. The nonalcoholic fatty liver disease patients were randomized into two groups: treated (60 patients) and not treated (30 patients). We performed a nutritional assessment and evaluated clinical parameters, routine home tests, the homeostatic model assessment of insulin resistance, NAFLD fibrosis score and fibrosis-4, transient elastography and controlled attenuation parameter, thiobarbituric acid reactive substances, tumor necrosis factor α, transforming growth factor β, interleukin-18 and interleukin-22, matrix metalloproteinase 2, epidermal growth factor receptor, insulin growth factor-II, cluster of differentiation-44, high mobility group box-1, and Endocan. Compared to the healthy controls, the nonalcoholic fatty liver disease patients had statistically significant differences for almost all parameters evaluated at baseline ($p < 0.05$). Six months after the baseline, the proportion of nonalcoholic fatty liver disease patients treated that underwent a statistically significant improvement in metabolic markers, oxidative stress, endothelial dysfunction, and worsening of disease was greater than not treated nonalcoholic fatty liver disease patients ($p < 0.05$). Even more relevant results were obtained for the same parameters by analyzing patients with a concomitant diagnosis of metabolic syndrome ($p < 0.001$). The benefit that derives from the use of RealSIL 100D could derive from the action on more systems able to advance the pathology above all in that subset of patients suffering from concomitant metabolic syndrome.

1. Introduction

Nonalcoholic fatty liver disease (NAFLD) represents the major cause of chronic liver disease in the Western countries [1, 2]. Very likely, it will occupy a leading position in the near future among the causes of cirrhosis and hepatocellular carcinoma (HCC) in increasingly younger patients [3]. An important contribution to the progression of the disease from simple steatosis (NAFL) to nonalcoholic steatohepatitis (NASH) is given by the alteration of the oxide-reductive imbalance that involves the cells of various organs and apparatus [4, 5]. However, the mechanisms responsible for this pathological evolution are not yet completely clear. The current attention of clinicians and researchers is oriented towards the possibility of using serum instruments and biomarkers able to provide valuable information on the extent of liver fat accumulation, systemic inflammation, and endothelial dysfunction [6–8]. In fact, NAFLD is closely linked with cardiovascular pathology, representing an independent risk factor for the development of chronic and acute diseases [9, 10]. This linkage is represented, precisely, by the endothelial dysfunction, which, in turn, is caused by the systemic "low-grade inflammation" that is supported both by the alteration of metabolic homeostasis and by the high production of reactive oxygen species in NAFLD patients [11]. In the recent past, scientific research has led to the identification of different serological markers of endothelial dysfunction, of which the most important elevated findings in subjects with NAFLD were high mobility group box 1 (HMGB-1), Endocan, and anti-endothelial cell antibodies (AECAs) [12]. The correct planning of the diagnostic, prognostic, and therapeutic procedures for NAFLD still represents a huge challenge for the scientific community, and in accordance with the clinical practice guidelines, the only therapeutic approach considered effective for this type of patients is nowadays constituted by dietary interventions and exercise. However, studies of our group have shown how the use of 12 months of a therapy with silybin conjugated with phospholipids, and vitamin E, in subjects with histological diagnosis of NASH, is able to improve the NAFLD activity score (NAS), the lipidomic profile, and the serum oxidative state as well as different metabolic parameters in these patients due to the well-known effect of silybin as an antioxidant, antifibrotic, and anti-inflammatory compound [13–15]. Moreover, a vitamin D deficiency in patients with NAFLD and metabolic syndrome exists. Vitamin D is closely related through its receptor to the fibrogenic mechanisms supported by the transforming growth factor-beta (TGF-β) in the liver. In particular, it would mediate a reduction in the TGF-β-induced fibrotic deposition as it happens during the progression of the disease towards fibrosis and cirrhosis [16, 17]. Therefore, it seems plausible that the administration of substances such as silybin and its association with vitamin D could positively influence the course of the disease by stopping or slowing the evolution of NASH in cirrhosis. For these reasons, the aim of our study was to evaluate the effect derived from the administration for six months of silybin with vitamin D and vitamin E (RealSIL 100D®) on metabolic markers of oxidative stress, endothelial dysfunction, and markers of the disease worsening in NAFLD patients.

2. Materials and Methods

2.1. Patients. This prospective study is in compliance with ethical guidelines of the Declaration of Helsinki (1975) and has been approved by the ethical committee of the University of Campania "L. Vanvitelli" in Naples (protocol no. 531/2016). 90 consecutive patients with histological diagnosis of NAFLD and 60 patients with diagnosis of reflux disease (not in therapy) as healthy controls followed up at Hepatogastroenterology Divisions of University of Campania "Luigi Vanvitelli" were enrolled between January and October 2017, according to inclusion/exclusion criteria, after signing informed consent. The NAFLD patients were randomized into two groups: treated (60 patients) and not treated (30 patients) (2 : 1 ratio treated vs. not treated). Inclusion criteria were age between 18 and 80 years and diagnosis of NAFLD. Exclusion criteria were use of hepatoprotective drugs; presence of tumors or chronic inflammatory disease such as inflammatory bowel disease, rheumatoid arthritis, systemic lupus erythematosus, or other major systemic diseases; ongoing infections; acute or chronic kidney disease; alcohol or drug abuse history; other causes of chronic liver damage; and psychological/psychiatric problems that could invalidate the informed consent. The definition of the presence/absence of NAFLD and the staging of the disease were diagnosed after the exclusion of other causes of liver diseases, by serological tests and clinical data and by performing a liver biopsy. Medical history, alcohol consumption, drug intake, current drug treatments, smoking habits, and blood pressure were investigated. Weight, height, and waist-to-height ratio (WHtR) were directly measured using standardized devices. The body mass index (BMI) was also calculated by dividing the weight (kg) by the square of height (m). Additional data included routine laboratory tests (blood glucose and insulin, ferritin, C reactive protein (CRP), total cholesterol, low-density lipoprotein (LDL), triglycerides, aspartate (AST) and alanine aminotransferases (ALT), gamma glutamyl transpeptidase (γGT), blood count, and vitamin D) and were obtained by blood peripheral venous samples. The homeostatic model assessment for insulin resistance (HOMA-IR), NAFLD fibrosis score (NFS), and fibrosis-4 (FIB-4) score were calculated in accordance with the specific formulas [18, 19]. It was not prescribed any type of dietary regimen or physical exercise during the study period, both for treated patients and controls. All the analyzed parameters were repeated at baseline (T0) evaluation, after 6 months (T6) of therapy, and at the end of the follow-up period (T12).

2.2. Histological Assessment. The absence or presence of NASH was evaluated according to standard histopathologic criteria, and severity of the disease was assessed using the NAS established by Kleiner, as the sum of scores of steatosis, lobular inflammation, and hepatocellular ballooning [20]. NASH was considered as diagnostic for NAS > 5. Fibrosis was scored according to Brunt et al. as stage 0 (none), stage 1 (zone 3 perisinusoidal or portal fibrosis), stage 2 (zone 3 perisinusoidal and periportal fibrosis without bridging), or stage 3 (bridging fibrosis). Hepatocyte ballooning was scored as 0 (none), 1 (few), or 2 (many) [21].

2.3. FibroScan and Controlled Attenuation Parameter Evaluation. FibroScan transient elastography (TE) was performed using the FibroScan version 502 (Echosens, Paris, France) with standard probes (M and XL probes) [22]. The XL probe was used when the distance from the skin to the liver capsule exceeded 2.5 cm, as measured by sonographic imaging, and/or when BMI was >30. FibroScan was performed by an expert physician without knowledge regarding the results of the histological picture. The objective was to obtain ten acceptable measurements (defined as a successful LS measurement), with the maximum number of attempts set at 20. The criteria proposed by Boursier et al. were used to consider the measurement "very reliable" ($IQR/M \leq 0.1$), "reliable" ($0.1 < IQR/M \leq 0.3$ or $IQR/M > 0.3$ with LS median < 7.1 kPa), or "poorly reliable" ($IQR/M > 0.3$ with LS median ≥ 7.1 kPa) [23]. Based on controlled attenuation parameter (CAP) scores, we classified the enrolled patients in S0, no steatosis (0%–10% fat; 0–237 dB/m); S1, mild steatosis (11%–33% fat; 238–259 dB/m); S2, moderate steatosis (34%–66% fat; 260–292 dB/m); and S3, severe steatosis (>67% fat; ≥293 dB/m) in accordance with calculation of the attenuation of ultrasonic signals used for TE [24].

2.4. Nutritional Assessment. In all subjects, food intake was evaluated by an electronic program (WinFood, Medimatica s.r.l., Martinsicuro, Italy). On the basis of the quantities and qualities of foods consumed, the program elaborates the energy intake and the percentage of macronutrients and micronutrients and calculates the elements in each food. The complete elaboration of intakes shows the list of diet components, the ratio among components and calories, and the subdivision in breakfast, lunch, and dinner. We recorded the food intake of a complete week, including working days and the weekend. Data were compared with the tables of food consumption and recommended dietary intakes of the Italian National Institute of Nutrition and Food Composition Database in Italy [25]. Alcohol use was evaluated with a standardized precodified questionnaire (complete AUDIT test) [26]. The quantity of daily alcohol intake was calculated based on a "drink" that corresponds to about 12 g of pure ethanol [27]. The assessment was repeated at baseline (T0) evaluation, after 6 months (T6), and at the end of the follow-up period (T12).

2.5. Thiobarbituric Acid Reactive Substance Assessment. The thiobarbituric acid reactive substance (TBARS) assay was performed using 10 μl of serum. The cromogen TBARS was quantified using a spectrophotometer at a wavelength of 532 nm with 1,1,3,3-tetramethoxyprophane as a standard. The amount of TBARS was expressed as nmol/μg of protein. Presented data are the mean (m) ± standard deviation (SD), resulting from three independent experiments. All the analyzed parameters were repeated at baseline (T0) evaluation, after 6 months (T6), and at the end of the follow-up period (T12).

2.6. Worsening Markers and Endothelial Dysfunction Assessment. We determined tumor necrosis factor-alpha (TNF-α), TGF-β, interleukin- (IL-) 18, IL-22, matrix metalloproteinase 2 (MMP-2), epidermal growth factor receptor (EGFR), insulin growth factor-II (IGF-II), cluster of differentiation- (CD-) 44, HMGB-1, and Endocan concentration after collecting peripheral blood samples and centrifuging them for serum extraction. Sera were tested by the enzyme-linked immunosorbent assay (ELISA), according to the manufacturer's instructions (CLOUD-CLONE CORP. (EGFR and HMGB-1), R&D SYSTEMS a biotechnic brand Quantikine ELISA (IGF-II, IL-18, TGF-β, MMP-2, IL-22, and TNF-α), and https://MyBioSource.com (TBARS AND Endocan)) [28–30]. All the analyzed parameters were repeated at baseline (T0) evaluation, after 6 months (T6), and at the end of the follow-up period (T12).

2.7. Experimental Design. We performed a baseline comparison of analyzed parameters between the NAFLD patient group and healthy control one.

Among enrolled NAFLD patients, 60 were randomized to have oral administration of RealSIL 100D® (303 mg of silybin-phospholipid complex, 10 mg of vitamin D, and 15 mg of vitamin E) twice a day for six months, and 30 to not have any type of intervention. The amount of vitamin E in the drug molecule is not used to obtain a therapeutic effect because it is very low; on the contrary, it was used in order to obtain a molecular stability of the drug in accordance with pharmacoengineers that designed the product.

Then, all patients were followed up for another 6 months without therapy. At the baseline, we performed a nutritional assessment. During the period of the study, patients were on free diet on the basis of dietary habits prior to the enrollment, and any type of physical exercise was prescribed during the study period. Moreover, we performed at the baseline (T0), at the end of the treatment period (T6), and after six months of follow-up (T12) the clinical, biochemical, liver fibrosis/steatosis, oxidative stress, and endothelial dysfunction assessment (Figure 1). In the evaluation of all the studied parameters, we considered as "improved" the normalization of the specific variable under the upper limit of the normality range level.

2.8. Statistical Analysis. The number of patients (90; 60 in the interventional arm and 30 in the observational one) was calculated on the basis of one of the endpoints of the study, namely, the reduction in CAP. A supposed significant reduction was calculated on the basis of the CAP validation studies that showed how a difference of about 20 dB/m identified a difference between steatosis classes with a good diagnostic performance (S1: 220-240 dB/m, S2: 230-260 dB/m, and S3: 260-300 in the various studies) [31]. On the basis of those data, we calculated that the number of patients needed to measure a statistically significant difference of about 20 dB/m before and after treatment, with a power of 90% and an alpha error of 0.01 in a two-tailed test for paired samples in repeated measures (before and after treatment), was 27 patients per arm (calculation performed with STATA v14 package for Mac: Power And Sample size calculation for means, repeated measures-StataCorp. 2015. Stata Statistical Software: Release 14. College Station, TX: StataCorp LP). Subsequently, to improve the possibilities of collecting significant differences also in the laboratory parameters, it was decided to enroll 30 patients in the observation arm and to double the number (60) in the interventional arm. Parametric and nonparametric tests were performed to

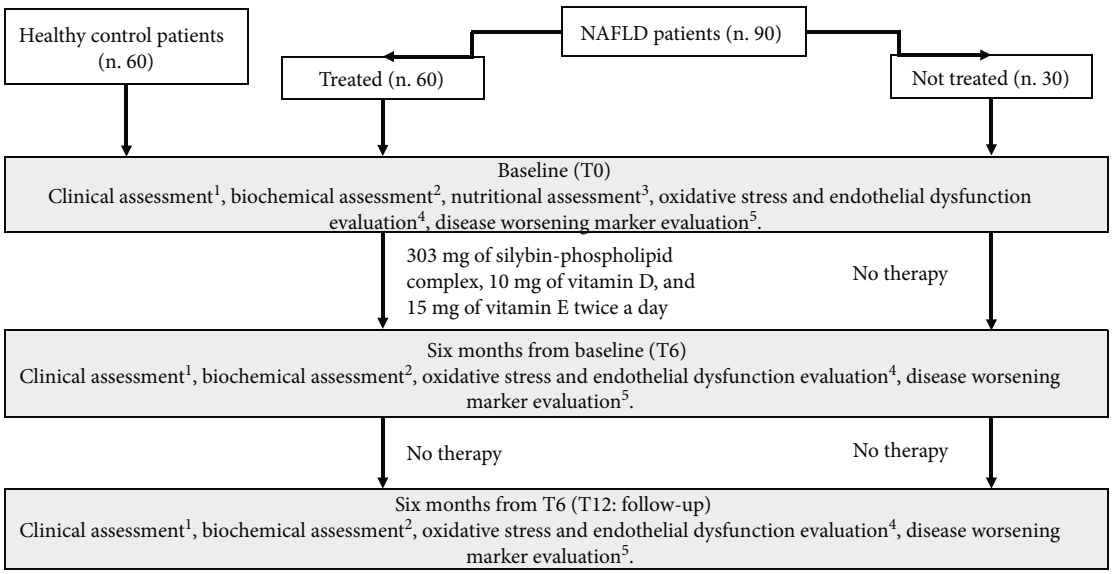

[1]Weight, height and waist-to-height ratio, body mass index, blood pressure measurement
[2]Blood glucose and insulin, HOMA-IR, ferritin, C reactive protein, total cholesterol, low density lipoprotein, triglycerides, aspartate and alanine aminotransferases, gamma-glutamyl transpeptidase, blood count, vitamin D and TNF-α
[3]WinFood analysis
[4]TBARS, HMGB-1, Endocan
[5]FibroScan controlled attenuation parameter, EGFR, CD-44, IL-18, IGF-II, IL-22, TGF-β, MMP-2, FIB-4, NFS

Figure 1: Study design flowchart. NAFLD: nonalcoholic fatty liver disease; HOMA-IR: homeostatic model assessment for insulin resistance; TNF-α: tumor necrosis factor-alpha; HMGB-1: high mobility group box 1; TBARS: thiobarbituric acid reactive substances; EGFR: epidermal growth factor receptor; CD: cluster of differentiation; IL: interleukin; IGF: insulin growth factor; TGF-β: transforming growth factor-beta; MMP-2: metalloproteinase 2; FIB-4: fibrosis 4 index; NFS: NAFLD fibrosis score.

compare the continuous variables when appropriate. In particular, the Student t-test and Mann–Whitney U test were performed to compare continuous variables; chi-square with Yates correction or the Fisher-exact test was performed to compare categorical variables. Data were reported as the mean ± standard deviation for continuous variables with a normal distribution and as the median and interval for those with "nonnormal" distribution. To assess if continuous variables were normally or not normally distributed, we preliminarily performed a Kolmogorov-Smirnov "goodness of fit" test for normality. Statistical significance was defined when "$p < 0.05$" in a "two-tailed" test with a 95% confidence interval. Statistical analyses were performed using the Statistical Program for Social Sciences (SPSS®) 20.0 for Macintosh® (SPSS Inc., Chicago, Illinois, USA).

3. Results and Discussion

3.1. Results. The general characteristics of the enrolled patients are shown in Table 1.

Compared to the population of healthy control patients, NAFLD patients had statistically significant differences ($p < 0.05$) for almost all the parameters evaluated at the baseline: BMI, body weight, AST, ALT, insulin, HOMA-IR, total cholesterol, triglycerides, vitamin D, CRP, TNF-α, EGFR, CD-44, IL-18, IGF-II, IL-22, TGF-β, MMP-2, Endocan, HMGB-1, and TBARS (Table 1). No statistically significant differences were found regarding the daily caloric intake and the type of daily calories between the two groups of NAFLD patients (treated vs. not treated) (Table 2). Furthermore, the repetition of the nutritional assessment at the three observation times envisaged by the study (T0, T6, and T12) did not reveal significant changes in dietary habits for both the groups: treated and the not treated NAFLD. Regarding the clinical parameters evaluated (BMI, WHtR, weight, and blood pressure), no significant differences were found between the two NAFLD groups and, within each group, between the three observation study times. Six months after the baseline, the proportion of treated NAFLD patients who experienced a statistically significant improvement in ALT and γGT was greater compared to not treated NAFLD patients ($p = 0.046$ and $p = 0.032$, respectively). On the other hand, there was no significant change in AST in the two groups of patients at six months from the baseline (T6) ($p = 0.073$) (Figure 2(a)). At the end of the follow-up period (T12), the proportion of NAFLD patients treated that showed a significant improvement of ALT and γGT was significantly reduced, becoming similar to that of the not treated ($p = 0.143$; $p = 0.091$). The AST did not undergo significant changes at the baseline, T6, and T12 (Figure 2(b)). With regard to metabolic parameters, the proportion of patients treated that showed a statistically significant improvement in insulin, HOMA-IR, vitamin D, and degree of steatosis assessed by CAP at six months from the baseline was greater than that in not treated patients, even if for this last parameter a complete normalization was not observed after six months of treatment ($p = 0.032$, $p = 0.044$, $p = 0.038$, and $p = 0.042$, respectively) (Figure 3(a)). This difference remained statistically significant at T12 ($p = 0.041$,

Table 1: General characteristics of the enrolled patients (mean ± SD).

Variable	Healthy controls (no. 60)	NAFLD population (no. 90)	NAFLD treated patients (no. 60)	Not treated NAFLD patients (no. 30)
Age (y)	47 ± 15	54 ± 11	51 ± 6	47 ± 10
Sex (M/F)	30/30	48/42	29/31	19/11
Weight (kg)	71 ± 10.6	88.98 ± 15.08	80.61 ± 13.82	82.07 ± 11.54
BMI (kg/m^2)	26.4 ± 3.9	32.38 ± 4.56	28.92 ± 6.65	29.43 ± 4.65
WHtR	0.81 ± 0.11	0.94 ± 0.06	0.91 ± 0.16	0.93 ± 0.08
Systolic blood pressure (mmHg)	120 ± 13	141 ± 14	138 ± 16	140 ± 9
Controlled attenuation parameters (dB/m)	168.25 ± 52.05	281.75 ± 60.05	282.65 ± 52.53	279.63 ± 58.76
AST (IU/l)	28 ± 11	44 ± 18	44 ± 9	43 ± 10
ALT (IU/l)	29 ± 14	47 ± 19	45 ± 14	48 ± 16
γGT (IU/l)	30 ± 13	36 ± 5	31 ± 17	39 ± 5
FPG (mg/dl)	72 ± 12	89 ± 26	87 ± 13	90 ± 11
Insulinemia (μU/ml)	12 ± 4	25 ± 8	24 ± 5	26 ± 3
HOMA-IR	0.9 ± 0.2	2.4 ± 0.6	2.5 ± 0.1	2.3 ± 0.4
TCH (mg/dl)	112 ± 30	142 ± 17	138 ± 27	146 ± 22
TG (mg/dl)	87 ± 13	87 ± 13	87 ± 13	87 ± 13
LDL (mg/dl)	89 ± 11	92 ± 9	95 ± 11	90 ± 16
Vitamin D (ng/ml)	88 ± 19	26 ± 15	23 ± 12	27 ± 9
CRP (μg/mg)	0.23 ± 0.02	1.89 ± 0.25	1.76 ± 0.32	2.01 ± 0.06
Ferritin (μg/l)	143 ± 34	156 ± 25	150 ± 32	158 ± 41
TNF-α (pg/ml)	12.7 ± 2.2	65.7 ± 22.6	63.5 ± 1.2	68.2 ± 1.8
EGFR (ng/ml)	10.6 ± 5	28.9 ± 2	27.3 ± 4.2	29.8 ± 5.3
CD-44 (ng/ml)	6.1 ± 1.8	12.9 ± 0.7	10.8 ± 0.9	13.3 ± 1
IL-18 (pg/ml)	70.1 ± 38.9	165.6 ± 26.7	159.8 ± 18.9	167.2 ± 22.8
IGF-II (pg/ml)	192.1 ± 43.6	265.9 ± 44.7	261.6 ± 34.6	266.9 ± 32.2
IL-22 (pg/ml)	19.3 ± 6.2	28.8 ± 7.6	29.3 ± 5.2	26.6 ± 4.8
TGF-β (pg/ml)	112.3 ± 42.3	188.8 ± 32.1	192.4 ± 41.1	184.2 ± 37.6
MMP-2 (ng/ml)	15.1 ± 3.7	27.4 ± 2.8	29.3 ± 2.3	25.7 ± 3.9
FIB-4	1.17 ± 0.21	1.27 ± 0.34	1.31 ± 0.18	1.24 ± 0.21
NFS	-1.145 ± 0.02	-1.149 ± 0.06	-1.152 ± 0.05	-1.138 ± 0.04
Stiffness (kPa)	3.4 ± 1.2	5.5 ± 2.6	5.9 ± 0.8	5.1 ± 1.1
Endocan (pg/ml)	372.8 ± 189.3	564.9 ± 196.7	572.3 ± 144.8	541.1 ± 178.9
HMGB-1 (pg/ml)	832.7 ± 242.2	1756.8 ± 212.8	1766.7 ± 282.8	1741.4 ± 142.6
TBARS (nmol/μg)	50.6 ± 24	194.6 ± 32	199.7 ± 27	191.6 ± 14

NAFLD: nonalcoholic fatty liver disease; BMI: body mass index; WHtR: waist-to-height ratio; AST: aspartate aminotransferase; ALT: alanine aminotransferase; γGT: gamma glutamyl transpeptidase; FPG: fasting plasma glucose; HOMA-IR: homeostatic model assessment for insulin resistance; TCH: total cholesterol; TG: triglycerides; LDL: low-density lipoprotein; CRP: C reactive protein; TNF-α: tumor necrosis factor-alpha; EGFR: epidermal growth factor receptor; CD-44: cluster of differentiation 44; IL-18: interleukin-18; IGF-II: insulin growth factor-II; IL-22: interleukin-22; TGF-β: transforming growth factor-beta; MMP-2: metalloproteinase-2; HMGB-1: high mobility group box-1; TBARS: thiobarbituric acid reactive substances.

$p = 0.043$, $p = 0.033$, and $p = 0.048$, respectively) (Figure 3(b)). With regard to glycaemia, total cholesterol, triglycerides, and LDL, there were no significant changes at the three observation times for both NAFLD groups. Among the parameters of systemic inflammation, the proportion of improved patients at T6 compared to the baseline was greater in the treated group compared to the not treated regarding CRP and TNF-α ($p = 0.03$ and $p = 0.037$, respectively) (Figure 4(a)). These parameters in the treated group became similar to not treated patients at T12 ($p = 0.112$ and $p = 0.657$, respectively) (Figure 4(b)). There were no significant changes in ferritin at the three observation times for both NAFLD groups. Among the markers of worsening/disease progression, the proportion of treated patients which presented a significant improvement

Table 2: Nutritional assessment of the enrolled patients (mean ± SD).

Variable	Healthy controls (no. 60)	NAFLD population (no. 90)	NAFLD treated patients (no. 60)	Not treated NAFLD patients (no. 30)
Daily intake (kcal)	2116.5 ± 679.5	2746 ± 164	2667 ± 174	2765 ± 144
Total daily proteins (% of total energy intake)	23 ± 11.5	26.3 ± 2.9	24.3 ± 2.3	23.3 ± 5.4
Soluble carbohydrates (g/day)	89.5 ± 26.5	98.9 ± 13.4	89.3 ± 12.4	88.8 ± 16.5
Saturated fatty acids (% of total energy intake)	8 ± 3.95	10.5 ± 1.9	12.3 ± 1.2	12.4 ± 2.4
Monounsaturated fatty acids (% of total energy intake)	4.55 ± 1.3	14.5 ± 4.6	12.8 ± 3.5	13.2 ± 3.8
Polyunsaturated fatty acids (% of total energy intake)	22.5 ± 6.5	7.1 ± 4.2	7.5 ± 4.3	6.5 ± 4.1
Folic acid (μg per day)	342 ± 101.5	328.6 ± 134.5	332.6 ± 134.5	316.6 ± 134.5
Vitamin A (μg per day)	723 ± 199.5	881.4 ± 344.5	798.4 ± 284.3	898.5 ± 351.2
Vitamin C (μg per day)	118 ± 50.5	145.7 ± 49	145.7 ± 49	145.7 ± 42
Thiamine (μg per day)	0.9 ± 0.4	1.6 ± 0.7	1.3 ± 0.2	1.8 ± 0.5
Riboflavin (μg per day)	3.5 ± 2.5	2.6 ± 1.3	2.6 ± 1.3	2.6 ± 1.3
Vitamin B6 (μg per day)	2 ± 0.5	1.2 ± 0.2	0.9 ± 0.5	1.3 ± 0.1

NAFLD: nonalcoholic fatty liver disease.

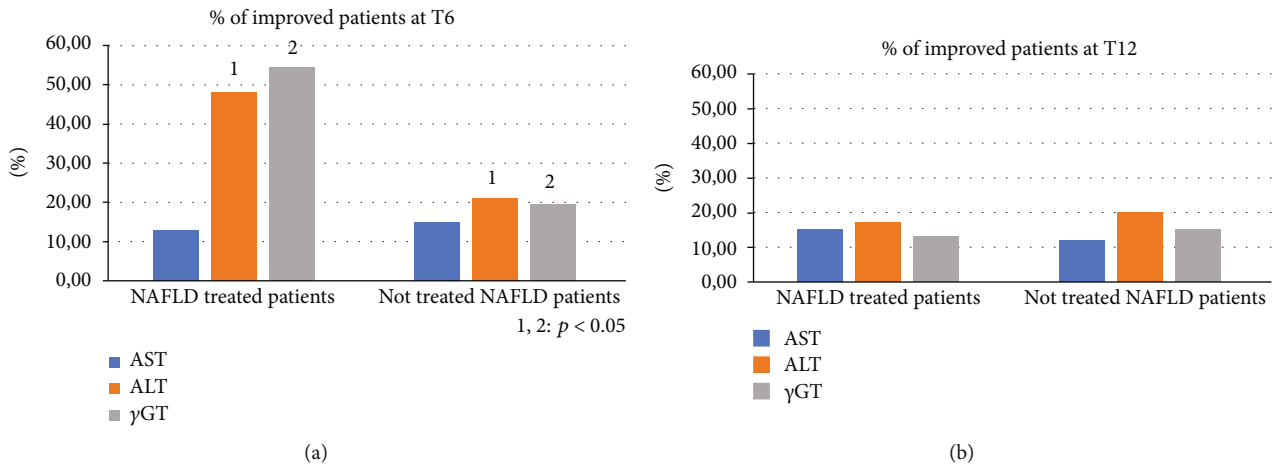

Figure 2: Comparison between the two NAFLD group patients with improvement of aspartate/alanine aminotransferase and gamma glutamyl transpeptidase. NAFLD: nonalcoholic fatty liver disease; AST: aspartate aminotransferase; ALT: alanine aminotransferase; γGT: gamma glutamyl transpeptidase.

at T6 compared to the baseline of EGFR, IL-18, IGF-II, TGF-β, and MMP-2 was greater than the not treated patients ($p = 0.044$, $p = 0.041$, $p = 0.032$, $p = 0.033$, and $p = 0.021$, respectively) (Figure 5(a)). At T12, this data was confirmed ($p = 0.046$, $p = 0.039$, $p = 0.042$, $p = 0.043$, and $p = 0.036$, respectively) (Figure 5(b)). On the contrary, no significant changes were found at the three observation times for CD-44, IL-22, FIB-4, NFS, and stiffness in the two groups of patients. Finally, the proportion of patients who showed at T6 compared to the baseline a significant improvement in Endocan, HMGB-1, and TBARS was greater in the group of patients treated compared to NAFLD controls ($p = 0.045$, $p = 0.043$, and $p = 0.031$) (Figure 6(a)). At T12, the proportion of patients with improvement of these parameters returned to be similar in the two NAFLD study groups ($p = 0.14$, $p = 0.082$, and $p = 0.091$) (Figure 6(b)).

Sixteen out of 30 (53.3%) not treated NAFLD patients showed the criteria for the diagnosis of metabolic syndrome (MS). Among these, 14/16 (87.5%) presented a histological picture of NASH, with values of NAFLD activity score (NAS) ≥ 6. None of the patients enrolled in this group was classified as F4 in accordance with Metavir staging. Furthermore, 31/60 (51.6%) NAFLD treated patients over the histologically diagnosed NAFLD presented the criteria for the diagnosis of MS. Among them, 30/31 (97%) presented a histological picture of NASH, with NAS values ≥ 6. Regarding

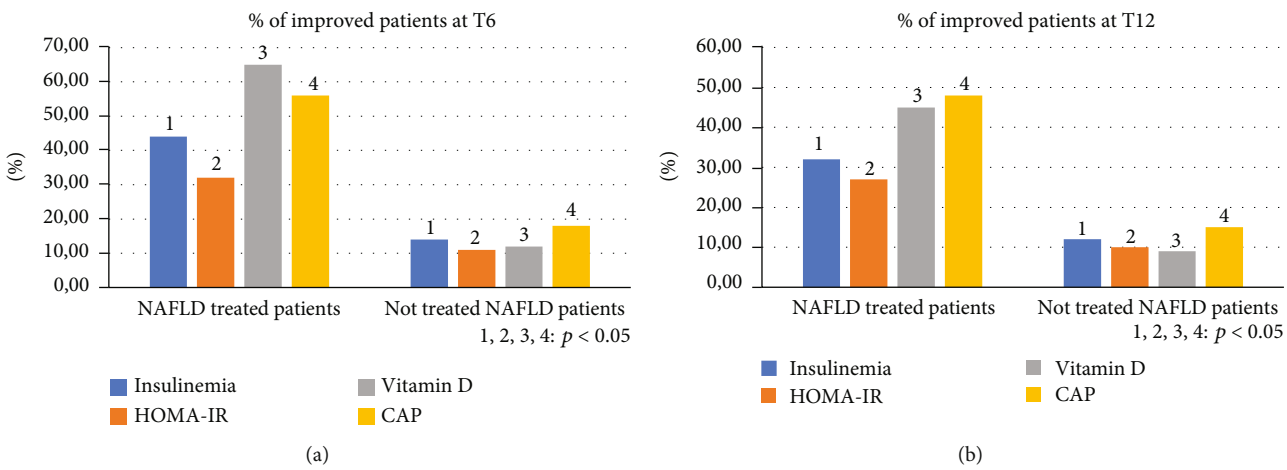

Figure 3: Comparison between the two NAFLD group patients with improvement of insulinemia, the homeostatic model assessment for insulin resistance, vitamin D, and controlled attenuation parameter. NAFLD: nonalcoholic fatty liver disease; HOMA-IR: homeostatic model assessment for insulin resistance; CAP: controlled attenuation parameter.

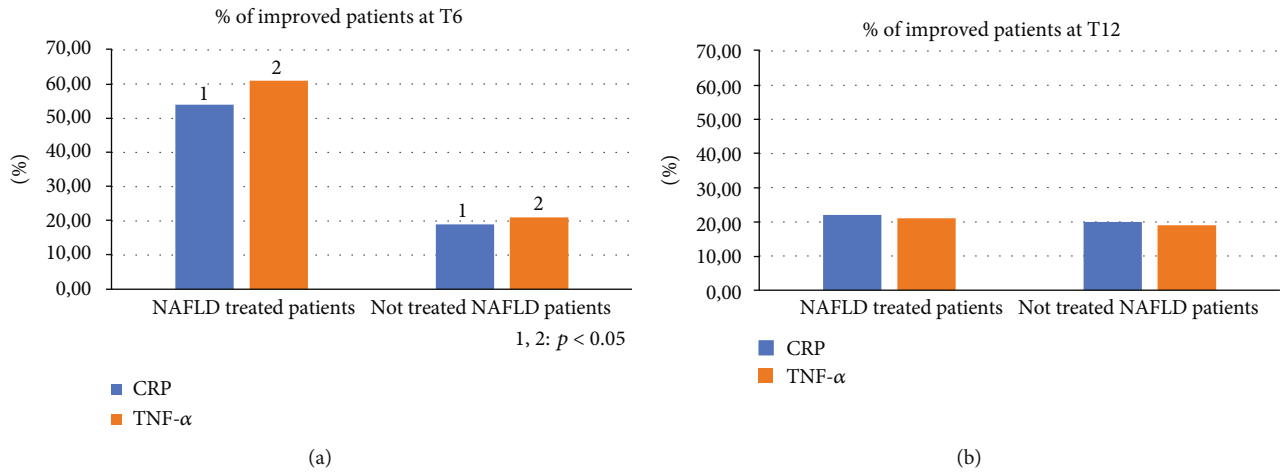

Figure 4: Comparison between the two NAFLD group patients with improvement of C reactive protein and tumor necrosis factor-alpha. NAFLD: nonalcoholic fatty liver disease; CRP: C reactive protein; TNF-α: tumor necrosis factor-alpha.

the histological staging of fibrosis, only one of the enrolled patients was classified as F4 in accordance with Metavir staging. In the NASH population with MS, higher fibrosis stages have been observed compared to patients with simple steatosis (Figure 7). Analyzing the population subset with MS (47/90 NAFLD study population patients, 16/30 not treated patients; 31/60 treated patients), we observed higher proportions of patients improved at T6 in comparison to the baseline in the group of treated patients compared to the not treated group for the following parameters: insulinemia, HOMA-IR, vitamin D, CRP, TNF-α, TGF-β, Endocan, HMGB-1, and TBARS ($p < 0.001$) (Figure 8(a)). This observation remained statistically significant even at T12 ($p < 0.001$) (Figure 8(b)).

4. Discussion

NAFLD has been the emerging cause of chronic liver disease for several years and will be responsible for the onset of new cases of HCC in the near future, eventually becoming the first indication for liver transplantation [32, 33]. NAFLD often fits into a pathological context that is much more complex than that of other liver diseases. In fact, it is frequently part of a pathological condition involving multiple systems identified with the term MS [34, 35]. This harmful union, whose pathogenesis is still not completely clear, is responsible for two very important consequences. While on the one hand speaking about a "metabolically ill" patient may mean having to consider in the prognosis even extrahepatic diseases such as cardiovascular diseases, on the other, the lack of knowledge of many of the mechanisms responsible for the onset of such conditions and the complex interaction between them does not allow, at present, to design a suitable therapy capable of impacting decisively on the natural history of the disease, stopping its course [36, 37]. The worrying clinical scenario that is recalled when thinking about NAFLD has led in recent years to a great scientific fervor in search of the most appropriate treatment for this type of patients [38]. Several

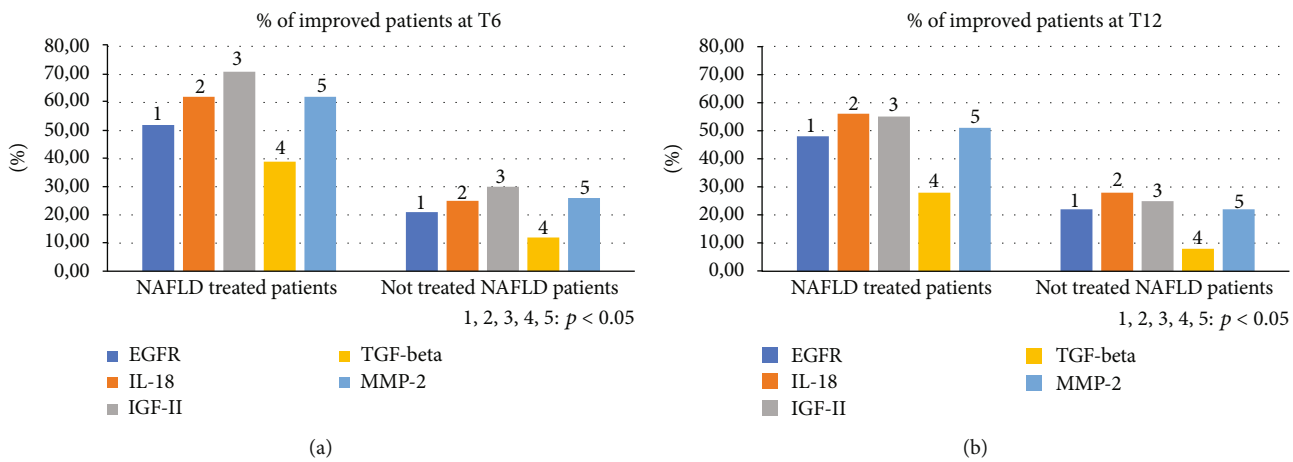

Figure 5: Comparison between the two NAFLD group patients with improvement of epidermal growth factor receptor, interleukin-18, insulin growth factor-II, transforming growth factor-beta, and matrix metalloproteinase-2. NAFLD: nonalcoholic fatty liver disease; EGFR: epidermal growth factor receptor; IL-18: interleukin-18; IGF-II: insulin growth factor-II; TGF-beta: transforming growth factor-beta; MMP-2: matrix metalloproteinase-2.

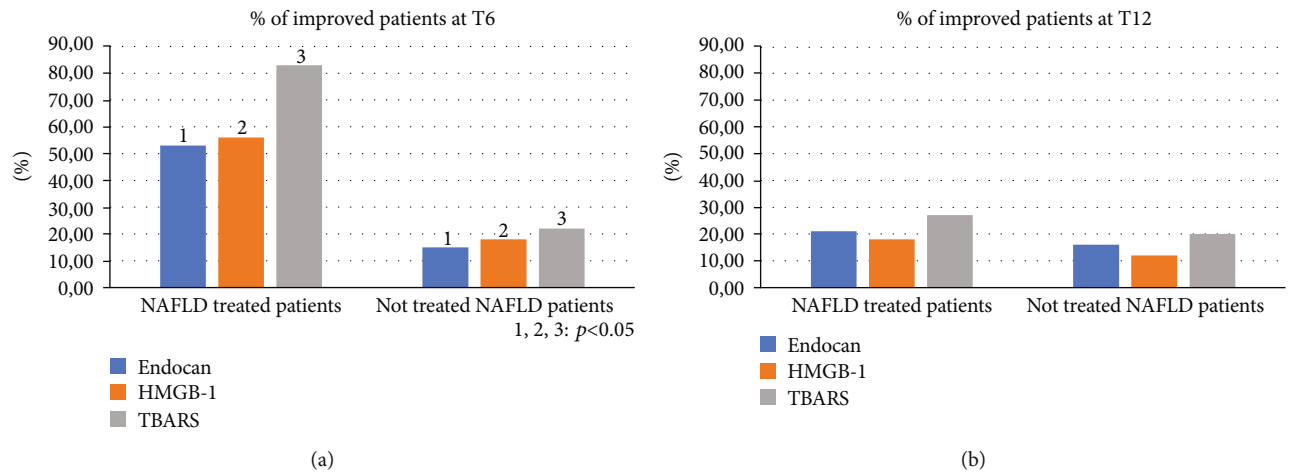

Figure 6: Comparison between the two NAFLD group patients with improvement of Endocan, high mobility group box-1, and thiobarbituric acid reactive substances. NAFLD: nonalcoholic fatty liver disease; HGMB-1: high mobility group box-1; TBARS: thiobarbituric acid reactive substances.

therapeutic attempts have been made in the recent past without obtaining significant results, sometimes even controversial. This is the case, for example, of long-term treatment with insulin-sensitizers, vitamin E, pioglitazone, or their association [38–41].

Several studies reported the role of the intestinal microbiota as a very important factor involved in the genesis of the inflammatory cascades correlated with the NAFLD and the MS, but there are not yet sufficient scientific evidences to support the transferability of the results highlighted by some studies on this topic in daily clinical practice [42]. As if this was not enough, even if many molecules are currently being studied for NAFLD long-term therapy, the majority of the ongoing trials will still require several years before allowing the approval of prescription drugs in this setting [43]. Consequently, the only universally accepted therapy available in this medical picture is represented by diet and physical exercise which have an extraordinary impact on the progression of NAFLD, also slowing down the onset of hepatic and extrahepatic complications [44, 45]. The beneficial effects of herbal product, in particular silybin, on the liver and systemic metabolism have long been studied by many research groups. Silybin antioxidant, insulin-sensitizing, and hepatoprotective capacity, in addition to its high safety profile for long-term administration, led it to represent a "greedy therapeutic opportunity" in the context of metabolic diseases, especially NAFLD [46]. In a multicenter, phase III, double-blind clinical trial, our group had already highlighted how a 12-month treatment with silybin phytosome complex (silybin plus phospholipids) coformulated with vitamin E was able to induce improvement in liver enzymes blood levels, insulin resistance, and liver histology [14]. In this study, we have shown how our population of NAFLD subjects showed a statistically significant difference at the baseline compared

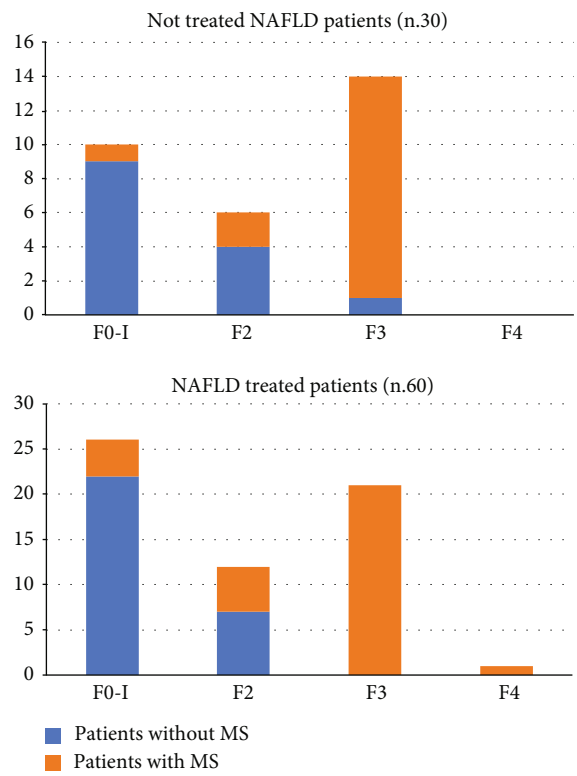

Figure 7: Fibrosis degree distribution in the two NAFLD groups with or without metabolic syndrome. NAFLD: nonalcoholic fatty liver disease; MS: metabolic syndrome.

to a population of hepatologically healthy subjects (with only reflux disease not being treated) for several of the parameters evaluated. Specifically, NAFLD patients demonstrated greater BMI, body weight, insulin, HOMA-IR, total cholesterol, triglycerides, CRP, TNF-α, EGFR, CD-44, IL-18, IGF-II, IL-22, TGF-β, MMP-2, Endocan, HMGB-1, and TBARS, with the evidence, moreover, of lower average levels of vitamin D. This pathological picture fully reflects the data present in the scientific literature showing how patients affected by NAFLD are more exposed to oxidative stress, systemic inflammation, and endothelial dysfunction and have a higher blood level of inflammatory cytokines and fibrosis markers compared to healthy subjects, thus being more predisposed to all the pathologies supported by these harmful factors [47–50]. Taking therefore in analysis the NAFLD population randomized in two arms: treated (no. 60) and not treated (nos. 30), there were not found statistically significant differences regarding the daily caloric intake and the type of calories taken daily. Furthermore, food habits of all the enrolled subjects did not change during the study period as we did not recommend patients to adopt a different lifestyle than they had before enrollment to not invalidate the analysis of the results of our study. Furthermore, we did not find any significant variation in the clinical parameters evaluated during the study between the two NAFLD groups. The group of NAFLD treated patients with respect to the not treated NAFLD patients showed a statistically greater proportion of subjects with normalization of the following parameters at six months: ALT, γGT, insulinemia, HOMA-IR, and vitamin D, with an associated reduction in CAP. A similar observation was found for CRP, TNF-α, EGFR, IL-18, IGF-II, TGF-β, MMP-2, Endocan, HMGB-1, and TBARS. At T12, we observed a clear reduction in the proportion of improved NAFLD treated patients compared to not treated NAFLD patients for ALT, γGT, CRP, TNF-α, Endocan, HMGB-1, and TBARS. Otherwise, the advantage gained during the six months of treatment was maintained at T12 for insulinemia, HOMA-IR, vitamin D, CAP, EGFR, IL-18, IGF-II, TGF-β, and MMP-2. These evidences show how the use of RealSIL 100D for six months was able, due to the known antioxidant, anti-inflammatory, and insulin-sensitizing effects of silybin, to slow down the pathological process by acting on multiple therapeutic targets. This could mean that RealSIL 100D would be able not only to slow down the progression of liver damage but also to improve the sensitivity of peripheral tissues to insulin by inhibiting the formation of free radicals and acting as scavengers for the latter, reducing lipid peroxidation and membrane permeability [51, 52]. Furthermore, it would be able to act on hepatic stellate cells by inhibiting the extracellular signal-related kinase (ERK) activity, MAP/ERK kinase (MEK), and Raf phosphorylation, reducing the migration of leukocytes to the site of inflammation and reducing TGF-β-induced synthesis of type I procollagen as well as MMP-2 secretion [53]. These biological activities are responsible for controlling the inflammatory cascade, the deposition of fat accumulation in the hepatocytes, and the reduction of hepatic and extrahepatic deposition of fibrotic tissue [47–50]. An interesting point is represented by the fact that the improvement of the markers of disease worsening assessed is maintained well beyond the end of the treatment period. How much this reduction results in effective fibrolysis and/or lipolysis or reduction in the risk of HCC development is not known, and further studies are needed. However, it is reasonable to hypothesize how the reduction of the factors that trigger and sustain fibrogenesis can be associated in the long term with a lower deposition of collagen fibers in the organic parenchyma and in the vascular walls. On the contrary, in our clinical setting, the anti-inflammatory and antioxidant effect exerted by silybin seems much more closely connected to its daily administration, running out in a period of time less than six months once the treatment has been interrupted, which would involve the need for a longer administration. Also of great importance is the effect that silybin exerts on the endothelial homeostasis [12]. It now seems scientifically proven, in fact, that the patient suffering from NAFLD, especially in the case of concomitant presence of MS, is a patient burdened by a high cardiovascular risk [9]. The proportion of treated NAFLD patients that showed a marked improvement of Endocan and HMGB-1 compared to not treated NAFLD patients was significantly greater. However, this observation was canceled at the end of the follow-up period, demonstrating, once again, a clear dependence on the administration of the drug. This condition entails the need in the prognostic evaluation of the patient to refer to more medical specialties that should work in concert in order to act on more points

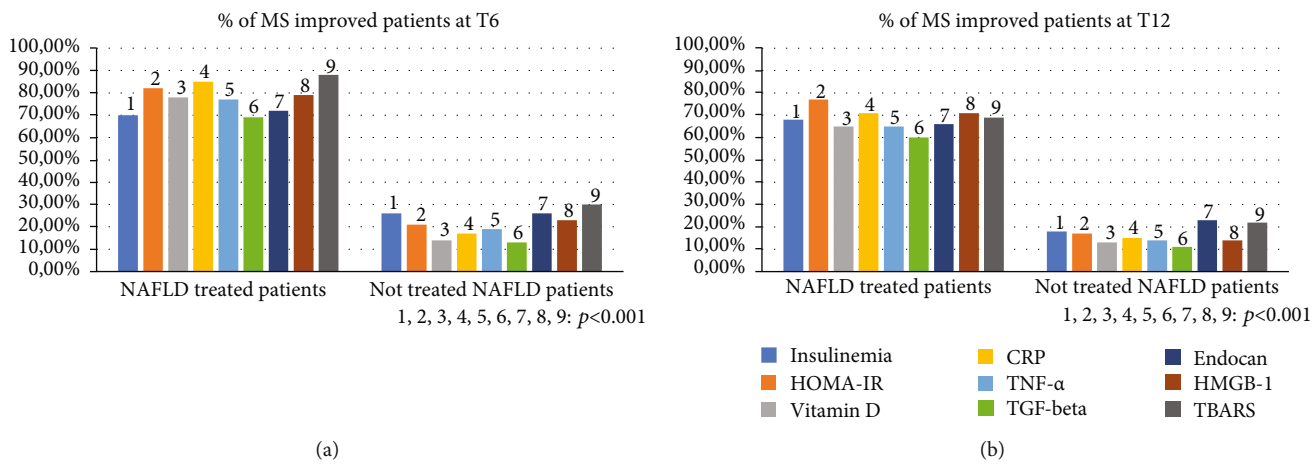

(a) (b)

Figure 8: Comparison between the two NAFLD group patients with metabolic syndrome which presented an improvement of insulinemia, the homeostatic model assessment for insulin resistance, vitamin D, C reactive protein, tumor necrosis factor-alpha, transforming growth factor-beta, Endocan, high mobility group box-1, and thiobarbituric acid reactive substances. NAFLD: nonalcoholic fatty liver disease; MS: metabolic syndrome; HOMA-IR: homeostatic model assessment for insulin resistance; CRP: C reactive protein; TNF-α: tumor necrosis factor-alpha; TGF-beta: transforming growth factor-beta; HGMB-1: high mobility group box-1; TBARS: thiobarbituric acid reactive substances.

in the contrast of the pathology. In this regard, in our clinical setting, the proportion of NAFLD patients treated with concomitant MS that improved in the parameters evaluated with respect to the not treated NAFLD patients with concomitant MS was clearly greater, with levels of statistical significance higher than those obtained from the analysis of the results on the general NAFLD population. This last observation would lead to the hypothesis that the actual benefit that results from a therapy with RealSIL 100D is higher in patients affected by concomitant MS in which NAFLD would be able to progress more rapidly towards more advanced stages of disease in the absence of an appropriate therapeutic intervention.

5. Conclusions

In the era of modern hepatology, NAFLD represents the most frequent cause of chronic liver disease in the Western world. The need to understand the pathogenetic mechanisms that support the disease and to connect it with other organs and systems is inextricably linked to the possibility of developing an appropriate therapeutic plan, able to slow down or stop the course of the disease. The close connection between the cardiovascular system and the liver is certainly a key to direct the development of new therapeutic regimes capable of providing concrete answers to the questions of clinicians, as well as the main reason why the management of this pathological condition should be approached with a multidisciplinary perspective. In this picture, the use of treatment strategies that demonstrate to have more therapeutic targets could represent an important turning point for the correct clinical management of NAFLD, especially in a subset at greater risk of pathological evolution.

Data Availability

The numerical data used to support the findings of this study are included within the article.

Conflicts of Interest

The authors declare no conflict of interest.

Acknowledgments

Research activity of Dr. Antonietta G. Gravina was supported by the Valere Program.

References

[1] A. Federico, M. Dallio, M. Masarone, M. Persico, and C. Loguercio, "The epidemiology of non-alcoholic fatty liver disease and its connection with cardiovascular disease: role of endothelial dysfunction," *European Review for Medical and Pharmacological Sciences*, vol. 20, no. 22, pp. 4731–4741, 2016.

[2] B. A. Neuschwander-Tetri, "Non-alcoholic fatty liver disease," *BMC Medicine*, vol. 15, no. 1, p. 45, 2017.

[3] Z. Younossi, Q. M. Anstee, M. Marietti et al., "Global burden of NAFLD and NASH: trends, predictions, risk factors and prevention," *Nature Reviews. Gastroenterology & Hepatology*, vol. 15, no. 1, pp. 11–20, 2018.

[4] M. Masarone, V. Rosato, M. Dallio et al., "Role of oxidative stress in pathophysiology of nonalcoholic fatty liver disease," *Oxidative Medicine and Cellular Longevity*, vol. 2018, Article ID 9547613, 14 pages, 2018.

[5] H. Kitade, G. Chen, Y. Ni, and T. Ota, "Nonalcoholic fatty liver disease and insulin resistance: new insights and potential new treatments," *Nutrients*, vol. 9, no. 4, p. 387, 2017.

[6] A. Canbay, J. Kalsch, U. Neumann et al., "Non-invasive assessment of NAFLD as systemic disease-a machine learning perspective," *PLoS One*, vol. 14, no. 3, article e0214436, 2019.

[7] S. J. Lee and S. U. Kim, "Noninvasive monitoring of hepatic steatosis: controlled attenuation parameter and magnetic resonance imaging-proton density fat fraction in patients with nonalcoholic fatty liver disease," *Expert Review of Gastroenterology & Hepatology*, vol. 13, no. 6, pp. 523–530, 2019.

[8] P. S. Dulai, S. Singh, J. Patel et al., "Increased risk of mortality by fibrosis stage in nonalcoholic fatty liver disease: systematic review and meta-analysis," *Hepatology*, vol. 65, no. 5, pp. 1557–1565, 2017.

[9] N. Motamed, B. Rabiee, H. Poustchi et al., "Non-alcoholic fatty liver disease (NAFLD) and 10-year risk of cardiovascular diseases," *Clinics and Research in Hepatology and Gastroenterology*, vol. 41, no. 1, pp. 31–38, 2017.

[10] L. A. Adams, Q. M. Anstee, H. Tilg, and G. Targher, "Non-alcoholic fatty liver disease and its relationship with cardiovascular disease and other extrahepatic diseases," *Gut*, vol. 66, no. 6, pp. 1138–1153, 2017.

[11] M. Persico, M. Masarone, A. Damato et al., "Non alcoholic fatty liver disease and eNOS dysfunction in humans," *BMC Gastroenterology*, vol. 17, no. 1, p. 35, 2017.

[12] M. Dallio, M. Masarone, G. G. Caprio et al., "Endocan serum levels in patients with non-alcoholic fatty liver disease with or without type 2 diabetes mellitus: a pilot study," *Journal of Gastrointestinal and Liver Diseases*, vol. 26, no. 3, pp. 261–268, 2017.

[13] P. Stiuso, I. Scognamiglio, M. Murolo et al., "Serum oxidative stress markers and lipidomic profile to detect NASH patients responsive to an antioxidant treatment: a pilot study," *Oxidative Medicine and Cellular Longevity*, vol. 2014, Article ID 169216, 8 pages, 2014.

[14] C. Loguercio, P. Andreone, C. Brisc et al., "Silybin combined with phosphatidylcholine and vitamin E in patients with non-alcoholic fatty liver disease: a randomized controlled trial," *Free Radical Biology & Medicine*, vol. 52, no. 9, pp. 1658–1665, 2012.

[15] M. Dallio, M. Masarone, S. Errico et al., "Role of bisphenol A as environmental factor in the promotion of non-alcoholic fatty liver disease: in vitro and clinical study," *Alimentary Pharmacology & Therapeutics*, vol. 47, no. 6, pp. 826–837, 2018.

[16] F. A. Cimini, I. Barchetta, S. Carotti et al., "Relationship between adipose tissue dysfunction, vitamin D deficiency and the pathogenesis of non-alcoholic fatty liver disease," *World Journal of Gastroenterology*, vol. 23, no. 19, pp. 3407–3417, 2017.

[17] A. Beilfuss, J. P. Sowa, S. Sydor et al., "Vitamin D counteracts fibrogenic TGF-β signalling in human hepatic stellate cells both receptor-dependently and independently," *Gut*, vol. 64, no. 5, pp. 791–799, 2015.

[18] R. K. Sterling, E. Lissen, N. Clumeck et al., "Development of a simple noninvasive index to predict significant fibrosis in patients with HIV/HCV coinfection," *Hepatology*, vol. 43, no. 6, pp. 1317–1325, 2006.

[19] P. Angulo, J. M. Hui, G. Marchesini et al., "The NAFLD fibrosis score: a noninvasive system that identifies liver fibrosis in patients with NAFLD," *Hepatology*, vol. 45, no. 4, pp. 846–854, 2007.

[20] "Nonalcoholic steatohepatitis clinical research network," *Hepatology*, vol. 37, no. 2, p. 244, 2003.

[21] E. M. Brunt, C. G. Janney, A. M. Bisceglie, B. A. Neuschwander-Tetri, and B. R. Bacon, "Nonalcoholic steatohepatitis: a proposal for grading and staging the histological lesions," *The American Journal of Gastroenterology*, vol. 94, no. 9, pp. 2467–2474, 1999.

[22] Z. J. Cao, J. Li, Y. Wang et al., "Serum hepatocyte apoptosis biomarker predicts the presence of significant histological lesion in chronic hepatitis B virus infection," *Digestive and Liver Disease*, vol. 48, no. 12, pp. 1463–1470, 2016.

[23] J. Boursier, J. P. Zarski, V. de Ledinghen et al., "Determination of reliability criteria for liver stiffness evaluation by transient elastography," *Hepatology*, vol. 57, no. 3, pp. 1182–1191, 2013.

[24] M. Sasso, V. Miette, L. Sandrin, and M. Beaugrand, "The controlled attenuation parameter (CAP): a novel tool for the non-invasive evaluation of steatosis using Fibroscan," *Clinics and Research in Hepatology and Gastroenterology*, vol. 36, no. 1, pp. 13–20, 2012.

[25] (SINU) SIdNU, "Tabelle LARN 2014," 2014, http://www.sinu.it/html/pag/tabelle_larn_2014_rev.asp.

[26] J. B. Saunders, O. G. Aasland, T. F. Babor, J. R. De La Fuente, and M. Grant, "Development of the alcohol use disorders identification test (AUDIT): WHO collaborative project on early detection of persons with harmful alcohol consumption–II," *Addiction*, vol. 88, no. 6, pp. 791–804, 1993.

[27] C. Loguercio, M. di Pierro, M. P. di Marino et al., "Drinking habits of subjects with hepatitis C virus-related chronic liver disease: prevalence and effect on clinical, virological and pathological aspects," *Alcohol and Alcoholism*, vol. 35, no. 3, pp. 296–301, 2000.

[28] D. Bechard, V. Meignin, A. Scherpereel et al., "Characterization of the secreted form of endothelial-cell-specific molecule 1 by specific monoclonal antibodies," *Journal of Vascular Research*, vol. 37, no. 5, pp. 417–425, 2000.

[29] H. Tilg and A. M. Diehl, "Cytokines in alcoholic and nonalcoholic steatohepatitis," *The New England Journal of Medicine*, vol. 343, no. 20, pp. 1467–1476, 2000.

[30] D. S. Manning and N. H. Afdhal, "Diagnosis and quantitation of fibrosis," *Gastroenterology*, vol. 134, no. 6, pp. 1670–1681, 2008.

[31] Y. Wang, Q. Fan, T. Wang, J. Wen, H. Wang, and T. Zhang, "Controlled attenuation parameter for assessment of hepatic steatosis grades: a diagnostic meta-analysis," *International Journal of Clinical and Experimental Medicine*, vol. 8, no. 10, pp. 17654–17663, 2015.

[32] C. Margini and J. F. Dufour, "The story of HCC in NAFLD: from epidemiology, across pathogenesis, to prevention and treatment," *Liver International*, vol. 36, no. 3, pp. 317–324, 2016.

[33] Q. M. Anstee, H. L. Reeves, E. Kotsiliti, O. Govaere, and M. Heikenwalder, "From NASH to HCC: current concepts and future challenges," *Nature Reviews. Gastroenterology & Hepatology*, vol. 16, no. 7, pp. 411–428, 2019.

[34] M. Asrih and F. R. Jornayvaz, "Metabolic syndrome and non-alcoholic fatty liver disease: Is insulin resistance the link?," *Molecular and Cellular Endocrinology*, vol. 418, pp. 55–65, 2015.

[35] D. Kim, A. Touros, and W. R. Kim, "Nonalcoholic fatty liver disease and metabolic syndrome," *Clinics in Liver Disease*, vol. 22, no. 1, pp. 133–140, 2018.

[36] T. Wong, R. J. Wong, and R. G. Gish, "Diagnostic and treatment implications of nonalcoholic fatty liver disease and

nonalcoholic steatohepatitis," *Gastroenterology & Hepatology*, vol. 15, no. 2, pp. 83–89, 2019.

[37] A. Shetty and W. K. Syn, "Current treatment options for non-alcoholic fatty liver disease," *Current Opinion in Gastroenterology*, vol. 35, no. 3, pp. 168–176, 2019.

[38] S. Sookoian and C. J. Pirola, "Repurposing drugs to target non-alcoholic steatohepatitis," *World Journal of Gastroenterology*, vol. 25, no. 15, pp. 1783–1796, 2019.

[39] N. Alkhouri, E. Lawitz, and M. Noureddin, "Looking into the crystal ball: predicting the future challenges of fibrotic NASH treatment," *Hepatology Communications*, vol. 3, no. 5, pp. 605–613, 2019.

[40] S. Gheibi, H. E. Gouvarchin Ghaleh, B. M. Motlagh, A. F. Azarbayjani, and L. zarei, "Therapeutic effects of curcumin and ursodexycholic acid on non-alcoholic fatty liver disease," *Biomedicine & Pharmacotherapy*, vol. 115, p. 108938, 2019.

[41] Y. Sumida and M. Yoneda, "Current and future pharmacological therapies for NAFLD/NASH," *Journal of Gastroenterology*, vol. 53, no. 3, pp. 362–376, 2018.

[42] A. Federico, M. Dallio, G. G. Caprio, V. M. Ormando, and C. Loguercio, "Gut microbiota and the liver," *Minerva Gastroenterologica e Dietologica*, vol. 63, no. 4, pp. 385–398, 2017.

[43] S. Singh, N. A. Osna, and K. K. Kharbanda, "Treatment options for alcoholic and non-alcoholic fatty liver disease: a review," *World Journal of Gastroenterology*, vol. 23, no. 36, pp. 6549–6570, 2017.

[44] M. Romero-Gomez, S. Zelber-Sagi, and M. Trenell, "Treatment of NAFLD with diet, physical activity and exercise," *Journal of Hepatology*, vol. 67, no. 4, pp. 829–846, 2017.

[45] European Association for the Study of the Liver (EASL), European Association for the Study of Diabetes (EASD), and European Association for the Study of Obesity (EASO), "EASL-EASD-EASO Clinical Practice Guidelines for the management of non-alcoholic fatty liver disease," *Obesity facts*, vol. 9, no. 2, pp. 65–90, 2016.

[46] A. Federico, M. Dallio, and C. Loguercio, "Silymarin/Silybin and chronic liver disease: a marriage of many years," *Molecules*, vol. 22, no. 2, p. 191, 2017.

[47] B. Bhushan, S. Banerjee, S. Paranjpe et al., "Pharmacologic Inhibition of Epidermal Growth Factor Receptor Suppresses Nonalcoholic Fatty Liver Disease in a Murine Fast-Food Diet Model," *Hepatology*, 2019.

[48] S. Patouraux, D. Rousseau, S. Bonnafous et al., "CD44 is a key player in non-alcoholic steatohepatitis," *Journal of Hepatology*, vol. 67, no. 2, pp. 328–338, 2017.

[49] K. Yamanishi, S. Maeda, S. Kuwahara-Otani et al., "Interleukin-18-deficient mice develop dyslipidemia resulting in nonalcoholic fatty liver disease and steatohepatitis," *Translational Research*, vol. 173, pp. 101–114.e7, 2016.

[50] A. Adamek and A. Kasprzak, "Insulin-like growth factor (IGF) system in liver diseases," *International Journal of Molecular Sciences*, vol. 19, no. 5, p. 1308, 2018.

[51] C. Loguercio and D. Festi, "Silybin and the liver: from basic research to clinical practice," *World Journal of Gastroenterology*, vol. 17, no. 18, pp. 2288–2301, 2011.

[52] C. P. Colturato, R. P. Constantin, A. S. Maeda Jr. et al., "Metabolic effects of silibinin in the rat liver," *Chemico-Biological Interactions*, vol. 195, no. 2, pp. 119–132, 2012.

[53] A. Federico, M. Trappoliere, C. Tuccillo et al., "A new silybin-vitamin E-phospholipid complex improves insulin resistance and liver damage in patients with non-alcoholic fatty liver disease: preliminary observations," *Gut*, vol. 55, no. 6, pp. 901-902, 2006.

Hindawi
Oxidative Medicine and Cellular Longevity
Volume 2019, Article ID 2580409, 18 pages
https://doi.org/10.1155/2019/2580409

Research Article

Danshenol A Alleviates Hypertension-Induced Cardiac Remodeling by Ameliorating Mitochondrial Dysfunction and Suppressing Reactive Oxygen Species Production

Kai Chen,[1,2] Yiqing Guan,[1] Yunci Ma,[3] Dongling Quan,[4] Jingru Zhang,[4] Shaoyu Wu,[4] Xin Liu,[1] Lin Lv,[4] and Guohua Zhang[1]

[1]*School of Traditional Chinese Medicine, Southern Medical University, Guangzhou, China*
[2]*Hong Kong University-Shenzhen Hospital, Shenzhen, China*
[3]*Southern Medical University Nanfang Hospital, Guangzhou, China*
[4]*School of Pharmaceutical Sciences, Southern Medical University, Guangzhou, China*

Correspondence should be addressed to Guohua Zhang; zghgz@163.com

Received 5 April 2019; Revised 24 July 2019; Accepted 6 August 2019; Published 11 September 2019

Guest Editor: Sabato Sorrentino

Current therapeutic approaches have a limited effect on cardiac remodeling, which is characteristic of cardiac fibrosis and myocardial hypertrophy. In this study, we examined whether Danshenol A (DA), an active ingredient extracted from the traditional Chinese medicine *Radix Salviae*, can attenuate cardiac remodeling and clarified the underlying mechanisms. Using the spontaneously hypertensive rat (SHR) as a cardiac remodeling model, DA ameliorated blood pressure, cardiac injury, and myocardial collagen volume and improved cardiac function. Bioinformatics analysis revealed that DA might attenuate cardiac remodeling through modulating mitochondrial dysfunction and reactive oxygen species. DA repaired the structure/function of the mitochondria, alleviated oxidative stress in the myocardium, and restored apoptosis of cardiomyocytes induced by angiotensin II. Besides, DA inhibited mitochondrial redox signaling pathways in both the myocardium and cardiomyocytes. Thus, our study suggested that DA attenuates cardiac remodeling induced by hypertension through modulating mitochondrial dysfunction and reactive oxygen species.

1. Introduction

Cardiovascular disease is still a serious threat to senior citizens in aging countries [1]. Cardiac remodeling, caused by hypertension, coronary disease, valvulopathy, and other stimuli, takes part in the occurrence and development of various cardiovascular diseases and even results in chronic heart failure [2]. Unfortunately, an ideal solution for therapeutic cardiac remodeling is lacking. The pathophysiology of cardiac remodeling includes cardiomyocyte hypertrophy and apoptosis, as well as extracellular fibrosis, which are considered the major predictive indicators of mortality in sufferers of cardiovascular diseases [3, 4]. Therefore, researchers believed that cardiac function could be ameliorated by inhibiting cardiac remodeling.

Evidence has been increasing that oxidative stress serves as an important mechanism for myocardial remodeling and cardiac failure [5, 6]. As a matter of fact, oxidative stress occurs in all cardiovascular tissue and regulates a variety of cell functions such as cytodifferentiation, multiplication, caducity, and apoptosis under physiological conditions [7]. In cardiac remodeling, oxidative stress is always intensive, which is manifested as mitochondrial dysfunction and excessive generated reactive oxygen species (ROS). These effects ultimately lead to cardiac contractile failure and structural damage [8, 9]. Accordingly, targeting cardiac oxidative stress as a strategy to inhibit hypertensive cardiac remodeling has attracted considerable attention over the past decade.

Over the past decades, natural plant medicines have been extensively applied and popularized in numerous countries.

The World Health Organization encourages the utilization of natural medicine as a promising adjuvant treatment strategy [10, 11]. *Radix Salviae* (Danshen) is a kind of traditional Chinese herb applied extensively in the treatment of cardiovascular diseases in China. As a drug for cardiovascular diseases, the compound Danshen dropping pill is currently undergoing phase III trials in clinical centers over nine countries. It is expected to become the first Chinese medicine authenticated by the Food and Drug Administration [12]. Danshenol A (DA) is an abietane-type diterpene ester separated from *Radix Salviae*. In contrast with the well-known tanshinone form of *Radix Salviae*, for instance, tanshinone I, tanshinone IIA, and cryptotanshinone, few studies have reported the biological effects of Danshenol. Previous reports indicated that the anti-inflammatory properties of DA are superior to those of tanshinone IIA, thereby prompting that DA has potential efficacy for atherosclerosis [13]. Another study revealed that DA can protect endothelial cells from oxidative stress by directly scavenging ROS [14]. Preliminary research conducted by our group found that treatment with DA significantly improves ventricular function in SHR and reduces ROS levels. The results aroused our interests. We surmise that the underlying mechanisms of DA attenuating cardiac remodeling are related to the oxidative stress pathway.

Our manuscript is intended at investigating the protective effects of DA on cardiac remodeling induced by hypertension and identifying whether the underlying mechanisms are associated with the oxidative stress pathway.

2. Materials and Methods

2.1. Reagents and Drugs. DA (CAS:189308-08-5, purity ≥ 98%) was purchased from EMMX Biotechnology LLC (Santiago, USA). Captopril tablets (12.5 mg) as the positive control were provided by Bristol-Myers Squibb Co. Ltd. (lot 1209031).

The biochemical kits for the detection of lactate dehydrogenase (LDH, batch number: A020-2), creatine kinase (CK, batch number: A032), CK-MB (batch number: H197), alanine aminotransferase (ALT, batch number: C009-2), aspartate aminotransferase (AST, batch number: C010-2), creatinine (Cr, batch number: C011-2), blood urea nitrogen (BUN, batch number: C013-2), and ROS (batch number: E004) were obtained from Nanjing Jiancheng Biotech Co. Ltd. (Nanjing, China). Biochemical kits of MitoCheck Complex I activity (lot 700930), MitoCheck Complex II activity assay kit (lot 700940), MitoCheck Complex II/III activity assay kit (lot 700950), and citrate synthase activity (lot 700990) were obtained from Cayman Chemical Company (Ann Arbor, Michigan).

2.2. Animal Grouping and Administration. Animal feeding and experimental procedures were conformed to institutional animal ethics committee guidelines, which acted in accordance with the Care and Use of Laboratory Animals published by the United States National Institutes of Health (NIH Publications No. 85-23, revised 1996).

Forty male spontaneously hypertensive rats (SHR) and eight male Wistar-Kyoto (WKY) rats at the age of 16 weeks were bought from Vital River Laboratory Animal Technology Co. Ltd. The rats were conventionally raised for 5 days in a SPF laboratory animal room at first, where the environment was set procedurally at 24°C ± 2°C and 35% ± 5% humidity under a regular 12 h/12 h light/dark schedule. All rats have free access to sterile water and forage.

Using a randomized complete control study, the forty SHR were assigned into five groups: SHR group (cardiac remodeling model, $n = 8$), CAP group (SHR+captopril, 13.5 $mg{\cdot}kg^{-1}{\cdot}day^{-1}$, $n = 8$), DAL group (SHR+DA low dose, 0.3 $mg{\cdot}kg^{-1}{\cdot}day^{-1}$, $n = 8$), DAM group (SHR+DA medium dose, 1 $mg{\cdot}kg^{-1}{\cdot}day^{-1}$, $n = 8$), and DAH group (SHR+DA high dose, 3 $mg{\cdot}kg^{-1}{\cdot}day^{-1}$, $n = 8$). The WKY group (blank control, $n = 8$) consisted of male Wistar-Kyoto rats. DA or captopril was orally administrated daily for 12 weeks, while the WKY and SHR groups received the equal volume of normal saline.

2.3. Blood Pressure and Echocardiography Measurements. After 12 weeks of administration, systolic blood pressure (SBP), diastolic blood pressure (DBP), and mean blood pressure (MBP) were determined using noninvasive tail pressure equipment (ALC-NIBP, Shanghai Alcott Biotechnology Co. Ltd., Shanghai, China). In brief, animals were preheated at 38°C for 8 minutes in a thermostat pad, and three stable consecutive measurements of blood pressure including SBP and DBP were recorded. Also, ejection fraction (EF) and fractional shortening (FS) were detected via color Doppler ultrasound diagnostic instrument in M-mode with a 10 MHz probe (S40 Exp).

2.4. Serum Sample Analysis. After treatment for 12 consecutive weeks, the blood samples were gathered from the caudal vein of rats and centrifugated at 3000 rpm/min for 12 min. Then, the serum was collected carefully from the supernatant and stored at −80°C. Myocardial injury was evaluated with the serum concentration of LDH, CK, and CK-MB, whereas liver and renal functions were examined using ALT, AST, Cr, and BUN.

2.5. Histopathological Detection. Executed with narcotic overdose, hearts from the rats were separated and weighed to determine the HW/BW index (the rate of heart weight to body weight). The left ventricle tissue was dissociated partially and fixed with 4% polyformaldehyde for 48 h. Then, the tissue was embedded in paraffin, sliced at 5 mm, and stained with Masson's trichrome (Solarbio, USA) to visualize fibrillar collagen. The extent of fibrosis was observed in 8 random fields of vision each sample and quantitated as the collagen volume fraction (CVF) using a light microscope (CX31, Olympus) at 40x magnification and ImageJ software (National Institutes of Health, Bethesda).

2.6. Analysis of Molecular Mechanisms. To clarify the molecular mechanisms of DA on cardiac remodeling, molecular targets of DA were obtained from the Traditional Chinese Medicine Systems Pharmacology Database and Analysis Platform (TCMSP, http://lsp.nwu.edu.cn/index.php) [15] and Bioinformatics Analysis Tool for Molecular mechANism

of Traditional Chinese Medicine (BATMAN-TCM, http://bionet.ncpsb.org/batman-tcm) [16]. The targets were further screened using the PharmMapper server (http://lilab.ecust.edu.cn/pharmmapper/) [17]. Subsequently, we executed KEGG analysis by a plug-in ClueGO in Cytoscape 3.6.1 (https://cytoscape.org) [18] to show the signaling pathways related to DA on cardiac remodeling ($P < 0.05$, min overlap ≥ 3).

2.7. Electron Microscopy. Anterior walls of the left ventricle were transferred into 2.5% glutaraldehyde and 1% paraformaldehyde for 24 h. After washing at least twice with 0.1 M PBS at 4°C, 1% OsO_4-buffered solution (pH 7.4) was used to postfix the tissue samples for 1 h. The resins were embedded and sectioned through the EM Ultramicrotome LKB-2088 and stained using 1% toluidine blue solution. The ultrathin sections were then stained with uranyl acetate and lead citrate twice. Eventually, the morphology of mitochondria in the myocardium was observed using an electron microscope (Hitachi H-7500).

2.8. Mitochondrial Complex Activity. Mitochondria in heart tissue were extracted as described above, and the activity of the mitochondrial complex was examined by corresponding biochemical kits. In brief, complex I activity was measured as the oxidation extent of nicotinamide adenine dinucleotide. Complex II activity was measured as the diminution in artificial electron acceptor L2 6-dichlorophenolindophenol. Complex III activity was determined as the reduction of cytochrome c. Complex IV was determined by the reduction in acetyl-CoA, which was measured as the content of oxaloacetate.

2.9. Adenine Nucleotide Analysis. The heart tissue and cardiomyocytes were collected and immersed in 0.6 M $HClO_4$ (4 mL/g, 4°C), then homogenized directly and transferred into a centrifuge at 10000 r/min for 15 min. The supernatant was neutralized and filtered after centrifugation under the same conditions. The test solution was completely separated with isocratic elution via 96% 0.05 M KH_2PO_4 (pH 6.5) and 4% methanol for 20 min in high-performance liquid chromatography (HPLC) with a Waters C18 column (250 × 4.6 mm, 5 μm). Content of adenosine triphosphate (ATP), adenosine diphosphate (ADP), and adenosine monophosphate (AMP) was measured at 254 nm via an external standard method for quantification. The energy charge was calculated as ((ATP + ADP)/2)/(ATP + ADP + AMP) [19].

2.10. Determination of Oxidative Stress in the Myocardium. After treatment for 12 consecutive weeks, myocardium samples were collected as mentioned above. The level of oxidative stress was determined by measuring the concentrations of ROS, malondialdehyde (MDA), and 4-hydroxynonenal (4-HNE) in the myocardium of rats.

2.11. Cell Culture. Primary cultures of rat cardiomyocytes were conducted in accordance with previous studies. In brief, neonatal Sprague-Dawley rats were sacrificed. The hearts were rapidly separated from the rats and washed using phosphate-buffered saline. Then, cardiac tissues were minced via amicrobic scissors and digested using Hanks' solution with 0.1% trypsin at 37°C for 3 min. Cells were isolated by digestion for 8–10 times and transferred to Dulbecco's modified Eagle medium containing 10% fetal bovine serum (FBS). The cardiomyocytes were then cultivated in culture flasks with a density of 1×10^5 cells/cm^2 and plated into an incubator where the environment was maintained at 37°C with 5% CO_2.

2.12. Detection of Apoptosis. The apoptosis rate of cardiomyocytes was determined via an Annexin V-FITC Apoptosis Detection Kit and a flow cytometer. Cardiomyocytes were cultivated in six-well culture plates with Dulbecco's modified Eagle medium with 10% FBS for 48 h. The medium was replaced with serum-free medium and cultivated for 24 h. Then, cells were pretreated with DA (1, 3, and 10 μmol/L) and captopril (5 μmol/L) for 35 min, followed by 0.1 μmol/L angiotensin II (Ang II) for another 48 h. After incubation, cells were cleaned with PBS and resuspended. Then, fluorescein-conjugated annexin V (5 mL) and propidium iodide reagent (5 mL) were added to cell suspensions. The mixture above was incubated for 15 min protected from light. Finally, the rate of apoptosis was determined and quantified by FACScan flow cytometry (Beckman Coulter).

2.13. Western Blot. The total proteins were isolated from the myocardial tissue and cardiomyocytes. After quantitation, protein samples were analyzed using 15% gradient gel and then transferred into the polyvinylidene fluoride (PVDF) membrane via a gel transfer device. Then, PVDF membranes were incubated via primary antibodies against Bax, Bcl-2, (GTP)p-Ras, Ras, p-Raf, Raf, p-Mek, Mek, p-Erk, Erk, Ask1, p-Jnk, Jnk, p-p38, p38, and GAPDH overnight at 4°C. After that, the primary antibodies were cleaned with Tween20/TBS solution, and then secondary antibodies were incubated for another 1 h. Using developing solution, the expression of proteins was measured via an Odyssey infrared imaging system (LI-COR Biosciences) and normalized to the GAPDH protein level.

2.14. Statistical Analysis. Results are presented as the mean ± standard deviation. Statistical analysis was conducted using one-way ANOVA and Dunnett's test. P value less than 0.05 was defined by having the difference of statistics. Statistical analysis was determined via GraphPad Prism 5.01 for Windows.

3. Results

3.1. Effect of DA on Blood Pressure and Cardiac Function. Dose-related alternations in SBP, DBP, and MBP for the six groups are exhibited in Figures 1(a) and 1(b). After treatment for 12 consecutive weeks, SBP, DBP, and MBP in the SHR group were obviously higher than those in the WKY group (Figure 1(a)–1(c)). With DA administration, blood pressure was decreased, which showed a dose-dependent manner, but the overall effects were not as credible as those in the CAP group.

EF and FS were used to evaluate the impairment of cardiac function, and the impairment of EF and FS suggested

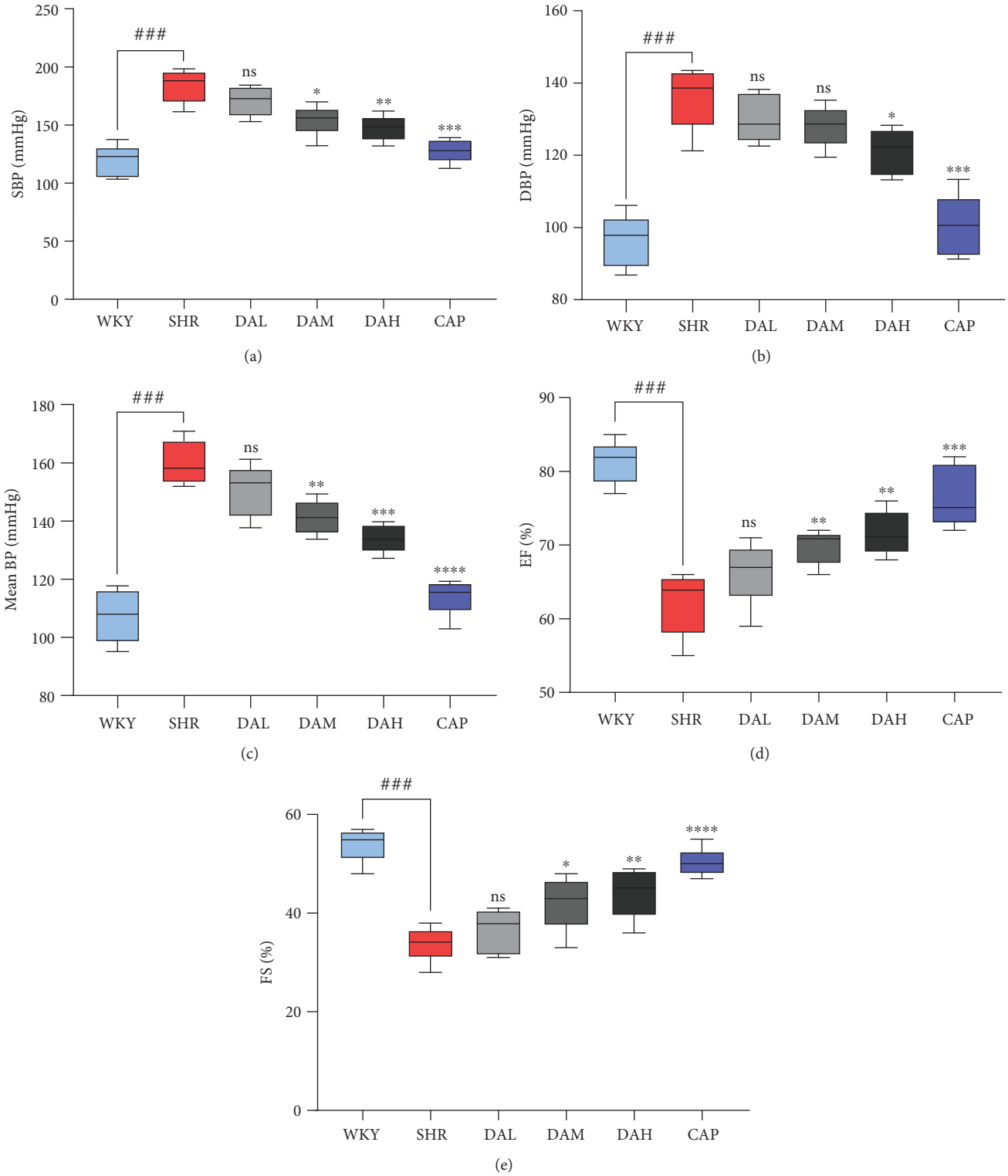

Figure 1: Continued.

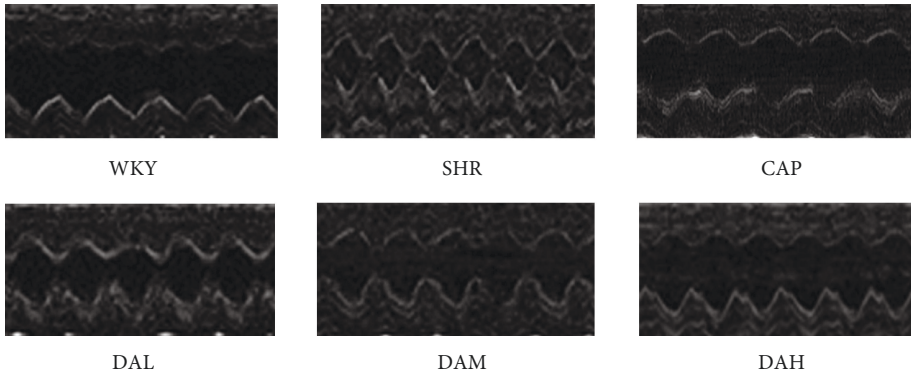

(f)

Figure 1: Effects of DA treatment on blood pressure and cardiac function during administration for 12 consecutive weeks: (a) SBP; (b) DBP; (c) MBP; (d) EF; (e) FS; (f) image of ultrasound cardiogram. $n = 7$. $^{\#\#\#}P < 0.001$ vs. WKY, $^{\#\#}P < 0.01$ vs. WKY, and $^{\#}P < 0.05$ vs. WKY; $^{***}P < 0.001$ vs. SHR, $^{**}P < 0.01$ vs. SHR, and $^{*}P < 0.05$ vs. SHR.

cardiac functional insufficiency. As shown in Figures 1(d) and 1(e), EF and FS in SHR were substantially deficient than those in WKY, whereas DA and CAP treatments increased EF and FS. Representative ECG images in M-mode are shown in Figure 1(f).

3.2. Effects of DA Treatment on Cardiac, Hepatic, and Renal Functions. To estimate the protection of DA on the heart and its safety for the liver and kidney, indexes of a myocardial enzymogram (CK, CK-MB, and LDH), liver function (ALT, AST), and kidney function (Cr, BUN) were detected in the present study. As shown in Figure 2, the serum concentration of CK and CK-MB increased obviously in SHR compared with WKY ($P < 0.001$), indicating that hypertension induced heart damage (Figure 2(a)). With treatment, DA improved cardiac function as evidenced by the reduction in serum CK and CK-MB, whereas the CAP group was the most effective group.

3.3. Effects of DA Treatment on Cardiac Remodeling. Consistent with the alternations in blood pressure and cardiac function, significant deterioration of cardiac remodeling under histological analysis was determined in the SHR compared with the WKY group (Figure 3(a)), as evidenced by the increase in the ratio of HW/BW (Figure 3(c)). The treatment of DA prevented cardiac remodeling and decreased HW/BW compared with SHR.

Masson's trichrome-stained sections (Figure 3(b)) and CVF (Figure 3(d)) showed that the content of cardiac collagen (staining in blue color) under DA treatment was obviously relieved compared with the SHR group (40x magnification), which showed a dose-dependent manner.

3.4. Molecular Mechanisms of DA on Cardiac Remodeling. Using the TCMSP database and BATMAN-TCM, we obtained 25 potential molecular targets of DA (Table 1). Molecular docking was carried out to increase the reliability of the results. Twelve molecular targets, namely, Ptgs1, Kcnc2, F10, Ptgs2, Diap1, Daf-2, Pik3cg, Mfn1, Ace, Cox17, Arnt, and Prkca, were screened as molecular targets of DA (Table 2). Signaling pathways enriched from the molecular targets are shown in Figure 4 and Table 3. Consequently, protein targeting to the mitochondrion and regulation of the response to ROS may be the potential signaling pathway underlying DA treatment of cardiac remodeling.

3.5. Effect of DA on Mitochondrial Morphology and Mitochondrial Complex Activity. Electron microscopy observations on the cardium showed obvious morphological changes in the SHR group compared with the WKY group (Figure 5(a)). The density of the mitochondrium was obviously decreased in the cardium of the SHR group compared with the WKY group. Furthermore, the structure of the cardium in the SHR group showed defective striation, reduced cristae structures, and disappearance of the z line compared with that in the WKY group. By contrast, DA treatment restored the damage to mitochondrial morphology and cardium structure.

Maximal activities of complexes I–VI were determined in cardiac mitochondria to evaluate the function of cardiac mitochondria. Mitochondrial complex enzyme activities decreased in the SHR group than in the WKY group, whereas DA treatment enhanced the activities, which showed a dose-dependent manner. (Figure 5(b)–5(e)).

3.6. Effect of DA on Mitochondrial Function and Oxidative Stress. The measurement of adenine nucleotide variants was conducted to evaluate the energy production in myocardial mitochondria. As a result, DA treatments increased ATP and ADP content in the myocardium, while ATP and ADP content in the SHR group was obviously lower than that in the WKY group (Figure 6(a)). Besides, the AMP content was more abundant in the SHR group compared with the WKY group, whereas DA treatment reduced it. Overall, DA groups, especially the high dose groups, demonstrated higher energy charge compared with the SHR group (Figure 6(b)). Consequently, the expression of ROS, MDA, and 4-HNE obviously increased in the SHR group (Figure 6(c)–6(e)), but the upregulated expression was less pronounced in the DA groups.

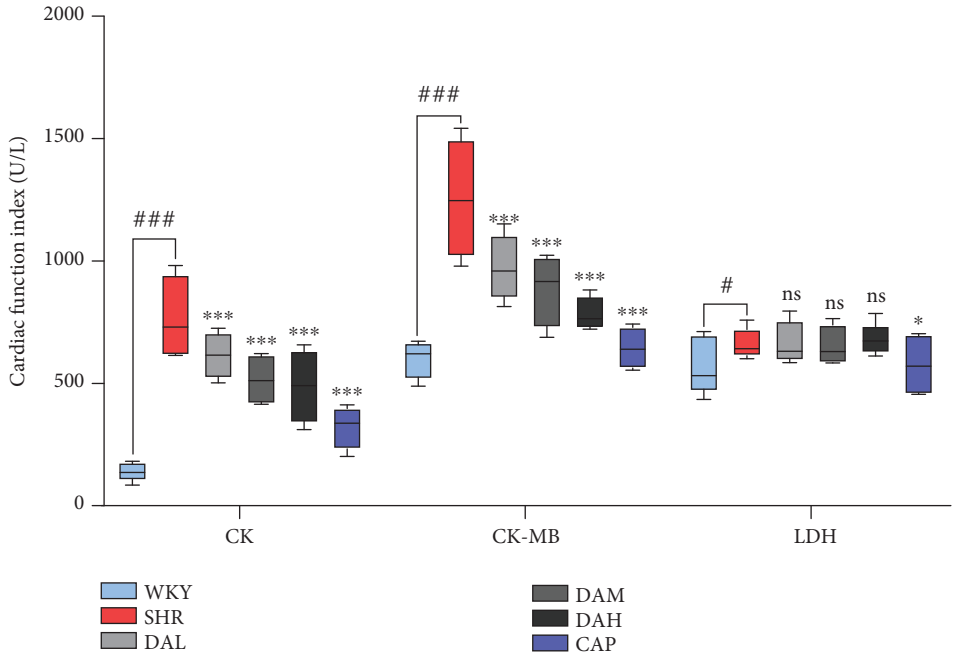

(a)

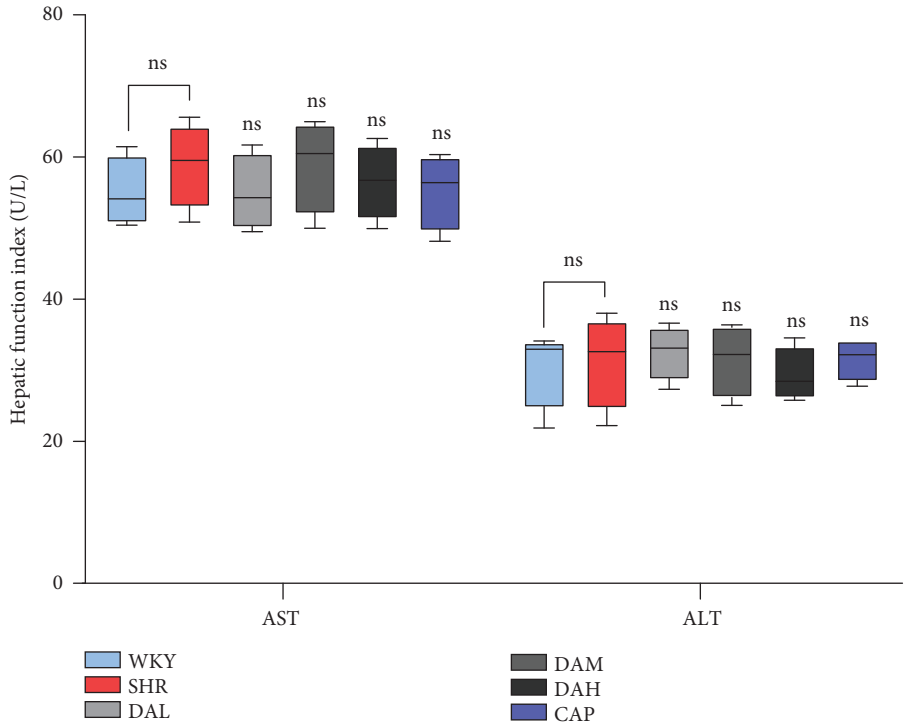

(b)

Figure 2: Continued.

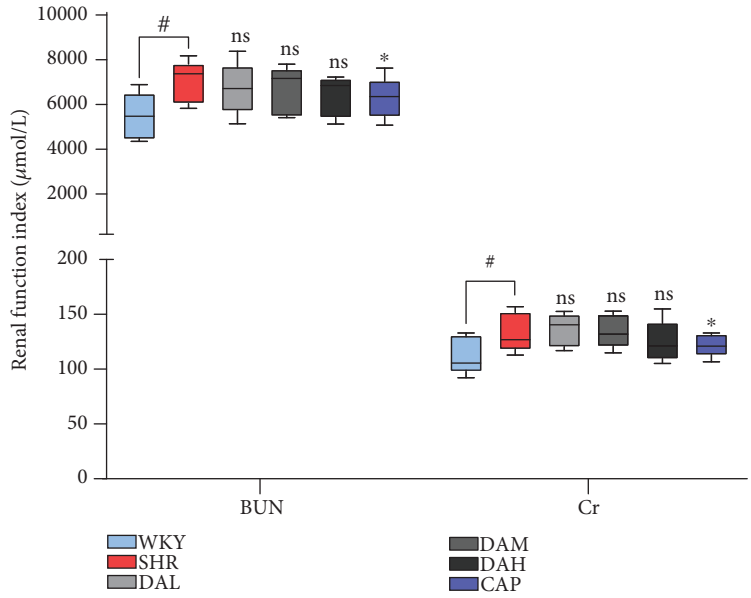

(c)

Figure 2: Effect of DA treatment on the serum biochemical index at 12 weeks. (a) Cardiac function index including CK, CK-MB, and LDH; (b) hepatic function index including AST and ALT; (c) renal function index including Cr and BUN. $^{\#\#\#}P < 0.001$ vs. WKY, $^{\#\#}P < 0.01$ vs. WKY, and $^{\#}P < 0.05$ vs. WKY; $^{***}P < 0.001$ vs. SHR, $^{**}P < 0.01$ vs. SHR, and $^{*}P < 0.05$ vs. SHR.

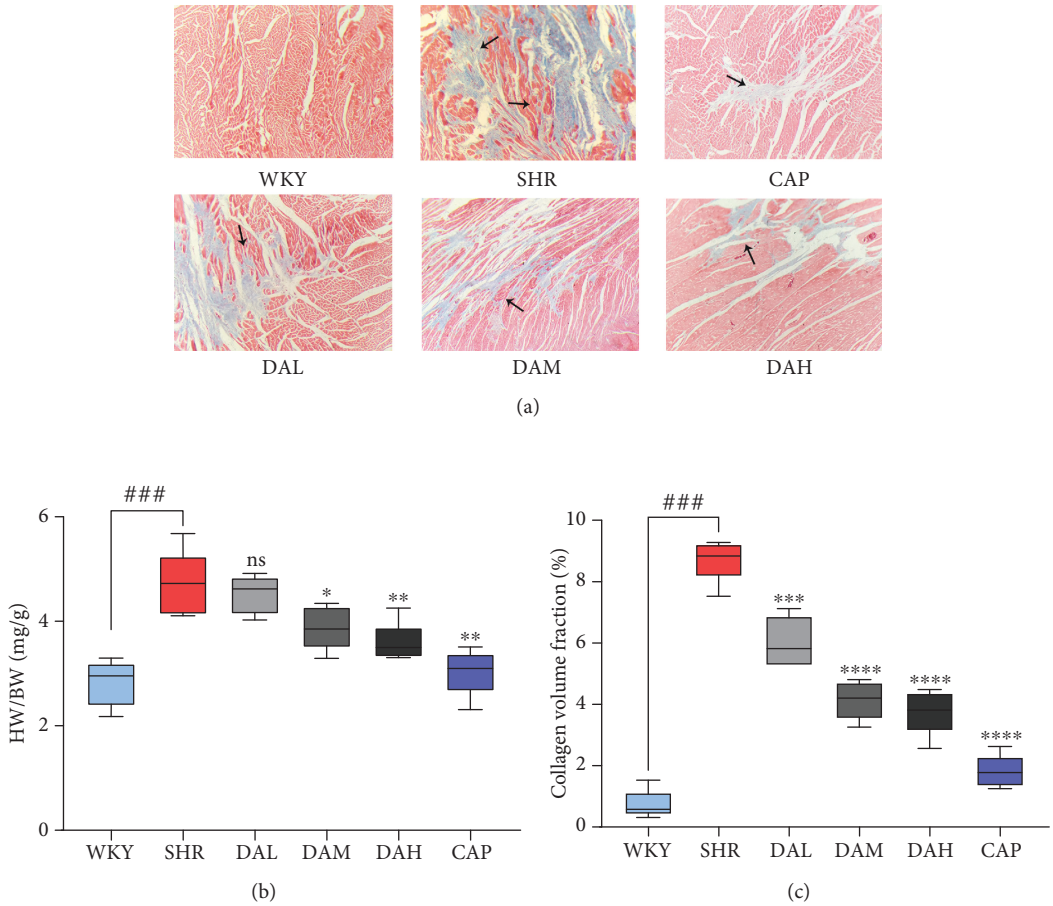

Figure 3: Effects of KXF treatment on cardiac remodeling. (a) Masson staining images under 200x magnification and the areas of collagen deposition were indicated by the black arrow; (b) HW/BW; (c) CVF. Results are presented as the mean ± SEM ($^{*}P < 0.05$, $^{**}P < 0.01$, and $^{***}P < 0.001$ vs. SHR; $^{\#\#\#}P < 0.001$ vs. WKY).

Table 1: Targets of DA from TCMSP and BATMAN-TCM.

TCMSP	BATMAN-TCM
Ptgs1, Kcnc2, Scn5a, F10, Ptgs2, Rxra, Pik3cg, Ncoa1, and Kcnma1	Diap1, Bak1, Ptgs2, Ucp2, Mfn1, Mfn2, Mapl, Rxra, Ace, Pde3a, Daf-2, Adra1b, Aif, Hif1a, Arnt, Prkca, Cox17, Eif4e

Table 2: Targets of DA validated by PharmMapper server.

PharmMapper server
Ptgs1, Kcnc2, F10, Ptgs2, Diap1, Daf-2, Pik3cg, Mfn1, Ace, Cox17, Arnt, Prkca

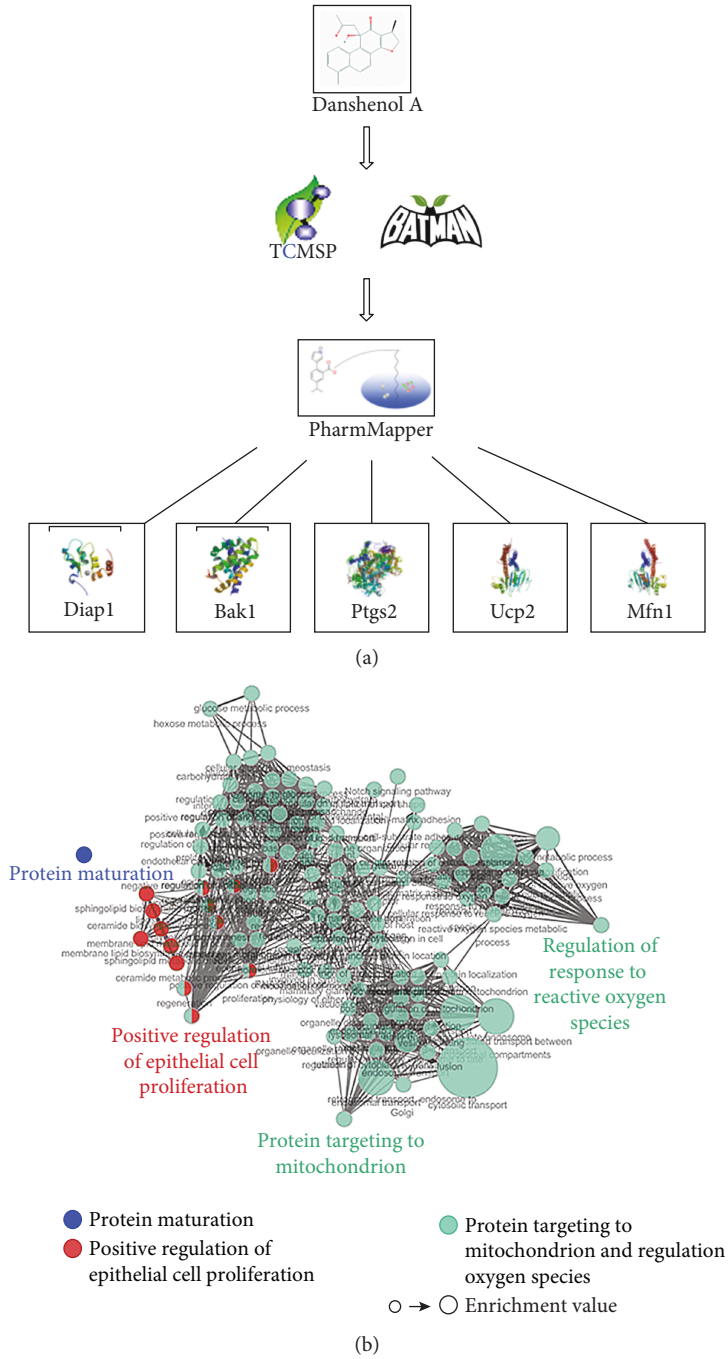

Figure 4: KEGG analysis of signaling pathways related to DA on cardiac remodeling. (a) Flow chart of reverse molecular docking using PharmMapper. (b) Significant enrichment of protein targets in the network diagram.

Table 3: Enrichment analysis of protein targets related to DA.

Function	Count	FDR
Protein targeting to mitochondrion/regulation of response to reactive oxygen species	6	0.002487
Positive regulation of epithelial cell proliferation	4	0.042185
Protein maturation	4	0.041617
Amoebiasis	3	0.026515
AGE-RAGE signaling pathway	3	0.031415
MAPK signaling pathway	3	0.003792
HIF-1 signaling pathway	3	0.019821
EGFR tyrosine kinase inhibitor resistance	2	0.032885

3.7. Effect of DA on Cardiomyocyte Apoptosis. Incubation with Ang II (0.1 μmol/L) for 48 h enhanced the apoptotic rate of cardiomyocytes (Figures 7(a) and 7(b)) with increased expression of apoptotic protein Bax and decreased expression of apoptosis inhibitory protein Bcl-2. By contrast, pretreatment with DA (1, 3, and 10 μmol/L) obviously decreased the apoptotic rate of cardiomyocytes incubated by Ang II, which was accompanied with the decreased expression of Bax and increased expression of Bcl-2 (Figure 7(c)–7(e)).

3.8. Effect of DA on Mitochondrial Redox Signaling Pathways. Mitochondrial redox signaling pathways are mainly regulated by Ras, Raf, Mek, Erk, Ask1, Jnk, and p38. The result of Western blot showed that the protein levels of p-Ras, p-Raf, p-Mek, p-Erk, Ask1, p-Jnk, and p-p38 were raised in the SHR group than in the WKY group, while pretreatment with DA decreased those (Figure 8). A similar result was observed in cardiomyocytes (Figure 9).

4. Discussion

Cardiac remodeling, an adaptive response of the heart to pressure overload, is a result from physiological or pathological stimuli [20], which presented as abnormal thickening of the ventricular wall and reduced volume of the ventricular chamber [21]. Although the physiological processes maintain enhanced heart function, cardiac remodeling can be decompensated and deteriorated into heart failure under pathological conditions [22]. Pathological hypertrophy is accompanied by the high fetal gene expression, excessive fiber deposition, and cardiac dysfunction. Research also suggested that the pathogenesis of cardiac remodeling is related to oxidative stress [6]. We used the SHR models to illustrate the ameliorated cardiac dysfunction effect of DA and its antioxidant capacity in vivo.

SHR is a mature hypertensive model that was introduced in 1963, in which myocardial damage occurs and eventually leads to cardiac remodeling after 16 weeks [23]. Hence, SHR was used as a cardiac remodeling model in this study. Captopril is an angiotensin-converting enzyme inhibitor that is widely used in the treatment of hypertension and congestive heart failure. Captopril was utilized as a positive control due to its ability to reverse cardiac fibrosis function.

The present study indicated that DA treatment significantly decreased SBP and DBP in SHR, but the effects were inferior to captopril. EF and FS are the fractions of outbound blood pumped from the heart in each cardiac cycle. EF and FS, which are measured by an echocardiogram, are general indicators of cardiac function [24]. As a result, EF and FS were enhanced in DA-treated groups compared with the SHR group, thereby illustrating that DA ameliorated cardiac function. Numerous cytokines have been demonstrated to be bound up with cardiac damage and cardiac dysfunction. Coinciding with previous studies, our data showed that the plasma content of CK, CK-MB, and LDH in the DA-administrated group was reduced compared with that in the SHR group. Meanwhile, Masson staining demonstrated a decrease in CVF in the DA-administrated group relative to the SHR group. Thus, DA treatment decreased cardiac injury markers of function in SHR, repaired the injured myocardium, and ameliorated cardiac function.

To explore the specific mechanism of DA on cardiac remodeling, bioinformatics technology was used in this study. TCMSP is an advanced platform of network pharmacology for Chinese herbal medicine which contains the correlations among drugs, targets, and diseases [15]. BATMAN-TCM, which captures TCM-related data obtained from different platforms, constructs a network model for integrative relationships among herbs, ingredients, targets, and diseases [16]. PharmMapper server conducts an in silico target prediction algorithm for a given small molecule through "probing" of the potential ligand binding sites via pharmacophore models [17]. Using these databases, we obtained potential molecular targets of DA. Functional enrichment analysis was carried out to show the mechanism of DA based on the targets, which, using a hypergeometric test to identify the significant enrichment pathway in differential proteins compared with all identified proteins, can identify the main biochemical metabolic pathways involved.

Accordingly, the analysis determined that the molecular targets were significantly enriched in functions associated with "protein targeting to mitochondrion/regulation of response to reactive oxygen species," "positive regulation of epithelial cell proliferation," "protein maturation," and "amoebiasis." Among them, "protein targeting to mitochondrion/regulation of response to reactive oxygen species" was highly enriched

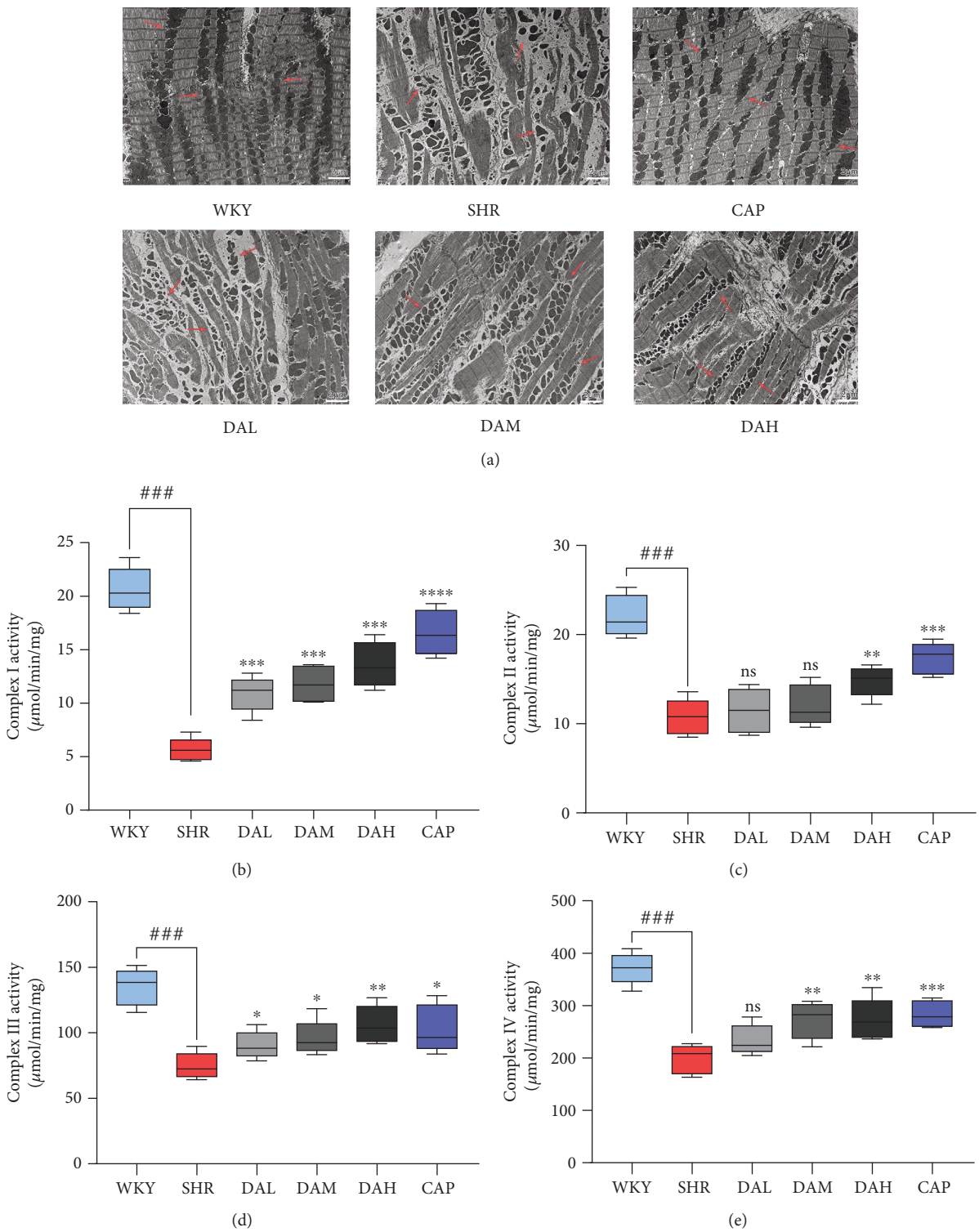

Figure 5: Changes in mitochondrial morphology and mitochondrial complex activity. (a) Ultrastructural analysis of myocardium under 8000x magnification and the areas of the mitochondrion were marked by the black arrow. (b–e) Maximal activities of complexes I-IV in cardiac mitochondria. $^{###}P < 0.001$ vs. WKY, $^{##}P < 0.01$ vs. WKY, and $^{#}P < 0.05$ vs. WKY; $^{***}P < 0.001$ vs. SHR, $^{**}P < 0.01$ vs. SHR, and $^{*}P < 0.05$ vs. SHR.

with a target level of 6 and considered one of the most essential pathways modulating the mechanism of DA. On the basis of the annotation data of gene ontology [25], the definition of "protein targeting to mitochondrion" is the process that modulates the frequency, rate, or extent of protein targeting to the mitochondrion, whereas "regulation of response to reactive oxygen species" is the process that modulates the frequency, rate, or extent of response to ROS. The

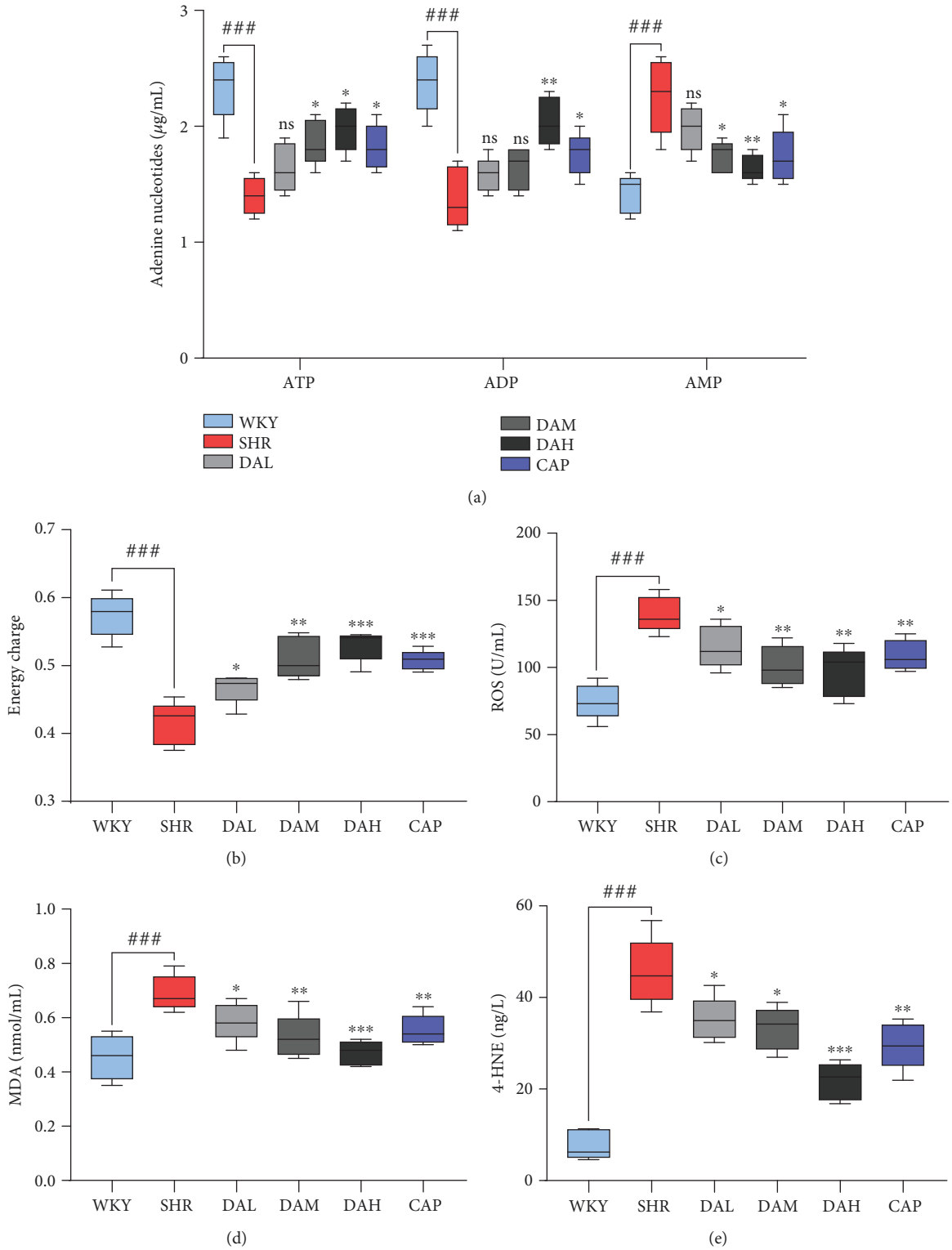

Figure 6: (a, b) ATP, ADP, and AMP concentrations and energy charge in the myocardium. (c–e) Oxidative stress indexes of MDA, ROS, and 4-HNE concentrations in the myocardium. $^{###}P < 0.001$ vs. WKY, $^{##}P < 0.01$ vs. WKY, and $^{#}P < 0.05$ vs. WKY; $^{***}P < 0.001$ vs. SHR, $^{**}P < 0.01$ vs. SHR, and $^{*}P < 0.05$ vs. SHR.

annotation of enrichment is quite a general concept, which only serves as a hint, so we focus on the relationship between the mitochondrion, ROS, cardiac remodeling, and DA through previous studies.

Growing evidence indicates that ROS is essential for the pathogenesis of cardiac remodeling, which may also exert an obvious effect in the progression from pathological remodeling to heart failure [26, 27]. For example, Dirican

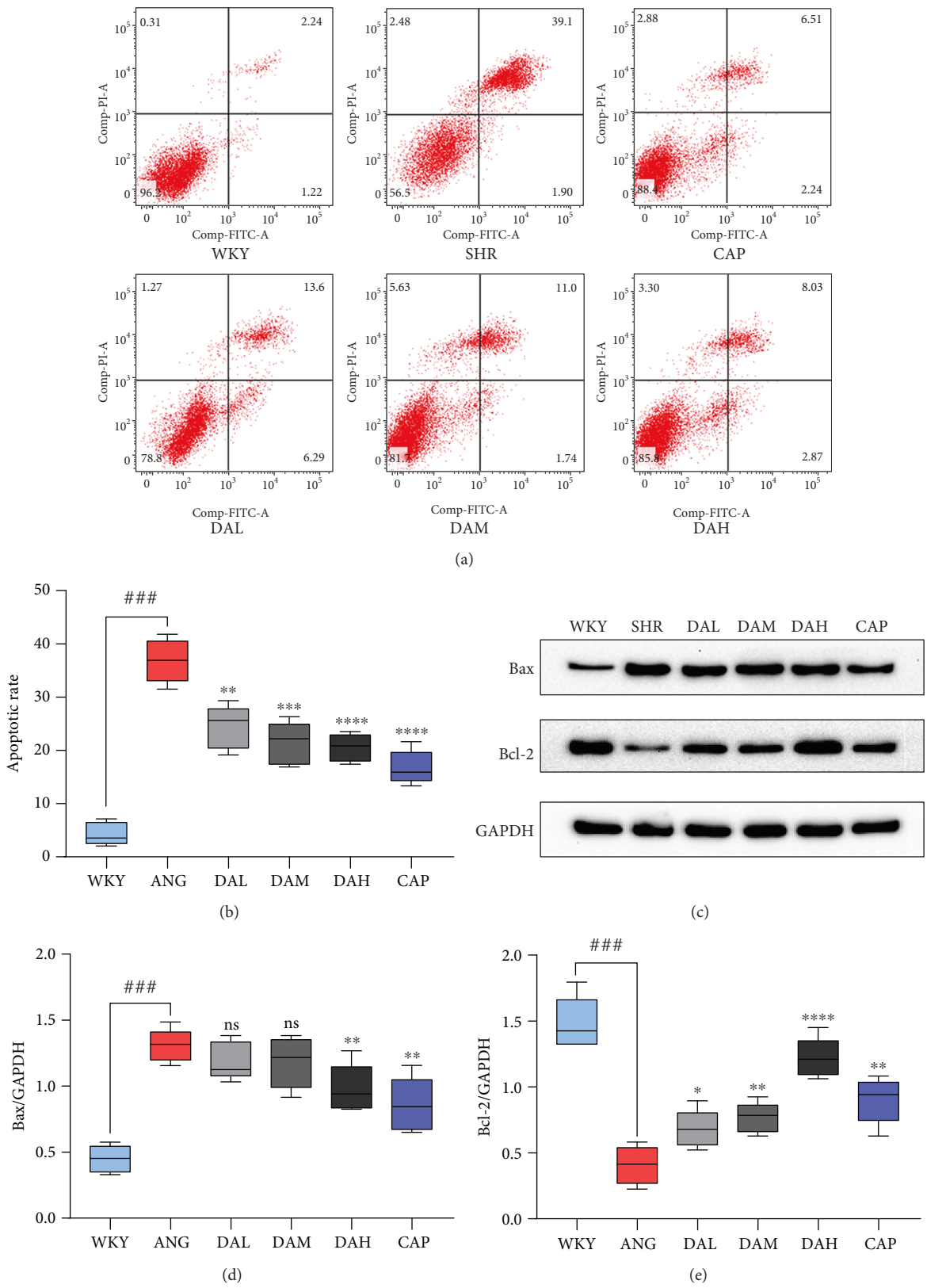

Figure 7: Effect of DA on cardiomyocyte apoptosis. (a, b) Ang II-induced cell apoptosis rate was quantified by flow cytometry. (c–e) Western blot analysis of apoptosis-related proteins: Bcl-2 and Bax in each groups. $^{###}P < 0.001$ vs. WKY, $^{##}P < 0.01$ vs. WKY, and $^{\#}P < 0.05$ vs. WKY; $^{***}P < 0.001$ vs. SHR, $^{**}P < 0.01$ vs. SHR, and $^{*}P < 0.05$ vs. SHR.

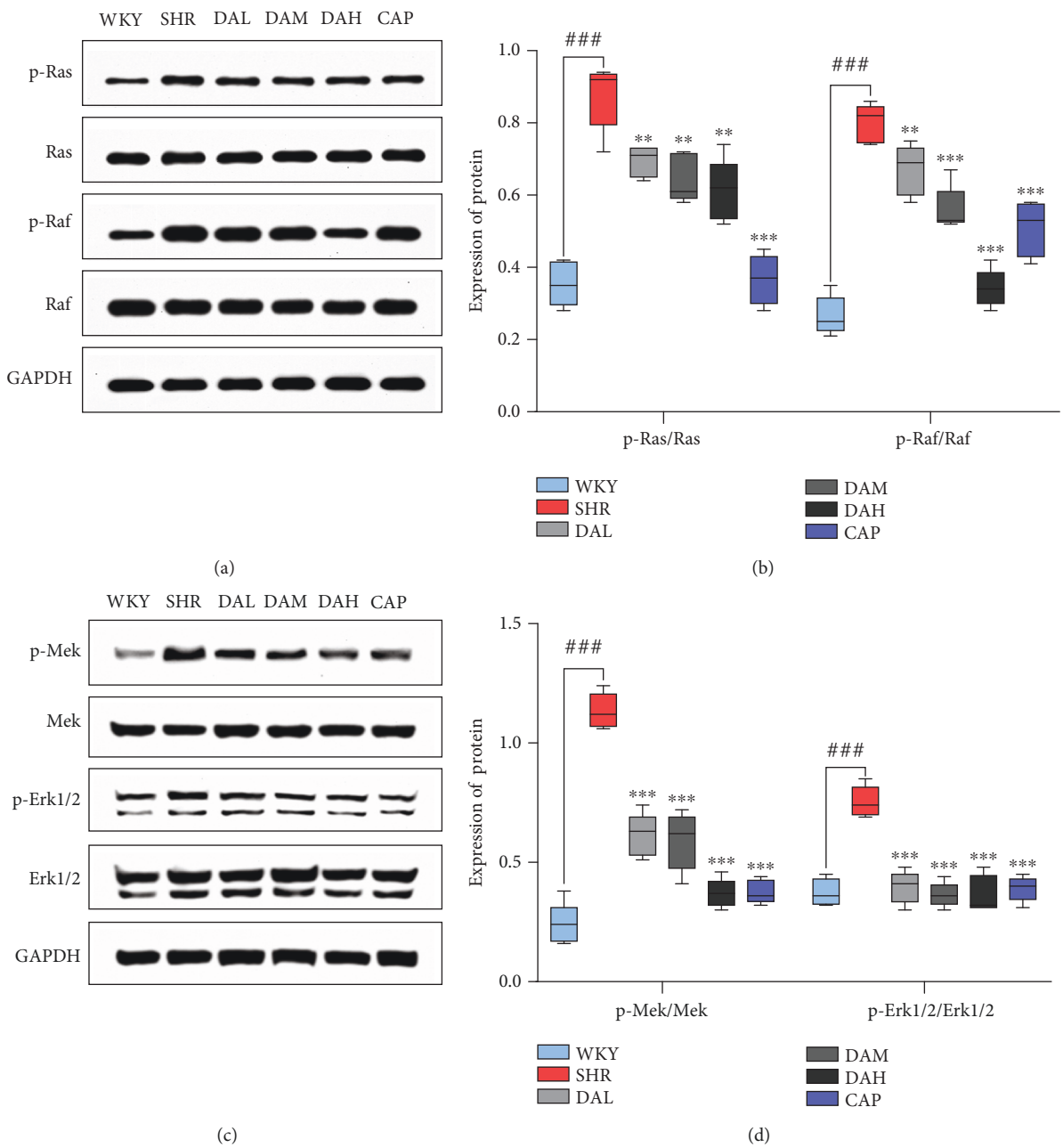

Figure 8: Continued.

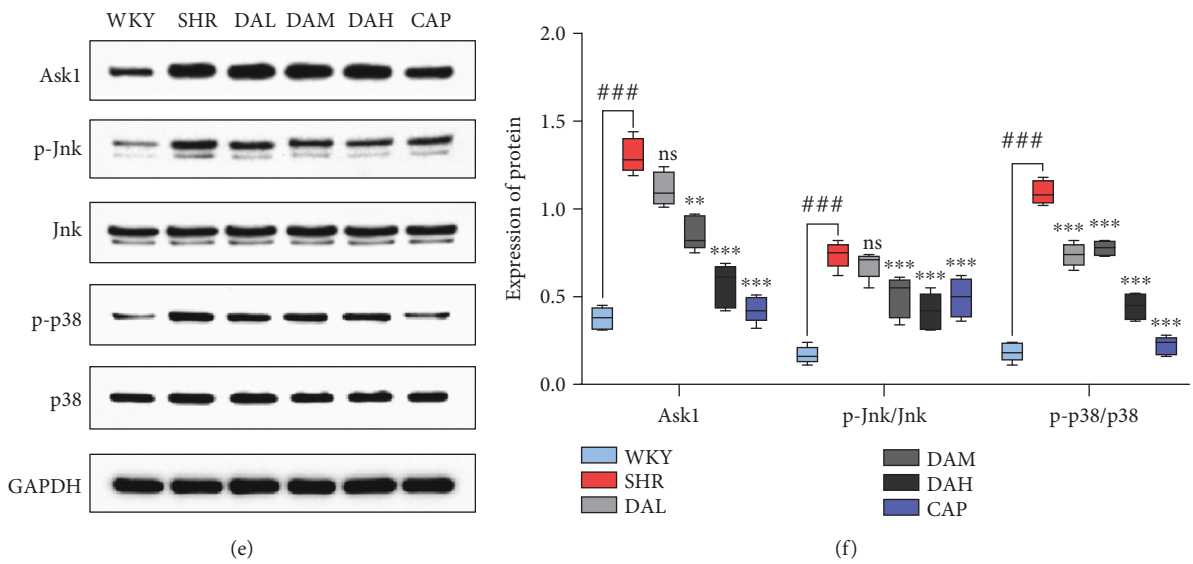

Figure 8: Mechanism of DA ameliorates cardiac remodeling involved in mitochondrial redox signaling pathways in the myocardium. Protein expression of (a, b) p-Ras, Ras, p-Raf, and Raf; (c, d) p-Mek, Mek, p-Erk, and Erk; and (e, f) Ask1, p-Jnk, Jnk, p-p38, and p38 in the myocardium. Results are presented as the mean ± SEM ($^{*}P < 0.05$, $^{**}P < 0.01$, and $^{***}P < 0.001$ vs. SHR; $^{*}P < 0.05$, $^{**}P < 0.01$, and $^{***}P < 0.001$ vs. Ang II; $^{###}P < 0.001$ vs. WKY and CON).

et al. reported a negative relevant relation between MDA and LVEF [28]. Yokota et al. found that the activation of SOD, catalase, and GSHIPx did not decrease in failing hearts, which indicated that oxidative stress in heart failure is mainly owing to the increase of prooxidant generation rather than to the reduction of antioxidant defenses [29]. Excess ROS can also attack the components of the mitochondria, which results in mitochondrial dysfunction and oxidative damage, and ultimately initiate cell death such as apoptosis [30]. Given the highest oxygen uptake rate of the heart in the body, cardiomyocytes have the highest volume density of mitochondria, accounting for 40%–60% of the total volume of cardiomyocytes [31]. Under compensatory effect, a small amount of ROS is generated from mitochondrial respiration and detoxification can be achieved through the endogenous scavenging mechanisms of cardiomyocytes [32]. Nevertheless, mitochondrial dysfunction will lead to the chronic release of ROS under decompensation. This toxicity accumulation can eventually cause cardiac remodeling and progression of heart failure [33]. During the early stages of pathological hypertrophy, mitochondrial failure is related to the decrease in complex enzyme activity and impairment of mitochondrial ATP generation [34]. Therefore, the mitochondria are a primary source of ROS in heart failure, which also indicates a pathophysiological relationship between mitochondrial dysfunction and oxidative stress. Our results indicated that mitochondria were also damaged in the case of myocardial injury, showing increased permeability of mitochondrial membranes (Figure 5); decreased activity of respiratory chain complexes I, II, III, and IV; and decreased energy metabolism and total energy charge in the SHR group compared with the WKY group. Compared with WKY, the ROS, MDA, and 4-HNE levels were significantly decreased in SHR. After treatment with DA for 3 months, the above indicators were all reversed.

Mitochondrial dysfunction will amplify apoptotic signals, and cardiomyocyte apoptosis plays a crucial role in cardiac remodeling and heart failure [35, 36]. Previous studies showed that Ang II could induce mitochondrial dysfunction, which presented with increased permeability of mitochondrial membranes [37]. In the present study, Ang II evidently increased the rate of apoptotic cells in cardiomyocytes accompanied by mitochondrial dysfunction, whereas DA treatments decreased the apoptosis ratio and enhanced mitochondrial dynamics.

Extensive reports implicated that ROS generated from mitochondrial dysfunction can result in the release of remodeling factors including Raf, Ras, Mek, Erk1/2, Ask1, JNK, and p38. Ask1 is intensively provoked by ROS, and it then activates MAPKs p38 and JNK. The deletion of Ask1 decreases p38 and JNK activation and improves cardiac remodeling induced by Ang II, which were validated in our results. Downstream signaling pathways mediated by ROS were activated under the pathological conditions of ventricular remodeling in vivo and in vitro. The downstream signaling pathways included the MAPK classical pathway, ASK1/JNK pathway, and p38 MAPK pathway, and the expression of proteins in those pathways significantly increased. All of these responses were significantly reversed by DA treatment in primary cardiomyocytes and in the myocardium of SHRs. Thus, DA may improve cardiac remodeling by modulating mitochondrial redox signaling pathways.

5. Conclusion

In summary, our study demonstrated that DA could improve cardiac function, ameliorate cardiac fibrosis, restore mitochondrial structure/function in SHR, and decrease the apoptosis of cardiomyocytes. These functions may be

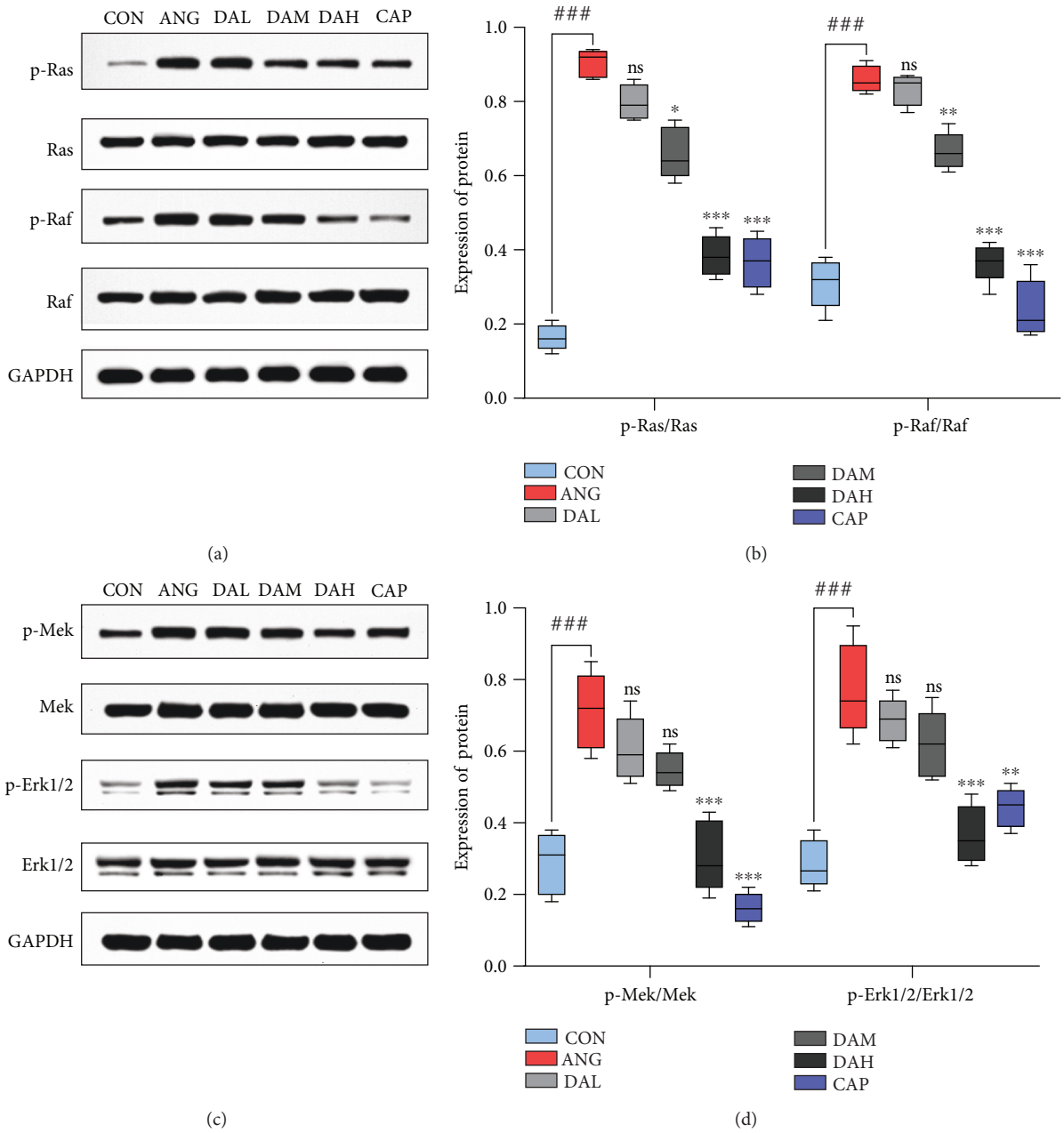

Figure 9: Continued.

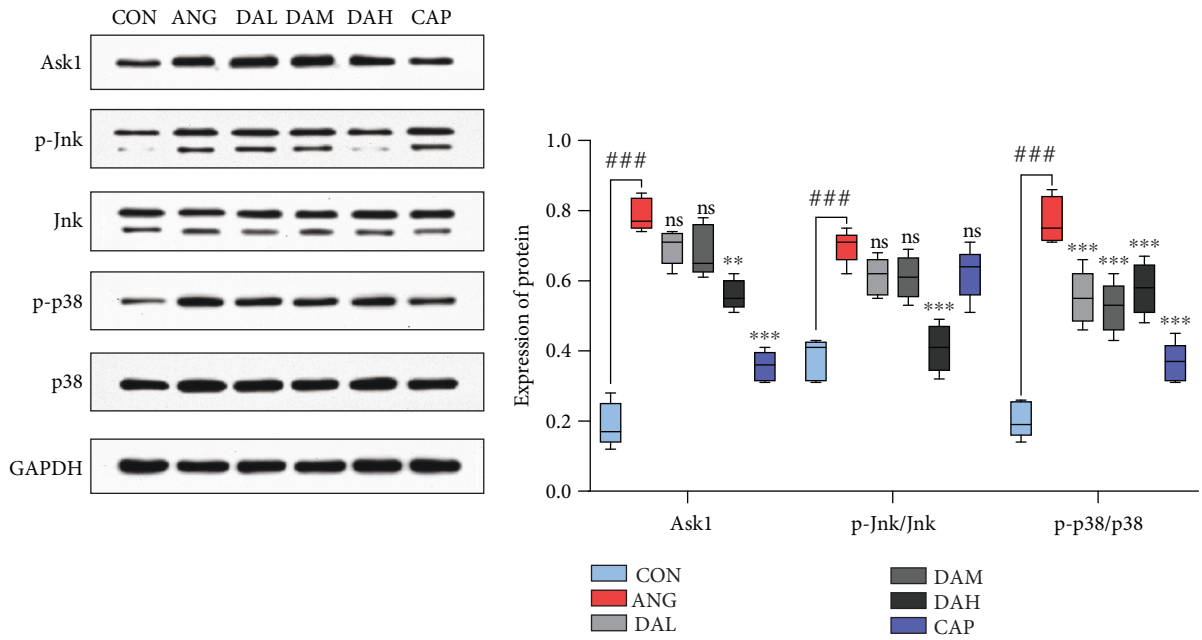

(e) (f)

Figure 9: Mechanism of DA ameliorates cardiac remodeling involved in mitochondrial redox signaling pathways in cardiomyocytes. Protein expression of (a, b) p-Ras, Ras, p-Raf, and Raf; (c, d) p-Mek, Mek, p-Erk, and Erk; and (e, f) Ask1, p-Jnk, Jnk, p-p38, and p38 in cardiomyocytes. Results are presented as the mean ± SEM ($^{*}P < 0.05$, $^{**}P < 0.01$, and $^{***}P < 0.001$ vs. SHR; $^{*}P < 0.05$, $^{**}P < 0.01$, and $^{***}P < 0.001$ vs. Ang II; $^{###}P < 0.001$ vs. WKY and CON).

completed by promoting mitochondrial dysfunction and reducing reactive oxygen species. We also proved that the mechanism may involve inhabitation of mitochondrial redox signaling pathways in cardiomyocytes and myocardium.

Abbreviations

DA: Danshenol A
SHR: Spontaneously hypertensive rat
WKY: Wistar-Kyoto
SBP: Systolic blood pressure
DBP: Diastolic blood pressure
MBP: Mean blood pressure
EF: Ejection fraction
FS: Fractional shortening
CK: Creatine kinase
CK-MB: Creatine kinase-MB
ALT: Alanine aminotransferase
AST: Aspartate aminotransferase
Cr: Creatinine
BUN: Blood urea nitrogen
ROS: Reactive oxygen species
4-HNE: 4-Hydroxynonenal
CVF: Collagen volume fraction
HPLC: High-performance liquid chromatography.

Data Availability

The data used to support the findings of this study are available from the corresponding authors upon request.

Conflicts of Interest

We declare that we have no financial and personal relationships with other people or organizations that can inappropriately influence our work; there is no professional or other personal interest of any nature or kind in any product, service, and/or company that could be construed as influencing the position presented in the manuscript.

Authors' Contributions

Kai Chen and Yiqing Guan contributed equally to this work.

Acknowledgments

We would like to appreciate all the participants of this study for their exceptional cooperation as well as valuable contributions. This work was supported by the National Nature Science Foundation of China (Nos. 81072937 and 81473246).

References

[1] C. W. Yancy, M. Jessup, B. Bozkurt et al., "2017 ACC/AHA/HFSA focused update of the 2013 ACCF/AHA guideline for the management of heart failure: a report of the American College of Cardiology/American Heart Association task force on clinical practice guidelines and the Heart Failure Society of America," *Journal of Cardiac Failure*, vol. 23, no. 8, pp. 628–651, 2017.

[2] J. Tomek and G. Bub, "Hypertension-induced remodelling: on the interactions of cardiac risk factors," *The Journal of Physiology*, vol. 595, no. 12, pp. 4027–4036, 2017.

[3] R. J. Reiter, L. C. Manchester, L. Fuentes-Broto, and D. X. Tan, "Cardiac hypertrophy and remodelling: pathophysiological consequences and protective effects of melatonin," *Journal of Hypertension*, vol. 28, Supplement 1, pp. S7–S12, 2010.

[4] J. S. Burchfield, M. Xie, and J. A. Hill, "Pathological ventricular remodeling," *Circulation*, vol. 128, no. 4, pp. 388–400, 2013.

[5] A. Kaplan, E. Abidi, R. Ghali, G. W. Booz, F. Kobeissy, and F. A. Zouein, "Functional, cellular, and molecular remodeling of the heart under influence of oxidative cigarette tobacco smoke," *Oxidative Medicine and Cellular Longevity*, vol. 2017, Article ID 3759186, 16 pages, 2017.

[6] M. Hori and K. Nishida, "Oxidative stress and left ventricular remodelling after myocardial infarction," *Cardiovascular Research*, vol. 81, no. 3, pp. 457–464, 2009.

[7] T. Münzel, G. G. Camici, C. Maack, N. R. Bonetti, V. Fuster, and J. C. Kovacic, "Impact of oxidative stress on the heart and vasculature: part 2 of a 3-part series," *Journal of the American College of Cardiology*, vol. 70, no. 2, pp. 212–229, 2017.

[8] N. Gurusamy and D. K. Das, "Autophagy, redox signaling, and ventricular remodeling," *Antioxidants & Redox Signaling*, vol. 11, no. 8, pp. 1975–1988, 2009.

[9] H. Tsutsui, T. Ide, and S. Kinugawa, "Mitochondrial oxidative stress, DNA damage, and heart failure," *Antioxidants & Redox Signaling*, vol. 8, no. 9-10, pp. 1737–1744, 2006.

[10] J. Chen, W. Cao, P. F. Asare et al., "Amelioration of cardiac dysfunction and ventricular remodeling after myocardial infarction by Danhong injection are critically contributed by anti-TGF-β-mediated fibrosis and angiogenesis mechanisms," *Journal of Ethnopharmacology*, vol. 194, pp. 559–570, 2016.

[11] A. Han, Y. Lu, Q. Zheng et al., "Qiliqiangxin attenuates cardiac remodeling via inhibition of TGF-β1/Smad3 and NF-κB signaling pathways in a rat model of myocardial infarction," *Cellular Physiology and Biochemistry*, vol. 45, no. 5, pp. 1797–1806, 2018.

[12] J. Luo, H. Xu, and K. Chen, "Systematic review of compound danshen dropping pill: a Chinese patent medicine for acute myocardial infarction," *Evidence-Based Complementary and Alternative Medicine*, vol. 2013, Article ID 808076, 15 pages, 2013.

[13] S. Ma, D. Zhang, H. Lou, L. Sun, and J. Ji, "Evaluation of the anti-inflammatory activities of tanshinones isolated from *Salvia miltiorrhiza* var. *alba* roots in THP-1 macrophages," *Journal of Ethnopharmacology*, vol. 188, pp. 193–199, 2016.

[14] W. Zhao, H. Feng, S. Guo, Y. Han, and X. Chen, "Danshenol A inhibits TNF-α-induced expression of intercellular adhesion molecule-1 (ICAM-1) mediated by NOX4 in endothelial cells," *Scientific Reports*, vol. 7, no. 1, article 12953, 2017.

[15] J. Ru, P. Li, J. Wang et al., "TCMSP: a database of systems pharmacology for drug discovery from herbal medicines," *Journal of Cheminformatics*, vol. 6, no. 1, 2014.

[16] Z. Liu, F. Guo, Y. Wang et al., "BATMAN-TCM: a bioinformatics analysis tool for molecular mechanism of traditional Chinese medicine," *Scientific Reports*, vol. 6, no. 1, article 21146, 2016.

[17] X. Wang, Y. Shen, S. Wang et al., "PharmMapper 2017 update: a web server for potential drug target identification with a comprehensive target pharmacophore database," *Nucleic Acids Research*, vol. 45, no. W1, pp. W356–W360, 2017.

[18] G. Bindea, B. Mlecnik, H. Hackl et al., "ClueGO: a Cytoscape plug-in to decipher functionally grouped gene ontology and pathway annotation networks," *Bioinformatics*, vol. 25, no. 8, pp. 1091–1093, 2009.

[19] D. E. Atkinson, "Energy charge of the adenylate pool as a regulatory parameter. Interaction with feedback modifiers," *Biochemistry*, vol. 7, no. 11, pp. 4030–4034, 1968.

[20] T. Stanton and F. G. Dunn, "Hypertension, left ventricular hypertrophy, and myocardial ischemia," *Medical Clinics of North America*, vol. 101, no. 1, pp. 29–41, 2017.

[21] M. Szibor, J. Pöling, H. Warnecke, T. Kubin, and T. Braun, "Remodeling and dedifferentiation of adult cardiomyocytes during disease and regeneration," *Cellular and Molecular Life Sciences*, vol. 71, no. 10, pp. 1907–1916, 2014.

[22] M. A. Horn, "Cardiac physiology of aging: extracellular considerations," *Comprehensive Physiology*, vol. 5, no. 3, 2015.

[23] C. H. Conrad, W. W. Brooks, J. A. Hayes, S. Sen, K. G. Robinson, and O. H. L. Bing, "Myocardial fibrosis and stiffness with hypertrophy and heart failure in the spontaneously hypertensive rat," *Circulation*, vol. 91, no. 1, pp. 161–170, 1995.

[24] F. R. Heinzel, F. Hohendanner, G. Jin, S. Sedej, and F. Edelmann, "Myocardial hypertrophy and its role in heart failure with preserved ejection fraction," *Journal of Applied Physiology*, vol. 119, no. 10, pp. 1233–1242, 2015.

[25] J. Lomax, "Get ready to GO! A biologist's guide to the Gene Ontology," *Briefings in Bioinformatics*, vol. 6, no. 3, pp. 298–304, 2005.

[26] L.-Y. Zhou, J. P. Liu, K. Wang et al., "Mitochondrial function in cardiac hypertrophy," *International Journal of Cardiology*, vol. 167, no. 4, pp. 1118–1125, 2013.

[27] H. Tsutsui, S. Kinugawa, and S. Matsushima, "Mitochondrial oxidative stress and dysfunction in myocardial remodelling," *Cardiovascular Research*, vol. 81, no. 3, pp. 449–456, 2008.

[28] A. Dirican, F. Levent, A. Alacacioglu et al., "Acute cardiotoxic effects of adjuvant trastuzumab treatment and its relation to oxidative stress," *Angiology*, vol. 65, no. 10, pp. 944–949, 2014.

[29] T. Yokota, S. Kinugawa, M. Yamato et al., "Systemic oxidative stress is associated with lower aerobic capacity and impaired skeletal muscle energy metabolism in patients with metabolic syndrome," *Diabetes Care*, vol. 36, no. 5, pp. 1341–1346, 2013.

[30] J. L. Pohjoismäki and S. Goffart, "The role of mitochondria in cardiac development and protection," *Free Radical Biology and Medicine*, vol. 106, pp. 345–354, 2017.

[31] S. M. Davidson, "Endothelial mitochondria and heart disease," *Cardiovascular Research*, vol. 88, no. 1, pp. 58–66, 2010.

[32] A. Nickel, M. Kohlhaas, and C. Maack, "Mitochondrial reactive oxygen species production and elimination," *Journal of Molecular and Cellular Cardiology*, vol. 73, pp. 26–33, 2014.

[33] S. Cadenas, "ROS and redox signaling in myocardial ischemia-reperfusion injury and cardioprotection," *Free Radical Biology and Medicine*, vol. 117, pp. 76–89, 2018.

[34] T. Doenst, T. D. Nguyen, and E. D. Abel, "Cardiac metabolism in heart failure: implications beyond ATP production," *Circulation Research*, vol. 113, no. 6, pp. 709–724, 2013.

[35] A. M. Rababa'h, A. N. Guillory, R. Mustafa, and T. Hijjawi, "Oxidative stress and cardiac remodeling: an updated edge," *Current Cardiology Reviews*, vol. 14, no. 1, pp. 53–59, 2018.

[36] S. L. C. Scofield, P. Amin, M. Singh, and K. Singh, "Extracellular ubiquitin: role in myocyte apoptosis and myocardial remodeling," *Comprehensive Physiology*, vol. 6, no. 1, pp. 527–560, 2015.

[37] L. Jia, Y. Li, C. Xiao, and J. Du, "Angiotensin II induces inflammation leading to cardiac remodeling," *Frontiers in Bioscience*, vol. 17, no. 1, pp. 221–231, 2012.

Hindawi
Oxidative Medicine and Cellular Longevity
Volume 2019, Article ID 1202676, 10 pages
https://doi.org/10.1155/2019/1202676

Research Article

Malaysian Tualang Honey Inhibits Hydrogen Peroxide-Induced Endothelial Hyperpermeability

Kogilavanee Devasvaran,[1] **Jun Jie Tan**,[2] **Chin Theng Ng**,[3] **Lai Yen Fong**,[4] **and Yoke Keong Yong**[1]

[1]*Department of Human Anatomy, Faculty of Medicine and Health Sciences, Universiti Putra Malaysia, 43400 Serdang, Selangor, Malaysia*
[2]*Advanced Medical and Dental Institute, Universiti Sains Malaysia, Bertam, 13200 Kepala Batas, Penang, Malaysia*
[3]*Physiology Unit, Faculty of Medicine, AIMST University, 08100 Bedong, Kedah, Malaysia*
[4]*Department of Pre-clinical Sciences, Faculty of Medicine and Health Sciences, Universiti Tunku Abdul Rahman, 43000 Kajang, Selangor, Malaysia*

Correspondence should be addressed to Yoke Keong Yong; yoke_keong@upm.edu.my

Received 10 May 2019; Accepted 20 June 2019; Published 18 August 2019

Guest Editor: Albino Carrizzo

Malaysian Tualang honey (TH) is a known therapeutic honey extracted from the honeycombs of the Tualang tree (Koompassia excelsa) and has been reported for its antioxidant, anti-inflammatory, antiproliferative, and wound healing properties. However, the possible vascular protective effect of TH against oxidative stress remains unclear. In this study, the effects of TH on hydrogen peroxide- (H_2O_2-) elicited vascular hyperpermeability in human umbilical vein endothelial cells (HUVECs) and Balb/c mice were evaluated. Our data showed that TH concentrations ranging from 0.01% to 1.00% showed no cytotoxic effect to HUVECs. Induction with 0.5 mM H_2O_2 was found to increase HUVEC permeability, but the effect was significantly reversed attenuated by TH ($p < 0.05$), of which the permeability with the highest inhibition peaked at 0.1%. In Balb/c mice, TH (0.5 g/kg-1.5 g/kg) significantly ($p < 0.05$) reduced H_2O_2 (0.3%)-induced albumin-bound Evans blue leak, in a dose-dependent manner. Immunofluorescence staining confirmed that TH reduced actin stress fiber formation while increasing cortical actin formation and colocalization of caveolin-1 and β-catenin in HUVECs. Signaling studies showed that HUVECs pretreated with TH significantly ($p < 0.05$) decreased intracellular calcium release, while sustaining the level of cAMP when challenged with H_2O_2. These results suggested that TH could inhibit H_2O_2-induced vascular hyperpermeability in vitro and in vivo by suppression of adherence junction protein redistribution via calcium and cAMP, which could have a therapeutic potential for diseases related to the increase of both oxidant and vascular permeability.

1. Introduction

Vascular diseases are among the leading causes of death worldwide, as they are linked to major illnesses such as atherosclerosis, hypertension, and rheumatoid arthritis [1]. These diseases occur upon an alteration in the homeostatic function in the vascular system. Vascular homeostasis is regulated by the endothelial cell monolayer integrity, which is responsible for the impermeable nature of blood vessels. Changes in endothelial integrity compromise vascular permeability, a physiological response commonly seen in inflammation and angiogenesis [1]. In recent years, growing evidence suggests that oxidative stress can contribute to increased vascular permeability via actin reorganization and Cav-1-associated dissociation of β-catenin [2].

Oxidative stress is defined as an imbalance between oxidants and antioxidants in cells due to overproduction of reactive oxygen species (ROS). ROS is also formed during normal cellular metabolism but is highly unstable due to its incomplete reduction of molecular oxygen. At physiological levels, ROS plays a dynamic role in modulating several signaling pathways, related to cell differentiation and growth [3].

Previous studies have shown that hydrogen peroxide (H_2O_2), generated by endothelial cells in response to inflammatory stimuli, increase paracellular permeability by promoting the loss of cell-cell adhesion and activation of actin-myosin-based cell retraction [1].

Antioxidants present in traditional medicine have been found to possess potent medicinal properties. Most countries have their own traditional remedies in treating various illnesses with minimal or no known side effects. In Malaysia, the Tualang tree (Koompassia excelsa), the tallest tree in Peninsular Malaysia with an average height of 265 ft, has gained popularity over the years for Tualang honey (TH), the natural product harvested from the honeycombs produced by *Apis dorsata* (giant rock bees) [4]. This therapeutic honey has been reported having the highest phenolic, flavonoid, and ascorbic acid content [5, 6] with an acidic nature at a pH between 3.2 and 4, which makes it bactericidal [7].

Currently, TH is widely studied for its beneficial properties, including promoting wound healing, antibacterial effects, and improved functions of human corneal epithelial cells [8–10]. Furthermore, TH also exhibits cardioprotective effect through ameliorating oxidative stress [11]. Therefore, this study is aimed at investigating the protective effects of Malaysian TH on H_2O_2-induced vascular dysfunction as well as its mechanism of action by elucidating the signaling pathway.

2. Materials and Methods

2.1. Cell Culture. The EndoGRO™ human umbilical vein endothelial cells (HUVECs) (Merck KGaA, Darmstadt, Germany) were cultured in an EndoGRO-LS Complete Culture Media Kit consisting of EndoGRO Basal Medium and its Supplement Kit (Merck KGaA, Darmstadt, Germany). Cells were grown in the incubator, supplemented with 5% CO_2 at 37°C. Cells were passaged when reaching approximately 80% confluence by using 0.05% trypsin (Biowest) to dissociate the cells. Passage 3-4 HUVECs were used to conduct all the experiments to maintain its originality.

2.2. Preparation of Malaysian Tualang Honey Solution. The Tualang honey (TH) used in this study was presented to us by Universiti Sains Malaysia (USM), where the source is from the Federal Agriculture Marketing Authorities of Malaysia (FAMA). TH solutions were prepared right before testing by diluting it to 10% (*v*/*v*) with cultured medium and sterilized by filtering it using a syringe filter (0.2 μm), followed by diluting it further to the required concentrations for cell culture [10]. In the animal study, TH was diluted in normal saline to concentrations 0.5 g/kg, 1.0 g/kg, and 1.5 g/kg based on a previous study [12] prior to testing.

2.3. Cell Viability Assay. HUVECs were seeded at 1×10^4 cells/well in a 96-well plate and kept in the incubator supplemented with 5% CO_2 at 37°C. The following day, culture medium containing the desired concentration of TH (0.001%-10.000%) was added and incubated for 24 h. Then, the medium was replaced by complete medium, to which the Thiazolyl blue tetrazolium bromide or MTT (Amresco, Ohio, USA) was at a final concentration of 0.4 mg/ml. After 4 h of incubation at 37°C in the dark, the medium was removed and the formazon product was dissolved in 100 μl of dimethylsulfoxide (DMSO). The absorbance was measured at 570 nm with a plate reader (SoftMax 5.0, VersaMax ELISA Microplate Reader, USA). Experiments were performed in triplicates and three independent tests. Cell viability was expressed as the percentage of formazon absorbance [13].

2.4. In Vitro Vascular Permeability Assay. The permeability of HUVEC monolayer was determined using an in vitro vascular permeability kit (96-well) (Merck KGaA, Darmstadt, Germany) and according to the method described by Yong et al. [14] with a slight modification. Briefly, cells were seeded at 5×10^4 cells/well onto collagen-coated inserts for 72 h. Cells were pretreated with TH at a concentration of 0.01-1.0% for 4 h, and endothelial hyperpermeability was induced with H_2O_2 at a concentration of 0.5 mM, followed by addition of FITC-dextran. The plate was incubated for 1 h, and to stop the reaction, the inserts were moved to another well. The fluorescent intensity was measured using a fluorescence microplate reader (Tecan 200, Infinite, Männedorf, Zürich, Switzerland) with an excitation wavelength of 485 nm and emission of 535 nm. Permeability is given as the quantity of FITC-dextran passing from the insert into the receiver well.

2.5. Immunofluorescence Staining of Actin Cytoskeleton. The immunofluorescence staining of filamentous actin (F-actin) was conducted according to the methods reported previously [15]. Briefly, HUVECs were cultured on fibronectin-coated round coverslips at 1.5×10^5 cells/well for 4 d at 37°C to reach confluence. After the indicated treatment period, cells were fixed with 3.7% paraformaldehyde (PFA) for 10 min, permeabilised with 0.1% Triton X-100 for 5 min, and stained for F-actin with fluorescein phalloidin (1 : 100, in methanol) for 20 min at room temperature. Next, cells were washed with PBS, and cell nuclei were stained with 4,6-diamidino-2-phenylindole (DAPI; 0.5 μg/ml, in PBS) for 3 min. The coverslips were mounted with a SlowFade Diamond antifade agent, and all the images were captured using a polarizing microscope (BX-51, Olympus, Japan) and processed with Cell^F software (Olympus, Japan).

2.6. Immunofluorescence Staining of Cav-1 and β-Catenin. HUVECs were grown, treated, and induced as described above. Subsequently, cells were fixed with 3.7% paraformaldehyde for 20 min, permeabilised with 0.10% Triton X-100 for 15 min, and blocked with 2% BSA for 1 h. A primary antibody for β-catenin (rabbit anti-β-catenin; 5 μg/ml, in 2% BSA) was stained and incubated overnight at 4°C; a secondary antibody (tetramethylrhodamine goat anti-rabbit IgG; 5 μg/ml, in 2% BSA) was then exposed for 2 h at room temperature. Next, a primary antibody for caveolin-1 (mouse anti-Cav-1; 5 μg/ml, in 2% BSA) was stained and incubated overnight at 4°C; a secondary antibody (FITC-goat anti-mouse IgG; 1 : 50, to 2% BSA) was stained for 2 h at room temperature. The nucleus staining with DAPI, mounting of coverslip, and capturing of image were all conducted as described above.

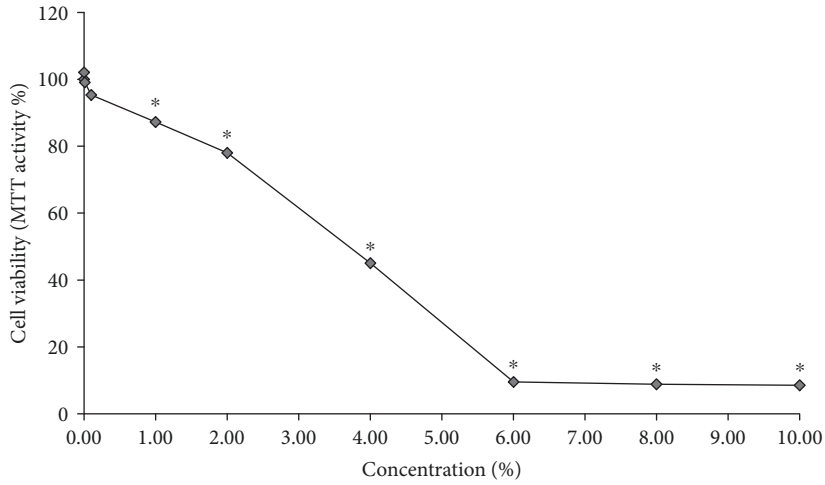

Figure 1: HUVEC viability after treatment with 0.001%-10.00% TH for 24 h. Data were generated from three independent experiments and expressed as the mean ± SEM where $^{*}p < 0.05$ is considered significant versus the no treatment control.

2.7. Measurement of Intracellular Calcium. Intracellular calcium was measured using the Fluo-4 Direct™ Calcium Assay Kit (Molecular Probes, Oregon, USA) according to the manufacturer's protocol. Briefly, HUVECs were plated at 5×10^4 cells/well and incubated overnight in 5% CO_2 at 37°C. The following day, the medium was substituted with a Fluo-4 Calcium assay reagent (1 : 1, to culture medium) in the dark and incubated for 30 min. Then, cells were pretreated with TH for 4 h and induced with H_2O_2 for 1 h. The fluorescence intensity of the supernatant was measured using a fluorescence microplate reader (Tecan 200, Infinite, Männedorf, Zürich, Switzerland) with an excitation wavelength of 494 nm and emission of 516 nm. The amount of intracellular calcium measured was proportional to the fluorescence intensity.

2.8. Measurement of Cyclic Adenosine Monophosphate (cAMP). The cAMP level was quantified using the Direct cAMP kit (ADI-900-066; Enzo Life Sciences, New York, USA). HUVECs were cultured, treated, and induced, and lysated cells (sample) were prepared as above. Samples were added to appropriate antibody-coated wells. cAMP conjugated to alkaline phosphatase (blue solution) was added prior to the rabbit polyclonal antibody (yellow solution). The antibody was left to bind to the cAMP in the sample. Subsequently, pNpp substrate was added and catalyzed by alkaline phosphatase to produce a yellow colour. Next, stop solution was added to stop the colour development, and the absorbance was measured at 405 nm with a plate reader (SoftMax 5.0, VersaMax ELISA Microplate Reader, USA). The level of cAMP is indirectly proportional to the signal produced (absorbance).

2.9. Experimental Animals. A total of 36 male Balb/c mice ($n = 6$/group) in the weight range of 20 to 25 g were bought from the Faculty of Veterinary, Universiti Putra Malaysia (Malaysia), and housed at the Animal House in the Faculty of Medicine and Health Sciences in 12 h dark-light condition (25 ± 2°C) with access to food and water ad libitum. The experimental protocol carried out was approved by University Putra Malaysia, Institutional Animal Care and Use Committee (IACUC), with the AUP No. R011/2015.

2.10. Miles Assay. Vascular leak was measured using the Miles assay by quantifying the extravasation of albumin-bound Evans blue into the interstitium from the vasculature of male Balb/c mice [16]. TH at 0.5, 1.0, and 1.5 g/kg was given orally for seven days and 40 min before H_2O_2 injection of the seventh day. Another group of mice was orally administered with 35 mg/kg of Trolox as a standard reference. The untreated control and disease groups received only normal saline. On the seventh day, the dorsal fur of the mice was removed using depilatory cream (Veet®, Reckitt Benckiser, UK). Evans blue (Santa Cruz Biotechnology, USA, 0.5% in PBS) was administered via the lateral tail vein and left to circulate for 30 min. Subsequently, H_2O_2 was injected intradermally in the dorsal skin. Mice were sacrificed after 10 min, and skin patches from the injection sites were removed and incubated in formamide at 55°C for 24 h. Extracted Evans blue was measured using a spectrophotometer (SoftMax 5.0, VersaMax ELISA Microplate Reader, USA) at 620 nm. The amount of dye extracted was expressed using the formula reported by Radu and Chernoff [17].

2.11. Statistical Analysis. Three independent tests were carried out for all experiments (triplicate). All data were expressed as the mean ± standard error of the mean (SEM), and comparisons between groups were analyzed using one-way analysis of variance (ANOVA) with a post hoc analysis using Dunnett's test. A p value less than 0.05 ($p < 0.05$) was considered significant.

3. Results

3.1. TH Is Not Cytotoxic to HUVECs. To study the cytotoxicity of TH, HUVECs were treated with 0.001%, 0.01%, 0.10%, 1.00%, 2.00%, 4.00%, 6.00%, 8.00%, and 10.00%. TH and the percentage of viable cells were assessed after 24 h. As reported in Figure 1, TH was not cytotoxic to HUVECs at

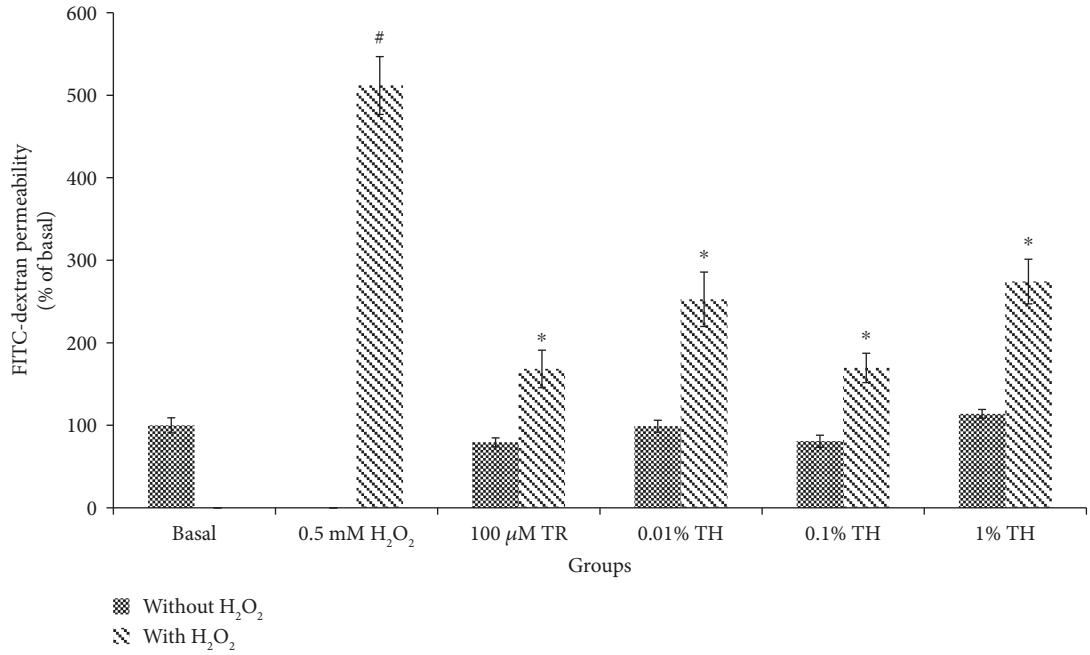

Figure 2: Quantification of FITC-dextran in HUVECs. The permeability (% of basal) of the cells treated with TH with and without the H_2O_2 group. Values are expressed as the mean ± SEM from three independent experiments. Hash (#) represents the significant difference compared with the basal group (untreated and with media only), $p < 0.05$; asterisk (∗) represents the significant difference compared to the H_2O_2 group, $p < 0.05$. Basal = untreated; TR = Trolox; TH = Tualang honey.

concentrations below 1.00% (cell viability of >87%). However, at 2.00% of TH, HUVEC viability was significantly reduced to 78.01% as compared to the untreated control ($p < 0.05$), and the calculated LD_{50} of TH was 3.7%.

3.2. TH Protects against Endothelial Barrier Disruption Induced by H_2O_2. To examine the permeability of HUVECs, the in vitro FITC-dextran-based vascular permeability assay was used. As shown in Figure 2, the permeability in HUVECs treated with TH was not significantly different ($p > 0.05$) from the control, suggesting that TH itself did not cause endothelial hyperpermeability. However, the permeability of HUVECs increased by 5-fold upon H_2O_2 induction to 511.85 ± 35.04% from the control 100.00 ± 9.16%. Pretreatment with TH at all tested concentrations significantly attenuated the increased permeability elicited by H_2O_2 ($p < 0.05$). The maximal inhibition of permeability was achieved with 0.10% TH, achieving a reduction to 169.69 ± 17.79% ($p < 0.05$).

3.3. TH Inhibits H_2O_2-Stimulated Actin Remodeling in HUVECs. As illustrated in Figure 3, a prominent cortical actin bundle was formed in control HUVECs, with a low level of stress fibers. In the H_2O_2 group (Figure 3(b)), stress fiber formation was dominant and led to gaps between cells. In groups of TH, at 0.01% (Figure 3(c)), the presence of stress fibers was more compared to the cortical actin; at 0.10% (Figure 3(d)), a suppression in the stress fiber formation was observed, which led to a minimal gap formation among cells, similar to the positive control, Trolox (Figure 3(f)); and at 1.00% (Figure 3(e)), the cells showed generally fewer and thinner stress fibers, also with some gaps formed between cells. Although H_2O_2 exposure caused the induction of cytoplasmic stress fibers and a less prominent cortical actin bundle, TH managed to block the effects of H_2O_2.

3.4. TH Inhibits H_2O_2-Induced Cav-1-Mediated Dissociation of β-Catenin in HUVECs. To understand the effect of TH on H_2O_2-induced endothelial barrier disruption and vascular permeability, the changes of Cav-1 and β-catenin colocalization in HUVECs were observed. Figure 4 shows that H_2O_2 decreased the colocalization of Cav-1 and β-catenin at the cell borders which coupled with the dissociation of barrier integrity that showed a rope ladder-like pattern as compared to the basal group. However, HUVECs pretreated with TH showed a marked increase in the association between Cav-1 and β-catenin. Interestingly, the greatest extent of colocalization between Cav-1 and β-catenin was observed at 0.10% TH, of which the extent of inhibition of H_2O_2-induced barrier disruption was similar to that of the positive control (Trolox).

3.5. TH Inhibits H_2O_2-Induced Intracellular Calcium Formation. To detect the intracellular calcium, the Fluo-4 calcium probe was used measured using a fluorescent plate reader. As shown in Figure 5, H_2O_2 stimulation resulted in a significant ($p < 0.05$) increase in the intracellular calcium by approximately twofold 211.11 ± 1.39% as compared to the basal 100.00 ± 4.81%. Pretreatment of TH significantly ($p < 0.05$) reduced the excessive intracellular calcium release with the highest percentage of intracellular calcium suppression of 102.12 ± 2.76% exhibited by TH at 0.10% and was comparable to the basal group.

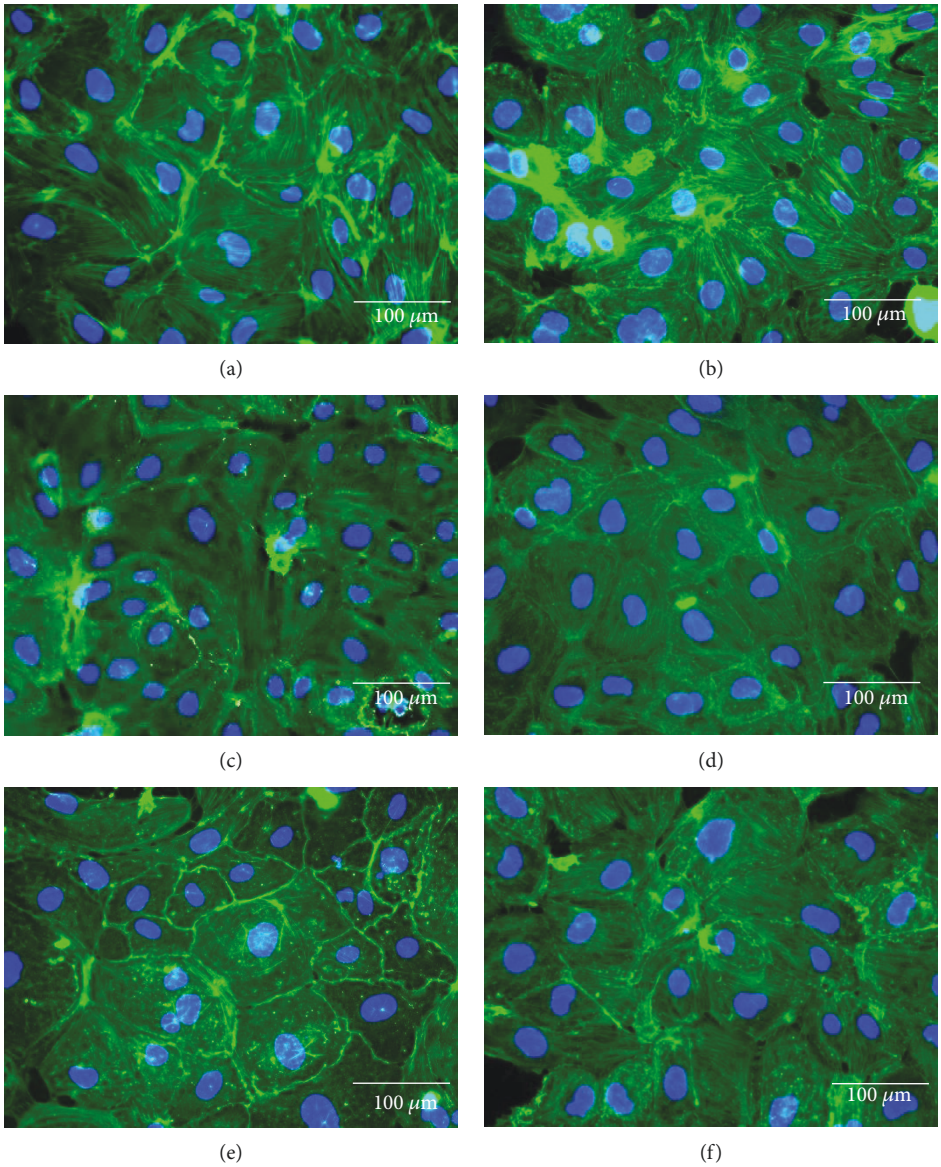

Figure 3: Effect of HUVECs pretreated with TH on H_2O_2-induced cytoskeletal remodeling and gap formation. Actin cytoskeleton (green) is shown merged with its nucleus (blue) stained with DAPI. Representative images were taken from one of three independent experiments at 400x magnification. Merged images were generated with Olympus BX-51 Cell-F imaging software. Images represent basal (a); H_2O_2 at 0.5 mM (b); and pretreatments+inducer: TH 0.01%+H_2O_2 (c), TH 0.10%+H_2O_2 (d), TH 1.00%+H_2O_2 (e), and TR+H_2O_2 (f). Basal = untreated; TH = Tualang honey; TR = Trolox.

3.6. TH Maintains cAMP Levels. To elucidate the mechanism of TH barrier protective effect, cAMP in HUVECs was quantified with and without induction by H_2O_2. As shown in Figure 6, exposure to H_2O_2 significantly ($p < 0.05$) decreased the production of cAMP in HUVECs by half as compared to the control group (from 15.36 ± 2.15 pmol/ml to 8.39 ± 0.81 pmol/ml). Although groups with TH alone at 0.01 and 1.00% significantly reduced the cAMP level in HUVECs ($p < 0.05$), the cAMP level in HUVECs treated with 0.10% TH showed no significant difference compared to control group. Interestingly, only HUVECs pretreated with 0.10% TH significantly ($p < 0.05$) attenuated the reduction in cAMP production to 12.23 ± 1.24 pmol/ml as compared to the untreated control, when both were challenged by H_2O_2. Similarly, in Trolox-treated HUVECs, a higher cAMP level was found when the cells were challenged with H_2O_2.

3.7. TH Protects against H_2O_2-Induced Vascular Leakage in Balb/c Mice. To test the protective effect of TH on endothelial barrier function in vivo, TH was pretreated in mouse models, and the vascular leakage, measured by Evans blue in tissues, was determined. All concentrations of TH including the reference drug (Trolox) showed no significant difference compared to the control group (basal level) (Figure 7). H_2O_2 caused a significant increase in dye leakage by almost 100% compared to the control group (from 1.50 ± 0.05 ng/g to 3.32 ± 0.13 ng/g) ($p < 0.05$). However, there was a significant decrease in dye leakage in mice pretreated with TH at 0.5, 1.0,

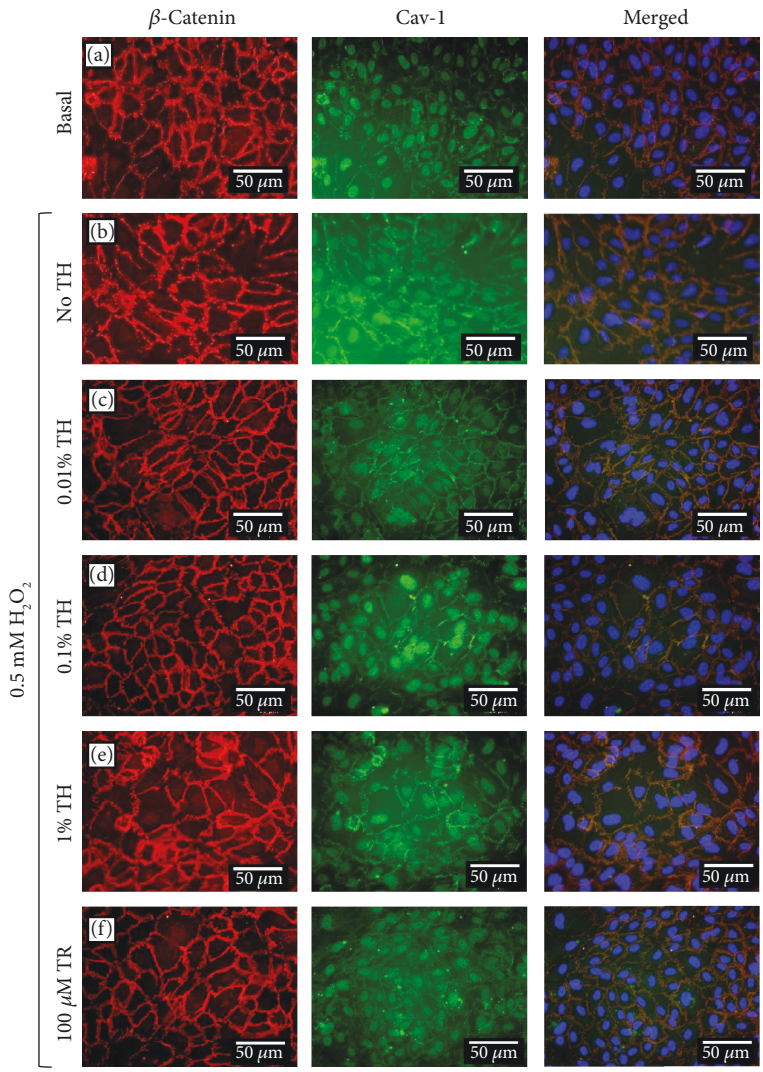

Figure 4: Localization of β-catenin and caveolin-1 in HUVECs pretreated with TH and induced with H_2O_2. Cellular localization of β-catenin (red) and Cav-1 (green) is shown merged with nucleus (blue) stained with DAPI. Merged images were generated with Olympus BX-51 Cell-F imaging software, whereby a third pseudocolour channel (orange) was used to show colocalization of red and green pixels. Representative images were taken from one of three independent experiments. Basal = untreated; TH = Tualang honey; TR = Trolox.

and 1.5 g/kg when compared to H_2O_2 alone with a suppression rate of 29%, 38%, and 49%, respectively ($p < 0.05$).

4. Discussion

Tualang honey (TH) has gained attention for its various properties such as wound healing [8], antibacterial properties [18], and antiproliferative properties [6]. However, the effects of TH at a cellular level and its potential as a vascular protective agent have not been studied. In this study, we evaluated the protective effect of TH on oxidative stress-induced increased endothelial permeability.

Exposure to a high level of oxidative stress such as hydrogen peroxide (H_2O_2) can cause contraction and separation of endothelial cells and results in increased endothelial permeability and exudation of fluid rich in plasma protein at the site of inflammation.

Our data showed that TH was capable to reduce HUVEC hyperpermeability when the cells were challenged with H_2O_2, with a concentration of only 0.10% of TH to yield the most potent inhibition rate similar to the basal permeability level. Similarly, *in vivo*, mice pretreated with TH also significantly ($p < 0.05$) reduced dye leakage from the microvessels following H_2O_2. Hence, both data (*in vitro* and *in vivo*) strongly suggest that TH can effectively suppress the exudative phase of acute inflammation, probably due to its high content of phenolic/flavonoid compounds, and radical scavenging activity [6].

Aghajanian et al. [19] demonstrated that endothelial cells exposed to H_2O_2 led to the remodeling of the actin filament, disrupted the cortical bond necessary for barrier integrity, increased intracellular tension and paracellular gap formation, and therefore, increased permeability. Once again, this process was reversed by TH, with its effect peaked at 0.10%,

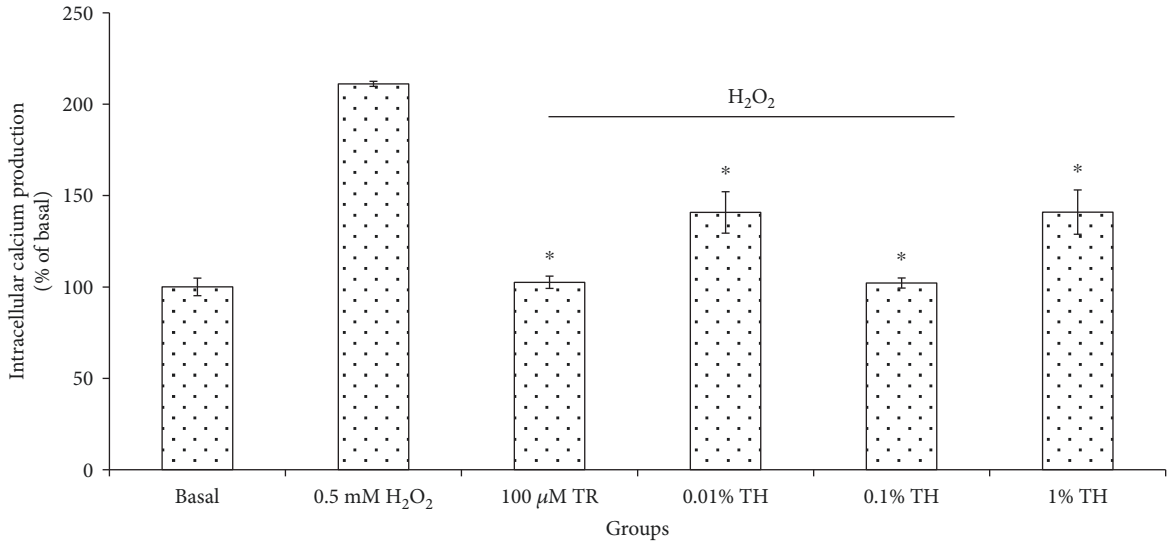

Figure 5: Percentage of intracellular calcium production in HUVECs pretreated with TH and induced with H_2O_2. The intracellular calcium (% of basal) of cells treated with TH shows a significant difference ($^*p < 0.05$) with the H_2O_2 group. Values are expressed as the mean ± SEM from three independent experiments. Asterisk (∗) represents the significantly different groups with the H_2O_2 group. Basal = untreated; TR = Trolox; TH = Tualang honey.

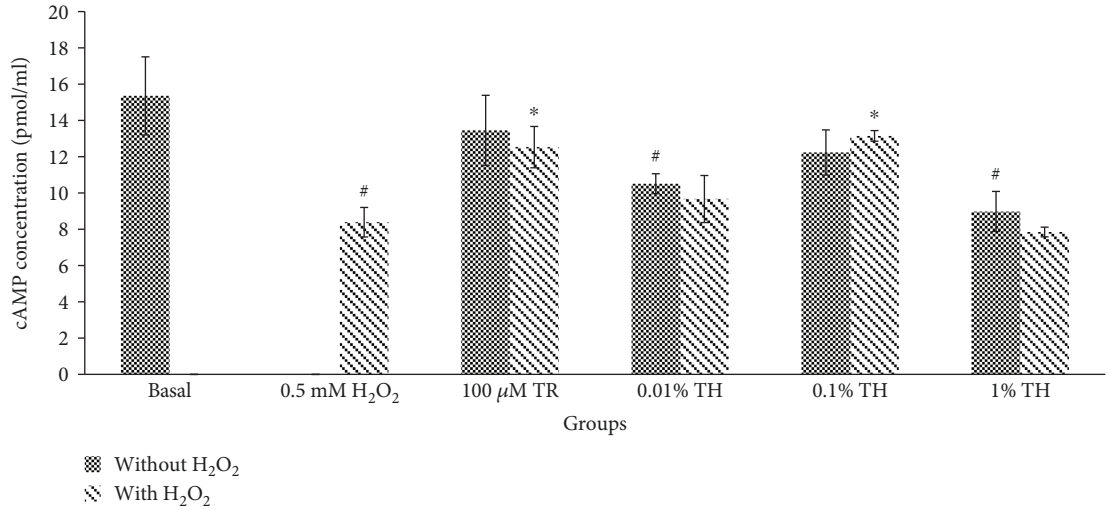

Figure 6: Amount of cAMP production in HUVECs. The cAMP concentration (pmol/ml) of cells treated with TH alone or induced with H_2O_2. Values are expressed as the mean ± SEM from three independent experiments. Hash (#) represents the significant difference compared to the untreated group (basal), $p < 0.05$; asterisk (∗) represents the significant difference compared to the H_2O_2 alone group, $p < 0.05$. Basal = untreated; TR = Trolox; TH = Tualang honey.

suggesting that the inhibition of HUVEC hyperpermeability by TH was via maintaining the actin filament, increasing the cortical actin bond which is important in maintaining the barrier integrity, and reducing the intracellular tension, thus leading to minimal intracellular gap formation [20].

Caveolae are abundant in endothelial cells, and they do play a part in vascular permeability. The formation of plasma membrane caveolae is driven by Cav-1 and is brought to the actin cytoskeleton, which regulates the interaction of cells with the extracellular matrix that eventually pulls together and modulates signaling molecules [21]. Cav-1 stabilizes the adherence junctions [22], and colocalization of Cav-1 and β-catenin, an adherent junction-associated protein, is important in maintaining the barrier integrity, specifically the interendothelial junctions [2]. Our study showed that H_2O_2 disrupts the colocalization between Cav-1 and β-catenin at the cell borders and dissociates barrier integrity in a rope ladder-like pattern. These events, again, were prevented by pretreatment of TH. The observation suggested that TH was able to reduce vascular hyperpermeability induced by H_2O_2 via increasing the colocalization between Cav-1 and β-catenin at the cell borders.

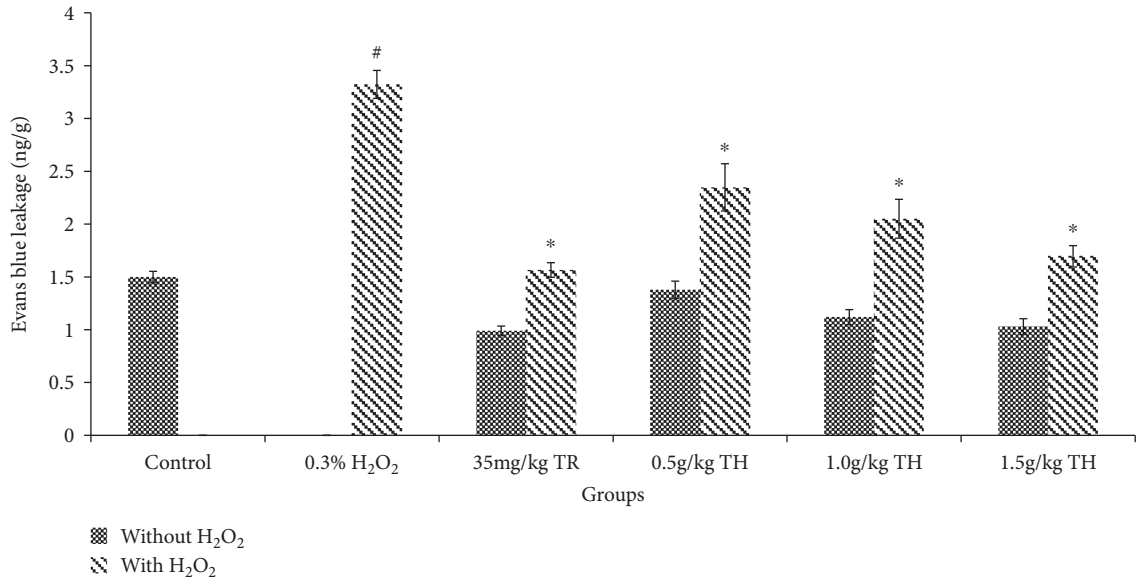

Figure 7: Quantitation of Evans blue extravasation in the skin of Balb/c mice. Mice treated with TH showed no significant difference ($p > 0.05$) compared with the untreated control group. $^{\#}p < 0.05$ vs. the control group; $^{*}p < 0.05$ vs. the H_2O_2 only group. Data were expressed as the mean ± SEM ($n = 6$). Control = untreated; TR = Trolox; TH = Tualang honey.

Several studies have shown that when endothelial cells are exposed to agonists like H_2O_2 [23], it raises the intracellular calcium concentration that causes increased endothelial permeability [23–25]. In the present study, the increase in the intracellular calcium level in HUVECs induced by H_2O_2 ($p < 0.05$) was abolished by TH and the level of intracellular calcium was almost reversed back to its basal level. Such maximal inhibition required only 0.10% of TH, suggesting that TH can reverse endothelial hyperpermeability through inhibiting H_2O_2-induced upregulation of intracellular calcium. Future investigation would be aimed at revealing if such suppression caused by TH occurs via inhibiting extracellular calcium influx or intracellular calcium production.

cAMP, a barrier-stabilizing molecule, could antagonize vascular leakage and protect endothelial barrier functions. By elevating cAMP levels, oxidant-induced permeability and edema formation can be reduced [26]. H_2O_2 is known to decrease cellular cAMP levels [27]. Another study demonstrated that the formation of cortical actin (F-actin cross linking protein, with cell protective effects) is a cAMP-dependent process [1]. In our study, pretreatment of TH alone on HUVECs reduced the cAMP production (0.01% and 1.0%); however, 0.10% of TH showed no significant difference as compared with the basal group even if there was a slight reduction (Figure 6). Interestingly, HUVECs induced with H_2O_2 were protected by TH especially at 0.10%, via maintaining the cAMP level. Low and high concentrations of TH (0.01% and 1.00%, respectively) failed to upregulate the cAMP level. This suggests that TH at its optimal concentration (0.10%) exhibited the maximal effect where it was able to maintain cAMP production which is comparable to the basal group.

Further investigation is needed to elucidate a clear TH-mediated signaling mechanism underlying our observation, e.g., redox-sensitive protein kinases such as mitogen-activated protein kinase (MAPK), using a more sophisticated tool to study the gene and protein expressions, and evaluate the differences in treatment response in animals of different genders to provide better translation insight to warrant clinical study in the future.

5. Conclusions

In summary, the present study provided the evidence that TH can inhibit H_2O_2-induced vascular permeability *in vivo* and *in vitro*. Such inhibition is via actin cytoskeleton reorganization, localization of β-catenin from Cav-1, and reduction of intracellular calcium influx while sustaining the cAMP levels. These discoveries may make a significant contribution to the pathogenesis of oxidant-dependent vascular diseases.

Data Availability

The data used to support the findings of this study are available from the corresponding author upon request.

Conflicts of Interest

The authors declare that there is no conflict of interest regarding the publication of this paper.

Acknowledgments

Kogilavanee Devasvaran was financed by the Graduated Research Fellowship of Universiti Putra Malaysia and MyBrain 15 from the Malaysian Ministry of Higher Education. The authors wish to thank Mr. Fahmi, Mr. Firdaus, and the supporting staff from the Anatomy and Histology Laboratory, Physiology Laboratory, and Cell Signaling Laboratory for their excellent technical support. This work was supported by

the Ministry of Education Malaysia under the Fundamental Research Grant Scheme (Project No. 04-02-13-1330FR) and Universiti Putra Malaysia under Geran Putra-IPS (GP-IPS/2015/9454900).

Supplementary Materials

Supplementary Materials Qualification of Evans blue extravasation in the skin of Balb/c mice. (a) Control group where mice were only treated with vehicle; (b) group pretreated with 35 mg/kg of TR; (c) group of mice pretreated with 0.5 g/kg of TH; (d) group of mice pretreated with 1.0 g/kg of TH; (e) group of mice pretreated with 1.5 g/kg of TH. Control = untreated; TR = Trolox; TH = Tualang honey. *(Supplementary Materials)*

References

[1] D. Mehta and A. B. Malik, "Signaling mechanisms regulating endothelial permeability," *Physiological Reviews*, vol. 86, no. 1, pp. 279–367, 2006.

[2] F. Wang, X. Song, M. Zhou et al., "Wogonin inhibits H_2O_2-induced vascular permeability through suppressing the phosphorylation of caveolin-1," *Toxicology*, vol. 305, pp. 10–19, 2013.

[3] H. Sauer, M. Wartenberg, and J. Hescheler, "Reactive oxygen species as intracellular messengers during cell growth and differentiation," *Cellular Physiology and Biochemistry*, vol. 11, no. 4, pp. 173–186, 2001.

[4] D. Kogilavanee and Y.-K. Yong, "Anti-inflammatory and wound healing properties of Malaysia Tualang honey," *Current Science*, vol. 110, no. 1, pp. 47–51, 2016.

[5] I. Khalil, S. A. Sulaiman, N. Alam et al., "Content and antioxidant properties of processed Tualang honey (AgroMas®) collected from different regions in Malaysia," *International Journal of Pharmacy and Pharmaceutical Sciences*, vol. 4, pp. 214–219, 2012.

[6] R. K. Kishore, A. S. Halim, M. S. N. Syazana, and K. N. S. Sirajudeen, "Tualang honey has higher phenolic content and greater radical scavenging activity compared with other honey sources," *Nutrition Research*, vol. 31, no. 4, pp. 322–325, 2011.

[7] S. P. Kek, N. L. Chin, Y. A. Yusof, S. W. Tan, and L. S. Chua, "Total phenolic contents and colour intensity of Malaysian honeys from the Apis spp. and Trigona spp. bees," *Agriculture and Agricultural Science Procedia*, vol. 2, pp. 150–155, 2014.

[8] N.-A. M. Nasir, A. S. Halim, K. K. B. Singh, A. A. Dorai, and M. N. M. Haneef, "Antibacterial properties of tualang honey and its effect in burn wound management: a comparative study," *BMC Complementary and Alternative Medicine*, vol. 10, no. 1, 2010.

[9] Y. T. Khoo, A. S. Halim, K. K. B. Singh, and N. A. Mohamad, "Wound contraction effects and antibacterial properties of Tualang honey on full-thickness burn wounds in rats in comparison to hydrofibre," *BMC Complementary and Alternative Medicine*, vol. 10, no. 1, 2010.

[10] J. J. Tan, S. M. Azmi, Y. K. Yong et al., "Tualang honey improves human corneal epithelial progenitor cell migration and cellular resistance to oxidative stress in vitro," *PLoS One*, vol. 9, no. 5, article e96800, 2014.

[11] M. I. Khalil, E. M. Tanvir, R. Afroz, S. A. Sulaiman, and S. H. Gan, "Cardioprotective effects of tualang honey: amelioration of cholesterol and cardiac enzymes levels," *BioMed Research International*, vol. 2015, Article ID 286051, 8 pages, 2015.

[12] T. K. Tan, M. Johnathan, M. S. Sayuti, and A. A. Nurul, "Immunomodulatory properties of Tualang honey in BALB/c mice," *Research Journal of Pharmaceutical Biological and Chemical Sciences*, vol. 6, pp. 209–216, 2015.

[13] K. Sarkar, S. R. Krishna Meka, A. Bagchi et al., "Polyester derived from recycled poly (ethylene terephthalate) waste for regenerative medicine," *RSC Advances*, vol. 4, no. 102, pp. 58805–58815, 2014.

[14] Y. K. Yong, H. S. Chiong, M. N. Somchit, and Z. Ahmad, "Bixa orellana leaf extract suppresses histamine-induced endothelial hyperpermeability via the PLC-NO-cGMP signaling cascade," *BMC Complementary and Alternative Medicine*, vol. 15, no. 1, 2015.

[15] L. Y. Fong, C. T. Ng, Y. K. Yong, M. N. Hakim, and Z. Ahmad, "Asiatic acid stabilizes cytoskeletal proteins and prevents TNF-α-induced disorganization of cell-cell junctions in human aortic endothelial cells," *Vascular Pharmacology*, vol. 117, pp. 15–26, 2019.

[16] J. Aman, J. van Bezu, A. Damanafshan et al., "Effective treatment of edema and endothelial barrier dysfunction with imatinib," *Circulation*, vol. 126, no. 23, pp. 2728–2738, 2012.

[17] M. Radu and J. Chernoff, "An *in vivo* Assay to Test Blood Vessel Permeability," *Journal of Visualized Experiments*, vol. 73, no. 73, 2013Journal of Visualized Experiments.

[18] H. T. Tan, R. A. Rahman, S. H. Gan et al., "The antibacterial properties of Malaysian tualang honey against wound and enteric microorganisms in comparison to manuka honey," *BMC Complementary and Alternative Medicine*, vol. 9, no. 1, 2009.

[19] A. Aghajanian, E. S. Wittchen, M. J. Allingham, T. A. Garrett, and K. Burridge, "Endothelial cell junctions and the regulation of vascular permeability and leukocyte transmigration," *Journal of Thrombosis and Haemostasis*, vol. 6, no. 9, pp. 1453–1460, 2008.

[20] N. Prasain and T. Stevens, "The actin cytoskeleton in endothelial cell phenotypes," *Microvascular Research*, vol. 77, no. 1, pp. 53–63, 2009.

[21] A. Navarro, B. Anand-Apte, and M. O. Parat, "A role for caveolae in cell migration," *The FASEB Journal*, vol. 18, no. 15, pp. 1801–1811, 2004.

[22] L. Song, S. Ge, and J. S. Pachter, "Caveolin-1 regulates expression of junction-associated proteins in brain microvascular endothelial cells," *Blood*, vol. 109, no. 4, pp. 1515–1523, 2007.

[23] A. L. Siflinger-Birnboim, H. A. Lum, P. J. Del Vecchio, and A. B. Malik, "Involvement of Ca2+ in the H_2O_2-induced increase in endothelial permeability," *American Journal of Physiology. Lung Cellular and Molecular Physiology*, vol. 270, no. 6, pp. L973–L978, 1996.

[24] K. Niwa, O. Inanami, T. Ohta, S. Ito, T. Karino, and M. Kuwabara, "p38 MAPK and Ca2+ contribute to hydrogen peroxide-induced increase of permeability in vascular endothelial cells but ERK does not," *Free Radical Research*, vol. 35, no. 5, pp. 519–527, 2001.

[25] C. M. Hecquet, G. U. Ahmmed, S. M. Vogel, and A. B. Malik, "Role of TRPM2 channel in mediating H_2O_2-induced Ca^{2+} entry and endothelial hyperpermeability," *Circulation Research*, vol. 102, no. 3, pp. 347–355, 2008.

[26] S. Hippenstiel, M. Witzenrath, B. Schmeck et al., "Adrenomedullin reduces endothelial hyperpermeability," *Circulation Research*, vol. 91, no. 7, pp. 618–625, 2002.

[27] R. C. Werthmann, K. Von Hayn, V. O. Nikolaev, M. J. Lohse, and M. Bünemann, "Real-time monitoring of cAMP levels in living endothelial cells: thrombin transiently inhibits adenylyl cyclase 6," *The Journal of Physiology*, vol. 587, no. 16, pp. 4091–4104, 2009.

Hindawi
Oxidative Medicine and Cellular Longevity
Volume 2019, Article ID 2567198, 9 pages
https://doi.org/10.1155/2019/2567198

Research Article

Moringa oleifera Seeds Improve Aging-Related Endothelial Dysfunction in Wistar Rats

Joseph Iharinjaka Randriamboavonjy,[1,2] Sandrine Heurtebise,[1] Pierre Pacaud,[1] Gervaise Loirand,[1,2] and Angela Tesse[1]

[1]*L'institut du thorax, INSERM, CNRS, UNIV Nantes, Nantes, France*
[2]*L'institut du thorax, CHU Nantes, Nantes, France*

Correspondence should be addressed to Angela Tesse; angela.tesse@univ-nantes.fr

Received 28 December 2018; Accepted 14 February 2019; Published 13 May 2019

Guest Editor: Albino Carrizzo

Vascular aging is characterized by functional and structural changes of the vessel wall, including endothelial dysfunction, with decreased endothelial $NO^{\cdot}$ bioavailability and elevated vasoconstrictor and inflammatory mediator production, vascular rigidity, and tone impairment. *Moringa oleifera* (MOI) is a little tree, and different parts of which are used in traditional medicine in tropical Africa, America, and Asia for therapeutic applications in several disorders including cardiovascular disease. The present study is aimed at assessing the effect of MOI on aging-associated alteration of the endothelial function in Wistar rats. Middle-aged Wistar rats (46-week-old males) have been fed with food containing or not 750 mg/kg/day of MOI seed powder for 4 weeks. A group of young Wistar rats (16-week-old) was used as control. Measurement of isometric contraction, western blot analysis, and immunostaining has then been performed in the aortas and mesenteric arteries to assess the endothelium function. MOI treatment improved carbachol-induced relaxation in both aortas and mesenteric arteries of middle-aged rats. In the aortas, this was associated with an increased Akt signalling and endothelial NO synthase activation and a downregulation of arginase-1. In the mesenteric arteries, the improvement of the endothelial-dependent relaxation was related to an EDHF-dependent mechanism. These results suggest a vascular protective effect of MOI seeds against the vascular dysfunction that develops during aging through different mechanisms in conductance and resistance arteries.

1. Introduction

Vascular aging corresponds to functional and structural changes of the arterial wall characterized by endothelial dysfunction and vascular rigidity [1, 2]. A primary mechanism responsible for aging-induced endothelial dysfunction is the decrease in the bioavailability and the production of nitric oxide ($NO^{\cdot}$), mainly resulting from the increased oxidative stress. NADPH-derived superoxide anions (O_2^-) interact with NO to form peroxynitrite ($ONOO^-$), which induces damaged protein accumulation and vascular inflammation and remodelling [3]. Peroxynitrite oxidizes the endothelial NO synthase (eNOS) cofactor BH4, thereby inactivating eNOS and reducing $NO^{\cdot}$ production [4, 5]. Moreover, BH4 reduction can result in eNOS uncoupling, leading to the generation of ROS rather than $NO^{\cdot}$ and thus perpetuating endothelial dysfunction [5]. Increased arginase expression and activity are also involved in endothelial dysfunction in aged vessels [6, 7]. Since arginase and eNOS compete for their common L-arginine (L-Arg) substrate, a rise in arginase activity or expression limits endothelial $NO^{\cdot}$ production in the vasculature [6–8]. Furthermore, the increased methylation of L-Arg and the resulting production of dimethyl L-Arg, observed in aged rats and humans, also contribute to the inhibition of eNOS activity [9].

In addition to decreased $NO^{\cdot}$ production and bioavailability, aging-associated endothelial dysfunction in resistance arteries also comprised oxidative stress-dependent impairment of prostacyclin and EDHF production that contributes to the defective endothelium-mediated vasorelaxation [5, 10].

Several studies suggested that polyphenols and other natural compounds contained in bioactive extracts and foods can protect against vascular aging through their anti-inflammatory and antioxidant properties as well as for their ability to improve eNOS activity and $NO^{\cdot}$ bioavailability [11–13]. *Moringa oleifera* (MOI) is a little tree used in Malagasy traditional medicine to treat several pathological states such as hypertension and inflammation [14, 15]. MOI seed oil showed free radical scavenging activity due to molecules such as flavonoids known to have antioxidant properties [16]. We previously described the cardiovascular protective effect of the oral administration of MOI seeds against cardiac complications induced by high blood pressure (left ventricle hypertrophy and fibrosis), vascular inflammation, and oxidative stress in spontaneously hypertensive rats (SHR), thus showing the anti-inflammatory and antioxidant action of a diet containing MOI seeds [17, 18].

The aim of the present work was to investigate the potential beneficial effects of MOI seeds administrated during 4 weeks against established aging-related vascular dysfunction in middle-aged Wistar rats (MAWR) by analysing endothelial function in conductance (aorta) and resistance (mesenteric) arteries.

2. Methods

2.1. Animals. Male Wistar rats (46 weeks old, middle-aged) were divided into two groups: a group receiving normal food (MAWR) and a group fed with food containing MOI seed powder (750 mg/day) mixed with standard pellet diet (MOI MAWR) for 4 weeks. This dose is within the range of concentrations classically used in experimental rodent models [18, 19]. A control group of young rats (16 weeks old, YWR), receiving normal food, was also used to check that middle-aged rats did indeed have arterial dysfunction. All groups received water ad libitum. At the end of the experimental protocol, all the rats were euthanized. The thoracic aorta and mesenteric arteries were then collected for vascular reactivity, western blot, and immunohistological analyses. All experiments were conducted in agreement with our Ethical Committee *Guide for the Care and Use of Laboratory Animals* (authorisation number 00909.01).

2.2. Arterial Reactivity. The aortas and first branches of superior mesenteric arteries were collected in physiological saline solution (in mM; 130 NaCl, 5.6 KCl, 1 $MgCl_2$, 2 $CaCl_2$, 11 glucose, and 10 Tris, pH 7.4 with HCl), cleaned, and cut in 2 mm long rings. Arterial rings were then mounted on multichannel isometric myograph, bathed in Krebs-Henseleit solution at 37°C bubbled with 95% O_2-5% CO_2, and connected to a force transducer (Pioden Controls Ltd., Canterbury, UK, for aortic rings; Danish Myo Technology, Aarhus, Denmark, for mesenteric artery rings). After equilibration, the contractile response to KCl (60 mM) was measured. Endothelial function was tested by measuring the relaxing response to cumulative doses of carbachol (CCh, 1 nM-10 μM, Sigma-Aldrich) of rings precontracted by phenylephrine (PhE, 1 μM, Sigma-Aldrich) in the absence and presence of L-N^G-nitroarginine methyl ester (L-NAME, 100 μM, Sigma-Aldrich) alone or in association with the cyclooxygenase (COX) inhibitor, indomethacin (10 μM, Sigma-Aldrich). Digital data were recorded by a MacLab/4e recorder and analysed using a LabChart v7 software (AD Instruments, Paris, France).

2.3. Staining and Confocal Microscopy Imaging. Frozen sections of the aortas (7 μm thick) were fixed with cold 100% methanol and incubated for 2 h at room temperature in blocking buffer (5% of albumin in PBS). Tissue sections were then incubated overnight (4°C) with a mouse monoclonal antibody against the phosphorylated-(Ser 1179)-eNOS (1 : 50, Santa Cruz Biotechnology) or a rabbit polyclonal antibody against phosphorylated-(Ser473)-Akt (p-Akt) protein (1/500, Cell Signaling). Three washes were followed by incubation (1 h, at room temperature, in the dark) with the secondary mouse or rabbit fluorescent Alexa fluor-647-conjugated antibody (1 : 500, Molecular Probes). A Nikon A1-RS inverted laser scanning confocal microscope was used for the optical sectioning of the tissue. Digital image recording was performed using the NIS element software. Images were analysed and processed by Fiji software.

2.4. Western Blot Analysis. The aortas were homogenized and lysed. Proteins (50 μg) were separated in precoated SDS-PAGE 4-15% (MiniPROTEAN® TGX™, Bio-Rad), transferred to nitrocellulose membrane, and then incubated (2 h at room temperature) in blocking buffer (5% nonfat dry milk in PBS). The membranes were probed overnight at 4°C with primary rabbit polyclonal antibody directed to arginase-1 (1/200, Santa Cruz Biotechnology). After 3 washes, immunoreactive bands were revealed with a secondary peroxidase-conjugated anti-rabbit IgG (1 : 5000, Beckman Coulter), detected by enhanced chemiluminescence system (ECL Plus, Amersham Biosciences), and quantified by densitometry. A polyclonal anti-α-tubulin antibody (1 : 5000, Sigma-Aldrich) was used to check protein gel loading and to normalize protein expression. The analysis of the blots was performed with Image Lab™ software v4.1 (Bio-Rad).

2.5. Data Analysis. The endothelial relaxation in response to cumulative doses of CCh was expressed as a percentage of the amplitude of PhE-induced precontraction. For the statistical analysis of these data, we used a two-way analysis of variance for repeated measures with subsequent Bonferroni post hoc test. To calculate the area under the curve (AUC) of the concentration-dependent relaxation in response to CCh, we used the GraphPad Prism 5.02 software. A one-way ANOVA with subsequent Bonferroni post hoc test or the ANOVA on ranks was performed for the AUC of relaxation and protein expression data. All statistical analysis were realized with SigmaStat 3.5 software. All values are presented as mean ± SD of n repetitive measurements, with n representing the number of rat samples. $^*p < 0.05$ was considered to be statistically significant.

3. Results

3.1. MOI Administration Restores CCh-Induced Relaxation in MAWR Aortas. We first assessed the effect of MOI

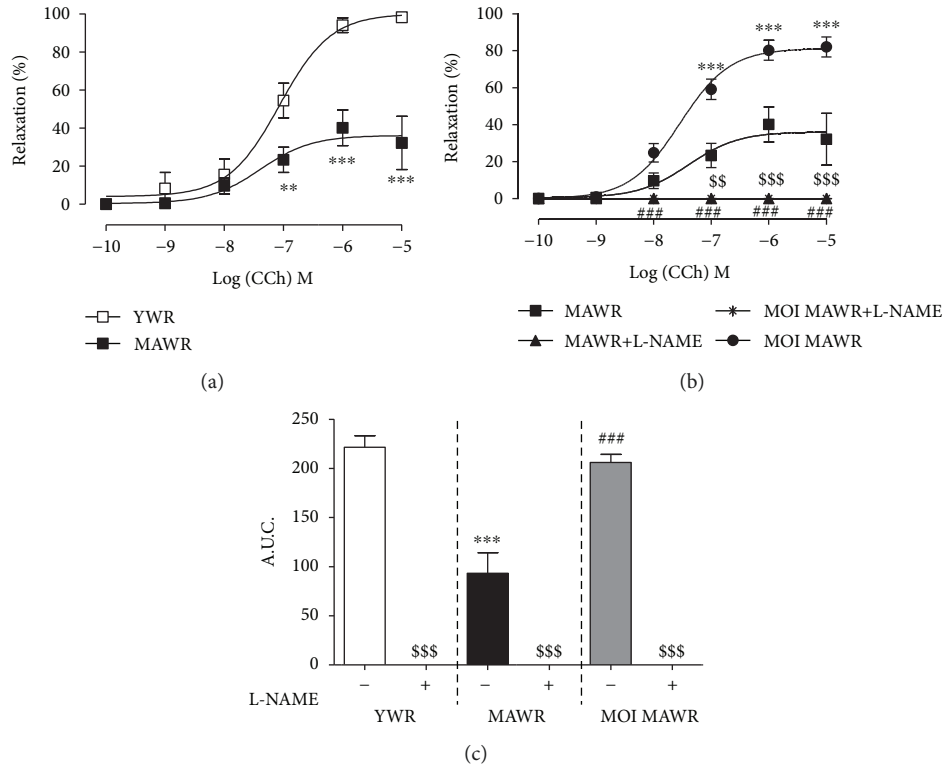

Figure 1: (a) Carbachol- (CCh-) induced relaxation in the aortas from young rats (YWR: 16 weeks old) and control middle-aged rats (MAWR, 50 weeks old; $^{**}p < 0.01$, $^{***}p < 0.001$, YWR versus MAWR). (b) Relaxation curves to CCh in the aortas from MAWR and MOI-treated middle-aged rats (MOI MAWR) in the absence and in the presence of L-NAME (100 μM) ($^{***}p < 0.001$, MOI MAWR versus MAWR; $^{###}p < 0.001$, MAWR versus MAWR+L-NAME; $^{\$\$}p < 0.01$, $^{\$\$\$}p < 0.001$, MOI MAWR versus MOI MAWR+L-NAME). (c) Histogram showing the area under the curve (AUC) of CCh-induced relaxation without and with L-NAME in YWR, MAWR, and MOI MAWR ($^{***}p < 0.001$, MAWR versus YWR; $^{###}p < 0.001$ MOI MAWR versus MAWR; $^{\$\$\$}p < 0.001$ without L-NAME versus with L-NAME in the same group. Results are expressed in mean ± SD; $n = 5$).

treatment on endothelial-dependent relaxation of aorta rings from MAWR by measuring the CCh-dependent relaxation in the three groups of rats and calculating the AUC in the absence and in the presence of L-NAME (Figure 1). As expected, CCh-induced endothelium-dependent relaxation was reduced in the aortas of MAWR compared to YWR aortas (Figures 1(a) and 1(c)). MOI seed administration almost completely restored CCh-induced relaxation in the aortas of MAWR that returned similar to that observed in YWR (Figures 1(b) and 1(c)). L-NAME completely abolished CCh-induced relaxation in the aortas from YWR, MAWR, and MOI MAWR (Figures 1(b) and 1(c) and Supplementary Figure 1) indicating that the relaxation response to CCh in the aorta is completely dependent of $NO^{\cdot}$ in the three groups of rats. These data suggest that the improvement of the endothelial function induced by MOI treatment in the aortas could result from the correction of aging-induced $NO^{\cdot}$ signalling defect.

3.2. MOI Administration Improves eNOS Signalling in the Aortas. To confirm the effect of MOI treatment on $NO^{\cdot}$ signalling, we directly assessed eNOS activity by immunostaining on cross sections of the aortas of active phosphorylated-(Ser1179)-eNOS and active phosphorylated-(Ser473)-Akt, one of the main kinases phosphorylating eNOS at Ser1179 [20] (Figures 2(a) and 2(b)). Both endothelial phosphorylated-(Ser1179)-eNOS and phosphorylated-(Ser473)-Akt staining observed in YWR were lost in MAWR but were restored in MOI MAWR (Figures 2(a) and 2(b)) suggesting a role of Akt-induced eNOS activation in the beneficial effect of MOI on endothelial function in MAWR. We next assessed the expression of arginase-1 that might also contribute to the reduced production of $NO^{\cdot}$ with aging [21] (Figure 2(c)). Arginase-1 expression, increased in MAWR aortas compared to YWR, was decreased to a level similar to YWR in MOI MAWR (Figure 2(c)). These data are consistent with a beneficial effect of MOI on eNOS activity in the aortas of MAWR.

3.3. MOI Administration Improves Endothelial Function in AWR Mesenteric Arteries. We also assessed the effect of MOI on the endothelial function of resistance arteries from MAWR. Both the dose-dependent relaxation curve to CCh and the AUC show that the relaxation induced by CCh was decreased in MAWR mesenteric arteries compared to YWR vessels (Figures 3(a) and 3(c)). MOI seeds improved the endothelial relaxation in the mesenteric arteries of MAWR compared to nontreated MAWR (Figures 3(b) and 3(c)). In YWR, L-NAME induced only a rightward shift of the concentration-relaxation curve to CCh without change of

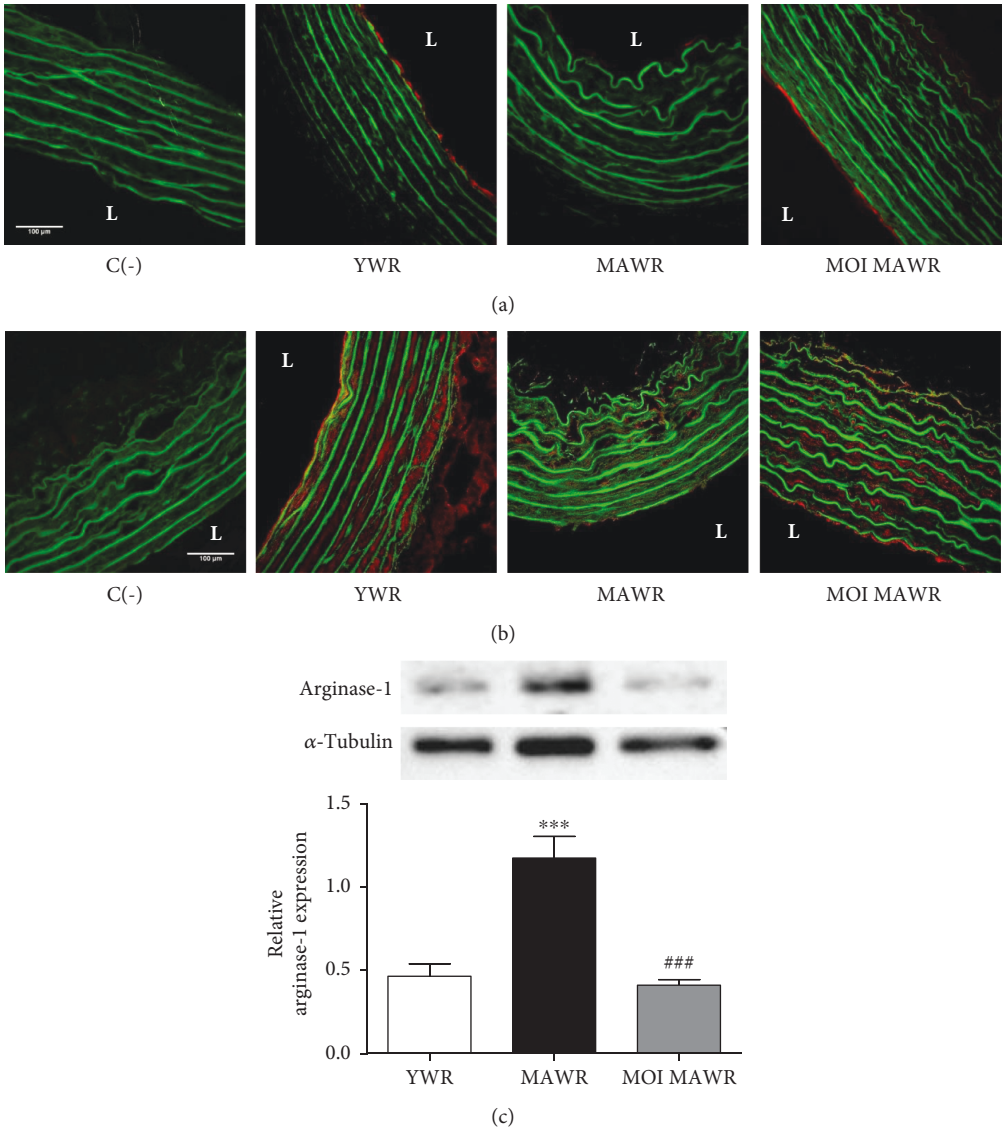

Figure 2: (a) Immunohistochemical representative red staining of phosphorylated-(Ser 1179)-eNOS or phosphorylated-(Ser 473)-Akt (b) in the aortas from YWR, control MAWR, and MOI MAWR. Green fluorescence corresponds to elastin autofluorescence. L = lumen of the vessel. C(-) is a negative control without the primary antibody. Scale bar = 100 μm. (c) Representative western blot and corresponding densitometric analysis of arginase-1 expression normalized to α-tubulin in the aortas of YWR, MAWR, and MOI MAWR (mean ± SD, $n = 3$; $^{***}p < 0.001$ MAWR versus YWR; $^{###}p < 0.001$ MOI MAWR versus MAWR).

the maximal relaxation, indicating that NO$^{\cdot}$ did not play a major role in CCh-induced relaxation of YWR mesenteric arteries (Supplementary Figure 2). Accordingly, the AUC was only decreased by ~25% by L-NAME in YWR mesenteric arteries (Figure 3(c)). In contrast, L-NAME strongly reduced the CCh-induced relaxation in MAWR as illustrated by the ~80% reduction of the maximal CCh-induced relaxation (Figure 3(b)) and the ~70% reduction of the AUC observed in the presence of L-NAME (Figure 3(c)). This suggests that aging increased the NO$^{\cdot}$ component of CCh-induced relaxation in the mesenteric arteries. MOI increased the relaxation response in MAWR mesenteric arteries, and L-NAME reduced only partially the CCh-induced relaxation in MOI MAWR, suggesting that the beneficial effect of MOI on the endothelial function was not mainly mediated by NO$^{\cdot}$ signalling but involved other mechanism(s) (Figures 3(b) and 3(c)).

3.4. MOI Administration Enhances EDHF-Dependent Relaxation in MAWR Mesenteric Arteries. We hypothesized that MOI improved endothelium-dependent relaxation in the mesenteric arteries of MAWR by increasing the contribution of EDHF. We therefore directly measured the EDHF-dependent component of the CCh-induced relaxation in the presence of both L-NAME and INDO to block both NO$^{\cdot}$- and COX-deriving relaxing factors, respectively (Figure 4). The EDHF-mediated relaxation of the mesenteric arteries in response to CCh was significantly decreased in MAWR compared to YWR, indicating that in mesenteric arteries CCh-induced relaxation was essentially dependent

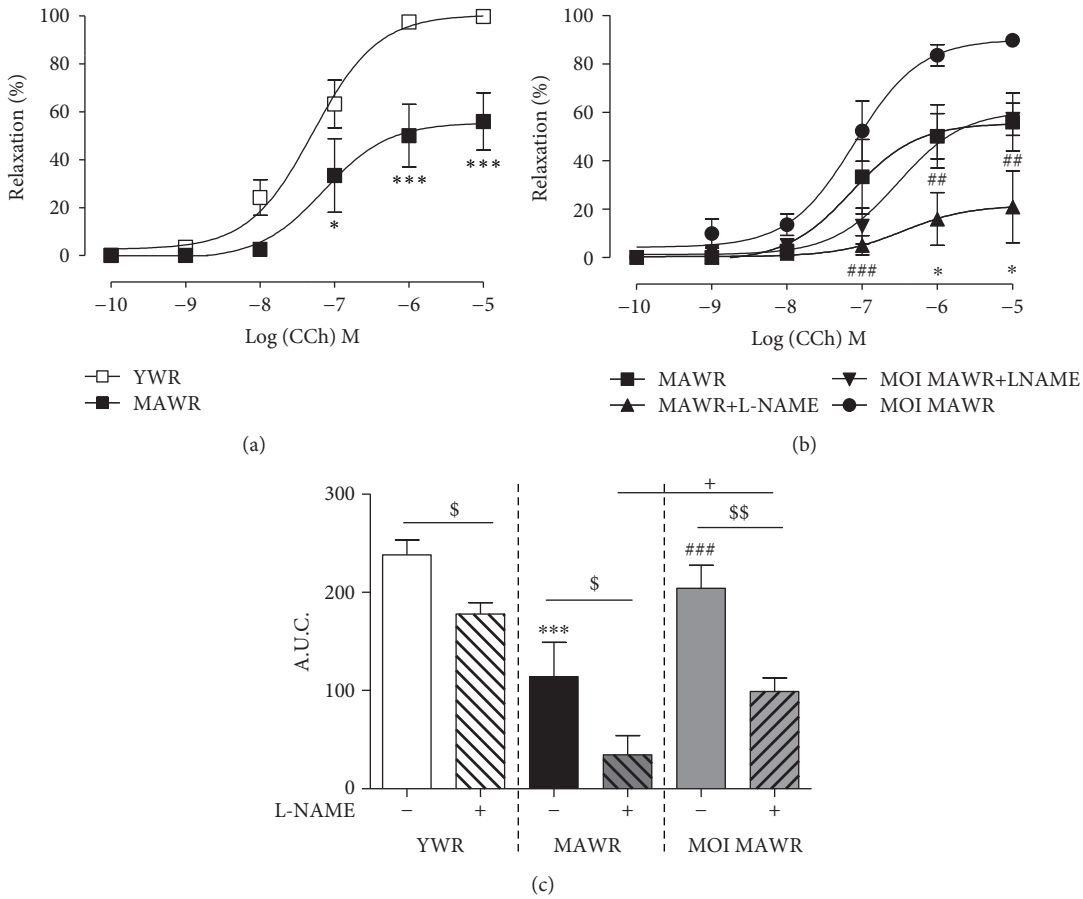

Figure 3: (a) Carbachol- (CCh-) induced relaxation in the mesenteric arteries of YWR and control MAWR ($^{*}p < 0.05$, $^{***}p < 0.001$, MAWR versus YWR). (b) Relaxation curves to CCh in the mesenteric arteries from MAWR and MOI MAWR in the absence and in the presence of L-NAME (100 μM) ($^{*}p < 0.05$, MAWR+L-NAME versus MAWR; $^{\#\#}p < 0.01$, $^{\#\#\#}p < 0.001$, MOI MAWR+L-NAME versus MOI MAWR). (c) Histograms showing the area under the curve (AUC) without and with L-NAME for YWR, MAWR, and MOI MAWR ($^{***}p < 0.001$, MAWR versus YWR; $^{\#\#\#}p < 0.001$, MOI MAWR versus MAWR; $^{\$}p < 0.05$, $^{\$\$}p < 0.01$, without L-NAME versus with L-NAME in the same group; $^{+}p < 0.05$ MOI MAWR+L-NAME versus MAWR+L-NAME). Results were expressed in mean ± SD of $n = 5$ rats.

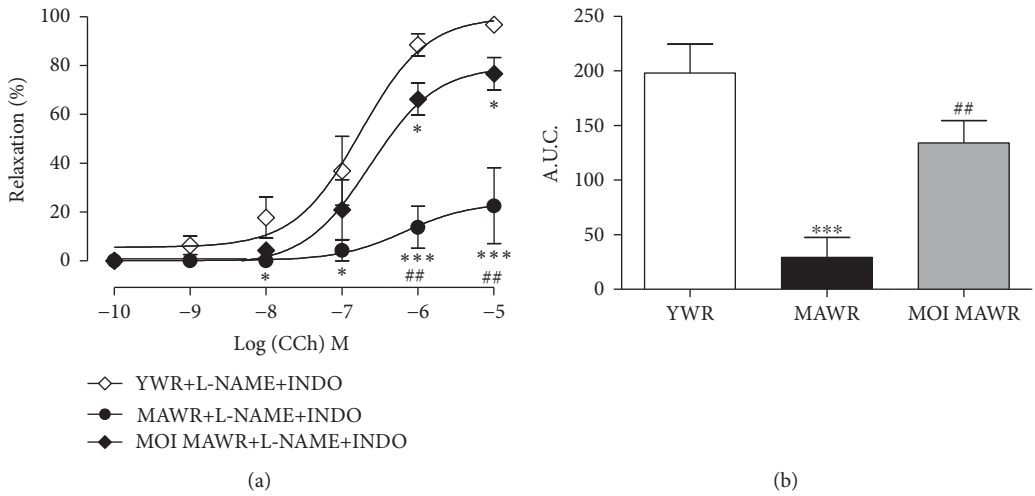

Figure 4: (a) EDHF-dependent relaxation to carbachol (CCh) in the mesenteric arteries from YWR, MAWR, and MOI MAWR obtained in the presence of L-NAME and indomethacin (INDO), L-NAME+INDO ($^{*}p < 0.05$, $^{***}p < 0.001$, versus YWR+L-NAME+INDO). (b) Histograms showing the area under the curve (AUC) of CCh-dependent relaxation of YWR, MAWR, and MOI MAWR mesenteric artery in the presence of L-NAME and INDO (L-NAME+INDO) ($^{***}p < 0.001$, MAWR+L-NAME+INDO versus YWR+L-NAME+INDO; $^{\#\#}p < 0.01$, MOI MAWR+L-NAME+INDO versus MAWR+L-NAME+INDO; results are expressed in mean ± SD with $n = 5$ per group).

on EDHF in YWR and that aging strongly reduced this EDHF-mediated relaxation (Figures 4(a) and 4(b)). MOI not totally but strongly restored EDHF-mediated relaxation in MAWR (Figures 4(a) and 4(b)). These data thus indicate that the altered endothelium-dependent relaxation response to CCh in MAWR mesenteric arteries resulted from a loss of its EDHF-mediated component which was partially corrected by MOI.

4. Discussion

Our study provides evidence for the beneficial arterial effects of MOI seed administration in MAWR with an established aging-induced endothelial dysfunction in both the aorta and mesenteric arteries. Diet containing MOI seeds improves the endothelial function in MAWR by boosting eNOS activity in the aorta and enhancing EDHF-dependent relaxation in the mesenteric arteries. These data suggest a different effect of MOI seeds on the endothelial aging process in conductance and resistance arteries.

Vascular aging consists of a set of changes in the mechanical and structural properties of the vascular wall including a decrease in endothelium-dependent relaxation by reducing the bioavailability of $NO^{\cdot}$ and/or EDHF depending on the arterial bed [4, 10, 22]. As previously described [23, 24], we confirm that the endothelium-dependent CCh-induced relaxation in the aortas was exclusively mediated by $NO^{\cdot}$ both in YWR and MAWR. Aging was associated with a reduction of endothelium-dependent $NO^{\cdot}$ signalling attested by the loss of the CCh-induced relaxation and the decrease of phosphorylation of eNOS and its upstream kinase Akt, in agreement with the role of Akt/eNOS signalling impairment in aging-induced endothelial dysfunction [20, 25]. MOI administration corrected the Akt/eNOS defect and restored $NO^{\cdot}$-mediated endothelium-dependent relaxation in MAWR. NO signalling has been identified as a target of the beneficial action of polyphenol-rich diets on endothelial function and cardiovascular protection [26, 27]. Indeed, similar improvements of endothelial function by activating the Akt/eNOS pathway were previously demonstrated in a diet supplemented with other natural substances such as (R)-α-lipoic acid contained in several vegetal foods and other polyphenols such as delphinine and resveratrol contained in red wine [25, 28, 29]. Polyphenolic compounds contained in MOI seeds could thus be responsible for or participate in the beneficial effects of MOI seeds on Akt/eNOS signalling in the endothelium of MAWR [30, 31]. Indeed, MOI seeds contain glucosinolates (glucomoringin) and isothiocyanates known for their ability to improve endothelial-dependent relaxation in rat aortas [32].

In addition to the stimulation of Akt/eNOS signalling, we observed that MOI reduced arginase-1 expression which was upregulated in MAWR. This MOI-induced reduction of arginase-1 expression can therefore provide an additional mechanism by which MOI improves $NO^{\cdot}$ signalling, by increasing the amount of the eNOS substrate L-Arg required for $NO^{\cdot}$ biosynthesis. Targeting arginase is considered as an emergent strategy to elevate $NO^{\cdot}$ level in disorders involving endothelial dysfunction and thus as a potential target for the treatment of cardiovascular disease [33]. Several plant-derived substances, especially polyphenols, have been shown to inhibit arginase activity [34]. In particular, MOI leaf extracts inhibited arginase activity in a dose-dependent manner [35]. This effect has been ascribed to the polyphenols (gallic acid, catechin, chlorogenic acid, ellagic acid, epicatechin, rutin, quercitrin, isoquercitrin, quercetin, and kaempferol) identified in the extract. Here, we show that MOI seeds downregulate arginase-1 protein expression, suggesting that plant-derived polyphenols can reduce the deleterious effect of arginase-1 on endothelial $NO^{\cdot}$ signalling by inhibiting both its activity and its expression.

In the mesenteric arteries, MOI restored the EDHF-mediated CCh-induced relaxation that was decreased in MAWR. Although not demonstrated in this study, hydrogen peroxide (H_2O_2), known as the main hyperpolarizing factor in the mesenteric arteries, could be involved in the effect of MOI [10, 36]. Other mechanisms such as the upregulation of Ca^{2+}-activated small (SK_{Ca}), intermediate (IK_{Ca}), and large (BK_{Ca}) conductance potassium channels, Na^+/K^+ ATPase pump, and the myoendothelial gap junctions can be also involved in the NO-independent effect of MOI in the mesenteric arteries [37, 38]. Indeed, the improvement of aging-related endothelial dysfunction, particularly its EDHF component, produced by red wine polyphenolic compounds has been ascribed, at least in part, to the normalization of SK_{Ca} and IK_{Ca} expression, reduced in MAWR mesenteric arteries [10]. Similar to MOI, the beneficial effect of dietary supplementation with red wine polyphenolic compounds on endothelial dysfunction results from the potentialization of the EDHF-dependent relaxation in resistance arteries while it was due to the increase in $NO^{\cdot}$ bioavailability in conductance arteries [39]. Thus, the endothelial effect of dietary MOI on the EDHF pathway is probably also due to the polyphenolic compounds contained in MOI seeds, in agreement with the polyphenolic compound-related antioxidant and anti-inflammatory effects of a diet containing MOI seeds that we previously described [18]. Complementary experiments to measure plasma biomarkers of inflammation, oxidative stress, and endothelial dysfunction such as resistin, ICAM-1, VCAM-1, and E-selectin could be useful to refine the mechanism of action of MOI.

The beneficial effect of MOI on endothelium function has been observed in male MAWR. However, it has been described that male and female rodents are not equally prone to age-induced endothelial dysfunction [40]. It thus would be interesting to assess whether MOI seeds would also be able to improve endothelial function in female rats.

5. Conclusion

This study shows that dietary supplementation with MOI corrects aging-induced endothelial dysfunction. The beneficial effects of MOI seeds result from the upregulation of $NO^{\cdot}$ and EDHF signalling in the aorta and mesenteric artery, respectively. They are likely due to the polyphenolic compounds contained in MOI seeds. Our data suggest the

interest of dietary supplementation with MOI seeds in middle-aged or elderly people to limit aging-related endothelial dysfunction and prevent the development of cardiovascular disease. This could be particularly relevant in MOI-producing countries that may have limited access to pharmacological treatments and also in Western countries, as a nondrug mean for healthy aging.

Abbreviations

MAWR:	Middle-aged Wistar rats
CCh:	Carbachol
COX:	Cyclooxygenase
EDHF:	Endothelium-derived hyperpolarizing factor
eNOS:	Endothelial NO synthase
INDO:	Indomethacin
iNOS:	Inducible NO synthase
L-Arg:	L-arginine
L-NAME:	L-N^G-nitroarginine methyl ester
MOI:	*Moringa oleifera*
MOI MAWR:	Middle-aged Wistar rats treated with *Moringa oleifera* seeds
NO:	Nitric oxide
PHE:	Phenylephrine
RAS:	Renin/angiotensin system
ROS:	Reactive oxygen species
RWPs:	Red wine polyphenols
SOD:	Superoxide dismutase
AUC:	Area under the curve
YWR:	Young Wistar rats.

Data Availability

The data of the vascular relaxation, the area under the curves of relaxation, and the values of protein expression (arginase-1) will be available on request asking directly the corresponding author writing a mail at angela.tesse@univ-nantes.fr.

Disclosure

Preliminary results of the manuscript have been presented as an abstract in *Archives of Cardiovascular Diseases Supplements* [41].

Conflicts of Interest

The authors declare that there is no conflict of interest regarding the publication of this article.

Authors' Contributions

Gervaise Loirand and Angela Tesse contributed equally to this work.

Acknowledgments

We thank Philippe Hulin and Steven Nedellec and the platform MicroPicell (SFR Francois Bonamy, Nantes) for technical assistance in confocal microscopy. We also value the support provided by the animal facility unit of the University of Nantes. This work was supported by a grant from the INSERM and Région Pays de la Loire (PROVASC project).

Supplementary Materials

Supplementary Figure 1: carbachol- (CCh-) induced relaxation in the aortas from young rats (YWR: 16 weeks old) in the absence and in the presence of L-NAME (100 μM) ($^{***}p < 0.001$, +L-NAME versus without L-NAME. Results are expressed in mean ± SD with $n = 5$ per group). Supplementary Figure 2: carbachol- (CCh-) induced relaxation in the mesenteric arteries from young rats (YWR: 16 weeks old) in the absence and in the presence of L-NAME (100 μM) ($^{**}p < 0.01$, +L-NAME versus without L-NAME; results are expressed in mean ± SD with $n = 5$ per group). *(Supplementary Materials)*

References

[1] M. El Assar, J. Angulo, S. Vallejo, C. Peiro, C. F. Sànchez-Ferrer, and L. Rodriguez-Manas, "Mechanisms involved in the aging-induced vascular dysfunction," *Frontiers in Physiology*, vol. 3, 2012.

[2] M. D. Herrera, C. Mingorance, R. Rodriguez-Rodriguez, and M. Alvarez de Sotomayor, "Endothelial dysfunction and aging: an update," *Ageing Research Reviews*, vol. 9, no. 2, pp. 142–152, 2010.

[3] B. van der Loo, R. Labugger, J. N. Skepper et al., "Enhanced peroxynitrite formation is associated with vascular aging," *The Journal of Experimental Medicine*, vol. 192, no. 12, pp. 1731–1744, 2000.

[4] Y. Higashi, Y. Kihara, and K. Noma, "Endothelial dysfunction and hypertension in aging," *Hypertension Research*, vol. 35, no. 11, pp. 1039–1047, 2012.

[5] U. Forstermann and T. Munzel, "Endothelial nitric oxide synthase in vascular disease," *Circulation*, vol. 113, no. 13, pp. 1708–1714, 2006.

[6] C. Zhu, Y. Yu, J. P. Montani, X. F. Ming, and Z. Yang, "Arginase-I enhances vascular endothelial inflammation and senescence through eNOS-uncoupling," *BMC Research Notes*, vol. 10, no. 1, article 82, 2017.

[7] L. Santhanam, D. W. Christianson, D. Nyhan, and D. E. Berkowitz, "Arginase and vascular aging," *Journal of Applied Physiology*, vol. 105, no. 5, pp. 1632–1642, 2008.

[8] Z. Yang and X. F. Ming, "Arginase: the emerging therapeutic target for vascular oxidative stress and inflammation," *Frontiers in Immunology*, vol. 4, 2013.

[9] D. Tsikas, A. Bollenbach, E. Hanff, and A. A. Kayacelebi, "Asymmetric dimethylarginine (ADMA), symmetric dimethylarginine (SDMA) and homoarginine (hArg): the ADMA, SDMA and hArg paradoxes," *Cardiovascular Diabetology*, vol. 17, no. 1, 2018.

[10] D. A. Long, M. A. Newaz, S. S. Prabhakar et al., "Loss of nitric oxide and endothelial-derived hyperpolarizing factor-mediated responses in aging," *Kidney International*, vol. 68, no. 5, pp. 2154–2163, 2005.

[11] N. Idris Khodja, T. Chataigneau, C. Auger, and V. B. Schini-Kerth, "Grape-derived polyphenols improve aging-related endothelial dysfunction in rat mesenteric artery: role of

oxidative stress and the angiotensin system," *PLoS One*, vol. 7, no. 2, article e32039, 2012.

[12] B. Monsalve, A. Concha-Meyer, I. Palomo, and E. Fuentes, "Mechanisms of endothelial protection by natural bioactive compounds from fruit and vegetables," *Anais da Academia Brasileira de Ciências*, vol. 89, 1 Supplement, pp. 615–633, 2017.

[13] R. G. Feresin, J. Huang, D. S. Klarich et al., "Blackberry, raspberry and black raspberry polyphenol extracts attenuate angiotensin II-induced senescence in vascular smooth muscle cells," *Food & Function*, vol. 7, no. 10, pp. 4175–4187, 2016.

[14] P. Siddhuraju and K. Becker, "Antioxidant properties of various solvent extracts of total phenolic constituents from three different agroclimatic origins of drumstick tree (Moringa oleifera Lam.) leaves," *Journal of Agricultural and Food Chemistry*, vol. 51, no. 8, pp. 2144–2155, 2003.

[15] J. W. Fahey, "*Moringa oleifera*: a review of the medical evidence for its nutritional, therapeutic and prophylactic properties," *Trees for life Journal*, vol. 1, 2005.

[16] H. A. Ogbunugafor, F. U. Eneh, A. N. Ozumba et al., "Physicochemical and antioxidant properties in Moringa oleifera seed oil," *Pakistan Journal of Nutrition*, vol. 10, no. 5, pp. 409–414, 2011.

[17] J. I. Randriamboavonjy, G. Loirand, N. Vaillant et al., "Cardiac protective effects of Moringa oleifera seeds in spontaneous hypertensive rats," *American Journal of Hypertension*, vol. 29, no. 7, pp. 873–881, 2016.

[18] J. I. Randriamboavonjy, M. Rio, P. Pacaud, G. Loirand, and A. Tesse, "Moringa oleifera seeds attenuate vascular oxidative and nitrosative stresses in spontaneously hypertensive rats," *Oxidative Medicine and Cellular Longevity*, vol. 2017, Article ID 4129459, 10 pages, 2017.

[19] S. J. Stohs and M. J. Hartman, "Review of the safety and efficacy of Moringa oleifera," *Phytotherapy Research*, vol. 29, no. 6, pp. 796–804, 2015.

[20] M. B. Harris, H. Ju, V. J. Venema et al., "Reciprocal phosphorylation and regulation of endothelial nitric-oxide synthase in response to bradykinin stimulation," *Journal of Biological Chemistry*, vol. 276, no. 19, pp. 16587–16591, 2001.

[21] Z. S. Katusic, "Mechanisms of endothelial dysfunction induced by aging: role of arginase I," *Circulation Research*, vol. 101, no. 7, pp. 640-641, 2007.

[22] R. L. Matz, M. A. de Sotomayor, C. Schott, J. C. Stoclet, and R. Andriantsitohaina, "Vascular bed heterogeneity in age-related endothelial dysfunction with respect to NO and eicosanoids," *British Journal of Pharmacology*, vol. 131, no. 2, pp. 303–311, 2000.

[23] F. T. Ruschitzka, R. H. Wenger, T. Stallmach et al., "Nitric oxide prevents cardiovascular disease and determines survival in polyglobulic mice overexpressing erythropoietin," *Proceedings of the National Academy of Sciences*, vol. 97, no. 21, pp. 11609–11613, 2000.

[24] R. Das, G. M. Kravtsov, H. J. Ballard, and C. Y. Kwan, "L-NAME inhibits Mg(2+)-induced rat aortic relaxation in the absence of endothelium," *British Journal of Pharmacology*, vol. 128, no. 2, pp. 493–499, 1999.

[25] A. R. Smith and T. M. Hagen, "Vascular endothelial dysfunction in aging: loss of Akt-dependent endothelial nitric oxide synthase phosphorylation and partial restoration by (R)-α-lipoic acid," *Biochemical Society Transactions*, vol. 31, no. 6, pp. 1447–1449, 2003.

[26] M. Forte, V. Conti, A. Damato et al., "Targeting nitric oxide with natural derived compounds as a therapeutic strategy in vascular diseases," *Oxidative Medicine and Cellular Longevity*, vol. 2016, Article ID 7364138, 20 pages, 2016.

[27] M. H. Oak, C. Auger, E. Belcastro, S. H. Park, H. H. Lee, and V. B. Schini-Kerth, "Potential mechanisms underlying cardiovascular protection by polyphenols: role of the endothelium," *Free Radical Biology & Medicine*, vol. 122, pp. 161–170, 2018.

[28] M. Chalopin, A. Tesse, M. C. Martínez, D. Rognan, J. F. Arnal, and R. Andriantsitohaina, "Estrogen receptor alpha as a key target of red wine polyphenols action on the endothelium," *PLoS One*, vol. 5, no. 1, article e8554, 2010.

[29] C. M. Klinge, N. S. Wickramasinghe, M. M. Ivanova, and S. M. Dougherty, "Resveratrol stimulates nitric oxide production by increasing estrogen receptor alpha-Src-caveolin-1 interaction and phosphorylation in human umbilical vein endothelial cells," *The FASEB Journal*, vol. 22, no. 7, pp. 2185–2197, 2008.

[30] A. Leone, A. Spada, A. Battezzati, A. Schiraldi, J. Aristil, and S. Bertoli, "Moringa oleifera seeds and oil: characteristics and uses for human health," *International Journal of Molecular Sciences*, vol. 17, no. 12, p. 2141, 2016.

[31] M. Premi and H. K. Sharma, "Effect of extraction conditions on the bioactive compounds from Moringa oleifera (PKM 1) seeds and their identification using LC-MS," *Journal of Food Measurement and Characterization*, vol. 11, no. 1, pp. 213–225, 2017.

[32] A. T. Dinkova-Kostova and R. V. Kostov, "Glucosinolates and isothiocyanates in health and disease," *Trends in Molecular Medicine*, vol. 18, no. 6, pp. 337–347, 2012.

[33] J. Pernow and C. Jung, "Arginase as a potential target in the treatment of cardiovascular disease: reversal of arginine steal?," *Cardiovascular Research*, vol. 98, no. 3, pp. 334–343, 2013.

[34] B. R. Minozzo, D. Fernandes, and F. L. Beltrame, "Phenolic compounds as arginase inhibitors: new insights regarding endothelial dysfunction treatment," *Planta Medica*, vol. 84, no. 5, pp. 277–295, 2018.

[35] G. Oboh, A. O. Ademiluyi, A. O. Ademosun et al., "Phenolic extract from Moringa oleifera leaves inhibits key enzymes linked to erectile dysfunction and oxidative stress in rats' penile tissues," *Biochemistry Research International*, vol. 2015, Article ID 175950, 8 pages, 2015.

[36] C. R. Triggle, S. M. Samuel, S. Ravishankar, I. Marei, G. Arunachalam, and H. Ding, "The endothelium: influencing vascular smooth muscle in many ways," *Canadian Journal of Physiology and Pharmacology*, vol. 90, no. 6, pp. 713–738, 2012.

[37] H. A. Coleman, M. Tare, and H. C. Parkington, "Endothelium potassium channels, endothelium-dependent hyperpolarization and the regulation of vascular tone in health and in disease," *Australian Physiological and Pharmacological Society*, vol. 34, pp. 55–64, 2004.

[38] G. Edwards, M. Félétou, and A. H. Weston, "Endothelium-derived hyperpolarising factors and associated pathways: a synopsis," *Pflügers Archiv*, vol. 459, no. 6, pp. 863–879, 2010.

[39] A. Agouni, A. H. Lagrue-Lak-Hal, H. A. Mostefai et al., "Red wine polyphenols prevent metabolic and cardiovascular alterations associated with obesity in Zucker fatty rats (Fa/Fa)," *PLoS One*, vol. 4, no. 5, article e5557, 2009.

[40] Y. Takenouchi, T. Kobayashi, T. Matsumoto, and K. Kamata, "Gender differences in age-related endothelial function in the murine aorta," *Atherosclerosis*, vol. 206, no. 2, pp. 397–404, 2009.

[41] J. I. Randriamboavonjy, G. Loirand, S. Heurtebise, P. Pacaud, and A. Tesse, "0515 : Moringa oleifera seeds improve vascular function in aged Wistar rats," *Archives of Cardiovascular Diseases Supplements*, vol. 8, no. 3, p. 218, 2016.

Hindawi
Oxidative Medicine and Cellular Longevity
Volume 2019, Article ID 4275984, 15 pages
https://doi.org/10.1155/2019/4275984

Research Article

Buyang Huanwu Decoction Exerts Cardioprotective Effects through Targeting Angiogenesis via Caveolin-1/VEGF Signaling Pathway in Mice with Acute Myocardial Infarction

Jia-Zhen Zhu, Xiao-Yi Bao, Qun Zheng, Qiang Tong, Peng-Chong Zhu, Zhuang Zhuang, and Yan Wang

Department of Cardiology, The Second Affiliated Hospital and Yuying Children's Hospital of Wenzhou Medical University, Wenzhou 325027, China

Correspondence should be addressed to Yan Wang; wywzchina@sina.com

Received 27 September 2018; Revised 2 January 2019; Accepted 11 March 2019; Published 16 April 2019

Guest Editor: Sabato Sorrentino

Background. Acute myocardial infarction (AMI) remains a leading cause of morbidity and mortality worldwide. The idea of therapeutic angiogenesis in ischemic myocardium is a promising strategy for MI patients. Buyang Huanwu decoction (BHD), a famous Chinese herbal prescription, exerted antioxidant, antiapoptotic, and anti-inflammatory effects, which contribute to cardio-/cerebral protection. Here, we aim to investigate the effects of BHD on angiogenesis through the caveolin-1 (Cav-1)/vascular endothelial growth factor (VEGF) pathway in MI model of mice. *Materials and Methods*. C57BL/6 mice were randomly divided into 3 groups by the table of random number: (1) sham-operated group (sham, $n = 15$), (2) AMI group (AMI +sham, $n = 20$), and (3) BHD-treated group (AMI+BHD, $n = 20$). 2,3,5-Triphenyltetrazolium chloride solution stain was used to determine myocardial infarct size. Myocardial histopathology was tested using Masson staining and hematoxylin-eosin staining. CD31 immunofluorescence staining was used to analyze the angiogenesis in the infarction border zone. Western blot analysis, immunofluorescence staining, and/or real-time quantitative reverse transcription polymerase chain reaction was applied to test the expression of Cav-1, VEGF, vascular endothelial growth factor receptor 2 (VEGFR2), and/or phosphorylated extracellular signal-regulated kinase (p-ERK). All statistical analyses were performed using the SPSS 20.0 software and GraphPad Prism 6.05. Values of $P < 0.05$ were considered as statistically significant. *Results and Conclusion*. Compared with the AMI group, the BHD-treated group showed a significant improvement in the heart weight/body weight ratio, echocardiography images, cardiac function, infarct size, Mason staining of the collagen deposition area, and density of microvessel in the infarction border zone ($P < 0.05$). Compared with the AMI group, BHD promoted the expression of Cav-1, VEGF, VEGFR2, and p-ERK in the infarction border zone after AMI. BHD could exert cardioprotective effects on the mouse model with AMI through targeting angiogenesis via Cav-1/VEGF signaling pathway.

1. Introduction

Based on the fourth edition of universal definition of myocardial infarction (MI), acute MI (AMI) was defined as having clinical evidences of acute myocardial injury with at least one of the following items: clinical symptoms of myocardial ischemia, new ischemic changes in electrocardiogram (ECG), development of pathological Q waves, imaging evidences in accordance with an ischemic aetiology as new loss of surviving myocardium or new regional ventricular wall motion abnormality, and identification of a coronary thrombus by coronary angiography or autopsy [1]. Epidemiological findings from National Health and Nutrition Examination Survey 2011 to 2014 (National Heart, Lung, and Blood Institute tabulation) manifested that the overall prevalence of MI was 3.0% in US adults greater than or equal to 20 years old [2]. Reperfusion and revascularization therapy, including thrombolysis and/or percutaneous coronary intervention (PCI), should be administrated as quickly and effectively as possible to limit infarct size or prevent complete occlusion

[3]. Reduction in the mortality rate of AMI is one big success story of modern medicine [3]. However, the process of restoring coronary blood flow to the ischemic myocardium may lead to myocardial ischemia/reperfusion (I/R) injury such as myocardial stunning, no-reflow phenomenon, and reperfusion arrhythmias. Several strategies such as pharmacological treatment and mechanical therapies could reduce I/R injury in animal studies or small-scale clinical trials, but the results are inconclusive [4]. Thus, there is still a need to develop a novel cardioprotective strategy for AMI patients.

Angiogenesis is defined as the growth and proliferation of new blood vessels from preexisting vascular structures [5]. Therapeutic angiogenesis refers to utilizing angiogenic growth factors to increase the growth of collateral blood vessels and promote new vascularization, so as to improve blood flow and tissue perfusion [6]. Promoting angiogenesis in ischemic myocardium that lack sufficient perfusion remains a promising strategy for MI patients [7, 8]. Although there will be a spontaneous angiogenic response in AMI which could partly reestablish blood flow in myocardium, this protective response is usually insufficient to restore the physiological level of tissue perfusion [7]. However, limited medical therapies have yet been proved to be able to successfully promote angiogenesis in AMI patients [9].

Growing evidences have shown that Chinese herbal medicines (CHM) could provide therapeutic effect on AMI by targeting angiogenesis [10–12]. Buyang Huanwu decoction (BHD), originally recorded in *Yilin Gaicuo (Correction on Errors in Medical Classics)* written by Wang in 1830, is a famous Chinese herbal prescription, has been used for the treatment of various vascular diseases in China for hundreds of years [13], and now is still being used in China and other countries around the world. BHD is composed of seven kinds of Chinese herbs (Table 1): (a) huang qi (radix astragali, the dried roots of *Astragalus membranaceus* (Fisch.) Bunge), (b) dang gui (radix angelicae sinensis, the dried lateral roots of *Angelica sinensis* (Oliv.) Diels), (c) chi shao (radix paeoniae rubra, the dried roots of *Paeonia lactiflora* Pall), (d) chuan xiong (rhizoma chuanxiong the dried rhizomes of *Ligusticum striatum* DC), (e) hong hua (flos carthami, the dried flowers of *Carthamus tinctorius* L), (f) tao ren (peach kernel, the dried seeds of *Prunus persica* (L.) Batsch), and (g) di long (Lumbricus, the dried bodies of *Pheretima aspergillum* (E. Perrier)), all of which are recorded in http://www.theplantlist.org and *Chinese Pharmacopoeia*. Based on traditional Chinese medicine theory, BHD has the function of invigorating the body, enhancing blood circulation, and activating Qi flow through energy meridians. Growing evidence has suggested the cardio-/cerebral protective functions of BHD in humans and animal models [14–22]. Recent studies on pharmacology and biochemistry also have shown that the protective functions of BHD on cardiocerebrovascular disease at least in part through the following mechanisms: antioxidant [18, 23, 24], antiapoptosis [25, 26], anti-inflammatory [19, 27], and improving hemorheological disorders [19]. An overview of systematic reviews indicated that BHD could treat a wide range of vascular disorders such as acute ischemic stroke and angina pectoris through targeting vascularity [28]. Studies showed that BHD could promote angiogenesis through increasing the expression of VEGF, VEGFR2, Flk-1, bFGF, and angiopoietin-1 (Ang-1) in ischemic stroke models both in vivo and in vitro [14, 29–33]. The regulation of BHD on the vascular endothelial growth factor (VEGF) signaling pathway according to the pathway enrichment analysis deserves to be studied in order to fully apprehend its latent capacity on treatment and its correlation with angiogenesis [34].

Caveolin-1 (Cav-1), the signature protein of endothelial cell caveolae, is involved in many physiological and pathological processes such as antifibrosis [35], inflammation [36], and oxidative stress [37]. Recent studies [38, 39] have demonstrated that Cav-1 is highly expressed in the vasculature in the process of blood vessel growth and could regulate the angiogenic activity of endothelial cells. Loss of Cav-1 would lead to the inhibition of vessel development and vascular remodeling [40]. Furthermore, Cav-1 plays a pivotal role in the signaling pathway of VEGF/VEGFR2-stimulated angiogenesis and is associated with angiogenic biological activities [41]. Resveratrol, a Cav-1 agonist, significantly elevated eNOS and VEGF protein levels in hypercholesterolemic rats with focal myocardial ischemic injury [42]. These evidences suggested that the Cav-1/VEGF pathway might play a critical role in angiogenesis after myocardial ischemic injury. Thus, in the present study, we aim to investigate the effects of BHD on angiogenesis through the Cav-1/VEGF pathway on the MI model of mice.

2. Materials and Methods

2.1. Animals. Thirty adult C57BL/6 male mice at 6-8 weeks of age and 20-25 g weight were obtained from Shanghai Slack Laboratory Animal Research Center and housed in the laboratory animal center of Wenzhou Medical University. All the mice were kept under 12 h light/dark cycles, temperature 22 $\pm 1^{\circ}$C, and provided with food and water ad libitum. The animals used were treated in accordance with the *Guide for the Care and Use of Laboratory Animals*, published by the National Institutes of Health (NIH). The study instructions were approved by the Animal Ethics Committee of the laboratory animal center of Wenzhou Medical University (number wydw2014-0058). All efforts were made to minimize the suffering of animals used.

2.2. Drugs and Reagents. BHD which consists of huang qi (radix astragali seuhedysari), dang gui (radix angelica sinensis), chi shao (radix paeoniae rubra), chuan xiong (rhizoma ligustici chuanxiong), hong hua (flos carthami), tao ren (semen persicae), and di long (Lumbricus) with a dispensing ratio of 120 : 6 : 4.5 : 3 : 3 : 3 : 3 was purchased from Sanjiu Medical & Pharmaceutical Co. Ltd., Shenzhen, China (granule preparations, approval number: country medicine accurate character Z44020711); CD31 antibody (ab28364), Cav-1 polyclonal antibody (ab2910), and VEGF polyclonal antibody (ab46154) were purchased from Abcam (UK); extracellular regulated protein kinases (ERK1/2) monoclonal antibody (4695), phosphorylated extracellular regulated protein kinases (p-ERK1/2) monoclonal antibody (4370), glyceraldehyde phosphate dehydrogenase (GAPDH) monoclonal

Table 1: Overview of Buyang Huanwu decoction.

Chinese name	Common name	Latin name/family/medicinal parts	Amount (%)
Huang qi	Radix astragali	Astragalus membranaceus (Fisch.) Bunge/Leguminosae/dried roots	120 g (84.2%)
Dang gui	Radix angelicae sinensis	Angelica sinensis (Oliv.) Diels/Apiaceae/dried lateral roots	6 g (4.2%)
Chi shao	Radix paeoniae rubra	Paeonia lactiflora Pall/Paeoniaceae/dried roots	4.5 g (3.2%)
Chuan xiong	Rhizoma chuanxiong	Ligusticum striatum DC/Apiaceae/dried rhizomes	3 g (2.1%)
Hong hua	Flos carthami	Carthamus tinctorius L/Compositae/dried flowers	3 g (2.1%)
Tao ren	Peach kernel	Prunus persica (L.) Batsch/Rosaceae/dried seeds	3 g (2.1%)
Di long	Lumbricus	Pheretima aspergillum (E. Perrier)/dried bodies	3 g (2.1%)

antibody (5174), and vascular endothelial growth factor receptor 2 (VEGFR2) monoclonal antibody (2479) were purchased from Cell Signaling Technology (USA).

2.3. AMI Model Establishment. Establishment of the AMI model referred to the previous publication [43]. Briefly, mice were anesthetized by isoflurane, and respiration was assisted with a ventilator (Inspira, Harvard Apparatus, Holliston, MA) in a volume-controlled mode at 80 strokes per minute. After fixation, thoracotomy was done at the 3rd intercostal space via the left lateral chest wall to expose the pericardium and heart. The AMI model was established by perpetually ligating the left anterior descending coronary artery (LAD) in 2 mm from its origin (near the main pulmonary artery) with a 7-0 silk suture, resulting in the development of pale color in the distal part of ligation.

All C57BL/6 mice ($n = 55$) were randomly divided into 3 groups by the table of random number: (1) sham-operated group (sham, $n = 15$), the LAD was encircled by a 7-0 silk suture without ligation; (2) AMI group (AMI+sham, $n = 20$), gavage with 0.2 ml 0.9% normal saline (once a day) 3 days before modeling until 14 days after modeling; and (3) BHD-treated group (AMI+BHD, $n = 20$), gavage with 0.2 ml BHD (20 g/kg, once a day) 3 days before modeling until 14 days after modeling.

2.4. Doppler Echocardiography Study. Fourteen days after modeling, mice undergo transthoracic echocardiography by the M-mode transducer (Acuson Sequoia 512, Sonos, Germany) after induction of anesthesia. At the papillary muscle level, M-mode tracings through short-axis view were recorded through the anterior and posterior left ventricle (LV) walls to measure LV end-diastolic dimension (LVEDd), LV end-systolic dimension (LVESd), LV fraction shortening (LVFS), and LV ejective fraction (LVEF) with the Simpson approach. All measurements were done by an experienced doctor who was blinded to the experimental design.

2.5. Determination of Myocardial Infarct Size. Euthanasia was done on the mice at 14 days after modeling through intraperitoneal injection of excessive pentobarbital sodium. The heart of the mice was separated from the aortic arch, major blood vessels, and extracardiac connective tissue and rinsed in phosphate-buffered saline to wash away the blood-stain. The heart tissues were semifreezed in a −20°C freezer for 30 minutes and then cut into 5 slices (1 mm thick) in a perpendicular way to the long axis. The slices were incubated in 1% 2,3,5-triphenyltetrazolium chloride solution (TTC) at 37°C for 15 minutes. After carefully evaluating the whole surface area, segments with brick red staining were identified as viable (noninfarcted area) and those without staining were identified as nonviable (infarcted area). Finally, the 3rd slice of each heart was chosen to calculate the infarct size (infarcted area/(noninfarcted area + infarcted area)) by the Image-Pro Plus 6.0 software (Media Cybernetics, Silver Spring, USA).

2.6. Myocardial Histopathology. The left ventricle including the region of MI was embedded in paraffin. The samples were then sectioned into 5 μm thick slices. Masson staining and hematoxylin-eosin (HE) staining were applied separately. Morphological changes of nuclei and cytoplasm around the marginal zone of MI in HE staining were observed by an optical microscope (Olympus, Japan). Image-Pro Plus 6.0 software (Media Cybernetics, Silver Spring, USA) was used to calculate the percentage of collagen deposition around the marginal zone of MI to assess the degree of fibrosis in the infarcted myocardium.

2.7. Western Blot Analysis. Total protein isolated from the myocardium was separated by SDS-PAGE and transferred to a polyvinylidene difluoride (PVDF) membrane. The membranes were then blocked with 5% fat-free milk and incubated overnight at 4°C with primary antibodies including Cav-1 (1 : 1000), VEGF (1 : 1000), VEGFR2 (1 : 1000), GADPH (1 : 10000), ERK1/2 (1 : 1000), and p-ERK1/2 (1 : 2000). After washing with TBST for three times, the membranes were incubated with secondary antibodies (1 : 10000) for 2 h at room temperature. ChemiDoc™ XRS+ Imaging System was used to visualize the signals. Javas freely available NIH ImageJ software (NIH, Bethesda, MD, USA) was used to quantify the intensity of immune reactivity.

2.8. Immunofluorescence Staining. After routine dewaxing and hydration, the antigens in myocardial tissue sections were repaired by sodium citrate buffer at 100°C. After washing thrice with PBS, tissues were treated with 3% hydrogen peroxide for 30 min. 1% bovine serum albumin (BSA) was used to block the antigen. The tissues were then incubated with CD31 antibody (1 : 300), Cav-1 antibody (1 : 500),

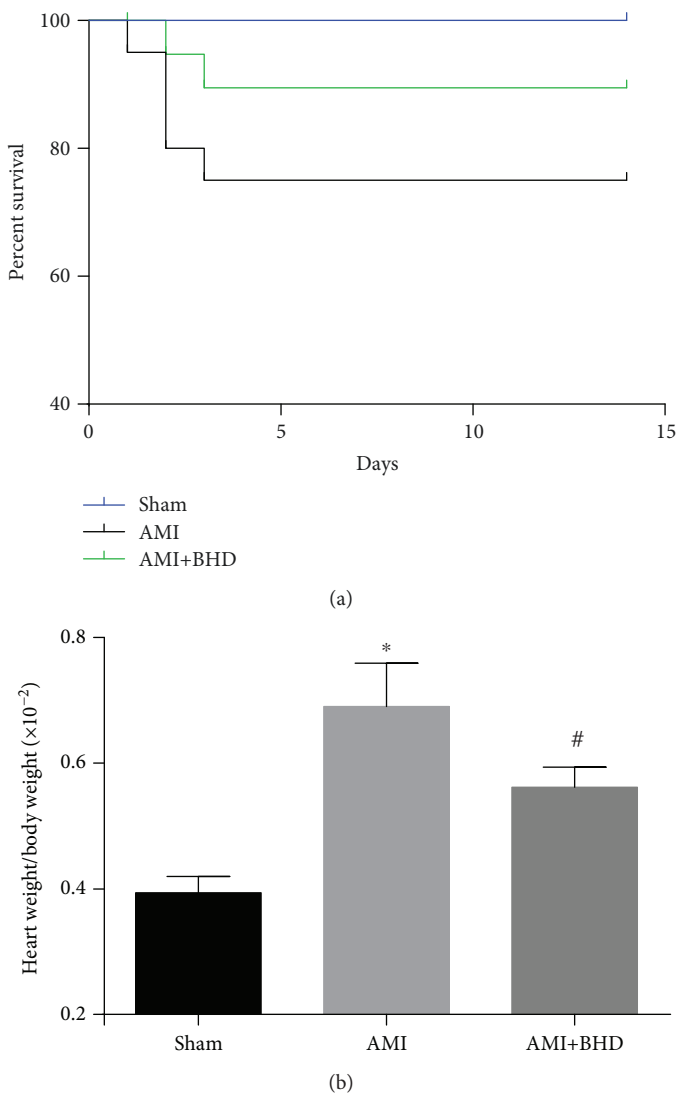

Figure 1: Survival rate and heart weight/body weight ratio at 14 days after AMI in mice (sham: $n = 15$, AMI: $n = 15$, and BHD+AMI: $n = 18$). (a) The survival rate of mice in the BHD-treated group compared with the AMI group (log-rank: $P = 0.0829$); (b) the heart weight/body weight ratio of mice (mean ± SD). $^{*}P < 0.05$, compared with the sham group; $^{\#}P < 0.05$, compared with the AMI group.

VEGF antibody (1 : 400), VEGFR2 antibody (1 : 200), and p-ERK antibody (1 : 200) at 4°C and then followed by 60 min of incubation with Alexa Flour 647- or 488-conjugated antibody (1 : 400) at 37°C. To visualize the nuclei, the cells were counterstained with 4′,6-diamidino-2-phenylindole (DAPI) for 5 min in the dark. The images were captured using a fluorescence microscope and then analyzed with the Image-Pro Plus 6.0 software (Media Cybernetics, Silver Spring, USA).

2.9. Real-Time Quantitative Reverse Transcription Polymerase Chain Reaction (RT-qPCR). Total RNA was isolated using the TRIzol reagent (Invitrogen, USA). RNA samples from each group were reverse transcribed into cDNA using the PrimeScript™ RT reagent Kit (TAKARA, Japan). Quantitative RT-qPCR was performed on a LightCycler thermal cycler system (Bio-Rad, USA) using SYBR® Premix Ex Taq™ II (TAKARA, Japan) and gene-specific primers. Gene-specific primers were as follows: Cav-1: forward, 5′-GACCTAATCCAACCATCAT-3′ and reverse, 5′-AGCAAGAACATTACCTCAA-3′; VEGF: forward, 5′-GACTATTCAGCGGACTCA-3′ and reverse, 5′-AAGAACCAACCTCCTCAA-3′; VEGFR2: forward, 5′-AATGATTGTTGGCGATGAA-3′ and reverse, 5′-GTGAGGATGACCGTGTAG-3′; and β-actin: forward, 5′-ACCTGCCCTTTAGAACTT-3′ and reverse, 5′-GCTCCAGGGACTATCTTT-3′.

2.10. Statistical Analysis. All data were expressed as mean ± standard deviation (SD). Difference between two groups was analyzed using two-tailed Student's t-test. Multiple groups were compared using one-way analysis of variance (ANOVA) and followed by LSD post hoc comparisons when appropriate. All statistical analyses were performed using the SPSS 20.0 software and GraphPad Prism 6.05. Values of $P < 0.05$ were considered as statistically significant.

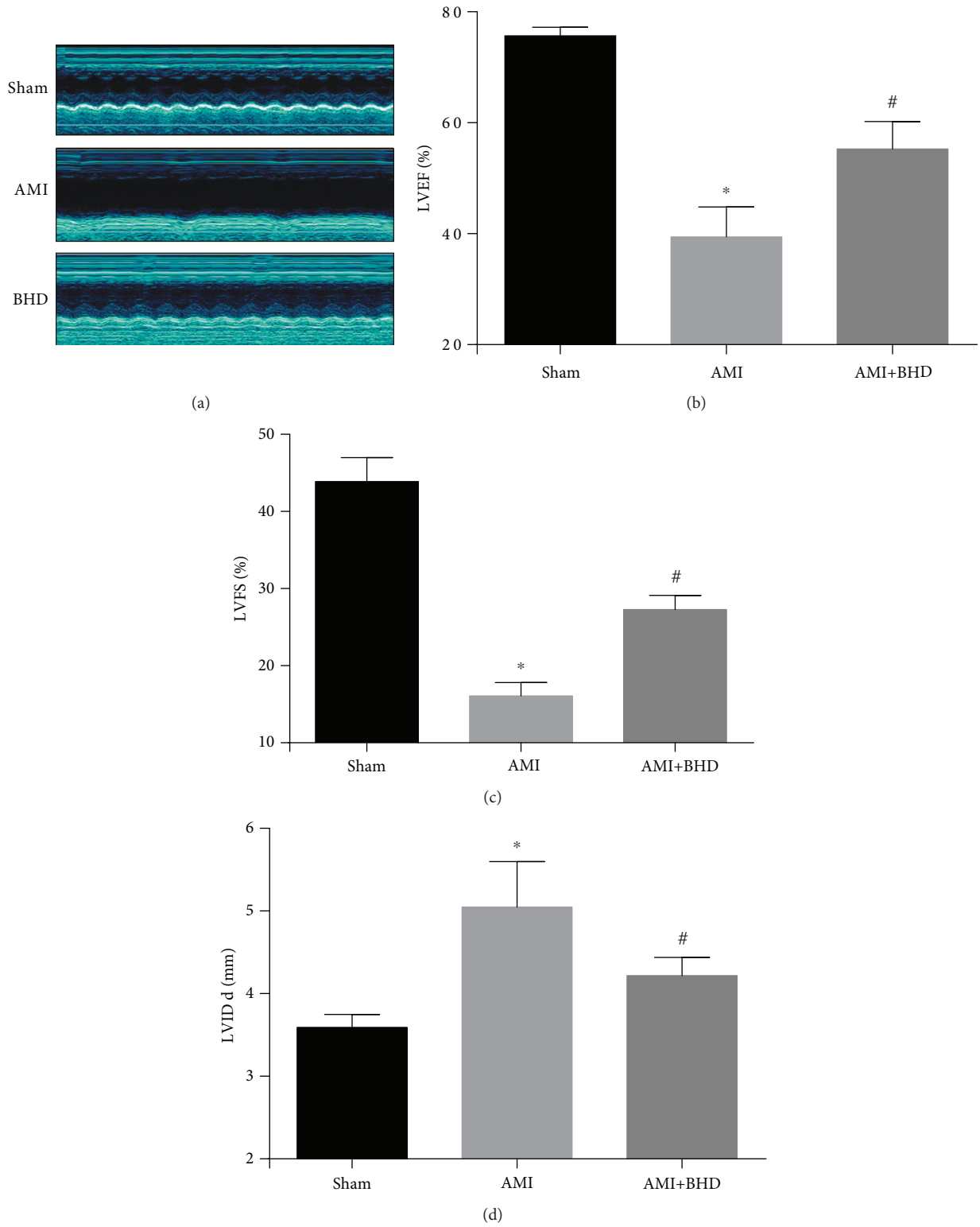

Figure 2: Continued.

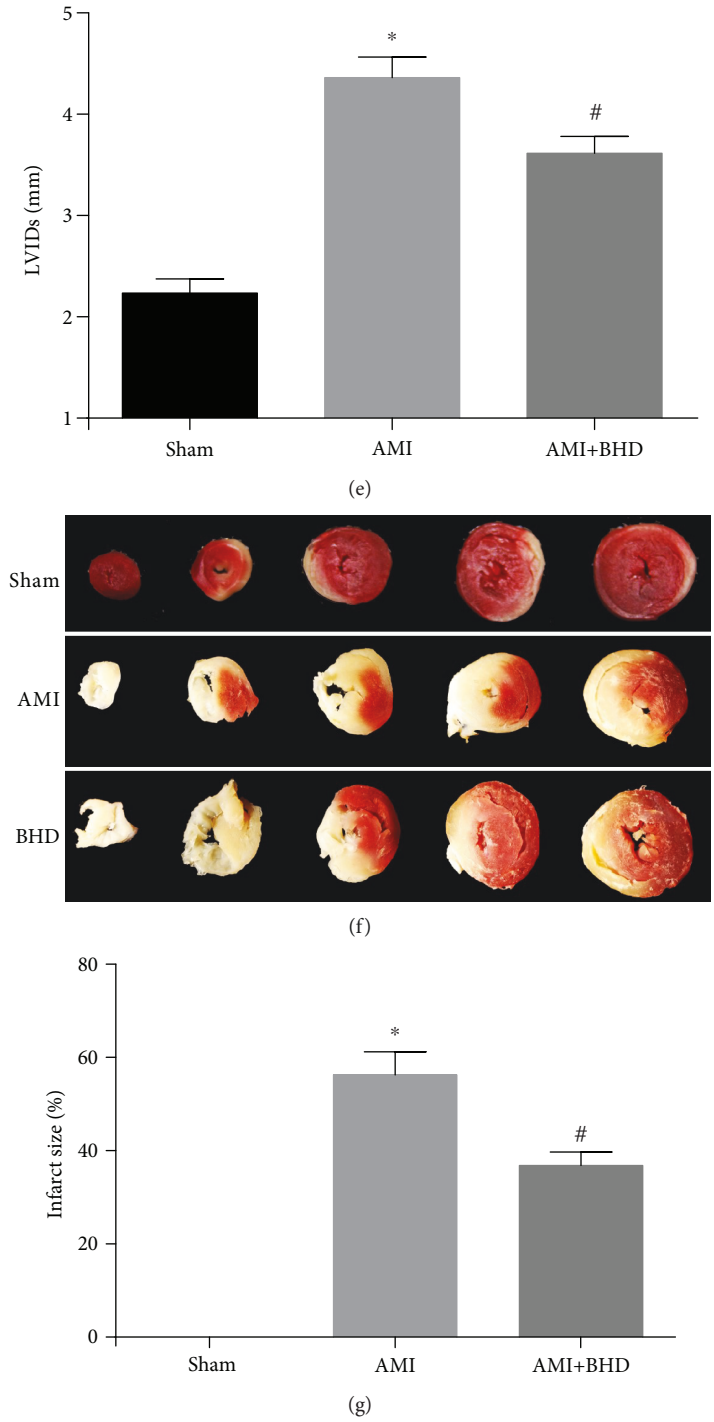

Figure 2: Cardiac function and infarct size at 14 days after AMI in mice. (a) M-mode echocardiographic images of the mice in each group. (b) The analysis of LVEF ($n = 6$). (c) The analysis of LVFS ($n = 6$). (d) The analysis of LVIDd ($n = 6$). (e) The analysis of LVIDs ($n = 6$). (f) Representative image of infarct size by cardiac 2,3,5-triphenyltetrazolium chloride (TTC) staining. (g) The analysis of the infarcted size (sham: $n = 5$, AMI: $n = 5$, and BHD+AMI: $n = 6$). $^{*}P < 0.05$, compared with the sham group; $^{\#}P < 0.05$, compared with the AMI group.

3. Result

3.1. Effect of BHD on the Survival Rate and the Heart Weight/Body Weight Ratio after AMI. After 14 days, all mice in the sham group survived, while the BHD-treated group exhibited a trend towards an improved overall survival rate after the induction of AMI, but differences did not reach statistical significance (log-rank: $P = 0.0829$, Figure 1(a)). The heart weight/body weight ratio was significantly decreased in the BHD-treated group compared with the AMI group ($P < 0.05$, Figure 1(b)).

3.2. Effect of BHD on Cardiac Function and Infarct Size after AMI. As shown by echocardiography images (Figure 2(a)),

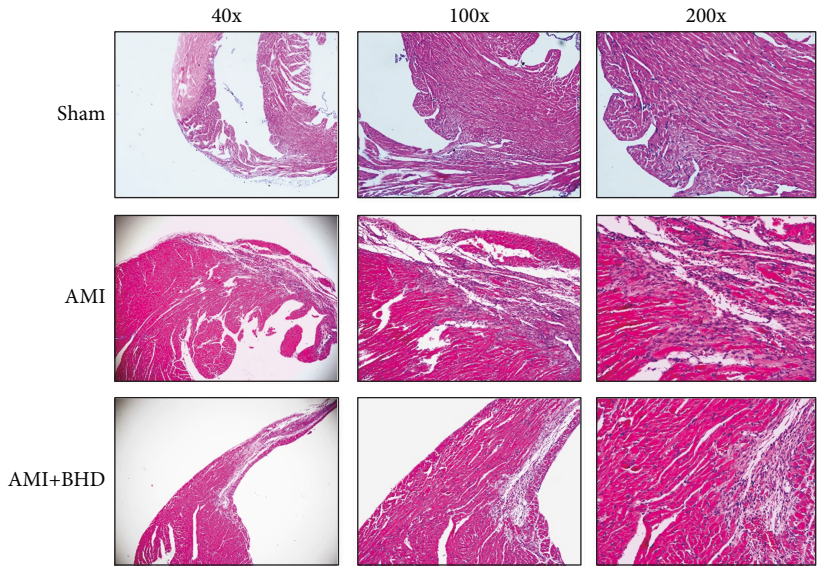

Figure 3: Histological changes in myocardial tissue at 14 days after AMI in mice (sham: $n = 4$, AMI: $n = 4$, and BHD+AMI: $n = 6$).

there was significant improvement of LVEF in the BHD-treated group (75.65 ± 0.64%) compared with the AMI group (39.40 ± 2.21%) at 14 days after AMI (Figure 2(b)). Significant improvements in cardiac function were also observed in LVFS, LVIDd, and LVIDs ($P < 0.05$). The infarct size in the AMI group was 56.20 ± 2.26% (Figures 2(g) and 2(h)). Compared with the AMI group, the infarct size (36.74 ± 1.22%) was markedly reduced in the BHD-treated group ($P < 0.05$).

3.3. Effect of BHD on Histological Changes and Fibrosis in Myocardial Tissue after AMI. By HE staining, the AMI group showed marked necrotic changes in myofibrils with severe infiltration of inflammation and interstitial edema (Figure 3). BHD-treated group exhibited only focal tissue necrosis, mild inflammatory infiltration, and interstitial edema (Figure 3). Compared with the AMI group, Mason staining of the collagen deposition area on myocardial fibrosis was significantly decreased in the BHD-treated group ($P < 0.05$, Figures 4(a) and 4(b)).

3.4. Effect of BHD on Angiogenesis after AMI. To verify whether myocardial protection of BHD is associated with angiogenesis in the infarction border zone, the immunohistochemical analysis was performed by CD31 staining. As shown in Figure 5(b), the density of microvessel in the BHD-treated group was much higher than that in the AMI group ($P < 0.05$).

3.5. Effect of BHD on Expression of Cav-1, VEGF, VEGFR2, and p-ERK in the Infarction Border Zone after AMI. Expression of Cav-1, VEGF, and VEGFR2 was elevated in the AMI group compared with the sham group ($P < 0.05$). Furthermore, the expression of Cav-1, VEGF, and VEGFR2 was further increased in the BHD-treated group compared with the AMI group ($P < 0.05$, Figures 6(a) and 6(b)). BHD treatment promoted the phosphorylation of ERK compared with the AMI group ($P < 0.05$, Figures 6(c) and 6(d)). Immunofluorescence indicated that the integrated optical density of Cav-1 (Figures 7(a) and 7(e)), VEGF (Figures 7(b) and 7(f)), VEGFR2 (Figures 7(c) and 7(g)), and p-ERK (Figures 7(d) and 7(h)) was significantly increased in the BHD-treated group compared with the AMI group ($P < 0.05$). RT-PCR showed that the mRNA level of Cav-1 (Figure 8(a)), VEGF (Figure 8(b)), and VEGFR2 (Figure 8(c)) in the BHD-treated group was significantly increased compared with the AMI group ($P < 0.05$).

4. Discussion

During AMI, the damage inflicted on the myocardium results in two processes: ischemia and the following reperfusion (I/R) [44]. The edema/sarcolemma rupture, calcium overload/hypercontracture, mitochondrial dysfunction, proteolysis (caspase, calpain), and apoptosis lead to a large amount of reduction of cardiomyocytes. And, the embolism, vasomotor disorder, leukocyte adherence/infiltration, stasis, and capillary rupture/hemorrhage appeared in coronary vascular caused severe myocardial injury [45]. Thus, cardiovascular protection drugs generally work through one or combined aspects of the above targets. In the present study, BHD reduced the myocardial fibrosis and inflammation, promoted angiogenesis in the infarction border zone via Cav-1/VEGF signaling pathway, then reduced the MI size, and improved the cardiac function. It may be because of these improvements that we finally observed a trend towards an improved overall survival rate of the BHD-treated group.

Cav-1 is a major component of the caveola membrane that is expressed in the majority of differentiated cells [46] and plays an important role in regulating the cellular signal transduction, endocytosis, transcytosis, and molecular transport [47]. The cardioprotective effects of Cav-1 in ischemic heart disease have been well reported [48] in both mouse and human specimens; an increase of Cav-1 in an infarcted

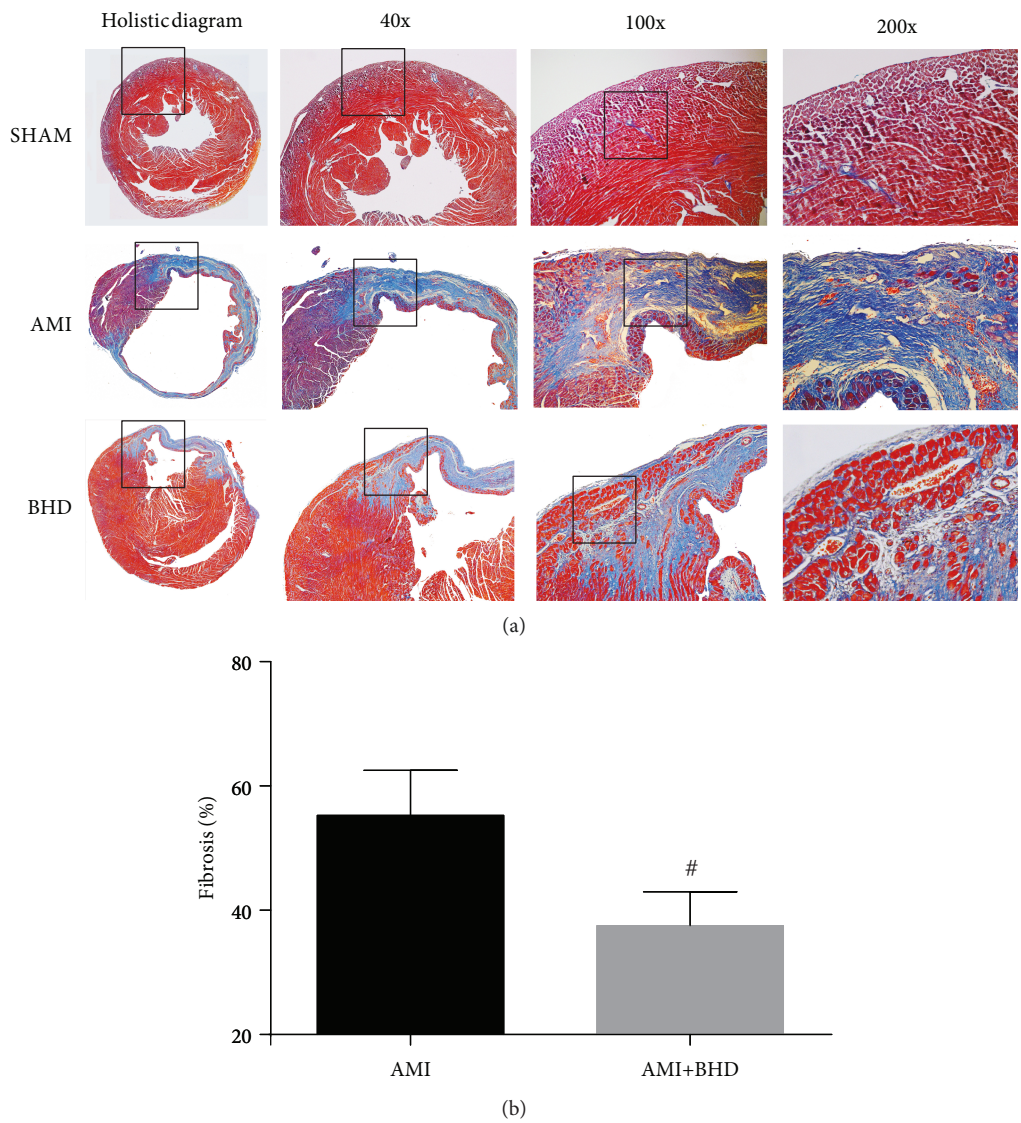

Figure 4: Fibrosis in myocardial tissue at 14 days after AMI in mice (mean ± SD; sham: $n = 4$, AMI: $n = 4$, and BHD+AMI: $n = 6$). (a) Representative images of Masson's trichrome staining. (b) Quantitative analysis of the collagen deposition area. $^{\#}P < 0.05$, compared with the AMI group.

area was detected in the early stage of MI [38]. Several studies have shown that the activation or preservation of Cav-1 played a protective role in myocardial I/R injury [49–51]. Subsequently, compared with the wild-type mice, Cav-1$^{-/-}$ mice showed a more severe cardiac dysfunction and a lower survival rate after MI [52]. In Cav-1$^{-/-}$ mice, a low-intensity pulsed ultrasound, which is a potential cardiac protection strategy, presented absent cardioprotective effects after myocardial ischemic injury [38]. Cav-1 is also a vital regulator of vascular endothelial homeostasis which controls angiogenesis and vessel function [53]. The adverse influence on angiogenesis after Cav-1 knockout has been confirmed in multiple disease models, including hindlimb ischemia [54], scleroderma fibroblasts [55], colitis [39], AMI [38], and cerebral ischemia [56]. In the present study, BHD increased angiogenesis and the expression of Cav-1 in the infarction border zone, suggesting that the cardioprotective effect of BHD targeted angiogenesis by Cav-1.

Previous studies also indicated that Cav-1 could reduce infarct volume and promote angiogenesis through the VEGF signaling pathway [57, 58]. Recent studies showed that the expression of Cav-1 and VEGF was significantly decreased after the use of the caveolin-1 inhibitor, resulted in increase in neurological deficit and infarction volume [59–61]. Other studies also confirmed this phenomenon at the genetic level. The ablation of Cav-1 gene in mice could result in an impairment in angiogenesis and reduction of VEGF expression [56, 62]. VEGF is a pivotal regulator of blood vessel formation during embryogenesis and angiogenesis [63]. Lots of evidences have shown that VEGF, through combining with its receptor VEGFR2, could trigger multiple downstream signals such as p-ERK, thereby promoting angiogenesis [64–66]. Taken together, these results indicate that Cav-1 could promote angiogenesis by upregulating the VEGF signaling pathway. The present study indicated that BHD increased the CAV-1, VEGF, VEGFR2, and p-ERK in the infarction border

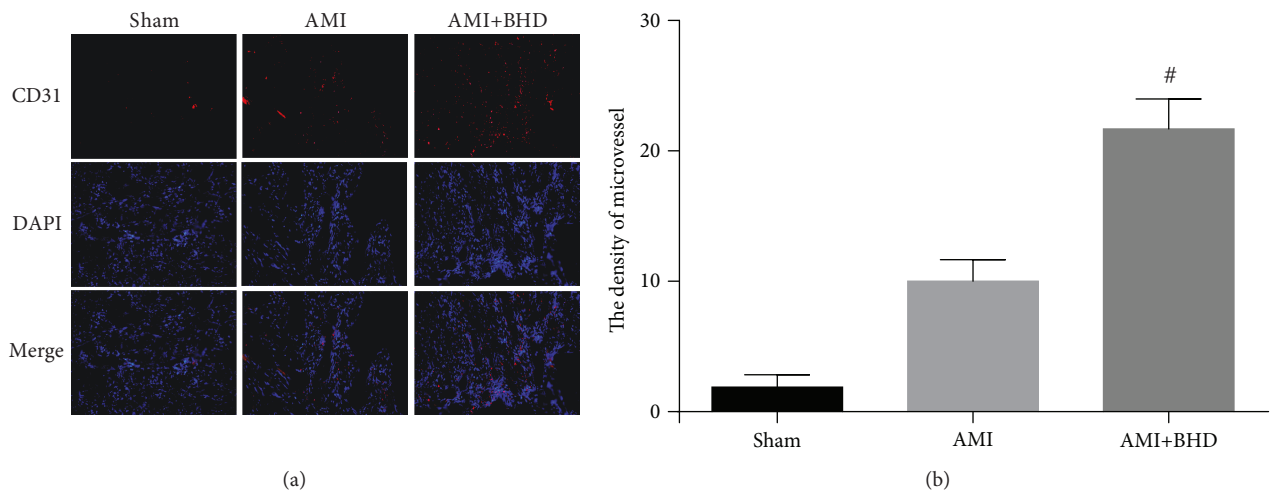

Figure 5: Density of microvessel in the infarction border zone at 14 days after AMI in mice (mean ± SD; sham: $n = 4$, AMI: $n = 4$, and BHD +AMI: $n = 6$). (a) Representative images of CD31 staining. (b) Quantitative analysis of the density of microvessel. $^{\#}P < 0.05$, compared with the AMI group.

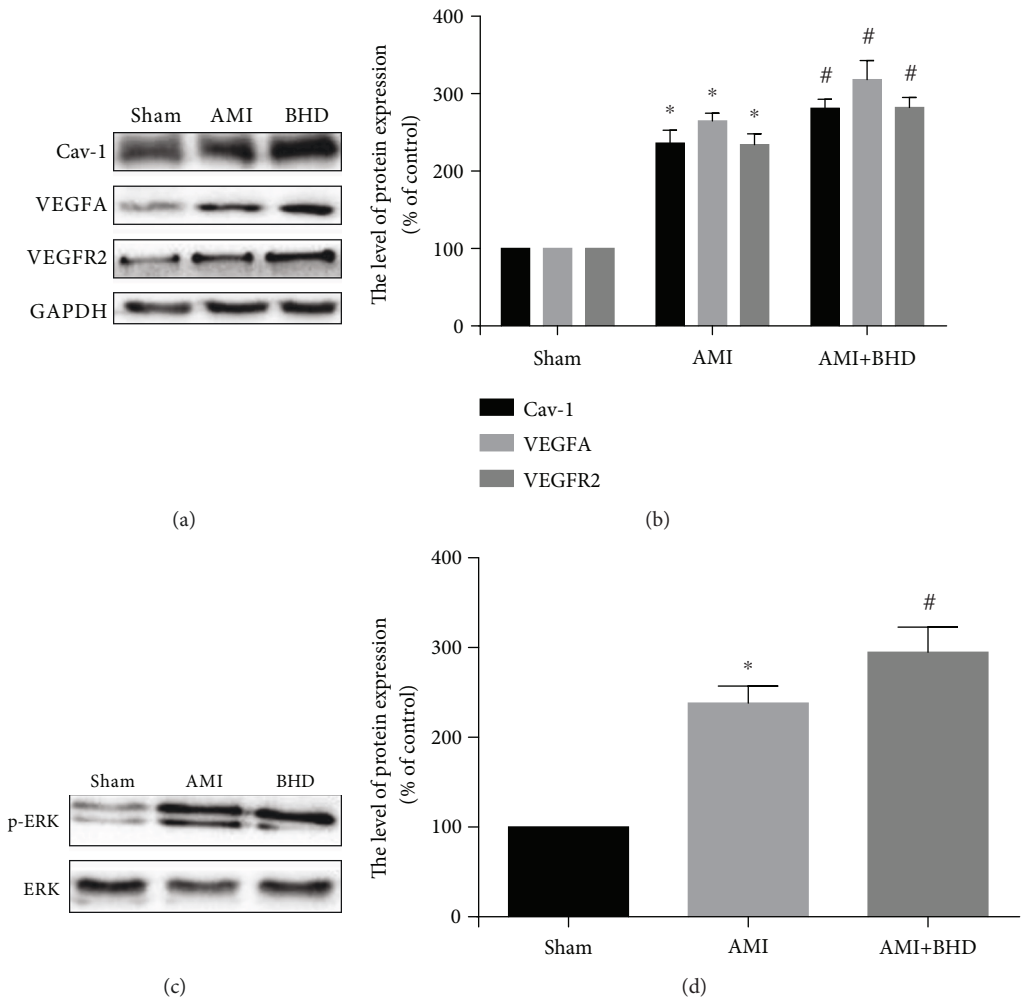

Figure 6: Western blot analysis of Cav-1, VEGF, VEGFR2, and p-ERK1/2 expression in the infarction border zone at 14 days after AMI in mice (mean ± SD, $n = 6$). (a) Western blot analysis of the expression of Cav-1, VEGF, and VEGFR2. (b) Quantitative analysis for the western blot results of Cav-1, VEGF, and VEGFR2. (c) Western blot analysis of the expression of p-ERK1/2. (d) Quantitative analysis for the western blot results of p-ERK1/2. $^{*}P < 0.05$, compared with the sham group; $^{\#}P < 0.05$, compared with the AMI group.

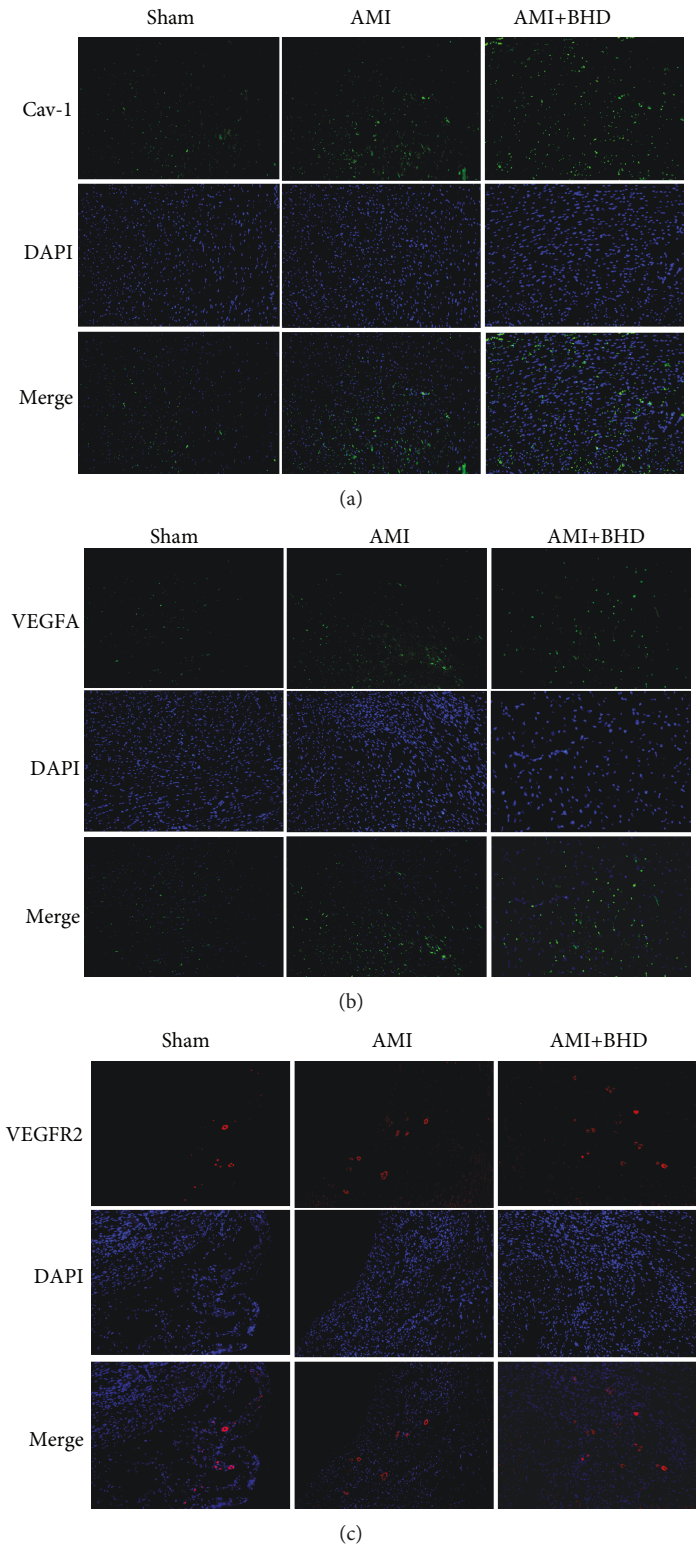

Figure 7: Continued.

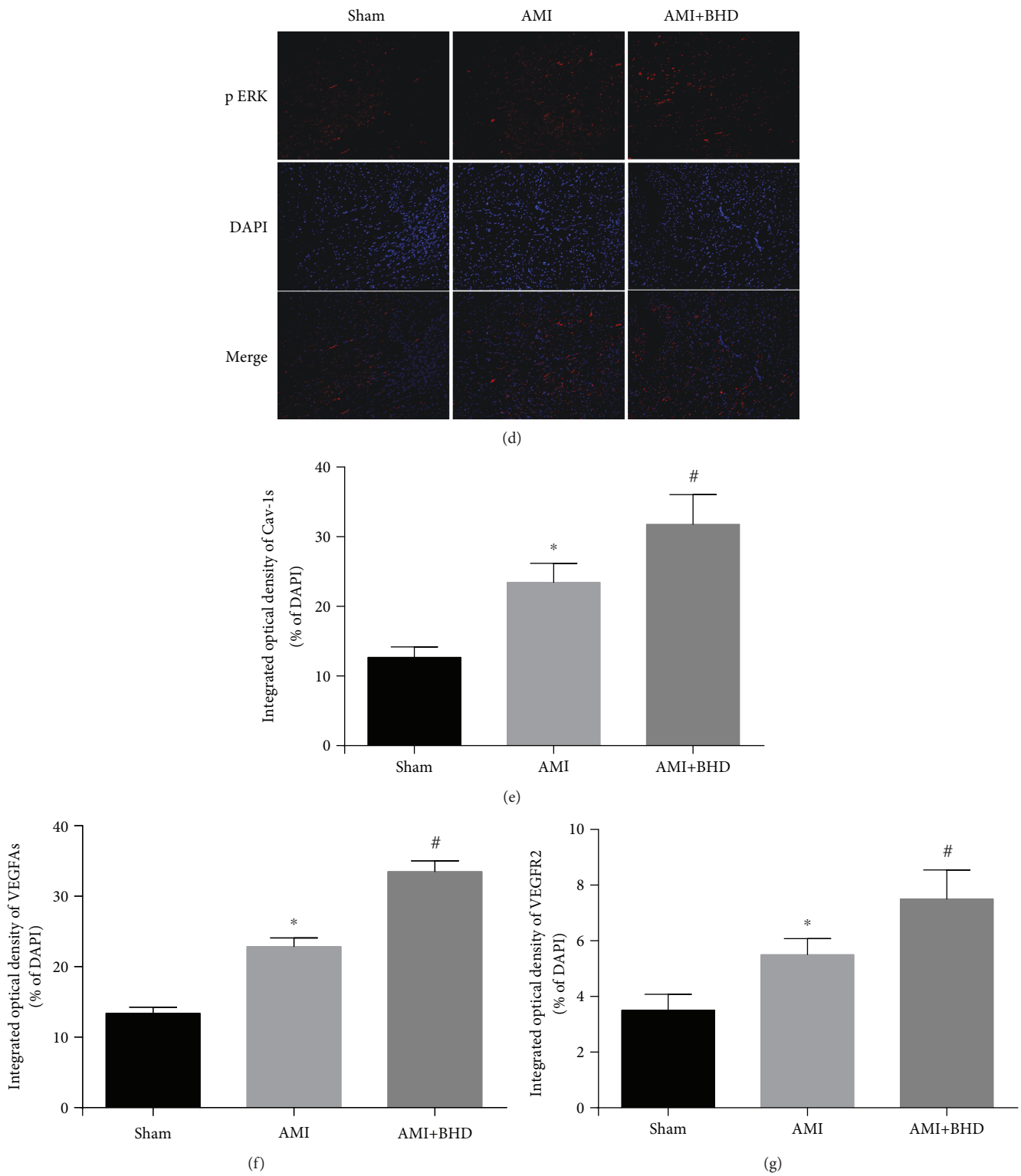

Figure 7: Continued.

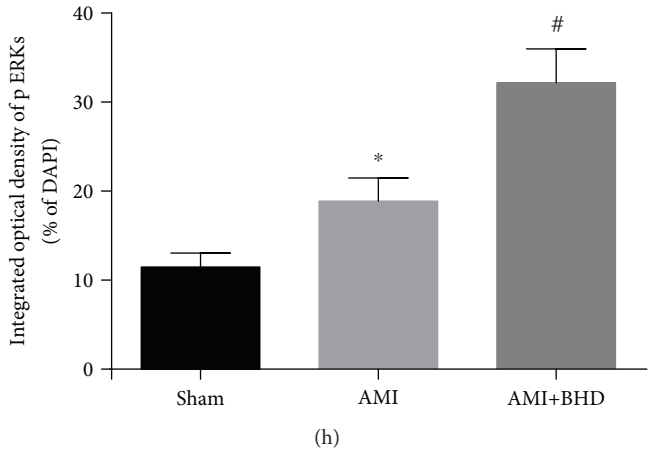

Figure 7: Immunofluorescence staining of Cav-1, VEGF, VEGFR2, and p-ERK1/2 in the infarction border zone at 14 days after AMI in mice (mean ± SD; sham: $n = 4$, AMI: $n = 4$, and BHD+AMI: $n = 6$). (a) Immunofluorescence staining of Cav-1. (b) Immunofluorescence staining of VEGF. (c) Immunofluorescence staining of VEGFR2. (d) Immunofluorescence staining of p-ERK1/2. (e) Quantitative analysis of Cav-1. (f) Quantitative analysis of VEGF. (g) Quantitative analysis of VEGFR2. (h) Quantitative analysis of p-ERK1/2. $^{*}P < 0.05$, compared with the sham group; $^{\#}P < 0.05$, compared with the AMI group.

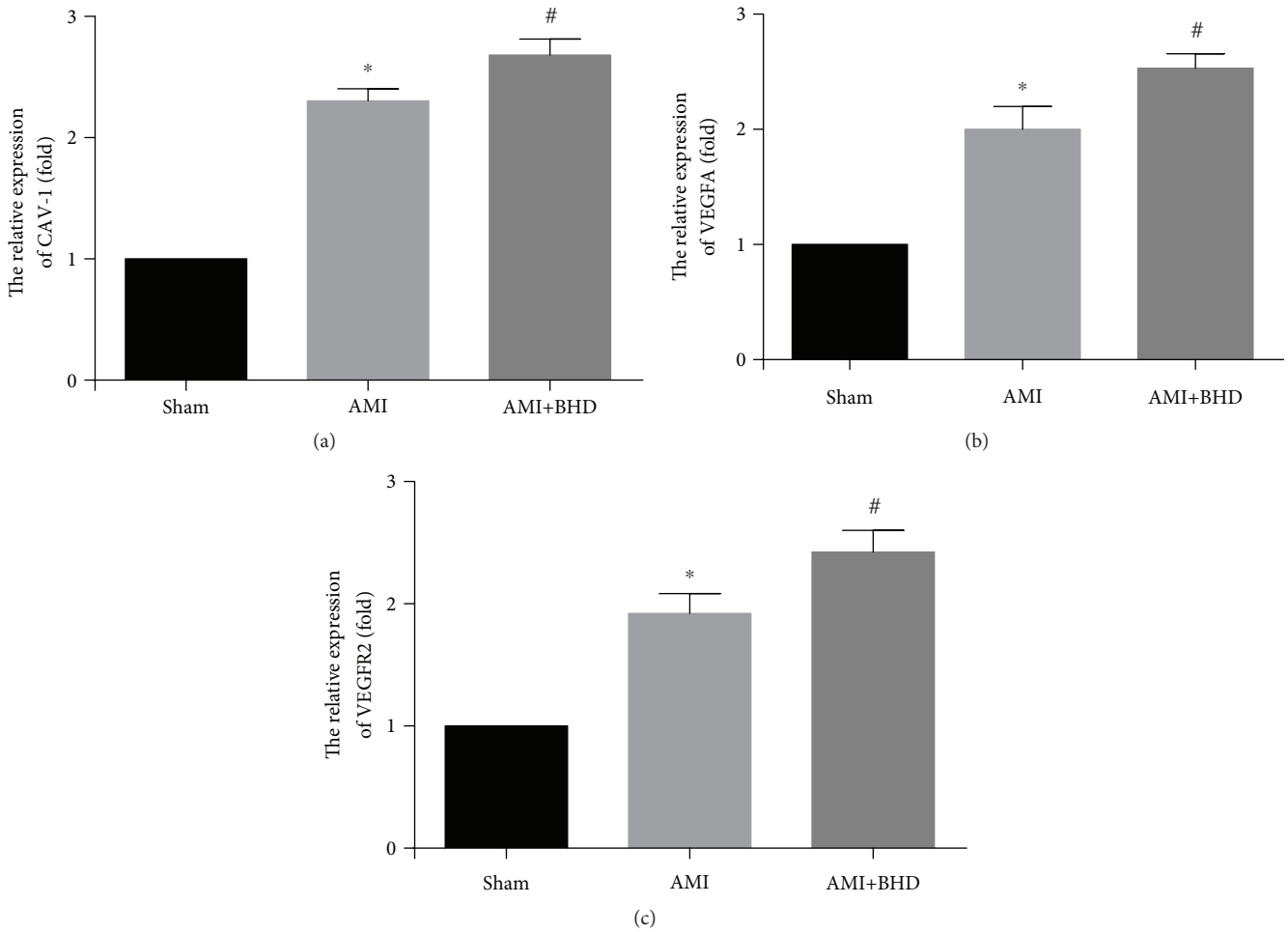

Figure 8: The mRNA expression of Cav-1, VEGF, and VEGFR2 at 14 days after AMI in mice (mean ± SD, $n = 6$). (a) The mRNA expression of Cav-1. (b) The mRNA expression of VEGF. (c) The mRNA expression of VEGFR2. $^{*}P < 0.05$, compared with the sham group; $^{\#}P < 0.05$, compared with the AMI group.

zone, suggesting that BHD could promote angiogenesis through the Cav-1/VEGF pathway.

Herbal formulae, with multicomponents and multitargets, may potentially satisfy the demands of complex disease treatment in an integrated manner. Furthermore, investigation on new molecular targets and principles indicated that a single angiogenic substance might be insufficient for inducing therapeutic angiogenesis [67]. Hundreds of constituents have been identified in BHD such as polysaccharides, astragalosides, and isoflavonoids in radix astragali seuhedysari [68], as well as phthalides and phenolic acids in radix angelicae sinensis and rhizoma ligustici chuanxiong, etc. [69, 70]. Network pharmacology can forecast multiple targets and pathways affected by the active components in TCM formulae. Among them, key targets/signaling pathways might be selected and should be experimentally validated.

5. Conclusion

The present study demonstrated that BHD could exert cardioprotective effects on the mouse model with AMI through targeting angiogenesis via Cav-1/VEGF signaling pathway.

Data Availability

The data used to support the findings of this study are available from the corresponding author upon request.

Conflicts of Interest

The authors declare that they have no conflicts of interest.

Authors' Contributions

JZZ and XYB contributed equally to this work. JZZ, XYB, QZ, QT, PCZ, ZZ, and YW designed the study; JZZ and XYB performed the experiments. QZ, QT, PCZ, and ZZ analyzed the data; JZZ, XYB, and QZ wrote the manuscript. Jia-Zhen Zhu and Xiao-Yi Bao contributed equally to this work.

Acknowledgments

This work was supported by the grant of the National Natural Science Foundation of China (81473491/81573750/81173395/H2902).

References

[1] K. Thygesen, J. S. Alpert, A. S. Jaffe et al., "Fourth universal definition of myocardial infarction," *Journal of the American College of Cardiology*, vol. S0735-1097, no. 18, pp. 36941–36949, 2018.

[2] E. J. Benjamin, M. J. Blaha, S. E. Chiuve et al., "Heart disease and stroke statistics-2017 update: a report from the American Heart Association," *Circulation*, vol. 135, no. 10, pp. e146–e603, 2017.

[3] G. W. Reed, J. E. Rossi, and C. P. Cannon, "Acute myocardial infarction," *Lancet*, vol. 389, no. 10065, pp. 197–210, 2017.

[4] B. Ibanez, S. James, S. Agewall et al., "ESC guidelines for the management of acute myocardial infarction in patients presenting with ST-segment elevation: the task force for the management of acute myocardial infarction in patients presenting with ST-segment elevation of the European Society of Cardiology (ESC)," *European Heart Journal*, vol. 39, no. 2, pp. 119–177, 2018.

[5] A. Birbrair, T. Zhang, Z. M. Wang et al., "Type-2 pericytes participate in normal and tumoral angiogenesis," *American Journal of Physiology-Cell Physiology*, vol. 307, no. 1, pp. C25–C38, 2014.

[6] Q. Lu, Y. Yao, Z. Hu et al., "Angiogenic factor AGGF1 activates autophagy with an essential role in therapeutic angiogenesis for heart disease," *PLOS Biology*, vol. 14, no. 8, article e1002529, 2016.

[7] K. Albrecht-Schgoer, W. Schgoer, J. Holfeld et al., "The angiogenic factor secretoneurin induces coronary angiogenesis in a model of myocardial infarction by stimulation of vascular endothelial growth factor signaling in endothelial cells," *Circulation*, vol. 126, no. 21, pp. 2491–2501, 2012.

[8] S. Araki, Y. Izumiya, S. Hanatani et al., "Akt1-mediated skeletal muscle growth attenuates cardiac dysfunction and remodeling after experimental myocardial infarction," *Circulation Heart Failure*, vol. 5, no. 1, pp. 116–125, 2012.

[9] R. Kornowski, "Therapeutic angiogenesis revisited," *Catheterization and Cardiovascular Interventions*, vol. 82, no. 6, pp. 907-908, 2013.

[10] D. Guo, C. E. Murdoch, T. Liu et al., "Therapeutic angiogenesis of Chinese herbal medicines in ischemic heart disease: a review," *Frontiers in Pharmacology*, vol. 9, p. 428, 2018.

[11] L. J. Yu, K. J. Zhang, J. Z. Zhu et al., "Salvianolic acid exerts cardioprotection through promoting angiogenesis in animal models of acute myocardial infarction: preclinical evidence," *Oxidative Medicine and Cellular Longevity*, vol. 2017, Article ID 8192383, 11 pages, 2017.

[12] K. J. Zhang, J. Z. Zhu, X. Y. Bao, Q. Zheng, G. Q. Zheng, and Y. Wang, "Shexiang baoxin pills for coronary heart disease in animal models: preclinical evidence and promoting angiogenesis mechanism," *Front Pharmacol*, vol. 8, p. 404, 2017.

[13] Q. R. Wang, *Yilin Gaicuo (Correction on Errors in Medical Classics)*, People's Medical Publishing House, Beijing, China, 2005.

[14] G. Cai, B. Liu, W. Liu et al., "Buyang Huanwu Decoction can improve recovery of neurological function, reduce infarction volume, stimulate neural proliferation and modulate VEGF and Flk1 expressions in transient focal cerebral ischaemic rat brains," *Journal of Ethnopharmacology*, vol. 113, no. 2, pp. 292–299, 2007.

[15] L. S. Chu, Y. J. Yin, Q. Ke, W. Chen, and F. Chen, "Effect of buyanghuanwu decoction on angiogenesis and Ang-1/Tie-2 expression after focal cerebral ischemia in mice," *Chinese Journal of Behavioral Medicine and Brain Science*, vol. 20, no. 3, pp. 202–204, 2011.

[16] G. Cai and B. Liu, "Buyang Huanwu Decoction increases vascular endothelial growth factor expression and promotes angiogenesis in a rat model of local cerebral ischemia," *Neural Regeneration Research*, vol. 5, no. 22, pp. 1733–1738, 2010.

[17] C. Z. Hao, F. Wu, J. Shen et al., "Clinical efficacy and safety of buyang huanwu decoction for acute ischemic stroke: a systematic review and meta-analysis of 19 randomized controlled trials," *Evidence-based Complementary and Alternative Medicine*, vol. 2012, Article ID 630124, 10 pages, 2012.

[18] Y. Liu, R. Lin, X. Shi et al., "The roles of buyang huanwu decoction in anti-inflammation, antioxidation and regulation of lipid metabolism in rats with myocardial ischemia," *Evidence-based Complementary and Alternative Medicine*, vol. 2011, Article ID 561396, 8 pages, 2011.

[19] W. R. Wang, R. Lin, H. Zhang et al., "The effects of Buyang Huanwu Decoction on hemorheological disorders and energy metabolism in rats with coronary heart disease," *Journal of Ethnopharmacology*, vol. 137, no. 1, pp. 214–220, 2011.

[20] G. Yang, Z. Fang, Y. Liu et al., "Protective effects of Chinese traditional medicine buyang huanwu decoction on myocardial injury," *Evidence-based Complementary and Alternative Medicine*, vol. 2011, Article ID 930324, 7 pages, 2011.

[21] H. Zhang, W. R. Wang, R. Lin et al., "Buyang Huanwu decoction ameliorates coronary heart disease with Qi deficiency and blood stasis syndrome by reducing CRP and CD40 in rats," *Journal of Ethnopharmacology*, vol. 130, no. 1, pp. 98–102, 2010.

[22] Y. C. Zhou, B. Liu, Y. J. Li et al., "Effects of buyang huanwu decoction on ventricular remodeling and differential protein profile in a rat model of myocardial infarction," *Evidence-based Complementary and Alternative Medicine*, vol. 2012, Article ID 385247, 11 pages, 2012.

[23] H. Cui, T. Liu, P. Li et al., "An intersectional study of LncRNAs and mRNAs reveals the potential therapeutic targets of buyang huanwu decoction in experimental intracerebral hemorrhage," *Cellular Physiology and Biochemistry*, vol. 46, no. 5, pp. 2173–2186, 2018.

[24] J. Shen, Y. Zhu, K. Huang et al., "Buyang Huanwu Decoction attenuates H_2O_2-induced apoptosis by inhibiting reactive oxygen species-mediated mitochondrial dysfunction pathway in human umbilical vein endothelial cells," *BMC Complementary and Alternative Medicine*, vol. 16, no. 1, p. 154, 2016.

[25] H. W. Wang, K. T. Liou, Y. H. Wang et al., "Deciphering the neuroprotective mechanisms of Bu-yang Huan-wu decoction by an integrative neurofunctional and genomic approach in ischemic stroke mice," *Journal of Ethnopharmacology*, vol. 138, no. 1, pp. 22–33, 2011.

[26] L. Fan, K. Wang, and B. Cheng, "Effects of buyang huanwu decoction on apoptosis of nervous cells and expressions of Bcl-2 and bax in the spinal cord of ischemia-reperfusion injury in rabbits," *Journal of Traditional Chinese Medicine*, vol. 26, no. 2, pp. 153–156, 2006.

[27] B. Dou, W. Zhou, S. Li et al., "Buyang huanwu decoction attenuates infiltration of natural killer cells and protects against ischemic brain injury," *Cellular Physiology and Biochemistry*, vol. 50, no. 4, pp. 1286–1300, 2018.

[28] J. H. Li, A. J. Liu, H. Q. Li, Y. Wang, H. C. Shang, and G. Q. Zheng, "Buyang huanwu decoction for healthcare: evidence-based theoretical interpretations of treating different diseases with the same method and target of vascularity," *Evidence-based Complementary and Alternative Medicine*, vol. 2014, Article ID 506783, 17 pages, 2014.

[29] Z. Q. Zhang, T. Tang, J. K. Luo et al., "Effect of qi-tonifying and stasis-eliminating therapy on expression of vascular endothelial growth factor and its receptors Flt-1, Flk-1 in the brain of intracerebral hemorrhagic rats," *Chinese Journal of Integrative Medicine*, vol. 13, no. 4, pp. 285–290, 2007.

[30] J. Yang, F. Gao, Y. Zhang, Y. Liu, and D. Zhang, "Buyang huanwu decoction (BYHWD) enhances angiogenic effect of mesenchymal stem cell by upregulating VEGF expression after focal cerebral ischemia," *Journal of Molecular Neuroscience*, vol. 56, no. 4, pp. 898–906, 2015.

[31] H. J. Cui, A. L. Yang, H. J. Zhou et al., "Buyang huanwu decoction promotes angiogenesis via vascular endothelial growth factor receptor-2 activation through the PI3K/Akt pathway in a mouse model of intracerebral hemorrhage," *BMC Complementary and Alternative Medicine*, vol. 15, no. 1, p. 91, 2015.

[32] F. Liao, Y. Meng, H. Zheng et al., "Biospecific isolation and characterization of angiogenesis-promoting ingredients in Buyang Huanwu decoction using affinity chromatography on rat brain microvascular endothelial cells combined with solid-phase extraction, and HPLC-MS/MS," *Talanta*, vol. 179, pp. 490–500, 2018.

[33] R. L. Wei, H. J. Teng, B. Yin et al., "A systematic review and meta-analysis of buyang huanwu decoction in animal model of focal cerebral ischemia," *Evidence-based Complementary and Alternative Medicine*, vol. 2013, Article ID 138484, 13 pages, 2013.

[34] Q. Guo, M. Zhong, H. Xu, X. Mao, Y. Zhang, and N. Lin, "A systems biology perspective on the molecular mechanisms underlying the therapeutic effects of buyang huanwu decoction on ischemic stroke," *Rejuvenation Research*, vol. 18, no. 4, pp. 313–325, 2015.

[35] D. Gvaramia, M. E. Blaauboer, R. Hanemaaijer, and V. Everts, "Role of caveolin-1 in fibrotic diseases," *Matrix Biology*, vol. 32, no. 6, pp. 307–315, 2013.

[36] S. G. Royce and C. J. Le Saux, "Role of caveolin-1 in asthma and chronic inflammatory respiratory diseases," *Expert Review of Respiratory Medicine*, vol. 8, no. 3, pp. 339–347, 2014.

[37] Z. C. Nwosu, M. P. Ebert, S. Dooley, and C. Meyer, "Caveolin-1 in the regulation of cell metabolism: a cancer perspective," *Molecular Cancer*, vol. 15, no. 1, p. 71, 2016.

[38] T. Shindo, K. Ito, T. Ogata et al., "Low-intensity pulsed ultrasound enhances angiogenesis and ameliorates left ventricular dysfunction in a mouse model of acute myocardial infarction," *Arteriosclerosis, Thrombosis, and Vascular Biology*, vol. 36, no. 6, pp. 1220–1229, 2016.

[39] J. H. Chidlow Jr, J. J. M. Greer, C. Anthoni et al., "Endothelial caveolin-1 regulates pathologic angiogenesis in a mouse model of colitis," *Gastroenterology*, vol. 136, no. 2, pp. 575–84.e2, 2009.

[40] S. E. Woodman, A. W. Ashton, W. Schubert et al., "Caveolin-1 knockout mice show an impaired angiogenic response to exogenous stimuli," *The American Journal of Pathology*, vol. 162, no. 6, pp. 2059–2068, 2003.

[41] S. A. Tahir, S. Park, and T. C. Thompson, "Caveolin-1 regulates VEGF-stimulated angiogenic activities in prostate cancer and endothelial cells," *Cancer Biology & Therapy*, vol. 8, no. 23, pp. 2286–2296, 2009.

[42] S. V. Penumathsa, S. Koneru, S. M. Samuel et al., "Strategic targets to induce neovascularization by resveratrol in hypercholesterolemic rat myocardium: role of caveolin-1, endothelial nitric oxide synthase, hemeoxygenase-1, and vascular endothelial growth factor," *Free Radical Biology & Medicine*, vol. 45, no. 7, pp. 1027–1034, 2008.

[43] E. Gao, Y. H. Lei, X. Shang et al., "A novel and efficient model of coronary artery ligation and myocardial infarction in the mouse," *Circulation Research*, vol. 107, no. 12, pp. 1445–1453, 2010.

[44] B. Ibáñez, G. Heusch, M. Ovize, and F. van de Werf, "Evolving therapies for myocardial ischemia/reperfusion injury," *Journal*

of the American College of Cardiology, vol. 65, no. 14, pp. 1454–1471, 2015.

[45] G. Heusch and B. J. Gersh, "The pathophysiology of acute myocardial infarction and strategies of protection beyond reperfusion: a continual challenge," *European Heart Journal*, vol. 38, no. 11, pp. 774–784, 2017.

[46] C. M. Thomas and E. J. Smart, "Caveolae structure and function," *Journal of Cellular and Molecular Medicine*, vol. 12, no. 3, pp. 796–809, 2008.

[47] P. W. Shaul and R. G. W. Anderson, "Role of plasmalemmal caveolae in signal transduction," *American Journal of Physiology-Lung Cellular and Molecular Physiology*, vol. 275, no. 5, pp. L843–L851, 1998.

[48] Y. Yang, Z. Ma, W. Hu et al., "Caveolin-1/-3: therapeutic targets for myocardial ischemia/reperfusion injury," *Basic Research in Cardiology*, vol. 111, no. 4, p. 45, 2016.

[49] K. R. Chaudhary, W. J. Cho, F. Yang et al., "Effect of ischemia reperfusion injury and epoxyeicosatrienoic acids on caveolin expression in mouse myocardium," *Journal of Cardiovascular Pharmacology*, vol. 61, no. 3, pp. 258–263, 2013.

[50] L. H. Young, Y. Ikeda, and A. M. Lefer, "Caveolin-1 peptide exerts cardioprotective effects in myocardial ischemia-reperfusion via nitric oxide mechanism," *American Journal of Physiology-Heart and Circulatory Physiology*, vol. 280, no. 6, pp. H2489–H2495, 2001.

[51] T. Murata, M. I. Lin, Y. Huang et al., "Reexpression of caveolin-1 in endothelium rescues the vascular, cardiac, and pulmonary defects in global caveolin-1 knockout mice," *The Journal of Experimental Medicine*, vol. 204, no. 10, pp. 2373–2382, 2007.

[52] J. F. Jasmin, G. Rengo, A. Lymperopoulos et al., "Caveolin-1 deficiency exacerbates cardiac dysfunction and reduces survival in mice with myocardial infarction," *American Journal of Physiology-Heart and Circulatory Physiology*, vol. 300, no. 4, pp. H1274–H1281, 2011.

[53] F. Braet, "Rac1, caveolin-1 and vascular endothelial growth factor-mediated liver sinusoidal endothelial cell angiogenesis," *Liver International*, vol. 29, no. 2, pp. 143-144, 2009.

[54] P. Sonveaux, P. Martinive, J. DeWever et al., "Caveolin-1 expression is critical for vascular endothelial growth factor-induced ischemic hindlimb collateralization and nitric oxide-mediated angiogenesis," *Circulation Research*, vol. 95, no. 2, pp. 154–161, 2004.

[55] V. Liakouli, J. Elies, Y. M. el-Sherbiny et al., "Scleroderma fibroblasts suppress angiogenesis via TGF-β/caveolin-1 dependent secretion of pigment epithelium-derived factor," *Annals of the Rheumatic Diseases*, vol. 77, no. 3, pp. 431–440, 2018.

[56] J.-F. Jasmin, S. Malhotra, M. Singh Dhallu, I. Mercier, D. M. Rosenbaum, and M. P. Lisanti, "Caveolin-1 deficiency increases cerebral ischemic injury," *Circulation Research*, vol. 100, no. 5, pp. 721–729, 2007.

[57] Y. Gao, Y. Zhao, J. Pan et al., "Treadmill exercise promotes angiogenesis in the ischemic penumbra of rat brains through caveolin-1/VEGF signaling pathways," *Brain Research*, vol. 1585, pp. 83–90, 2014.

[58] Q. Pang, H. Zhang, Z. Chen et al., "Role of caveolin-1/vascular endothelial growth factor pathway in basic fibroblast growth factor-induced angiogenesis and neurogenesis after treadmill training following focal cerebral ischemia in rats," *Brain Research*, vol. 1663, pp. 9–19, 2017.

[59] M. Liu, Y. Wu, Y. Liu et al., "Basic fibroblast growth factor protects astrocytes against ischemia/reperfusion injury by upregulating the caveolin-1/VEGF signaling pathway," *Journal of Molecular Neuroscience*, vol. 64, no. 2, pp. 211–223, 2018.

[60] Q. Xie, J. Cheng, G. Pan et al., "Treadmill exercise ameliorates focal cerebral ischemia/reperfusion-induced neurological deficit by promoting dendritic modification and synaptic plasticity via upregulating caveolin-1/VEGF signaling pathways," *Experimental Neurology*, vol. 313, pp. 60–78, 2019.

[61] Z. Chen, Q. Hu, Q. Xie et al., "Effects of treadmill exercise on motor and cognitive function recovery of MCAO mice through the caveolin-1/VEGF signaling pathway in ischemic penumbra," *Neurochemical Research*, vol. 44, no. 4, pp. 930–946, 2019.

[62] J. H. Chidlow Jr and W. C. Sessa, "Caveolae, caveolins, and cavins: complex control of cellular signalling and inflammation," *Cardiovascular Research*, vol. 86, no. 2, pp. 219–225, 2010.

[63] S. Dehghani, R. Nosrati, M. Yousefi et al., "Aptamer-based biosensors and nanosensors for the detection of vascular endothelial growth factor (VEGF): a review," *Biosensors and Bioelectronics*, vol. 110, pp. 23–37, 2018.

[64] S. Ikeda, M. Ushio-Fukai, L. Zuo et al., "Novel role of ARF6 in vascular endothelial growth factor-induced signaling and angiogenesis," *Circulation Research*, vol. 96, no. 4, pp. 467–475, 2005.

[65] J. Oshikawa, S. J. Kim, E. Furuta et al., "Novel role of p66Shc in ROS-dependent VEGF signaling and angiogenesis in endothelial cells," *American Journal of Physiology. Heart and Circulatory Physiology*, vol. 302, no. 3, pp. H724–H732, 2012.

[66] M. Simons, E. Gordon, and L. Claesson-Welsh, "Mechanisms and regulation of endothelial VEGF receptor signalling," *Nature Reviews Molecular Cell Biology*, vol. 17, no. 10, pp. 611–625, 2016.

[67] P. Carmeliet and R. K. Jain, "Molecular mechanisms and clinical applications of angiogenesis," *Nature*, vol. 473, no. 7347, pp. 298–307, 2011.

[68] C. Chu, L. W. Qi, E. H. Liu, B. Li, W. Gao, and P. Li, "Radix Astragali (Astragalus): latest advancements and trends in chemistry, analysis, pharmacology and pharmacokinetics," *Current Organic Chemistry*, vol. 14, no. 16, pp. 1792–1807, 2010.

[69] X. Ran, L. Ma, C. Peng, H. Zhang, and L. P. Qin, "*Ligusticum chuanxiong* Hort: a review of chemistry and pharmacology," *Pharmaceutical Biology*, vol. 49, no. 11, pp. 1180–1189, 2011.

[70] X. D. Liu, W. D. Li, and B. C. Cai, "Advances in research of chemical constituents and the pharmacological activities on cardio- and cerebro-vascular systems of *Angelicae Sinensis* Radix," *Journal of Nanjing Traditional Chinese Medicine University*, vol. 26, pp. 155–157, 2010.

Hindawi
Oxidative Medicine and Cellular Longevity
Volume 2019, Article ID 7658052, 11 pages
https://doi.org/10.1155/2019/7658052

Clinical Study

Chitosan Oligosaccharides Show Protective Effects in Coronary Heart Disease by Improving Antioxidant Capacity via the Increase in Intestinal Probiotics

Tiechao Jiang,[1,2] Xiaohong Xing,[1] Lirong Zhang,[3] Zhen Liu,[4] Jixue Zhao,[5] and Xin Liu[6]

[1]*Department of Cardiovascular, China-Japan Union Hospital of Jilin University, Changchun 130033, China*
[2]*Jilin Provincial Molecular Biology Research Center for Precision Medicine of Major Cardiovascular Disease, Changchun 130033, China*
[3]*Department of Pathology, China-Japan Union Hospital of Jilin University, Changchun 130033, China*
[4]*Department of Pediatrics, Liuhe District Hospital of Nanjing, Nanjing 211500, China*
[5]*Department of Pediatrics Surgery, The First Hospital of Jilin University, Changchun 130021, China*
[6]*Central Sterile Supply Department, China-Japan Union Hospital of Jilin University, Changchun 130033, China*

Correspondence should be addressed to Jixue Zhao; jixuezhao0431@yeah.net and Xin Liu; liuxinccjlu@126.com

Received 11 September 2018; Accepted 16 December 2018; Published 10 March 2019

Guest Editor: Gabriele G. Schiattarella

We explored the effects of chitosan oligosaccharides (COS) on coronary heart disease (CHD) patients. The component of COS was measured by matrix-assisted laser desorption ionization time-of-flight mass spectrometry (MALDI-TOF MS). CHD patients were evenly assigned into the COS group (COG) and the placebo group (CG). The duration of treatment was 6 months and therapeutic results were explored by measuring left ventricular ejection fraction (LVEF) value, Lee scores, quality of life (QOL), blood urea nitrogen, and serum creatinine. The intestinal flora were determined by 16s rDNA sequencing. The circulating antioxidant levels and lipid profiles were compared between two groups. There were 7 different degrees of polymerization (DP4-10) in COS. Lee scores, QOL scores, and LVEF values in the COG group were higher than those in the CG group ($P < 0.05$). COS treatment improved blood urea nitrogen and serum creatinine when compared with controls ($P < 0.05$). Circulating antioxidant levels were higher in the COG group than in the CG group. COS consumption increased the serum levels of SOD and GSH and reduced the levels of ALT and AST ($P < 0.05$). Meanwhile, lipid profiles were improved in the COG group. COS consumption increased the abundance of *Faecalibacterium*, *Alistipes*, and *Escherichia* and decreased the abundance of *Bacteroides*, *Megasphaera*, *Roseburia*, *Prevotella*, and *Bifidobacterium* ($P < 0.05$). On the other hand, COS consumption increased the probiotic species *Lactobacillus*, *Lactococcus*, and *Phascolarctobacterium*. The increased species have been reported to be associated with antioxidant properties or lipid improvement. COS had similar effects with chitohexaose on the growth rate of these species. Therefore, COS ameliorate the symptoms of CHD patients by improving antioxidant capacities and lipid profiles via the increase of probiotics in the intestinal flora.

1. Introduction

Coronary heart disease (CHD) is mainly caused by circulating cholesterol accumulation on the artery walls, narrow arteries, and reduced blood flow to the heart [1]. CHD is a major cause of death worldwide and its prevalence is still increasing with population ageing [2]. CHD is difficultly diagnosed [3], and most medical treatment can cause side effects. Angiotensin-converting enzyme 2 (ACE2) is a regulator of the renin angiotensin system and has been widely used in the prevention of CHD development. Recent work showed that ACE2 treatment could increase the hazard of unwanted long-term cardiovascular outcomes in CHD patients [4]. Aspirin is also widely used for CHD therapy as anti-inflammatory pharmaceutical. Administration of aspirin may result in altered reproductive profiles and serum

biochemistry [5]. Therefore, it is highly demanded to explore natural products with few side effects in the prevention of CHD risk and progression.

Chitosan is the second most abundant polysaccharide next to cellulose as a natural renewable resource. Chitosan oligosaccharides (COS) are effective antiatherosclerosis potential natural products [6] and have many valuable properties. COS exert obvious efficiency for preventing intestinal lipid absorption and improving liver lipid biosynthesis and accumulation [7] while lipid profile is an important risk factor of CHD [8]. Furthermore, COS have excellent biological properties presenting a promising prospect in antibacterial [9] and antioxidant biomaterials [10] with little cytotoxicity. Antioxidant therapy will be an effective way for CHD treatment since long-term hyperglycemia can result in the enhancement of oxidative stress [11]. Chitosan consumption can affect fecal microbiota and metabolites of humans [12], which may be associated with the changes of the intestinal flora. Intestinal flora disorder and disturbance also increase the CHD risk [13] and affect lipid metabolism [14] and antioxidant activities [15].

The above results suggest that COS are feasible and promising natural products for CHD patients. However, the effects of COS on CHD patients and the related molecular mechanisms remain unknown. Therefore, we explored the effects of COS on CHD patients and the changes of the intestinal flora. The improvement of the quality of life of CHD patients was compared with controls, and the levels of antioxidant and lipid profiles were measured.

2. Materials and Methods

2.1. Measurement of the Component of COS. Food-grade COS, chitohexaose hydrochloride (MW 1203.72), chitoheptaose hydrochloride (MW 1401.3), and chitooctaose hydrochloride (MW 1598.94) were purchased from Qingdao BZ Oligo Biotech Co. Ltd. (Qingdao, China). Thirty milligrams of COS or other oligosaccharides was dissolved in 1.0 mL ddH_2O and transferred to a chromatography flask for the analysis of matrix-assisted laser desorption ionization time-of-flight mass spectrometry (MALDI-TOF MS). Voyager DESTR type MALDI-TOF mass spectrometer was purchased from Applied Biosystems (Carlsbad, CA, USA). The following operating parameters were used: nitrogen laser (wavelength 337 nm, pulse width 3 ns), reflection mode vacuum 2.08×10^{-6} Torr, ion source acceleration voltage 20 kV, extraction voltage 92.1%, and the ion delay 125 s. The mass spectrometry signal was accumulated 50 times in a single scan, and the positive ion model was determined.

2.2. Participants. All procedures were approved by the human research ethical committee of China-Japan Union Hospital of Jilin University (Changchun, China) (the clinical register no. ChiCTR1900020902 at http://www.chictr.org.cn/searchprojen.aspx). All patients agreed to sign the written consent form. CHD patients were diagnosed by using electrocardiogram, myocardial enzymology markers, coronary angiography, and clinical manifestations.

2.3. Inclusion Criteria. The patients had clinical manifestations of typical pain, which mostly occurred in the early morning. Sudden and severe stern poststernal or precordial compression pain could be found but the cause was not obvious. Taking a rest or taking nitroglycerin tablets could not alleviate the symptoms. The patients were often upset, sweating, fearful, experienced chest tightness, or had a sense of death. Typical electrocardiogram showed that ST-segment elevation was arch-back-up with wide and deep Q wave (pathological Q wave) and T wave inversion. The levels of serum myocardial necrosis markers, myoglobin and troponin I (cTnI), or myocardial markers, such as cardiac troponin T (cTnT) and creatine kinase isoenzyme CK-MB, were significantly elevated.

2.4. Exclusion Criteria. The patients with the following condition were excluded: (1) gastrointestinal diseases, such as gastritis and gastric ulcer, and diarrhea in the past 4 weeks or a history of gastrointestinal surgery; (2) combined symptoms of heart failure; (3) cardiogenic shock; (4) previous coronary revascularization procedures (e.g., thrombolysis and PCI); (5) combined symptoms with autoimmune diseases; (6) other endocrine diseases such as thyroid disorder; (7) serious damage to organs such as the liver and kidney; (8) oral and intravenous antibiotic administration for nearly 1 week and adjustment of intestinal flora preparation and gastric mucosal protective agent for nearly 1 week; (9) hypertension, obesity, diabetes, and dyslipidemia; and (10) pregnant.

2.5. Patient Grouping. From March 4, 2016, to April 28, 2017, a total of 528 CHD patients were screened. The first primary endpoint was mortality, stroke, and myocardial infarction and the endpoint was determined according to a one-month observation after randomization. Finally, a sample size with 120 subjects was determined. COS have been sold widely in China as healthy products. The dosage of COS (1-2 g/day) was provided according to product instructions. COS mixtures administered orally at doses between 50 and 1,000 mg/kg b.w. will not produce any significant change in the autonomic or behavioral responses in animal models [16]. To maintain the safety of COS, the lowest dose of COS (2 g daily) was used. All patients were selected and evenly assigned into the COG (received 2 g COS daily) and CG (placebo) groups. The therapeutic duration was half a year.

2.6. Specimen Collection. Fresh stools were collected on the first morning after admission, and stool samples from all subjects were collected in closed fecal storage boxes within two-hour defecation (subjects took hospital diet and normal control diet). The samples were immediately stored in a -80°C refrigerator.

2.7. Extraction of Total DNA. Two-gram feces was placed in a 2.0 mL Safe-Lock tube, and glass beads were added and one-milliliter PBS (50 mM, pH 7.0) and vortexed evenly. The mixture was water bathed at 95°C for 10 min, and 20 μL proteinase K was added and incubated at 55°C for 10 min. After centrifugation at 12000 rpm for 15 min, the supernatant was placed in a two-milliliter test tube. Genomic

DNA was extracted and purified by using the kit from Promega (Madison, WI, USA). The quality of genomic DNA was determined by using Thermo NanoDrop 2000 Ultraviolet Micro Spectrophotometer (Thermo Fisher Scientific Inc., Waltham, MA, USA) and 1% agarose gel electrophoresis.

2.8. 16S rDNA Sequencing. The 16S rDNA amplification selection region is V3-V4 region, and a universal primer is used. The specific universal primers (forward primer: 5′-ACTCCT ACGGGRSGCAGCAG-3′; reverse primer: 5′-GGACTAC VVGGGTATCTAATC-3′) were used for 16S rDNA sequencing. The primers were completed by adding the index sequence and the linker sequence suitable for PE250 sequencing at the 5′ end of the primer. Using the diluted genomic DNA as a template, PCR was performed with KAPA HiFi HotStart ReadyMix PCR kit high-fidelity enzyme (Kapa Biosystems Inc., Boston, MA, USA). The PCR product was detected by 2% agarose gel electrophoresis, and the PCR product was recovered by gelatinization using an AxyPrep DNA Gel Recovery Kit (Axygen Scientific Co., CA, USA). After recovery, library quality checks were performed using a Thermo NanoDrop 2000 UV spectrophotometer and 2% agarose gel electrophoresis. PCR products were sequenced by using illumina HiSeq PE250 (Illumina, San Diego, CA, USA).

2.9. The Effects of COS on the Growth of Intestinal Flora. The strains *Bacteroides thetaiotaomicron* (CGMCC 1.5132, broken meat medium); *Escherichia coli* (CGMCC 1.12883, LB medium); *Megasphaera elsdenii* (CGMCC 1.2720, CGMCC medium 0288); and *Bifidobacterium bifidum* (CGMCC 1.5091, CGMCC medium 0244) were purchased from the China General Microbiological Culture Collection Center, Institute of Microbiology, Chinese Academy of Sciences (Beijing, China). The strains *Faecalibacterium prausnitzii* (ATCC 27768, ATCC medium: 2107 modified reinforced clostridial); *Alistipes shahii* (ATCC BAA-1179, ATCC medium 1490: modified chopped meat medium); and *Prevotella bivia* (ATCC 29303, ATCC medium 2107) were purchased from the American Type Culture Collection (ATCC) (Manassas, VA, USA). The strain *Roseburia intestinalis* (DSM 14610, medium 143) was purchased from Leibniz-Institut DSMZ-Deutsche Sammlung von Mikroorganismen und Zellkulturen GmbH (Inhoffenstraße, Braunschweig, Germany). *Escherichia coli* was cultured at a 200 rpm shaker at 37°C while other strains were cultured with anaerobic gas mixture, 80% N_2, 10% CO_2, and 10% H_2 at 37°C with corresponding media and 10 μg/mL chitohexaose hydrochloride, chitoheptaose hydrochloride, chitooctaose hydrochloride, and mixed 80 μg/mL chitosan oligosaccharide. The group without chitosan oligosaccharides was used as a control. The growth rate of all strains was measured by using a Real-Time Cell Analyzer (xCELLigence™, Roche Inc., Indianapolis, IN, USA) within 24 hours.

2.10. Lipid Profile Analysis. Serum triglycerides (TG), total cholesterol (TC), low-density lipoprotein cholesterol (LDL-C), and high-density lipoprotein cholesterol (HDL-C) were examined by using an automatic biochemical analyzer (Dimension, Schererville, IN, USA).

2.11. Analyses of Circulating Oxidative Levels. 2 mL blood was taken from individual patient. Circulating oxidative levels were examined by measuring the levels of superoxide dismutase (SOD), glutathione (GSH), alanine aminotransferase (ALT), and aspartate aminotransferase (AST). ELISA kits were purchased from Beyotime Institute of Biotechnology (Beijing, China).

2.12. Measurement of Therapeutic Effects. The normal therapy of CHD included oxygen inhalation, angiotensin-converting enzyme inhibitors (ACE-in), and implantable cardioverter defibrillator (ICD). Ejection fraction (EF) value and scores of quality of life (QOL) were evaluated by using the Minnesota Living with Heart Failure Questionnaire (MLHFQ) [17].

Left ventricular ejection fraction (LVEF) was detected by using radionuclide ventriculography with patients in the supine position [18]. Serum was separated from the blood sample via centrifugation at $4000 \times g$ for 10 min. Blood urea nitrogen (BUN) was analyzed by using the above automatic biochemistry analyzer via a BUN kit (Beckman Coulter Inc., Brea, CA, USA). Serum creatinine was measured by a creatinine kit (Biosino Bio-Technology, Beijing, China).

2.13. Statistical Analysis. All data were presented as mean values ± S.D. and analyzed by using SPSS 20.0 statistical package. The t-test was used for the comparison of mean values between the two groups and count number was analyzed using the χ^2 test. $P < 0.05$ was considered statistically significant.

3. Results

3.1. The Main Components of COS. There were seven main kinds of chitosan oligosaccharides in food-grade COS from DP4 (666.2 Da) to DP10 (1638.1 Da) (Figure 1(a)). The molecular weight of chitohexaose (990.1 Da, Figure 1(b)), chitoheptaose (1152.1 Da, Figure 1(c)), and chitooctaose (1314.1 Da, Figure 1(d)) were also accordant with theoretical values in a positive mode.

3.2. Clinical Characteristics. After the 6-month therapy, 4 and 6 patients left the COG and CG groups for other medical treatment, respectively. There was no significantly statistical differences for clinical characteristics of CHD patients between the COG and CG groups, including sex ratio, body mass index (BMI), age, diastolic blood pressure (DBP), and systolic blood pressure (SBP) (Table 1, $P > 0.05$). The cases for taking ACE-In, ARBS, beta-blockers, and diuretics were also comparable between the two groups ($P > 0.05$, Table 1).

3.3. Therapeutic Results. There was no significant difference ($P > 0.05$) in the mean values of BUN before COS therapy ($P < 0.05$, Table 2). After therapy, the values of mean BUN and serum creatinine were significantly reduced when compared with the placebo group ($P < 0.05$, Table 2). Before COS treatment, the statistical difference for Lee scores was insignificant between the COG and CG groups (Table 2, $P > 0.05$). After COS consumption, COS reduced more Lee scores than CG (Table 2, $P < 0.05$). Before COS consumption, the statistical difference for the QOL scores was

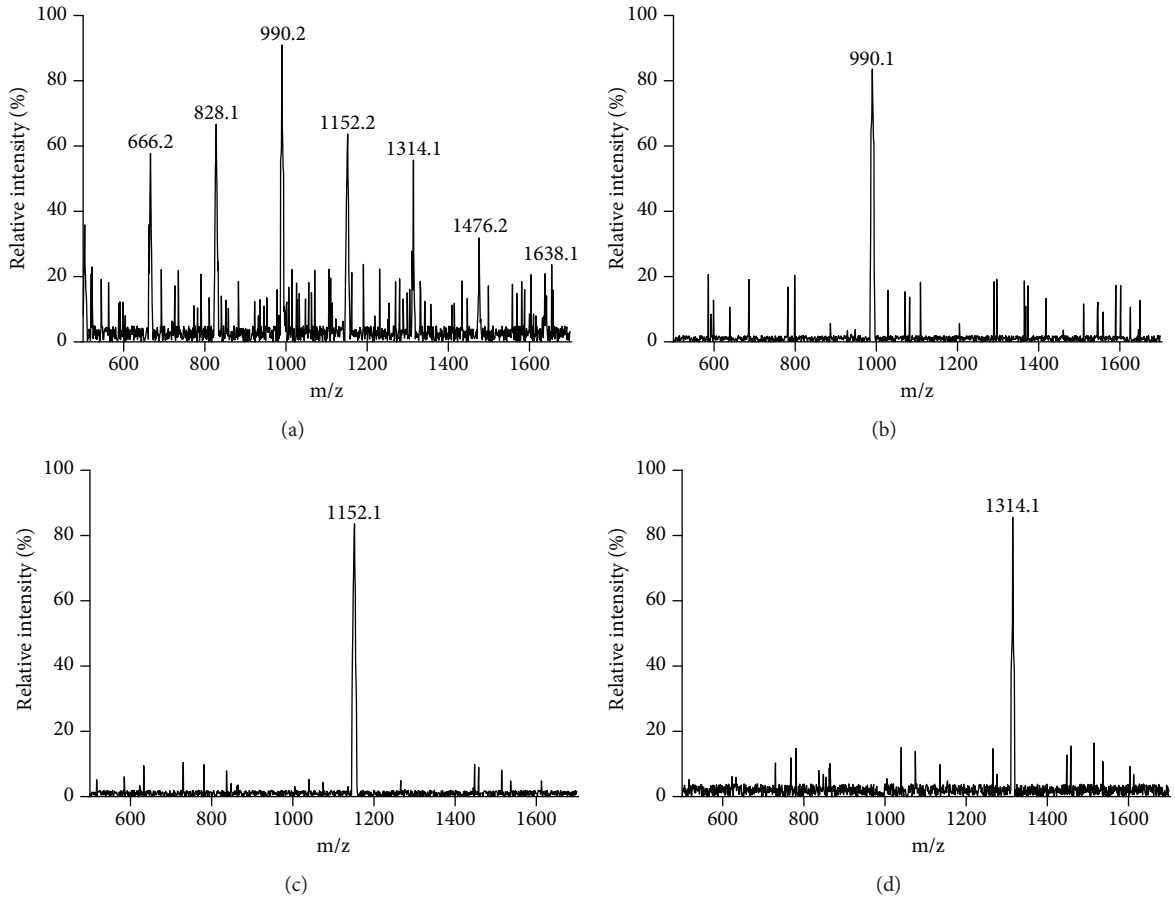

Figure 1: Matrix-assisted laser desorption ionization time-of-flight mass spectrometry (MALDI-TOF MS) analysis of the main components of chitosan oligosaccharides (COS). (a) The main components of food-grade COS with different degrees of polymerization DP4-10. (b) Chitohexaose with molecular weight $[M+H]^+ = 990.1$ Da. (c) Chitoheptaose with molecular weight $[M+H]^+ = 1152.1$ Da. (d) Chitooctaose with molecular weight $[M+H]^+ = 1314.2$ Da.

Table 1: Clinical characteristics between COS and placebo groups.

Parameters	COS	Placebo	χ^2 and t value	P value
Gender (male/female)	30/26	31/23	0.164	0.686
Age (yr)	39.29 ± 13.36	41.23 ± 12.98	-1.307	0.189
SBP (mm Hg)	125.21 ± 11.62	128.54 ± 12.76	-1.685	0.087
DBP (mm Hg)	87.23 ± 7.16	88.53 ± 7.38	-1.290	0.157
BMI	24.93 ± 2.94	24.52 ± 2.68	-1.564	0.198
Cr (μmol/L)	85.34 ± 13.58	87.24 ± 14.56	-1.344	0.156
HbA1C (%)	8.47 ± 0.93	8.75 ± 0.96	-0.664	0.256
ACE-In	7	8		
ARBS	3	6	2.47	0.48
Beta-blockers	5	6		
Diuretics	8	4		

Chi-square test and t-test were used to compare the significant difference between the two groups. BMI: body mass index; ACE-In: angiotensin-converting enzyme; ARBS: angiotensin receptor blockers. All data were presented as mean value ± S.D. There were significantly statistical differences between two groups if $P < 0.05$.

insignificant between the COG and CG groups (Table 2, $P > 0.05$). After 6-month COS consumption, COS increased more QOL scores than CG (Table 2, $P < 0.05$). Before COS consumption, the statistical difference for LVEF volume was insignificant between the COG and CG groups (Table 2, $P > 0.05$). After 6-month COS consumption, the values of LVEF were improved in the COG group higher than in the CG group (Table 2, $P < 0.05$).

Table 2: The therapeutic results of COS.

		Before treatment	After treatment	t values	P values
Blood urea nitrogen (mg/dL)	COS	19.13 ± 6.85	15.33 ± 6.24	6.42	0.02[b]
	Placebo	18.73 ± 6.54	17.25 ± 5.98	1.16	0.23
	t values	0.39	3.21		
	P values	0.54	0.02[a]		
Serum creatinine (mg/dL)	COS	1.41 ± 0.32	1.04 ± 0.27	8.65	0.01[b]
	Placebo	1.35 ± 0.27	1.29 ± 0.22	0.35	0.24
	t values	0.25	4.37		
	P values	0.66	0.02[a]		
Lee scores	COS	4.52 ± 1.87	2.18 ± 0.43	5.38	0.01[b]
	Placebo	4.27 ± 1.79	4.19 ± 0.78	0.25	0.31
	t values	0.26	4.12		
	P values	0.68	0.02[a]		
Quality-of-life (QOL) scores	COS	43.61 ± 3.38	21.73 ± 4.12	13.40	0.01[b]
	Placebo	42.50 ± 3.25	39.39 ± 4.36	0.45	0.29
	t values	0.36	2.13		
	P values	0.75	0.02[a]		
LVEF	COS	29.06 ± 9.34	36.82 ± 10.43	3.03	0.02[b]
	Placebo	28.74 ± 8.15	30.73 ± 10.21	1.10	0.08
	t values	0.92	2.17		
	P values	0.36	0.03[a]		

Note: LVEF: left ventricular ejection fraction. $n = 60$ for each group. [a]$P < 0.05$ vs. the placebo group and [b]$P < 0.05$ vs. before treatment. There were significantly statistical differences between the two groups if $P < 0.05$.

3.4. The Effects of COS Consumption on Intestinal Flora of CHD Patients. The statistical difference for the abundance of intestinal flora was insignificant between the two groups before therapy (Figure 2(a) $P > 0.05$). After 6-month therapy, the abundance of *Faecalibacterium*, *Alistipes*, and *Escherichia* was reduced, while the abundance of *Bacteroides*, *Megasphaera*, *Roseburia*, *Prevotella*, and *Bifidobacterium* was increased when compared with the CG group (Figure 2(b), $P < 0.05$). On the other hand, COS consumption increased the probiotic species *Lactobacillus*, *Lactococcus*, and *Phascolarctobacterium*. The results suggest that COS consumption can inhibit the abundance of harmful bacteria and increase the abundance or species of probiotics in CHD patients.

3.5. The Effects of COS on the Growth Rate of Intestinal Flora. In vitro test showed that COS mixture and chitooctaose (DP8) treatment inhibited the growth rate of *Escherichia coli* (Figure 3(a)), *Megasphaera elsdenii* (Figure 3(b)), and *Faecalibacterium prausnitzii* (Figure 3(c)) and promoted the growth of *Alistipes shahii* (Figure 3(d)), *Prevotella bivia* (Figure 3(e)), *Roseburia intestinalis* (Figure 3(f)), *Bacteroides thetaiotaomicron* (Figure 3(g)), and *Bifidobacterium bifidum* (Figure 3(h)). Meanwhile, chitooctaose had similar results with mixed COS. Comparatively, chitohexaose and chitoheptaose had no effects on these bacteria. The results suggest that COS affect intestinal flora via chitooctaose.

3.6. COS Consumption Improved Lipid Profiles of CHD Patients. Before COS consumption, the statistical difference was insignificant between the two groups ($P > 0.05$, Table 3). After 6-month therapy, the serum levels of TG, TC, and LDL-c were reduced while HDL-c was increased when compared with the control group ($P < 0.05$, Table 3). The results suggest that COS consumption can improve lipid profiles of CHD patients.

3.7. COS Consumption Increased Antioxidant Properties of CHD Patients. The statistical difference for the biomarkers of antioxidant and oxidative stress was insignificant between the two groups before therapy (Table 4, $P > 0.05$). After 6-month therapy, the circulating levels of SOD and GSH were increased while the levels of ALT and AST were reduced in the COG group when compared with the CG group ($P < 0.05$, Table 4). The results suggest that COS consumption can increase antioxidant properties of CHD patients.

4. Discussion

Chitosan has been widely used for CHD therapy as biomaterials of the drug delivery system [19, 20] and coronary artery bypass graft [21]. However, the direct effects of chitosan on CHD have seldom been reported. This study showed that COS consumption increased the values of LVEF in the COG group higher than in the CG group ($P < 0.05$). Medicine combined with COS effectively ameliorated CHD patients with lower LVEF. Lee scores and QOL scores were also increased in the COG group ($P < 0.05$, Table 2). Meanwhile, lipid profiles (Table 3) and antioxidant properties

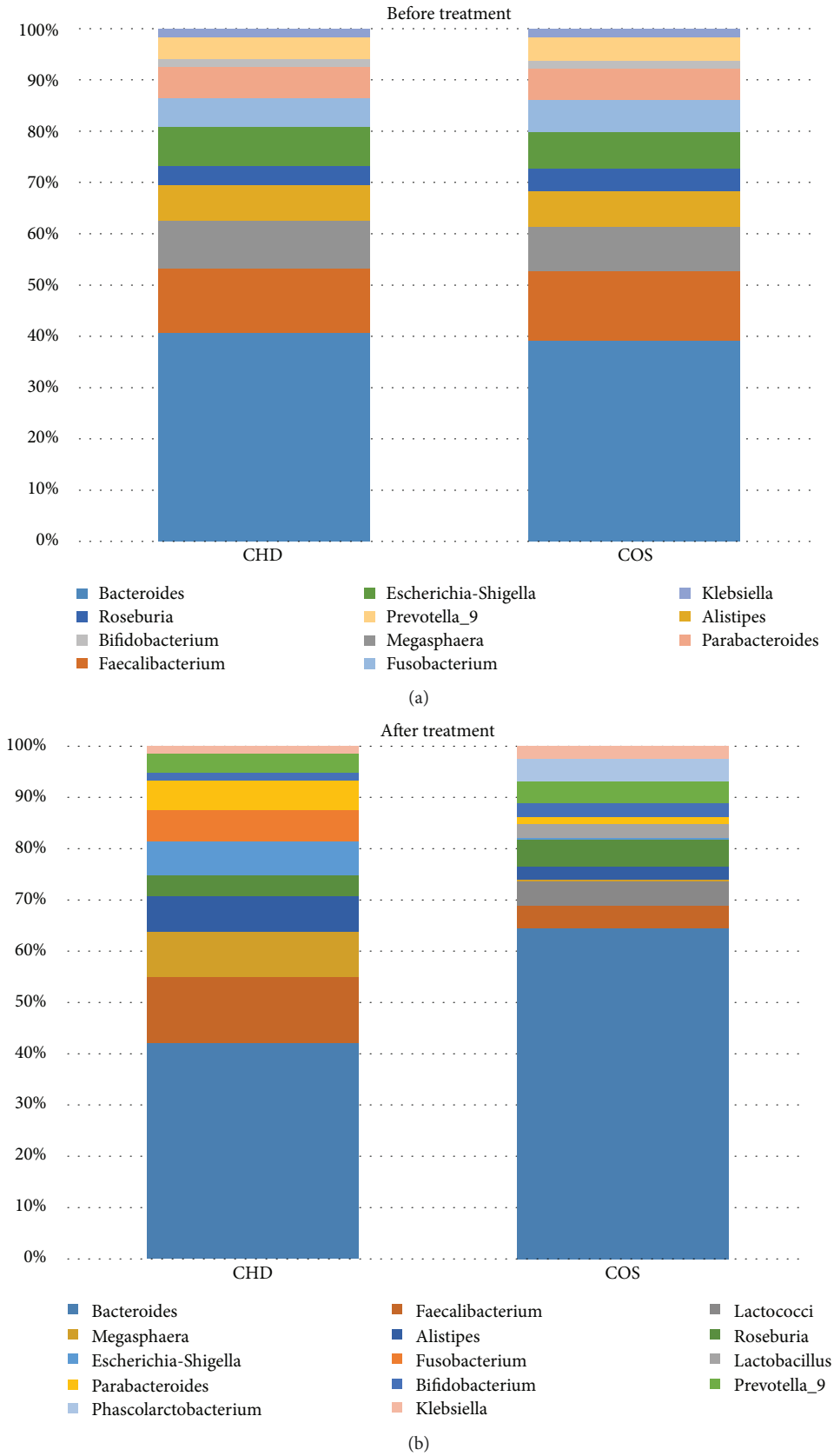

Figure 2: The effects of COS on intestinal flora. (a) The abundance of intestinal flora before COS treatment. (b) The abundance of intestinal flora after 6-month treatment.

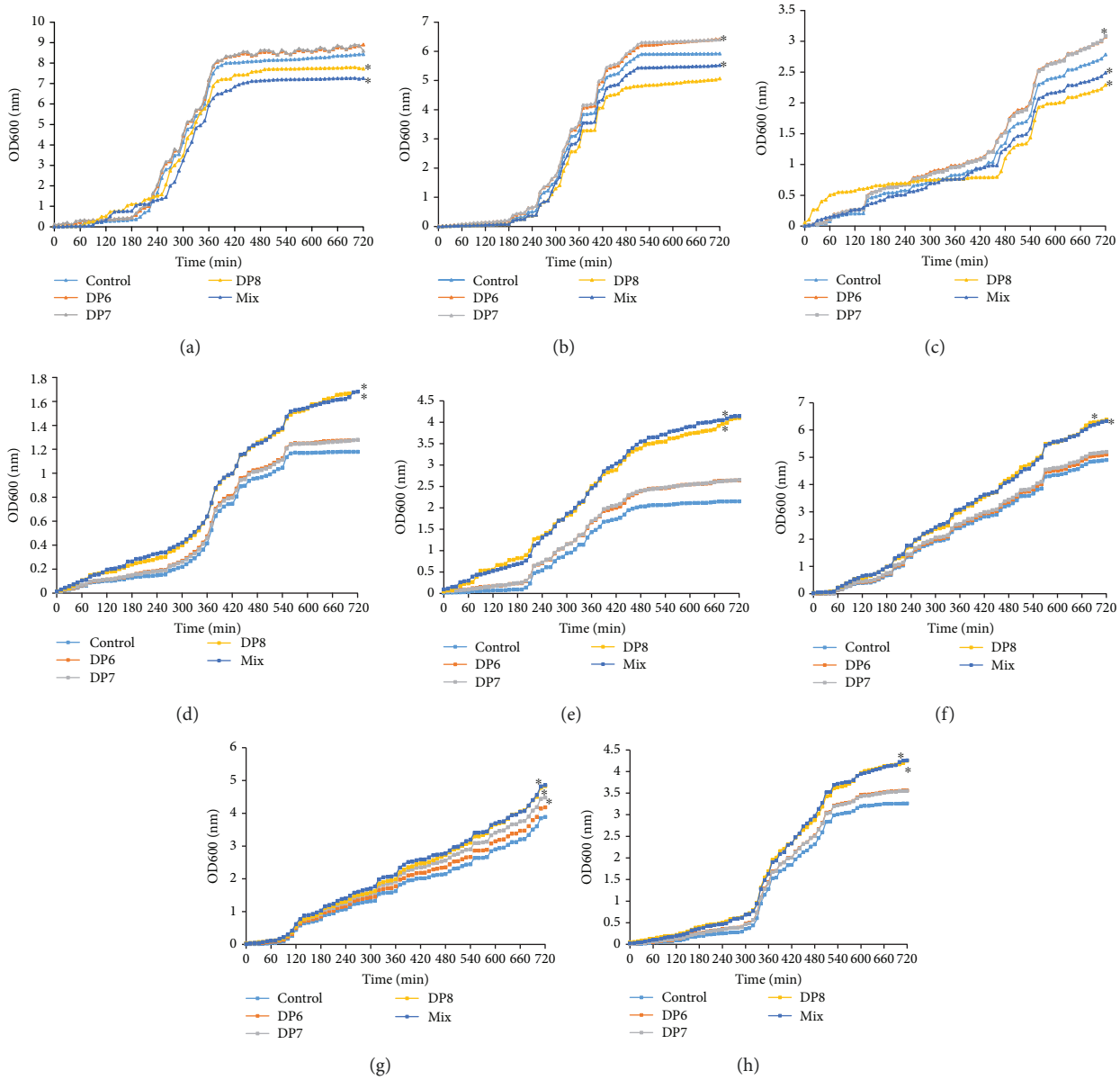

Figure 3: Real-time analysis of the effects of COS on the growth of intestinal flora. (a) The effects of COS on the growth of *Escherichia coli*. (b) The effects of COS on the growth of *Megasphaera elsdenii*. (c) The effects of COS on the growth of *Faecalibacterium prausnitzii*. (d) The effects of COS on the growth of *Alistipes shahii*. (e) The effects of COS on the growth of *Prevotella bivia*. (f) The effects of COS on the growth of *Roseburia intestinalis*. (g) The effects of COS on the growth of *Bacteroides thetaiotaomicron*. (h) The effects of COS on the growth of *Bifidobacterium bifidum*. Mix: food-grade COS, DP4-10 chitosan oligosaccharides; DP6: chitohexaose hydrochloride (MW 1203.72); DP7: chitoheptaose hydrochloride (MW1401.3); and DP8: chitooctaose hydrochloride (MW1598.94). $^{*}P < 0.05$ vs. the control group without COS.

(Table 4) were also improved in the COG group better than the CG group ($P < 0.05$). The results suggest that COS are effective to ameliorate symptoms of CHD patients by improving biochemical indices and the living ability of CHD patients.

LVEF is an important predicator for heart failure hospitalization and mortality in ambulatory adults with CHD [22]. CHD patients with low-level LVEF had a poor prognosis [23]. The present findings demonstrated that COS consumption improved LVEF values significantly when compared with controls (Table 2, $P < 0.05$). COS have been reported to have the clinical effects of pain relief [24], which will be beneficial for CHD patients with chest pain or chronic back pain [25, 26]. Chitosan microspheres were used for chronotherapy of chronic stable angina in an animal model [27] while angina is the common symptom of CHD patients [28, 29]. Fatigue is a prevalent and disabling symptom associated with CHD [30] while COS have been proved to delay fatigue in animal models [31]. All these results suggest that COS may have direct or indirect effect on improving CHD symptoms.

On the other hand, intestinal flora total load was found to be associated with CHD risk in obese patients [13]. Intestinal flora can produce short-chain fatty acids (SCFA) [32, 33] and

Table 3: Lipid profiles between two groups.

		COS	Placebo	t values	P values
Before therapy	TC (mmol/L)	5.42 ± 0.63	5.70 ± 0.81	-0.621	0.284
	TG (mmol/L)	2.34 ± 0.81	2.17 ± 0.92	-2.108	0.129
	LDL-C (mmol/L)	2.11 ± 0.62	2.31 ± 0.81	-1.834	0.167
	HDL-C (mmol/L)	1.83 ± 0.42	1.65 ± 0.38	-2.609	0.094
After therapy	TC (mmol/L)	4.89 ± 0.87	5.81 ± 0.72	-1.982	0.013
	TG (mmol/L)	2.01 ± 0.65	2.24 ± 0.83	-2.696	0.035
	LDL-C (mmol/L)	1.81 ± 0.54	2.40 ± 0.75	-1.992	0.031
	HDL-C (mmol/L)	2.13 ± 0.40	1.71 ± 0.46	-2.852	0.009

Note: there were significant statistical differences between two groups if $P < 0.05$.

Table 4: Antioxidant levels between two groups.

		COS	Placebo	t values	P values
Before therapy	SOD (U/mL)	12.25 ± 4.06	11.30 ± 4.21	0.79	0.46
	GSH (U/mL)	9.20 ± 2.99	9.35 ± 2.73	0.12	0.81
	ALT (U/mL)	68.79 ± 9.03	65.52 ± 8.76	0.35	0.47
	AST (U/mL)	198.21 ± 27.21	190.36 ± 20.38	0.83	0.12
After therapy	SOD (U/mL)	21.34 ± 3.78	13.49 ± 4.71	8.77	0.01
	GSH (ng/L)	15.26 ± 3.12	10.59 ± 2.01	6.25	0.01
	ALT (U/L)	61.03 ± 12.27	66.49 ± 8.24	4.31	0.02
	AST (U/L)	147.43 ± 21.73	188.52 ± 23.62	7.04	0.01

Note: there were significant statistical differences between two groups if $P < 0.05$.

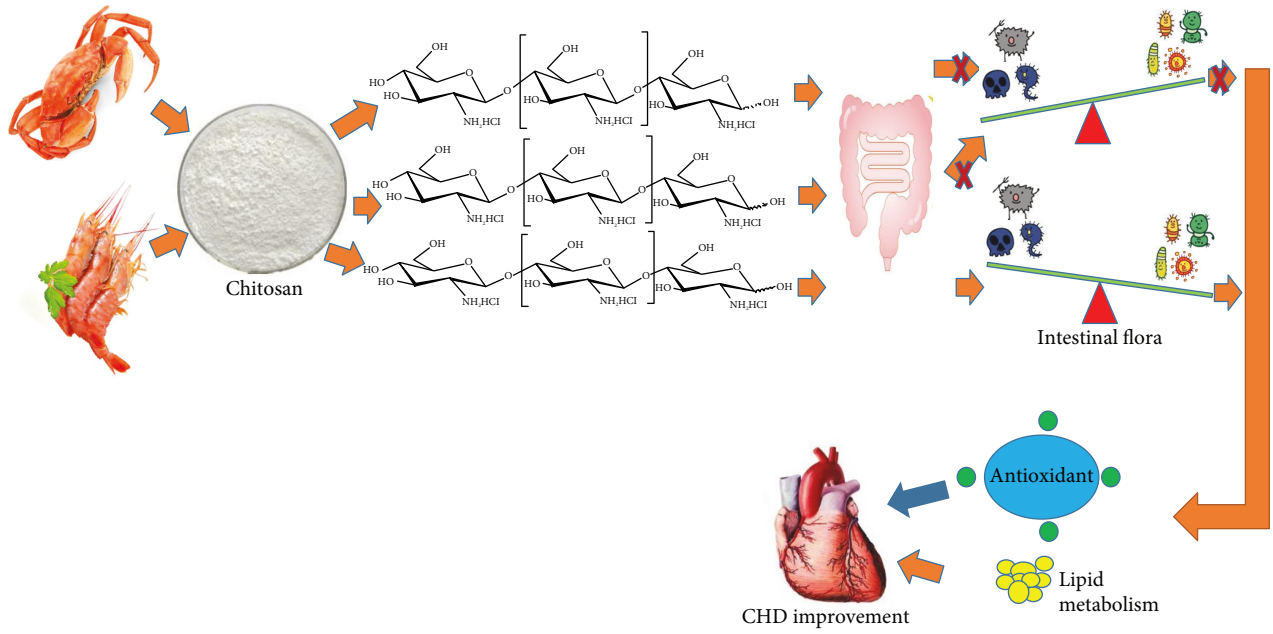

Figure 4: COS show health-promoting properties for coronary heart disease by affecting intestinal flora via chitooctaose. COS increase the levels of probiotics, which exert antioxidant properties and improve lipid profiles. All the function will be beneficial in the prevention of CHD.

bile acids [34, 35] involved in various metabolic pathways, endotoxin secretion and circulation, dopamine, the fasting-induced adipose factor (FIAF) [36], and adenosine monophosphate-activated protein kinase (AMPK) [37], which affect CHD risk factors such as hypertension [38], obesity [39], diabetes [40], and dyslipidemia [41]. Adjusting the

structure and function of the flora via probiotics, antibiotics or diet can provide ideal methods for the prevention of CHD. Therefore, the effects of COS on intestinal flora were explored in CHD patients.

After COS consumption, the abundance of *Faecalibacterium*, *Alistipes*, and *Escherichia* was reduced, while the abundance of *Bacteroides*, *Megasphaera*, *Roseburia*, *Prevotella*, and *Bifidobacterium* was increased (Figure 2(b)). Furthermore, COS consumption increased the probiotic species *Lactobacillus*, *Lactococcus*, and *Phascolarctobacterium*. *Faecalibacterium* was found to be linked with type 2 diabetes mellitus or other risk factors of heart disease [42]. Conversely, *Faecalibacterium* numbers were also found to be decreased in the patients with chronic heart disease [43]. Cardiac abnormalities were reported to be caused by bacterial myocarditis resulting from *E. coli* infection [44, 45]. A high-fiber diet and supplementation with the SCFA can increase the number of *Bacteroides acidifaciens* and prevent cardiovascular disease [46]. *Roseburia* reduced microbially derived, proinflammatory secondary bile acids and LDL-c, which are associated with heart disease [47]. *Bifidobacterium* exerted beneficial effects on the serum cholesterol metabolism by reducing the levels of TC and LDL-c in the patients with dyslipidemia [48]. *Bifidobacterium* had strong antioxidant properties by scavenging 2,2-diphenyl-1-picryl-hydrazyl (DPPH) radical, superoxide anion, and hydroxyl radical [49]. However, *Prevotella* was reported to be a potential risk bacterium of heart disease [50]. All the growth of these species could be affected by COS while COS had similar results with chitooctaose but not chitohexaose and chitoheptaose (Figure 3). Thus, the COS from crab and shrimp may ameliorate CHD by affecting intestinal flora, which improve lipid profiles and antioxidant activities of CHD patients (Figure 4).

More importantly, the increased probiotic species *Lactobacillus* and *Lactococcus* show health-promoting activities for CHD. *Lactobacillus* showed strong antioxidant function by upregulating the expression of glutathione reductase, glutathione S-transferase, glutamate-cysteine ligase catalytic subunit, and NAD(P)H quinone oxidoreductase 1 [51]. *Lactococcus acidophilus* was found to prevent the progression of arteriosclerosis and coronary heart disease by affecting lipid profiles and increasing the antioxidant abilities of hyperlipidemia animal model [52].

The lipid metabolism may be correlated with not only intestinal flora but also intestinal enzymes. Previous work showed that intestinal disaccharidases (such as sucrase and maltase) were significantly decreased animals being fed with COS [53]. COS were proved to have antihyperglycemia ability for inhibiting carbohydrate hydrolysis enzymes, such as sucrase and glucoamylase [54]. Based on these findings, further clinical trials are highly demanded to prove the mechanism.

There were some limitations to the present work. The effects of chitosan oligosaccharides DP4-5 and DP9-10 on intestinal flora were not investigated although the mixed COS had similar results with chitooctaose for the growth rate of intestinal flora. The effects of COS on the increased probiotic species *Lactobacillus*, *Lactococcus*, and *Phascolarctobacterium* were not measured and reason remained unknown. Considering the short time of the present study, the small sample size, and other influencing factors, further work is highly demanded to confirm the present results.

5. Conclusions

COS combined with conventional treatment improved the LVEF values, QOL scores, and Lee scores. COS consumption increased the types and numbers of probiotic species of intestinal flora, which may improve lipid profiles and antioxidant properties of CHD patients. COS had similar effects with chitohexaose on the growth rate of these species. Therefore, COS improve the symptoms of CHD patients by improving antioxidant capacities via the increase of probiotics in intestinal flora.

Data Availability

The data used to support the findings of this study are available from the corresponding author upon request.

Conflicts of Interest

There are no investigator conflicts of interest to declare on the part of any of the investigators.

Authors' Contributions

TJ and XX designed the study and drafted the manuscript. LZ, ZL, and JZ conducted the study and analyzed the data. JZ and XL commented and revised the manuscript. Tiechao Jiang and Xiaohong Xing contributed equally to this work.

References

[1] P. R. Lawler, A. O. Akinkuolie, P. M. Ridker et al., "Discordance between circulating atherogenic cholesterol mass and lipoprotein particle concentration in relation to future coronary events in women," *Clinical Chemistry*, vol. 63, no. 4, pp. 870–879, 2017.

[2] A. J. LeBlanc, N. Q. Kelm, and M. George, "Current themes in myocardial and coronary vascular aging," *Current Opinion in Physiology*, vol. 1, pp. 27–33, 2018.

[3] W. J. Zimoch, P. Kubler, M. Kosowski et al., "Pacjenci z nasilonymi zwapnieniami w naczyniu odpowiedzialnym za niedokrwienie, poddawani zabiegom angioplastyki wieńcowej z powodu zawału serca cechują się złym rokowaniem w obserwacji odległej," *Kardiologia Polska*, vol. 75, no. 9, pp. 859–867, 2017.

[4] J. Ramchand, S. K. Patel, P. M. Srivastava, O. Farouque, and L. M. Burrell, "Elevated plasma angiotensin converting enzyme 2 activity is an independent predictor of major adverse cardiac events in patients with obstructive coronary artery disease," *PLoS One*, vol. 13, no. 6, article e0198144, 2018.

[5] A. Vyas, H. Ram, A. Purohit, and R. Jatwa, "Adverse effects of subchronic dose of aspirin on reproductive profile of male rats," *Journal of Pharmaceutics*, vol. 2016, Article ID 6585430, 9 pages, 2016.

[6] Y. Yu, T. Luo, S. Liu et al., "Chitosan oligosaccharides attenuate atherosclerosis and decrease Non-HDL in ApoE-/- mice,"

Journal of Atherosclerosis and Thrombosis, vol. 22, no. 9, pp. 926–941, 2015.

[7] S. H. Liu, C. Y. Chiu, C. M. Shi, and M. T. Chiang, "Functional comparison of high and low molecular weight chitosan on lipid metabolism and signals in high-fat diet-fed rats," *Marine Drugs*, vol. 16, no. 8, 2018.

[8] M. H. Maleki, M. Mousavi, T. Kazemi, N. Azdaki, A. R. Sharifabad, and R. Hoshyar, "Comparison of atherogenic index and lipid profiles in candidates for coronary artery bypass graft surgery versus normal people," *Pakistan Journal of Pharmaceutical Sciences*, vol. 31, no. 5, pp. 1899–1902, 2018.

[9] J. Wongpreecha, D. Polpanich, T. Suteewong, C. Kaewsaneha, and P. Tangboriboonrat, "One-pot, large-scale green synthesis of silver nanoparticles-chitosan with enhanced antibacterial activity and low cytotoxicity," *Carbohydrate Polymers*, vol. 199, pp. 641–648, 2018.

[10] W. Tan, J. Zhang, Y. Mi, F. Dong, Q. Li, and Z. Guo, "Synthesis, characterization, and evaluation of antifungal and antioxidant properties of cationic chitosan derivative via azide-alkyne click reaction," *International Journal of Biological Macromolecules*, vol. 120, Part A, pp. 318–324, 2018.

[11] W. Liang, Y. J. Zhao, H. Yang, and L. H. Shen, "Effects of antioxidant system on coronary artery lesions in patients with abnormal glucose metabolism," *Aging Clinical and Experimental Research*, vol. 29, no. 2, pp. 141–146, 2017.

[12] S. Inoguchi, Y. Ohashi, A. Narai-Kanayama, K. Aso, T. Nakagaki, and T. Fujisawa, "Effects of non-fermented and fermented soybean milk intake on faecal microbiota and faecal metabolites in humans," *International Journal of Food Sciences and Nutrition*, vol. 63, no. 4, pp. 402–410, 2012.

[13] X. Li and C. Li, "Analysis of changes in intestinal flora and intravascular inflammation and coronary heart disease in obese patients," *Experimental and Therapeutic Medicine*, vol. 15, no. 5, pp. 4538–4542, 2018.

[14] M. Fukushima and M. Nakano, "Effects of the lipid-saccharide complex and unsaponifiable matter from sunflowers on liver lipid metabolism and intestinal flora in rats," *Bioscience, Biotechnology, and Biochemistry*, vol. 59, no. 5, pp. 860–863, 1995.

[15] X. W. Yang, N. Wang, W. Li, W. Xu, and S. Wu, "Biotransformation of 4,5-*O*-dicaffeoylquinic acid methyl ester by human intestinal flora and evaluation on their inhibition of NO production and antioxidant activity of the products," *Food and Chemical Toxicology*, vol. 55, pp. 297–303, 2013.

[16] J. C. Fernandes, H. Spindola, V. de Sousa et al., "Anti-inflammatory activity of chitooligosaccharides in vivo," *Marine Drugs*, vol. 8, no. 6, pp. 1763–1768, 2010.

[17] J. Mogle, H. Buck, C. Zambroski, R. Alvaro, and E. Vellone, "Cross-validation of the Minnesota Living With Heart Failure Questionnaire," *Journal of Nursing Scholarship*, vol. 49, no. 5, pp. 513–520, 2017.

[18] J. Naar, F. Málek, O. Lang et al., "Assessment of left ventricular diastolic function by radionuclide ventriculography in patients with chronic heart failure and reduced ejection fraction," *Vnitřní Lékařství*, vol. 60, pp. 110–113, 2014.

[19] J. Q. Gao, J. P. Zheng, H. G. Jin et al., "A new rapamycin-abluminally coated chitosan/heparin stent system accelerates early re-endothelialisation and improves anticoagulant properties in porcine coronary artery models," *Clinical and Investigative Medicine*, vol. 37, no. 6, pp. E395–E402, 2014.

[20] S. Meng, Z. Liu, L. Shen et al., "The effect of a layer-by-layer chitosan–heparin coating on the endothelialization and coagulation properties of a coronary stent system," *Biomaterials*, vol. 30, no. 12, pp. 2276–2283, 2009.

[21] E. P. Azevedo, R. Retarekar, M. L. Raghavan, and V. Kumar, "Mechanical properties of cellulose: chitosan blends for potential use as a coronary artery bypass graft," *Journal of Biomaterials Science, Polymer Edition*, vol. 24, no. 3, pp. 239–252, 2013.

[22] B. Ristow, S. Ali, M. A. Whooley, and N. B. Schiller, "Usefulness of left atrial volume index to predict heart failure hospitalization and mortality in ambulatory patients with coronary heart disease and comparison to left ventricular ejection fraction (from the Heart and Soul Study)," *The American Journal of Cardiology*, vol. 102, no. 1, pp. 70–76, 2008.

[23] J. F. Dopheide, P. Knopf, G. C. Zeller et al., "Low IL-10/TNFα ratio in patients with coronary artery disease and reduced left ventricular ejection fraction with a poor prognosis after 10 years," *Inflammation*, vol. 38, no. 2, pp. 911–922, 2015.

[24] Y. Okamoto, K. Kawakami, K. Miyatake, M. Morimoto, Y. Shigemasa, and S. Minami, "Analgesic effects of chitin and chitosan," *Carbohydrate Polymers*, vol. 49, no. 3, pp. 249–252, 2002.

[25] R. Schweier, G. Grande, C. Richter, S. G. Riedel-Heller, and M. Romppel, "In-depth statistical analysis of the use of a website providing patients' narratives on lifestyle change when living with chronic back pain or coronary heart disease," *Patient Education and Counseling*, vol. 101, no. 7, pp. 1283–1290, 2018.

[26] M. N. Kim, D. Cho, S. A. Kim et al., "PS 05-42 the usefulness of heart rate and blood pressure recovery in diagnosis of coronary artery disease in hypertensive women with suspected coronary artery disease: from Korean women's chest pain registry (KoROSE)," *Journal of Hypertension*, vol. 34, pp. E152–E153, 2016.

[27] S. Jose, M. T. Prema, A. J. Chacko, A. C. Thomas, and E. B. Souto, "Colon specific chitosan microspheres for chronotherapy of chronic stable angina," *Colloids and Surfaces B: Biointerfaces*, vol. 83, no. 2, pp. 277–283, 2011.

[28] L. P. Kimble, "A randomized clinical trial of the effect of an angina self-management intervention on health outcomes of patients with coronary heart disease," *Rehabilitation Nursing*, vol. 43, no. 5, pp. 275–284, 2018.

[29] Z. Zhang, P. Jones, W. S. Weintraub et al., "Predicting the benefits of percutaneous coronary intervention on 1-year angina and quality of life in stable ischemic heart disease: risk models from the COURAGE trial (Clinical Outcomes Utilizing Revascularization and Aggressive Drug Evaluation)," *Circulation: Cardiovascular Quality and Outcomes*, vol. 11, no. 5, article e003971, 2018.

[30] A. L. Eckhardt, H. A. Devon, M. R. Piano, C. J. Ryan, and J. J. Zerwic, "Fatigue in the presence of coronary heart disease," *Nursing Research*, vol. 63, no. 2, pp. 83–93, 2014.

[31] X. Chen, Z. Wen, and J. Xiong, "Chitosan oligosaccharides reduces the fatigue in a rat model," *Journal of Zhanjiang Teachers College*, vol. 26, no. 1, pp. 53–55, 2005.

[32] L. Kao, T. H. Liu, T. Y. Tsai, and T. M. Pan, "Beneficial effects of the commercial lactic acid bacteria product, Vigiis 101, on gastric mucosa and intestinal bacterial flora in rats," *Journal of Microbiology, Immunology and Infection*, no. 18, pp. 30195-30196, 2018.

[33] X. M. Ben, X. Y. Zhou, W. H. Zhao et al., "Supplementation of milk formula with galacto-oligosaccharides improves

intestinal micro-flora and fermentation in term infants," *Chinese Medical Journal*, vol. 117, no. 6, pp. 927–931, 2004.

[34] A. Balasso, M. Fritzsche, D. Liepsch, S. Prothmann, J. S. Kirschke, S. Sindeev et al., "High-frequency wall vibrations in a cerebral patient-specific aneurysm model," *Biomedical Engineering/Biomedizinische Technik*, 2018.

[35] M. Sidira, A. Galanis, P. Ypsilantis et al., "Effect of probiotic-fermented milk administration ongastrointestinal survival of *Lactobacillus casei* ATCC 393 and modulation of intestinal microbial flora," *Journal of Molecular Microbiology and Biotechnology*, vol. 19, no. 4, pp. 224–230, 2010.

[36] S. Alex, L. Lichtenstein, W. Dijk, R. P. Mensink, N. S. Tan, and S. Kersten, "ANGPTL4 is produced by entero-endocrine cells in the human intestinal tract," *Histochemistry and Cell Biology*, vol. 141, no. 4, pp. 383–391, 2014.

[37] Q. Li, T. Wu, R. Liu, M. Zhang, and R. Wang, "Soluble dietary fiber reduces trimethylamine metabolism via gut microbiota and co-regulates host AMPK pathways," *Molecular Nutrition & Food Research*, vol. 61, no. 12, 2017.

[38] C. Zhai, W. Shi, W. Feng et al., "Activation of AMPK prevents monocrotaline-induced pulmonary arterial hypertension by suppression of NF-κB-mediated autophagy activation," *Life Sciences*, vol. 208, pp. 87–95, 2018.

[39] E. C. Thomas, S. C. Hook, A. Gray et al., "Isoform-specific AMPK association with TBC1D1 is reduced by a mutation associated with severe obesity," *Biochemical Journal*, vol. 475, no. 18, pp. 2969–2983, 2018.

[40] E. M. Desjardins and G. R. Steinberg, "Emerging role of AMPK in brown and beige adipose tissue (BAT): implications for obesity, insulin resistance, and type 2 diabetes," *Current Diabetes Reports*, vol. 18, no. 10, p. 80, 2018.

[41] E. Yuan, X. Duan, L. Xiang et al., "Aged oolong tea reduces high-fat diet-induced fat accumulation and dyslipidemia by regulating the AMPK/ACC signaling pathway," *Nutrients*, vol. 10, no. 2, p. 187, 2018.

[42] Q. Yang, S. L. Lin, M. K. Kwok, G. M. Leung, and C. M. Schooling, "The roles of 27 genera of human gut microbiota in ischemic heart disease, type 2 diabetes mellitus, and their risk factors: a Mendelian randomization study," *American Journal of Epidemiology*, vol. 187, no. 9, pp. 1916–1922, 2018.

[43] X. Cui, L. Ye, J. Li et al., "Metagenomic and metabolomic analyses unveil dysbiosis of gut microbiota in chronic heart failure patients," *Scientific Reports*, vol. 8, no. 1, p. 635, 2018.

[44] V. Wiwanitkit, "E. coli outbreak and myocarditis: a story in cardiology," *The Anatolian Journal of Cardiology*, vol. 11, no. 8, p. 746, 2011.

[45] A. Uribarri, M. Martinez-Selles, R. Yotti, E. Perez-David, and F. Fernandez-Aviles, "Acute myocarditis after urinary tract infection by *Escherichia coli*," *International Journal of Cardiology*, vol. 152, no. 2, pp. e33–e34, 2011.

[46] F. Z. Marques, E. Nelson, P. Y. Chu et al., "High-fiber diet and acetate supplementation change the gut microbiota and prevent the development of hypertension and heart failure in hypertensive mice," *Circulation*, vol. 135, no. 10, pp. 964–977, 2017.

[47] H. D. Holscher, H. M. Guetterman, K. S. Swanson et al., "Walnut consumption alters the gastrointestinal microbiota, microbially derived secondary bile acids, and health markers in healthy adults: a randomized controlled trial," *The Journal of Nutrition*, vol. 148, no. 6, pp. 861–867, 2018.

[48] K. Wang, X. Yu, Y. Li et al., "Bifidobacterium bifidum TMC3115 can characteristically influence glucose and lipid profile and intestinal microbiota in the middle-aged and elderly," *Probiotics and Antimicrobial Proteins*, 2018.

[49] B. G. Wang, H. B. Xu, F. Xu, Z. L. Zeng, and H. Wei, "Efficacy of oral *Bifidobacterium bifidum* ATCC 29521 on microflora and antioxidant in mice," *Canadian Journal of Microbiology*, vol. 62, no. 3, pp. 249–262, 2016.

[50] T. N. Kelly, L. A. Bazzano, N. J. Ajami et al., "Gut microbiome associates with lifetime cardiovascular disease risk profile among Bogalusa Heart Study participants," *Circulation Research*, vol. 119, no. 8, pp. 956–964, 2016.

[51] X. Lin, Y. Xia, G. Wang et al., "*Lactobacillus plantarum* AR501 alleviates the oxidative stress of D-galactose-induced aging mice liver by upregulation of Nrf2-mediated antioxidant enzyme expression," *Journal of Food Science*, vol. 83, no. 7, pp. 1990–1998, 2018.

[52] J. Chen, Y. Wu, C. Yang, X. Xu, and Y. Meng, "Antioxidant and hypolipidemic effects of soymilk fermented via *Lactococcus acidophilus* MF204," *Food & Function*, vol. 8, no. 12, pp. 4414–4420, 2017.

[53] H. T. Yao, S. Y. Huang, and M. T. Chiang, "A comparative study on hypoglycemic and hypocholesterolemic effects of high and low molecular weight chitosan in streptozotocin-induced diabetic rats," *Food and Chemical Toxicology*, vol. 46, no. 5, pp. 1525–1534, 2008.

[54] J. G. Kim, S. H. Jo, K. S. Ha et al., "Effect of long-term supplementation of low molecular weight chitosan oligosaccharide (GO2KA1) on fasting blood glucose and HbA1c in *db/db* mice model and elucidation of mechanism of action," *BMC Complementary and Alternative Medicine*, vol. 14, no. 1, p. 272, 2014.